Distribution and chemistry of kimberlite indicator minerals in the southern Slave Province, NWT

Dana Campbell

A thesis submitted to the Department of Geology in partial fulfillment of requirements for the Degree of Master of Science

Lakehead University, Thunder Bay, Ontario

Abstract

As part of the greater Slave Province geophysical, surficial materials and permafrost study, a Northwest Territories Geological Survey (NTGS) led government-academic-industry research program, this study is intended to identify and interpret indicator mineral glacial dispersal trains using publicly available mineral chemistry data and discuss the uses of the NTGS kimberlite indicator mineral chemistry database (KIMC) for diamond exploration in the southern Slave Province.

In addition to the database, 21 till samples were collected from the southern Slave Province national topographic system map sheets 075M and 075N during the 2017 field season (17-DECS sample suite). Kimberlite indicator minerals (KIM) were recovered from the till samples and selected grains were subsequently analyzed using scanning electron microscopy and laser ablation techniques to identify mineral chemistry that is representative of KIMS in surficial sediment samples in the KIMC for the southern Slave. Mineral chemistry data collected during this study were evaluated and compared to those published in a database of the Slave Province by the NTGS. The database was created as a collaborative effort between the NTGS and exploration companies in order to compile an all-encompassing kimberlite indicator mineral database with raw mineral chemistry data. Mineral chemistry data retrieved from the NTGS database and from analysis of the 17-DECS sample suite were used to interpret kimberlite potential of the region. Ilmenite, chromite, Cr-diopside, olivine, and garnet grains in surficial sediment samples were assessed in terms of their chemistry and areal distribution in the Slave Province. The raw mineral chemistry data for garnets were classified according to their G-numbers and chromite, ilmenite, olivine, and Cr-diopside were classified as kimberlitic or non-kimberlitic. Data from indicator minerals in till samples collected during this study were classified using the same criteria.

Indicator minerals distribution patterns were mapped based on the classification of individual mineral grains. These maps show disparity in the amount of data contained in the database and the variation in kimberlite indicator mineral dispersal train direction, length, and composition between the north and south Slave. Kimberlite indicator mineral dispersal trains in the southern Slave Province are disjointed with highly variable indicator concentrations per sample location, and trend approximately westward. These trains are near monomineralic, often exclusively consisting of garnet. Trains in the northern Slave Province are more consistent in concentration (concentration increases with increasing distance down ice) and trend northwest and west. These trains have greater variety of kimberlitic mineral species. The direction, length, and composition of the trains reflects glacial processes (erosion, entrainment, transportation, deposition), permafrost conditions, and the nature of the source kimberlites. Of the kimberlite indicator minerals identified, garnet was the most abundant and informative mineral recovered from surficial sediment samples in the southern Slave Province. Overall, there was little variation in abundance of garnet G-number classes which could not be contributed to variations in sample density. However, garnet grains recovered from till samples in the southern Slave Province have lower sodium concentrations than till samples in the northern Slave. It has been proposed that the concentration of sodium in certain garnets is indicative of kimberlite diamond potential. Sodium concentrations of the southern Slave Province are below the diamond indicator threshold (Na_2O>0.07%). Although this may be indicative of a lower diamond potential, it may also be a result of differing geochemical compositions of the subcontinental lithospheric mantle.

Table of Contents

Table of Figures

Table of Tables

Acknowledgements

I would like to thank my supervisor Dr. Shannon Zurevinski for her support and guidance throughout this project. Her enthusiasm and knowledge made this project possible.

I would also like to thank Barrett Elliot from the Northwest Territories Geological Survey and CanNor for providing me with this opportunity, financial support, and guidance.

I would also like to thank Dave Sacco and Robin McKillop for taking me out into the field with them while conducting ground-truthing and geomorphological mapping in the NWT.

A big thank you goes out to Anne Hammond, Kristi Tavener, and Dr. Jonas Valiunas for their countless hours mounting mineral grains in epoxy. This is a tremendously tedious task, and they were patient, efficient, and friendly no matter how many vials of minerals I brought to them. Kristi is now a mineral mounting master, and it really showed in my samples. A special thanks is extended to Beth McClenaghan for her editing and input on this thesis. Beth is an expert in the world of kimberlites and her help and suggestions were an invaluable asset for this project.

I would also like to thank my family for their support throughout this project, I definitely would not be where I am today without their encouragement.

Chapter 1: Introduction

1.1 Objective

Over the past 30 years, large indicator mineral data sets have been compiled by diamond exploration companies, the Northwest Territories Geological Survey (NTGS) and the Geological Survey of Canada as part of diamond exploration programs. In order to help preserve some of the indicator mineral data from individual exploration programs, the data have been compiled and published by the NTGS in a publicly accessible database. This database was published to encourage and facilitate further mineral exploration in the Northwest Territories (NWT). The database includes surficial sediment sample location and related indicator mineral geochemical data from across the NWT and provides an opportunity to utilize regional data in order to make inferences about mineral deposits exploration using drift prospecting. Many studies of kimberlite indicator mineral dispersal have been completed in the northern Slave Province, mostly as a result of the 1990-2000s staking rush in the Lac des Gras region. These studies resulted in a greater understanding of till distribution, glacial transport directions, and kimberlite indicator mineral distribution and chemistry in the northern Slave Province. Several plan and 3D models have been created for the glacial dispersal of indicator mineral in the northern Slave Province and other regions of Canada (e.g. McClenaghan et al., 2002; Stea et al., 2009; Kelley et al., 2019). In contrast, the southern Slave Province has only begun to attract the attention of exploration companies and geoscientists. The distribution of till, glacial transport trends, and indicator mineral chemistry of the region are not well understood. In the southern Slave Province, the mechanics of till redistribution and cryoturbation may present a significant difference (in comparison to the northern Slave Province), and these differences could result in the need for different exploration approaches in the South.

This study is part of the Slave Province Surficial Materials and Permafrost study, a multi-disciplinary study that involves the assessment of surface sediment deposited during numerous past glaciations and permafrost that is being overseen by the NTGS. The objective of the study reported here is to identify kimberlite indicator distribution patterns, relative abundances, and mineral chemistry signatures, with an emphasis on garnet chemistry, within till of the southern Slave Province. Garnet chemistry in the Slave Province is highly variable, with most garnets being classified using G-numbers based on criteria by Grütter et al. (2004). This study was conducted utilizing the regional database available to the public through the Northwest Territories Geological Survey (NTGS, 2018) and comparing the database to results obtained from till samples collected as part of this southern Slave project in the summer of 2017. The volume of kimberlite indicator mineral chemistry data made available to the public in recent years is unprecedented and allows large-scale interpretations of kimberlite indicator mineral dispersal and chemistry in ways previously unattainable.

The comparison and visual representation of mineral chemistry variations between the north and south Slave Province KIMs are intended to be used as a preliminary tool in exploration. The variations in chemistry and dispersal patterns have implications as to where indicator minerals could potentially occur in the southern Slave Province. Additionally, the variations also display which kimberlite indicator(s) may be present in the southern Slave Province and in what relative abundance. Since glacial dispersal patterns are seemingly well known in parts of the northern Slave Province, these new data provide an opportunity for comparative analysis.

1.2 Drift Prospecting

Drift prospecting in glaciated terrain is a technique used in mineral exploration wherein mineralogy, geochemistry, and lithology of till are used to locate bedrock deposits and/or a distinct bedrock source. The dispersal of these indicator minerals and lithologies is a product of

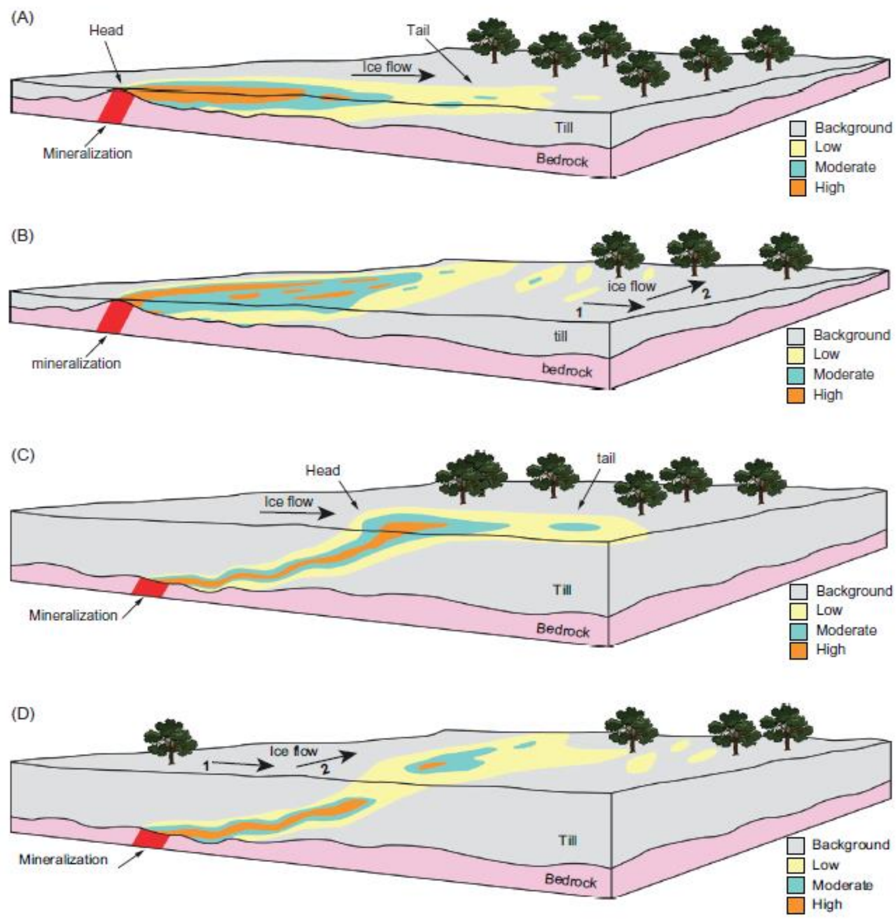

Figure 1.1: Conceptual models of glacial dispersal trains depicting a buried up-ice component, a head, and a tail. (A) thin till covered where host is dispersed by a single ice flow direction; (B) thin till cover where host is dispersed by two phases of ice flow; (C) thick till cover where host is dispersed by a single phase of ice flow; (D) thick till cover where host is dispersed by two phases of ice flow (McClenaghan and Paulen, 2018).

the entrainment, transport and deposition of bedrock debris by glacial processes (Figure 1.1).

In situ kimberlite can contain tens of thousands of indicator minerals per 10 kg sample (McClenaghan and Kjarsgaard, 2001). These minerals are more abundant and sufficiently dense to be concentrated by gravity methods (McClenaghan and Kjarsgaard, 2001). Kimberlite indicator minerals (KIMs) include xenocrysts derived from disaggregated peridotite and eclogite mantle xenoliths (olivine, enstatite, Cr-diopside, Cr-pyrope garnet, Cr-spinel, pyrope-almandine garnet, omphacitic pyroxene, and diamond); and the associated megacryst suite of minerals (low-Cr Ti-pyrope, Mg-ilmenite, Cr-diopside, phlogopite, zircon, and olivine); and kimberlite-derived olivine, spinel and ilmenite (McClenaghan and Kjarsgaard, 2001). These minerals are not necessarily indicative of kimberlite magmatism as they can also be found in other ultrabasic rocks of deep-seated origins (McClenaghan and Kjarsgaard, 2001). Minerals considered to be potential diamond indicator minerals (DIMs) are garnets classified as “G10D”, “G3D”, “G4D” and “G5D” according to the criteria of Grütter et al. (2004). Minerals classified as KIMs have some inherent diamond association, whereas minerals classified as DIMs have a higher statistical association to diamond.

Various models are used to estimate glacial dispersal distances and to assess the glacial entrainment and depositional processes (McClenaghan and Paulen, 2018). McClenaghan and Paulen (2018) have noted that the dispersal model that best represents observed glacial dispersal trains is the aggradational-constant entrainment decay model (Figure 1.2) of Stanley, (2009). In this model, the englacial debris and subglacial material (materials within and below the glacier, respectively) are treated as cells (Stanley, 2009; McClenaghan and Paulen, 2018). The cells form the basal part of the glacier and each contains a specific geochemical, mineralogical, or lithological composition (McClenaghan and Paulen, 2018). Each layer of till is composed of unit cells that are adjacent to each other, and material within the cell is entrained from bedrock by regelation, glacial creep, internal thrusting, abrasion, or from subjacent cells by internal shearing processes, and transported upwards by internal shearing (McClenaghan and Paulen, 2018). As the glacier flows down ice, the metal-rich debris is transported upwards in the glacier and down ice of the bedrock source (McClenaghan and Paulen, 2018).

Ice flow →

Till layers

10	0	0	0	0	0	0	0	0	2	3	6	8	10	11	11	10
9	0	0	0	0	0	0	0	1	3	5	8	10	11	11	11	9
8	0	0	0	0	0	0	0	2	5	8	10	12	12	11	10	8
7	0	0	0	0	0	0	1	4	8	11	13	13	12	10	8	6
6	0	0	0	0	0	0	3	7	11	14	14	13	11	8	6	4
5	0	0	0	0	0	1	6	12	16	16	14	11	8	6	4	3
4	0	0	0	1	1	2	12	18	18	16	12	8	6	4	2	1
3	0	0	1	3	6	9	21	22	18	13	8	5	3	2	1	0
2	0	2	7	13	19	26	30	21	13	7	4	2	1	1	0	0
1	0	17	32	44	53	61	27	12	5	2	1	0	0	0	0	0
	0	**100**	**100**	**100**	**100**	**100**	0	0	0	0	0	0	0	0	0	0
Bedrock		***Mineralization***					***Bedrock***									

Figure 1.2: Concentration of metal rich debris in till illustrating the aggradational-constant entrainment decay model down ice from mineralized bedrock. Mineralized bedrock is eroded and smeared down -ice as till layers are accreted, the size of the dispersal train increases down-ice, and the concentration of metal-rich material decreases by dilution down ice (McClenaghan and Paulen, 2018: Modified from Stanley, 2009). Red= highest concentration, white = lowest concentration.

In permafrost terrain, a particularly useful location for sampling relatively unoxidized till is in frostboils (McMartin and Campbell 2009; McClenaghan and Paulen, 2018). A frostboil is a feature that develops in the active layer of till in permafrost regions during the maximum summer thaw period (Shilts, 1978; McMartin and Campbell, 2009; McClenaghan and Paulen, 2018). Frostboils are the product of hydrostatic pressure in the summer thaw active layer pushing till up to the surface (Figure 1.3). Frostboils can be recognized on surface by a distinct rounded patch barren of any vegetation, surrounded by rock fragments and vegetation (Figure 1.4). Till within frostboils is generally homogenous and relatively unoxidized, making it possible to collect representative samples at shallow depths (~30 cm) from the centre of the frostboil (McClenaghan and Paulen, 2018). In an inactive frostboil, as depicted in Figure 1.4, the till is located below the thin soil profile.

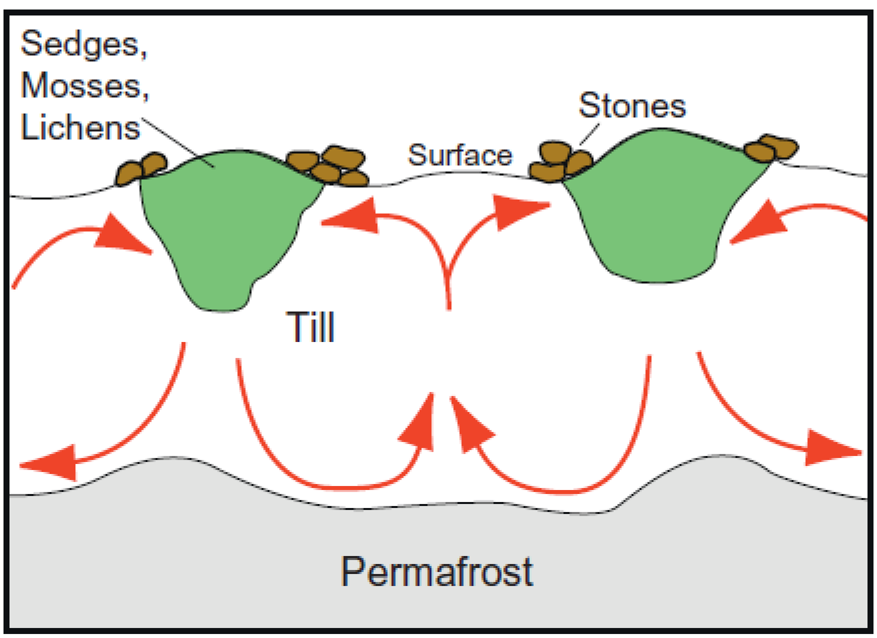

Figure 1.3: Frostboil schematic cross-section from McClenaghan and Paulen (2018), emphasizing the mixing and push of fresh till to the surface due to hydrostatic pressure during the summer thaw period.

Figure 1.4: Relict or inactive frostboil at till sample site 17-DECS-006.

Figure 1.5: Active frostboil with a high moisture content.

In this study, we explore the variability in potential extraction of indicator minerals from frostboils developed in till based on regional variations in active layer thickness. When a frostboil is active, it is thought to mix and push up material from the greatest depths of the active layer (0.5 to 1 m) in till, and in places where the till is thin (i.e. less than 0.5 m), the active processes that form the frostboils may extend into bedrock (Figure 1.3, Figure 1.5). In the Northwest Territories, there is a southward increase in active-layer thickness related to latitude. The variation in active-layer thickness is a product of the type of vegetation, organic layer thickness, soil moisture, and snow cover. In tundra soils, the mean maximum thaw depths are usually less than 80 cm (Nixon, 2000). In the southern Northwest Territories active layer thaw depths are often greater than 100 cm (Nixon, 2000). This variation in active layer thickness has the potential to affect the depth from which frost boils bring fresh till to surface and thus the indicator mineral (i.e. KIMs) content in till down ice of kimberlites.

1.3 Regional Bedrock Geology

1.3.1 Slave Province

The Slave Province is an Archean craton in the northwestern parrt of the Canadian Shield, between the Churchill Province (east) and the Interior platform (west) (Figure 1.6). The presence of diamondiferous kimberlites was first reported in the Slave Province in 1991 (Kjarsgaard and Levinson, 2002). The craton consists of steeply dipping metamorphosed volcanic rocks that strike north to northeast with metaturbidites and plutonic rocks separating units (Isachsen and Bowring, 1994). The Slave Craton consists of an anomalously high proportion of metamorphosed sedimentary rocks, with greenschist to lower amphibolite facies (Isachsen and Bowring, 1994). This province is host to numerous diamondiferous kimberlites and active diamond mines, including Ekati and Diavik in the central part and Gahcho Kué and Snap Lake in the southern part. The reconnaissance scale map shown in figure 1.6 consists of a compilation of rock units assembled by the NTGS from various open file reports. The most up to date legend for detailed rock unit classifications and descriptions can be found in Stubley and Irwin (2019). A short summary of the legend can be seen below in Table 1.1.

Table 1.1: Descriptions of select Rock Sub Classes from Stubley and Irwin (2019).

Descriptions of select Rock Sub Classes from Stubley and Irwin (2019)	
Rock Sub Class	Description
Tectonic	felsic and mafic mylonites; varied protoliths; subhorizontal lineations predominate; subvertical mylonite, augen gneiss; various protoliths (derived largely from K-feldspar porphyritic granite); mylonitic lineations not recognized; late brittle reactivation resulted in brecciation and quartz flooding along the fault zone; heterogeneous zone of "paragneiss" (dominated by quartz-biotite schist and amphibole-rich layers) and discontinuous pink- to orange-weathering hematitic granite; large-scale breccia textures; variably sheared oblique to foliation/gneissosity
Alkaline	gabbro and quartz syenite; gabbro, syenogranite, carbonatite, syenite, etc.; syenite; hedenbergite, ferrorichterite; biotite-alkaline amphibole-perthite granite; gabbro to syenogranite; heterogeneous suite of unfoliated hornblende-bearing intrusions
Alkaline-mafic	gabbro to syenogranite; heterogeneous suite of generally unfoliated hornblende-bearing rocks; hornblende syenite, quartz syenite, syenogabbro; variably foliated;
Granitoid	granite and granodiorite; biotite, muscovite +/-hornblende; heterogeneous multiphase granitoids (granite, granodiorite, tonalite); variably foliated (massive to moderately gneissic); common xenoliths in some area; grouped as the "Anton Complex" by Henderson (1985); biotite monzogranite; K-feldspar porphyritic; weakly to moderately foliated; massive homogeneous granite with >10% gneissic or foliated phases; minor supracrustal inclusions; generally leucocratic, medium to coarse grained; biotite and muscovite may both be present; multiple sheet-like intrusions parallel to tectonic fabric

Mafic	fine- to medium-grained gabbro with centimetre-scale hornblende phenocrysts; no significant magnetic enhancement; non-magnetic medium-grained gabbro; weak to no foliation; appears to intrude post-volcanic argillite; mapped as gabbro; extreme magnetism suggests ultramafic affinity; gabbro dyke; weakly magnetic; limited description available
Metamorphic	granitoid migmatite, heterogeneous, anatectic and injection leucosome; heterogeneous gneisses and granitoid rocks of various ages; garnet-bearing granite - granodiorite to garnet - biotite - sillimanite migmatitic gneiss +/-sediment rafts; foliated metagranite-tonalite, homogeneous with gneiss inclusions; unsubdivided mixed gneisses, granitoids and pegmatite
Mixed	heterogeneous mafic and pelitic gneiss, amphibolite; mostly of supracrustals origin; interbedded dacitic volcaniclastic rocks and greywacke-argillite; some chert; mixed pelitic and felsic schists
Sedimentary	pelitic to psammitic schist; local anatectic melt; rare aluminosilicate blasts; sillimanite - cordierite - garnet migmatite; >5% leucosome; local banded iron formation and gabbro; paragneiss derived from Yellowknife Supergroup metasedimentary rocks as inclusions or zones within granitoid suite
Ultramafic	strongly magnetic ultramafic intrusion; unsubdivided; strongly magnetic mafic/ultramafic body described as "komatiitic pyroxenite"; strongly Fe-carbonate granular altered ultramafic intrusion; local moderate fuchsite; moderately magnetic; pyroxenite plug, massive, coarse-grained (to 3 cm), brown to greenish black
Unknown	uncertain rock types
Volcanic	dacitic to rhyolitic tuffs; basalt to andesite; dark grey, brown, rarely green; massive or layered; possible pillowed flows locally; commonly amygdaloidal, plagioclase-phyric; rarely variolitic; locally strongly foliated; hypabyssal porphyry and lesser rhyolite to rhyodacite; feldspar phyric, and locally feldspar-quartz phyric; local fragmental textures and/or alignment of phenocrysts

The Ekati and Diavik mines are both in the Lac de Gras Kimberlite field (NTS 76D) (Figure 1.7). They lie within an area of Archean volcanic rocks and supracrustal mudstone turbiditic sedimentary rocks belonging to the Yellowknife Supergroup (Henderson, 1970; Padgham and Atkinson, 1991; Padgham and Fyson, 1992). The supracrustal rocks have undergone varying degrees of metamorphism and were intruded by a 2.61 Ga diorite-granodiorite and a 2.59 Ga biotite and muscovite+biotite monzogranite (Padgham and Fyson, 1992). Proterozoic diabase dyke swarms trending northeast, east, and north-northwest are found crosscutting the area with some dykes being as wide as 50m (Padgham and Fyson, 1992). Several kimberlites intrude these older rocks and are Cretaceous to Eocene in age (Padgham and Fyson, 1992; Armstrong and Chatman, 2001).

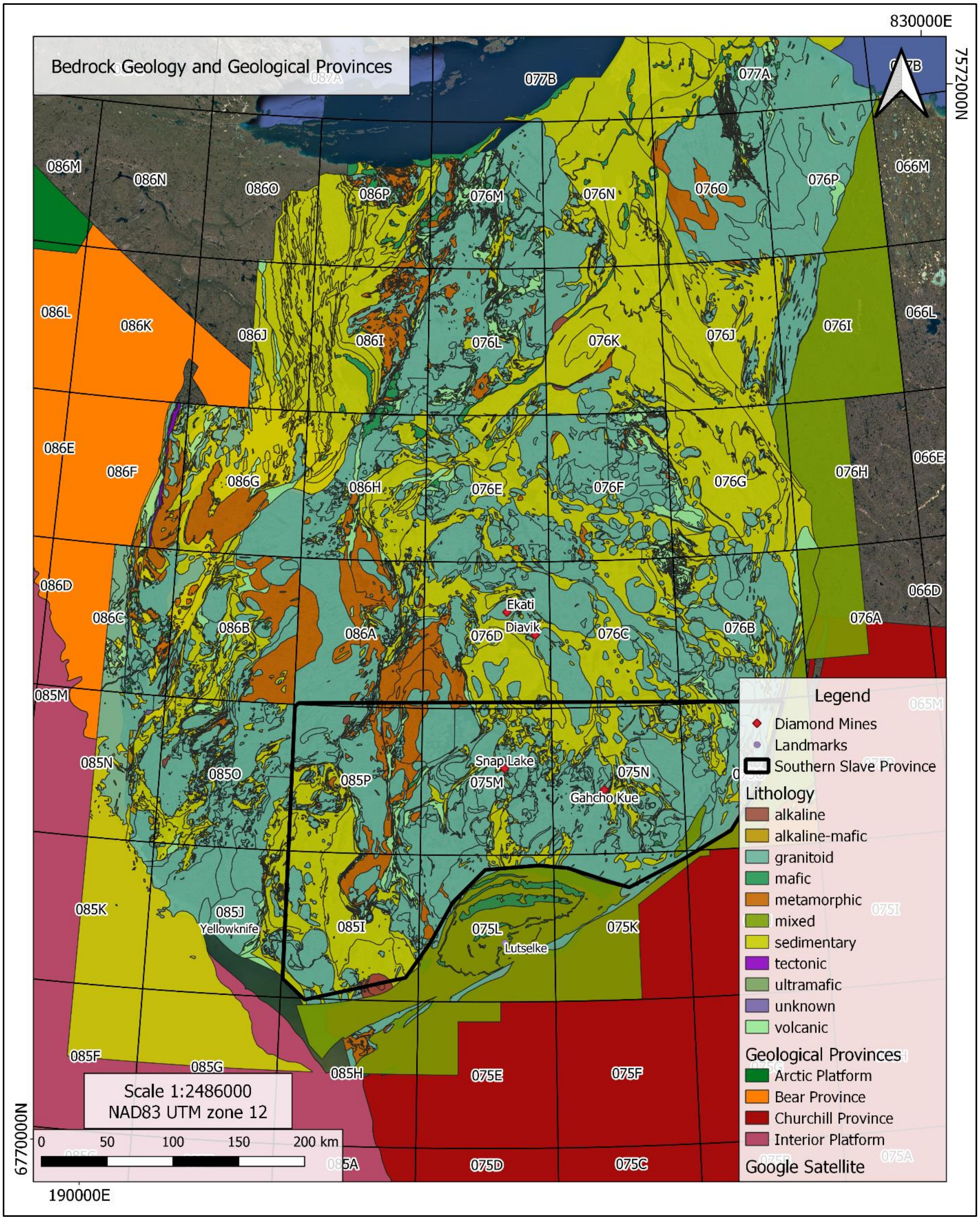

Figure 1.6: Reconaissance-scale bedrock geology of the Slave Province, NWT, Canada. Southern Slave Province represented in this study (outlined in black). Bedrock geology from NWT Open File 2005-001, NWT Geoscience Office (2018);and Stubley and Irwin (2019).

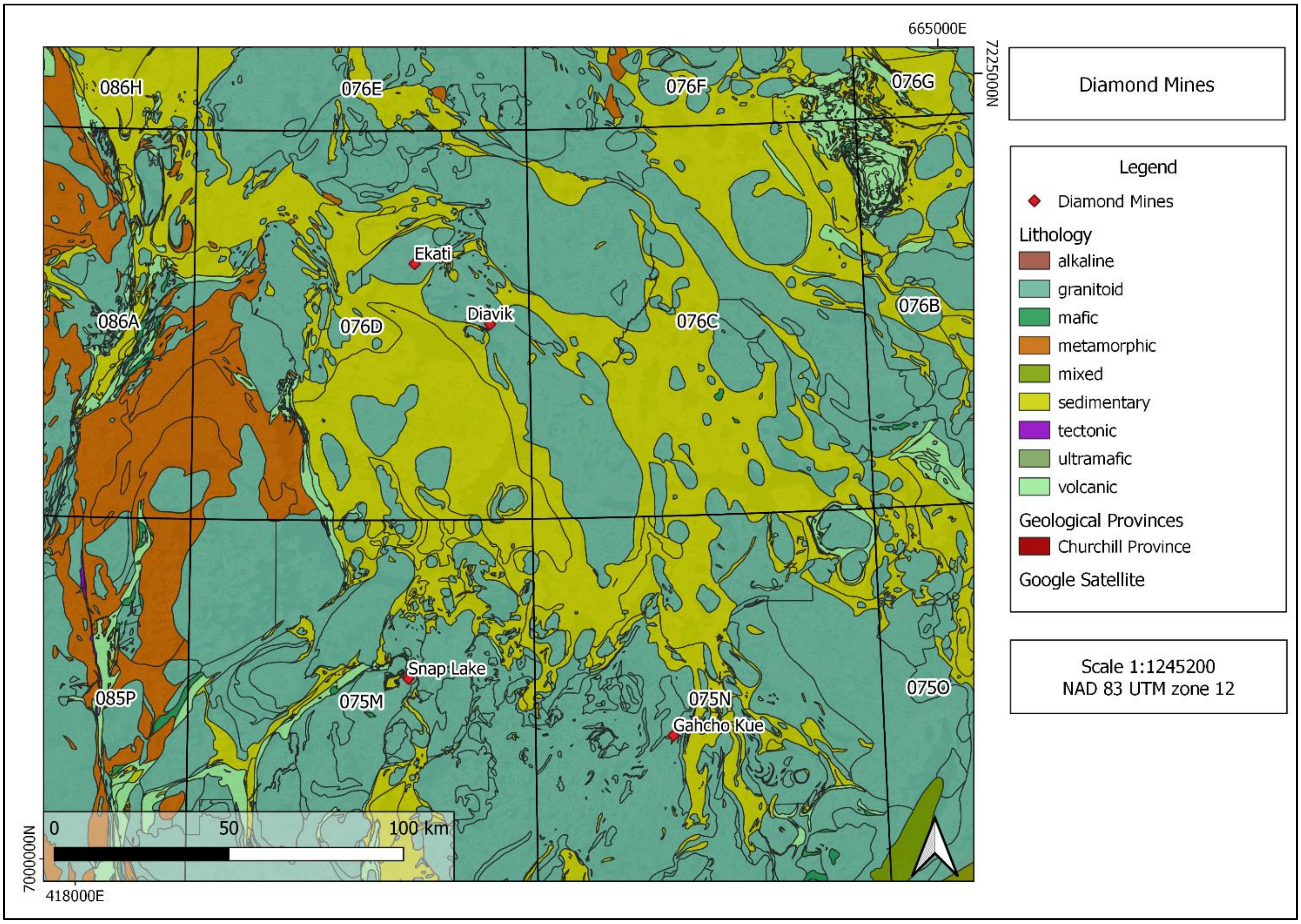

Figure 1.7: Diamond mine locations in the central and southeastern Slave Province, NWT, Canada. Bedrock geology data from the NWT Open File 2005-001, NWT Geoscience Office (2018); and Stubley and Irwin (2019).

Ekati is an active diamond mine with the Koala, Lynx, Misery, Pigeon, and Sable kimberlites currently being mined. The kimberlites of Ekati represent the only Phanerozoic igneous activity on the property and are more commonly intruded within pluton hosts (Nowicki et al., 2004). They are associated with lineaments, with intersections of two or more lineaments, and with intersections of lineaments with dykes (Nowicki et al., 2004). It is evident that kimberlites in the area are not exclusively associated with specific structural features (Nowicki et al., 2004). However, Nowicki et al. (2004) have noted an alignment of kimberlites along dykes of the north-northeast trending Lac de Gras swarm. Emplacement ages of the Ekati kimberlites range from 45 to 75 Ma with five different age groupings, based on the age dates of over 30 kimberlites (Nowicki et al., 2004). The Ekati kimberlites are pipe-shaped with a steep dip of ~75 to 85° and tapering inward walls with increasing depth (Nowicki et al., 2004). Till above the Ekati pipes has been measured to be as thick as 30 m by reverse circulation drilling (Crawford et al., 2009).

The Diavik mine is comprised of the A154 south, A154 north, A418, and most recently the A21 kimberlite pipes. The Diavik kimberlites are Eocene volcanic deposits intruded in Archean granitoid and metasedimentary rock (Rio Tinto, 2015). The kimberlites were subsequently covered by a Quaternary glacial till that is up to 40 m thick in the immediate area of the pipes (Rio Tinto, 2015). The Diavik pipes are steeply inclined to vertical cone-shaped intrusions, or pipes with the walls inclined and dipping at ~78 to 84° (Rio Tinto, 2015). The pipes range from 100 m to 150 m wide in plan and form complex elongated cone shapes with depths nearing 1000 m below surface (Rio Tinto, 2015).

1.3.2 Exploration history of the southern Slave Province

During the 1990-2000s, there was an emphasis on diamond claim staking in the Slave Province, specifically within what would become the Lac des Gras kimberlite field. Within the past 20 or so years, numerous geophysical surveys and till sampling surveys have been conducted over the southern Slave Province. The samples taken during this study were collected within the Munn Lake Property which consists of 19 mineral claims over approximately 14,030 ha around Munn Lake and Margaret Lake in the southern Slave Province (Miller, 2016). Historic work on the Munn Lake Property commenced in 1992 with airborne geophysical surveys and till and beach sediment sampling, followed by diamond drilling in 1993 (Miller, 2016). A kimberlite boulder, known as the Yuryi occurrence, was discovered on surface on the property in 1997 (Miller, 2016). Table 1.1 summarizes the exploration activity that has occurred on the Munn Lake Property. Within the Munn Lake Property, 19 airborne and 52 ground geophysical surveys have been conducted and a total of 4,918 till samples have been examined for their KIM content (Miller, 2016). In addition, there have been 79 holes diamond drilled in the claim area (Miller, 2016). During the 2015-2016 field season, till?? samples were collected on the Munn property on behalf of 877384 Alberta Ltd. and Zimtu Capital Corporation (Miller, 2016). A total of 55 till samples were collected with 38 being submitted for recovery of KIM and subsequent microprobe analysis (Miller, 2016). In total, approximately 20,567 line km of airborne geophysical surveys with 1,374.17 line km of ground geophysical surveys were completed on and around the Munn Lake Property (Miller, 2016). An approximate total of 11,818.37 m of diamond drilling was completed in 82 holes, with approximately 3,731.79 m of sonic drilling in 252 holes, and a total of 2,918 beach, esker, and till samples were collected (Miller, 2016). GPS inaccuracy during the 1990s resulted in historic sample locations being displaced by as much as 300 m (Miller, 2016).

Table 1.2: Summary of prior exploration activity on the Munn Lake Property in the southern Slave Province from Miller (2016).

Year	Summary of prior work-Munn Lake Property while part of the MacKay Lake Project
1992	Airborne electromagnetic and magnetic survey, 4,834 line km; 172 till and beach samples.
1993	Ground magnetic surveys, 9 grids, 73.35 line km; 130 till samples. 3 diamond drill holes, 218 m.
1994	Airborne electromagnetic, magnetic and VLF-EM survey, 4,575 line km. Ground magnetic surveys, 19 grids, 143.25 line km. Ground HLEM surveys, 149.37 line km; Helicopter borne magnetic surveys, 2 grids. 259 till samples, Diamond drilling, 3 holes, 406.75 m
Year	**Summary of prior work- Munn Lake Property while part of the Back Lake Project**
1992	Airborne electromagnetic and magnetic survey, 3,813 line km; 106 till, esker and beach samples.
1993	Ground magnetic surveys, 7 grids, 39.60 line km; 74 till samples.
1994	Airborne electromagnetic, magnetic and VLF-EM survey, 4,575 line km. Ground magnetic surveys, 4 grids, 26.10 line km; Ground HLEM surveys, 4 grids, 26.10 line km. Helicopter borne magnetic survey, 8 grids. 139 till samples.
1995	Diamond Drilling, 2 holes, 602.24 m. Intersected 2 intervals of kimberlite (1.51 – 4.40 m wide).
1996	Ground magnetic surveys, 45 grids, 429.14 line km. Ground HLEM surveys, 22 grids, 125.80 line km; Diamond drilling, 12 holes, and 2,711.49 m. 1,433 till samples. Helicopter borne magnetic survey, 368 line km. Airborne electromagnetic and magnetic survey, 4,224 line km.
1997	Airborne magnetic and electromagnetic survey, 1,269 line km. Diamond drilling, 15 holes, 2,129.70 m. Collection of kimberlitic boulder float (Yuryi occurrence) – diamond analysis returned 226 diamonds. Size and texture of the boulders suggest a kimberlite pipe as the source, not the Munn Lake Sill.
1998	Bathymetric survey of Grid 19. Diamond drilling, 21 holes, 1,985.5 m.
1999	Diamond Drilling, 26 holes, totalling 2,902.19 m. Delineation of the Munn Lake Sill over a strike length of 1.3 km and to a depth of 120 m. Eight holes intersected kimberlite with a true width ranging from 0.25 to 12 m. Sonic Drilling, 252 holes, totalling 3,731.79 m. Targeting a sill in the bottom of Munn lake, returned 14 diamonds in 67.3 kg of kimberlite.
2000	Ground magnetic survey, 15.84 line km; 134 till samples.
2001	Ground HLEM survey, 7.73 line km; 75 till samples.
2002	Airborne Digihem survey, 1,484 line km; Ground magnetic survey, 1 grid, 4.90 line km. Ground HLEM survey, 1 grid, 3.35 line km; 138 till samples.
2003	Ground magnetic survey, 16 grids, 131.65 line km; Ground HLEM survey, 15 grids, 43.58 line km. 140 till samples. Diamond drilling, 3 holes, totalling 495.00 m.
2004	Ground magnetic survey, 21 grids, 135.70 line km; Ground HLEM survey, 11 grids, 18.71 line km. 118 till samples. Diamond drilling, 3 holes, totalling 367.50 m.

1.3.3 Southern Slave Province

The study area is comprised of a small part of the southeastern Slave Province (Figure 1.6, Figure 1.7). The southern Slave Province is underlain by composite granite-greenstone terrane composed of volcano-sedimentary successions overlying older sialic basement (Armstrong and Kjarsgaard, 2003). There is a large region of Yellowknife super-group metamorphosed sedimentary and metamorphosed volcanic rocks that occur within granodiorite and gneissic rocks, with common northwest-trending dykes (Armstrong and Kjarsgaard, 2003).

Gahcho Kué is an active diamond mine located at Kennady Lake, approximately 280 km northeast of Yellowknife. The kimberlites of Gahcho Kué are intruded in the Archean granitic basement rock of the Slave Craton (Caro et al., 2004). There are six kimberlites of the Gahcho Kué cluster (5034, 5034-South, Tesla, Tuzo, Hearn, and Wallace) which may represent the oldest known kimberlites of the Slave Craton at up to ~542 Ma (5034 pipe) (Caro et al., 2004). Granitic xenoliths have been recovered from four kimberlites (5034, Hearne, Tuzo and Tesla) and each of the pipes is dominated by hypabyssal kimberlite (HK) and tuffisitic kimberlite breccia (TKB).

The Snap Lake diamond mine is currently under care and maintenance (as of December 2015) and is located 220 km northeast of Yellowknife. Snap Lake is a Cambrian (523 Ma) kimberlite dyke (Gernon et al., 2012) that dips ~15° to the northeast and has an average thickness of 2.8 m extending over 3.5 km (Fulop et al., 2018).

In addition to the above-mentioned kimberlite at the two mines, the southern Slave Province is host to several other kimberlites including the CL-25, Cl-174, CL-186, Kelvin Pipe, Faraday Pipe, MZ Sills, Doyle Sill, the Margaret Lake Dyke, and the Yuryi pipe (Figure 1.8).

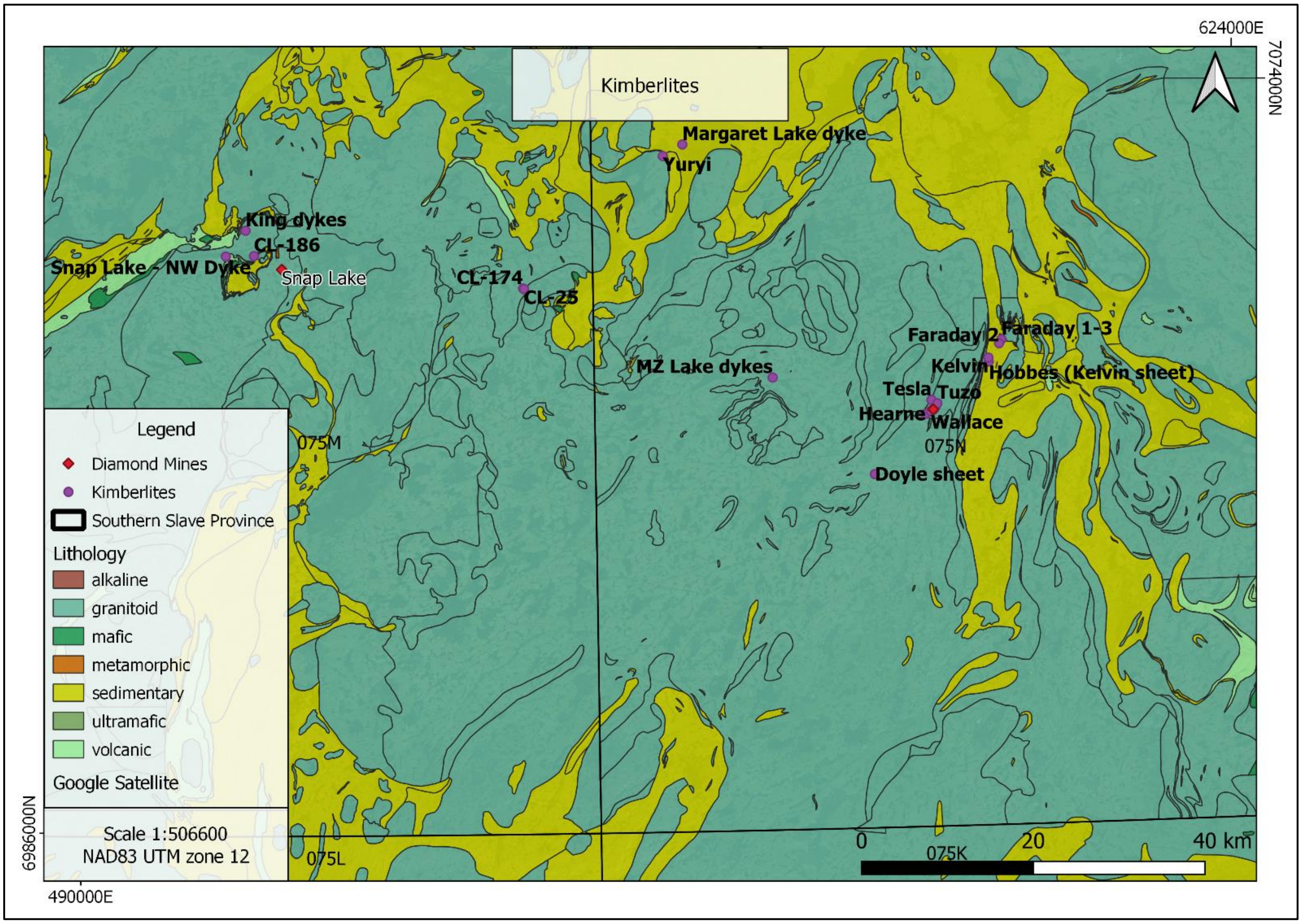

Figure 1.8: Known kimberlites of the southern Slave Province. Bedrock geology and data from NWT Open File 2005-001, NWT Geoscience Office (2018); Stubley and Irwin (2019).

1.4 Quaternary geology of the Slave Province

The most recent glaciation in North America was the Laurentide Ice Sheet, reaching its maximum extent around 26.5 and 19 ka during the Last Glacial Maximum (Clark et al., 2009; Gowan, 2013, Dyke, 2004). The Laurentide Ice Sheet covered most of Canada and extended into the northern United States (Gowan, 2013). It covered the entirety of the Slave Province and its advance and retreat has shaped the geomorphology of the region (Aylsworth and Shilts, 1989; Gowan, 2013; Knight, 2018) and dispersed kimberlite indicator minerals. Ice retreat in the southern Slave Province occurred approximately 10 000 to 8 000 years ago (Gowan, 2013). This age range is based on the age date of wood and marine shell samples from the region with an age of around 8000 to 10 000 calibrated years BP which provides the minimum timing of retreat for the region (Dredge et al., 1999; Gowan, 2013).

The northern Slave Province till has been subjected to numerous studies of glacial and kimberlite indicator mineral transport. Large portions of the Slave Province are believed to be overlain by a single till unit and associated streamlined landforms (Kerr and Knight, 2007). Kerr and Knight (2007) divided till into three subunits for the Slave Province based on surface morphology that reflects thickness and glacial process: veneer (<2 m thick), blanket (~8 m thick), and hummocky (~10+ m thick). Till in the Slave region is generally a matrix-supported diamicton with variable matrix grain size from sand to silt with minor clay, and compositionally reflects the local bedrock (Kerr et al., 1996; Kerr and Knight, 2007). Surface till units of the northern Slave province consist of till blanket, till veneer, or bare bedrock with patches of hummocky till (Figure 1.9).

There are several mapped ice-flow directions in the northern Slave Province, based largely on striation measurements. The earliest ice-flow direction is interpreted to be southwest. This older ice flow was followed by westward flow and subsequently by northwest flow (Ward et al., 1997). The most dominant flow is the westward flow.

The southern Slave Province till dominantly has a sand to silty sand matrix with <26% gravel. The thickness of till varies from thick (~5-10 m), blanket (2-5 m), or veneer (<2m) (Rampton and Sharpe, 2014). Till can be sampled regardless of thickness, although sampling till blanket may not yield as many KIMs as thinner till units (Rampton and Sharpe, 2014). This lower KIM content is due to a lack of local bedrock debris in the upper parts of thick till units (Rampton and Sharpe, 2014). Generally, samples collected from compact till close to the bedrock surface will contain materials derived closer to their up ice glacial source (Rampton and Sharpe, 2014). The proportion of bedrock exposure has been utilized in order to estimate thickness of till coverage in an area (Kerr and Knight, 2007; Knight, 2018). The oldest direction of ice flow is interpreted to be westward based on the orientation of roche moutonnées in the region (Knight, 2018). It has been noted by Knight (2018) that diamond exploration work supports an early east to west movement (Figure 1.10). The movement that occurred just prior to deglaciation is interpreted from the orientation of striations, crag and tails, and oriented landforms such as drumlinoids (Knight, 2018). The most recent ice flow direction in the study area is roughly towards 270° (Figure 1.10). Modelling of till and glacial landforms is currently being conducted in the southern Slave Province and surficial sediment and bedrock maps have recently been published by Sacco et al. (2018) encompassing the 17-DECS sample area (Figure 1.11, Figure 1.12).

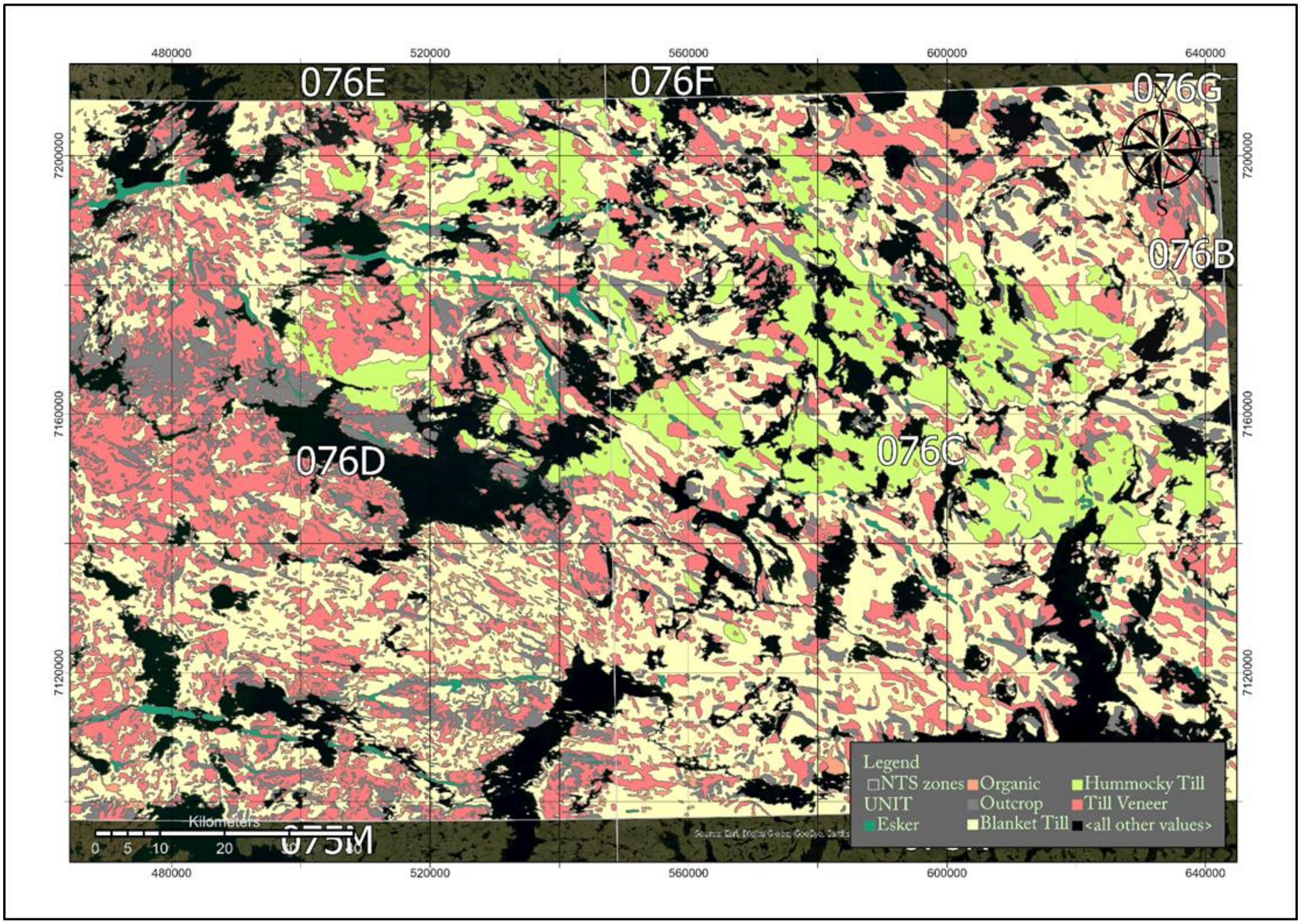

Figure 1.9: Distribution of surficial sediments and bedrock (from Kerr and Knight, 2007) in a heavily sampled region of the northern Slave Province (NTS map sheet 076D and 076C). Blanket till ~8 m thick, Hummocky till ~10 + m thick, and till veneer <2 m thick).

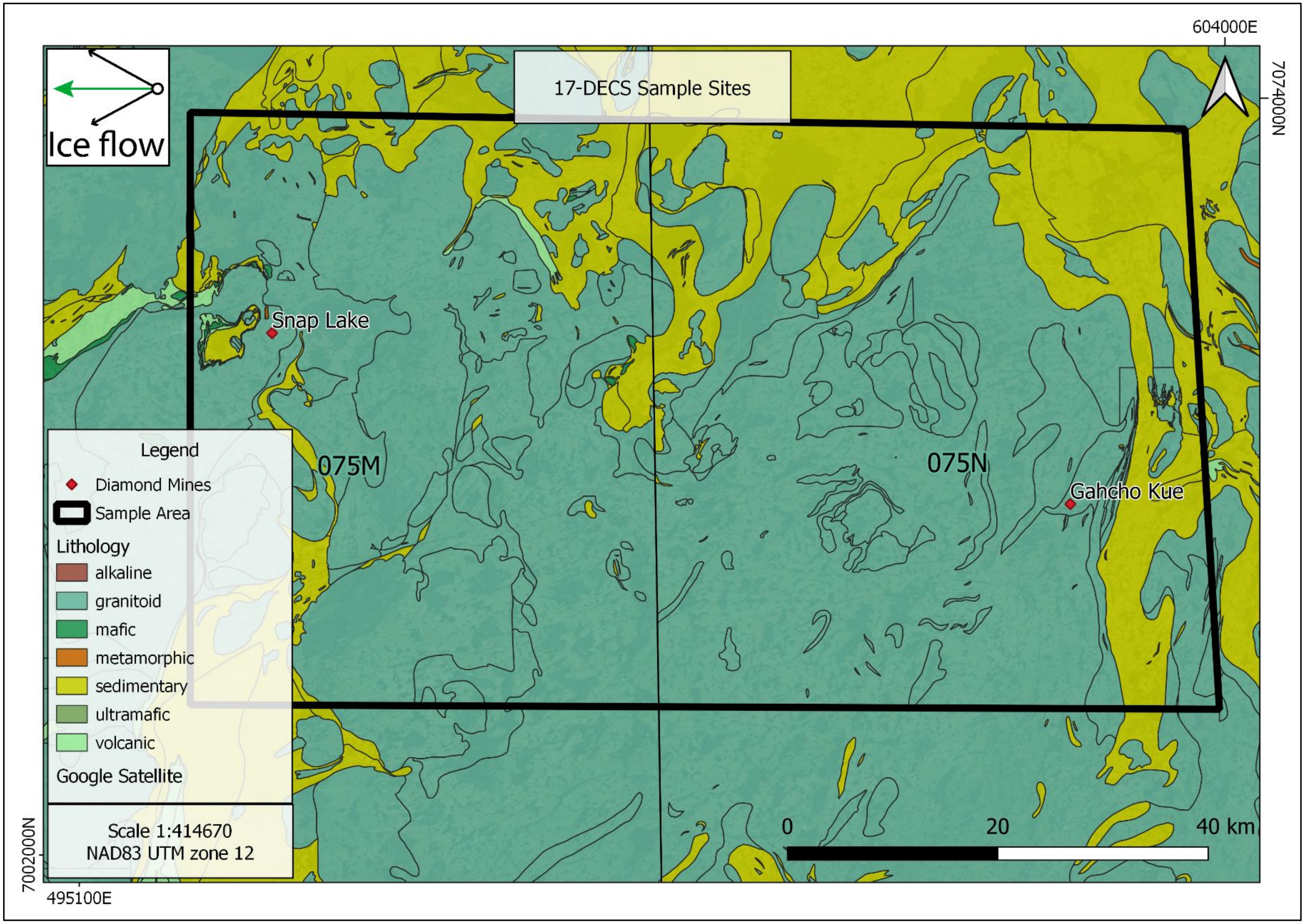

Figure 1.10: Bedrock geology of the southern Slave Province showing the 3 mapped ice-flow directions in the top left corner. Dominant and most recent ice-flow direction is shown in green. The sample area for 17-DECS are outlined in black. Data from NWT Open File 2005-001, NWT Geoscience Office (2018) and Stubley and Irwin (2019); glacial data from Knight (2018).

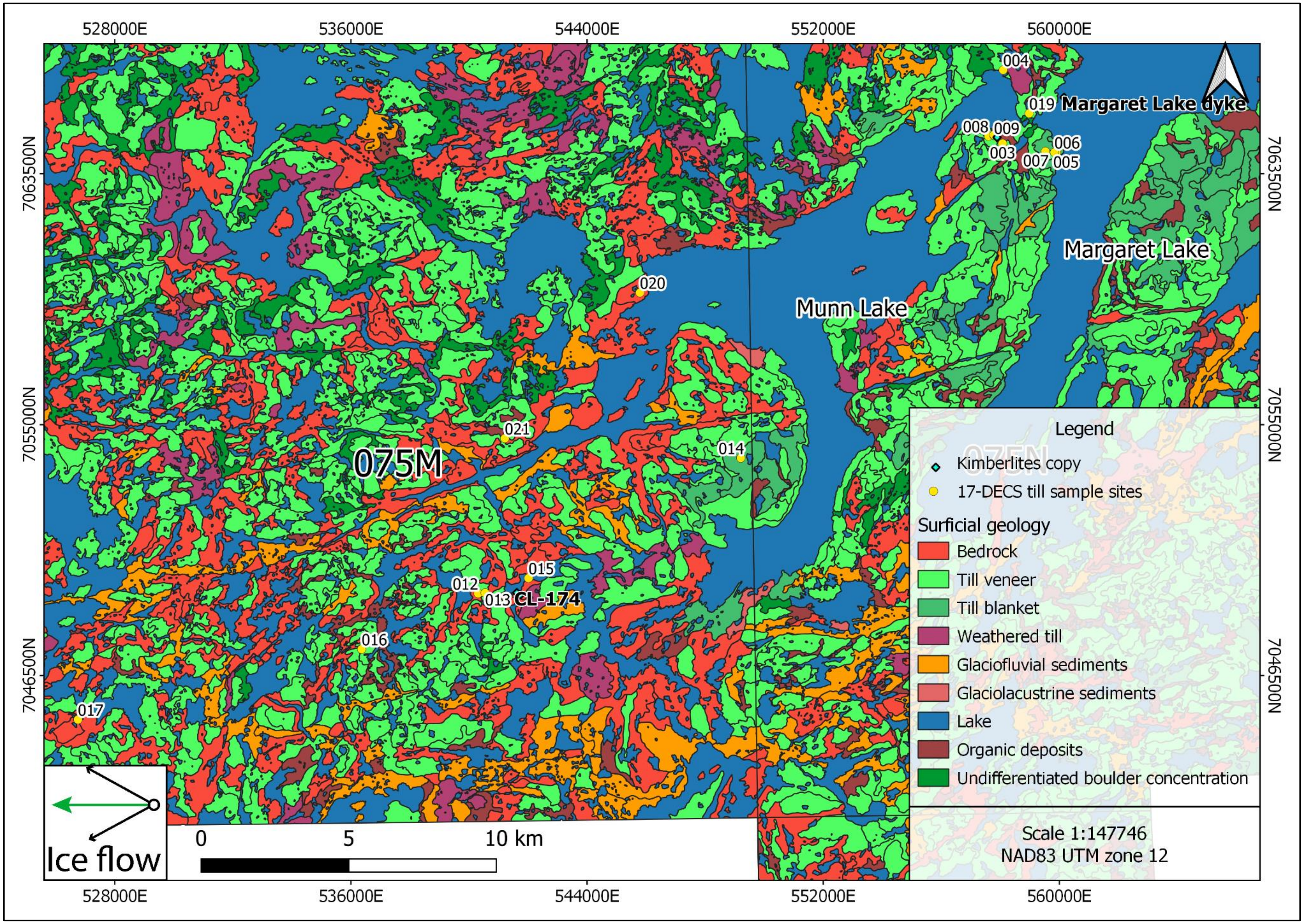

Figure 1.11: Distribution of surficial sediments and bedrock (from Sacco et al., 2018, NWT Open Report 2018-015) in the southern Slave Province in the 17-DECS sample area proximal to till samples furthest east. Ice flow direction is dominated by westward flows (green arrow) (Knight, 2018).

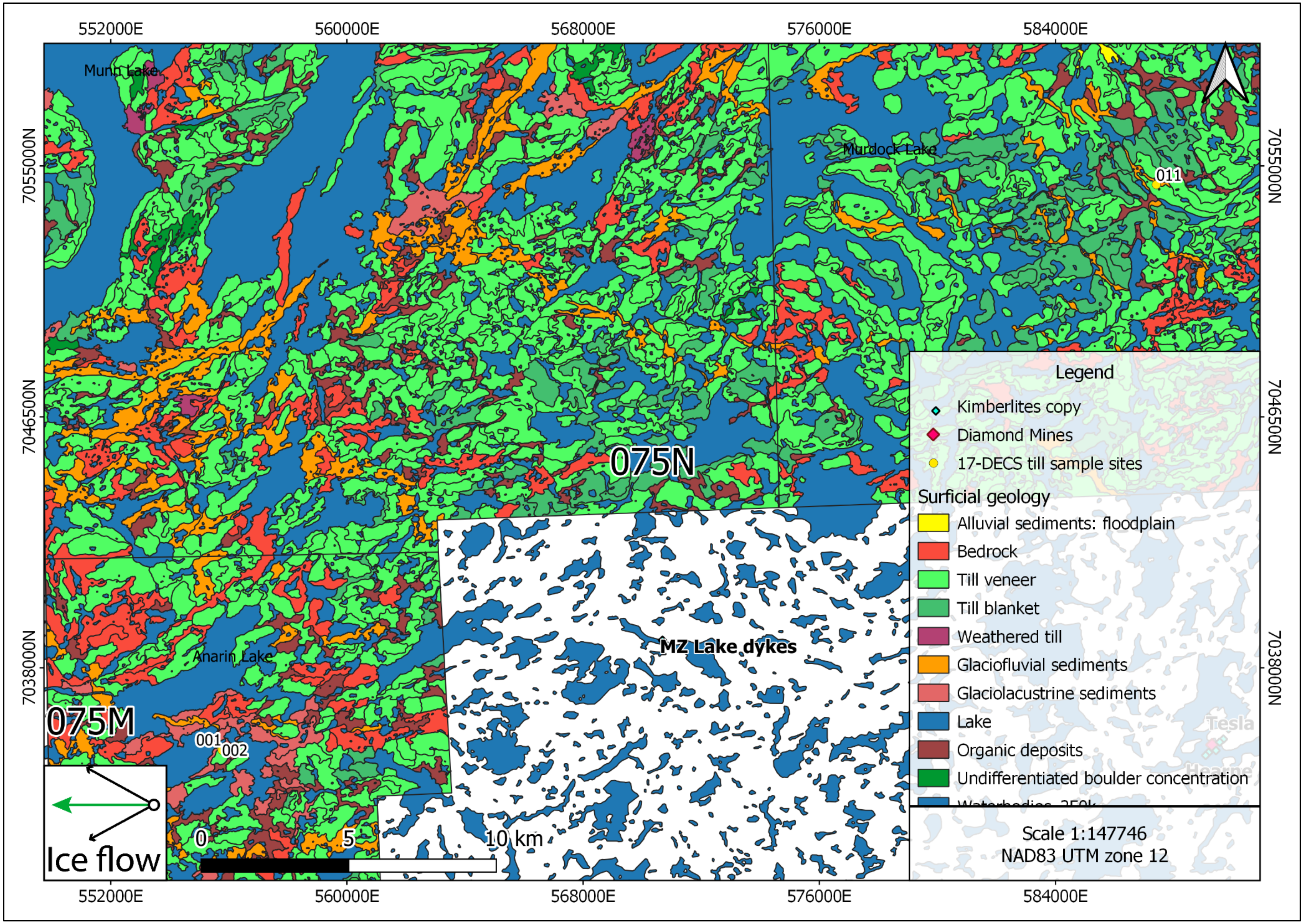

Figure 1.12: Distribution of surficial sediments and bedrock (from Sacco et al., 2018, NWT Open Report 2018-015) in the southern Slave Province in the 17-DECS sample area proximal to till samples furthest west. Ice flow direction is dominated by westward flows (green arrow) (Knight, 2018).

1.5 Kimberlite indicator mineral dispersal trains in the Slave Province (Review)

(1) Ranch Lake kimberlite

The Ranch Lake kimberlite dispersal train to the north of the Lac de Gras kimberlite field is a narrow ribbon-shape with relatively sharp edges that is believed to have formed during one phase of ice flow to the west (McClenaghan et al., 2002). The length of the Ranch Lake dispersal train is relatively long at 70 km (Table 1.3). McClenaghan et al. (2002) observed an increase in KIM down ice with 'spikes' in concentration between 15 and 20 km down-ice. Possible explanations presented for this unusual dispersal pattern by McClenaghan et al. (2002) are:

1. Glacially transported boulders of kimberlite were crushed during deposition between 15 and 20 km down-ice and contributed large concentrations of indicator minerals to the till. (However, no kimberlite boulders were noted on the surface in the area).
2. A second unknown kimberlite source west of the Ranch Lake kimberlite contributed large numbers of indicator minerals to the till.
3. Decreasing accessibility of the glacier to erode the kimberlite over time produce indicator mineral-rich till farther (15-20 km) down-ice and relatively indicator mineral-poor till closer (<15 km) to the kimberlite. Kimberlite is more easily eroded when compared to the surrounding country rocks and therefore kimberlite would preferentially erode initially, when the crater was very shallow. At that time kimberlite debris would be carried westward down ice producing a band of kimberlite rich debris. Through time glacial erosion of the kimberlite would produce a steed-sided, bedrock depression in the pipe relative to the surrounding bedrock and kimberlite would be less

accessible to erosion. As a result, subsequently entrained basal debris would contain less kimberlite debris. The debris transported farthest would have the highest kimberlite content.

(2) Slave Craton

Armstrong (2003) has previously compiled maps of the kimberlite indicator diamond database (KIDD) and the kimberlite indicator mineral chemistry database (KIMC) distribution across the Slave Province using a sample set of over 135 000 surficial sediment (mostly till) sample locations. These maps were subsequently used to make interpretations regarding kimberlite dispersal trains in the Slave Province. Kimberlite indicator dispersal trains may extend up to 100 km down ice of their source and widths of 20 to 50km (Armstrong, 2003). He also noted that most individual kimberlite indicator mineral trains have a pencil-shape (rather than fan) dispersal pattern, with length to width ratios of 8:1, typically, with aspect ratios of 23:1 in the southeastern Slave Province. The Lac de Gras field hosts volumetrically significant 'volcaniclastic' to re-worked volcaniclastic' kimberlite that has shed large quantities of indicator minerals (Armstrong, 2003). Older kimberlite fields in the Slave Craton are dominated by hypabyssal to diatreme facies kimberlite and are characterized by lower overall abundances of indicators (Armstrong 2003 and thus till down ice of these fields contain fewer KIMs.

(3) Tahera Claim Group

Till samples were collected around and down ice of what were subsequently discovered to be seven kimberlite pipes in the Tahera claim group area in the northeastern part of the Slave Province. Stea et al. (2009) conducted KIM detailed striation mapping and reinterpretations of the KIM dispersal patterns. They concluded that kimberlite dispersal fans showed complex geometry and are likely the result of one and sometimes multiple phases of ice flow (Stea et al., 2009).

A summary of the dispersal fan mapping conducted by Stea et al. (2009) can be seen in Table 1.3. The comparison of these dispersal fans and the ice flow features present in the area lead Stea et al. (2009) to the following conclusions:

1. KIM dispersal fan boundaries generally match or are enclosed within the range of local flow directions. The dispersal fans are narrow and linear in areas of unidirectional flow and broader in areas featuring multiple flow directions.

2. The main axis of KIM dispersal fans is generally parallel to the predominant phases of northwestward flow during the glacial maximum with the exception of one fan parallel to a late-glacial northward ice flow.

3. Some fans feature lobate projections reflecting earlier directions of ice flow.

4.Dispersal fan boundaries can be irregular and skip zones exist within the fans as demonstrated by background samples *between the source and the anomalies.*

The predominant regional ice flow is interpreted to be northwestward and played a major role in fan shape with significant fan relicts left from precursor southwest and westward ice flows (Stea et al., 2009). As ice flow shifted, debris from older fans was reworked by several processes (Stea et al., 2009):

1. Comminution.

2. Re-entrainment and transport of KIMs from previous

tills and the kimberlite source (inheritance).

3. Mixing (dilution) of previous tills with inert up-ice debris

(overprinting).

Table 1.3: Vector and scalar properties of the dispersal fans in the Tahera claim group areas and from tRanch Lake (McClenaghan et al., 2002). All distances in kilometers. Summary of ice flow directional indicators adjacent to fans from Stea et al. (2009).

Fan parameter	Ranch lake	Anuri	Unicorn	Muskox	Rush	Jericho	Contwoyto
Fan-azimuths	265°-275°	310°-359°	302°-335°	279°-319°	240°-322°	286°-346°	226°-3°
Fan-spread	10°	49°	33°	40°	82°	60°	137°
Main axis	265°	333°	322°	312°	293°	336°	351°
Max-width	2	7.7	1.8	5.7	8.9	3.4	2.8
Largst-anomaly	1380	1945	297	414	95	685	560
Dist-anomaly	19	1.7	0.7	1.8	2.9	2.0	0.9
Skip zone	?	-	0.1	0.8	2.0	0.8	0.5
Total-length	70	29	9.4	23.7	24.2	10.7	11.9
Local ice flow directions							
Azimuths	252°-280°	310°-5°	325°-357°	280°-5°	280°-5°	250°-338°	240°-10°
Vector-Mean	-	342°	333°	319°	319°	315°	301°
Number	-	94	8	134	134	20	20
Surface area of kimberlite pipes (hectares)							
	13	4.75	<1?	3	<1	3	0.48

(4) Deep overbruden drilling in central Lac de Gras region

Kelley et al. (2019) conducted an analysis of three-dimensional dispersal KIM patterns in the Lac de Gras region around the DO-18 and DO-27 kimberlite pipes. Using striations, grooves, plucked surfaces, and crescentic gouges on exposed bedrock surfaces, Kelley et al. (2019) identified three directions of ice flow with a clockwise shift through time from southwest to northwest (oldest to youngest). These observations agree with ice flow history reported by Dredge et al. (1995) and Ward et al. (1997).

Kimberlite indicator minerals used to model glacial dispersal were predominantly garnet and Cr-diopside because, as Kelley et al. (2019) noted, olivine could be sourced from other common olivine-bearing bedrock lithologies in the region, chromite grains yielded inconclusive results, and ~76% of ilmenite grains were not classified as kimberlitic. The highest KIM (p-pyrope and Cr-diopside) concentrations in till were found immediately surrounding the DO-18 and DO-27 pipes (Figure 1.13) (Kelley et al., 2019). Cr-diopside extended up to ~3 km northwest of DO-18 with concentrations rising in the till column over the first kilometer (Kelley et al., 2019).

Kelley et el. (2019) found that the highest KIM counts were within topographic depressions overlying kimberlites DO-18 and DO-27. Their study noted possible dispersal along the two youngest ice flow vectors, with no strong evidence of SW dispersal from kimberlite pipes. The youngest and dominant ice flow phase in the Lac de Gras Region is ~300° (Dredge et al., 1995; Ward et al., 1997; Kelley et al., 2019). They also reported evidence of northwesterly KIM dispersal (Kelley et al., 2019). In three dimensions, kimberlitic material is observed rising through the till column down ice (Kelley et al., 2019). An older westward ice flow phase was observed by Kelley et al. (2019). The westward dispersal of kimberlitic material was observed in the study area and best expressed in the thin till directly west of DO-1 and DO-27 (Kelley et al., 2019). A cluster of p-pyrope grains without kelyphite rims were observed at or near the land surface northwest of DO-27 and proximal to DO-18 on the east facing slope of the bedrock high in the centre of the study area (Kelley et al., 2019). This lack of kelyphite rims suggest that the kimberlite source is not proximal and contrasts with nearby till samples within the NW dispersal train and suggests reworking or modification of the till in the area (Kelley et al., 2019). The confidence given to identification of the westward dispersal is low due to the small number of samples in that area of the study (Kelley et al., 2019).

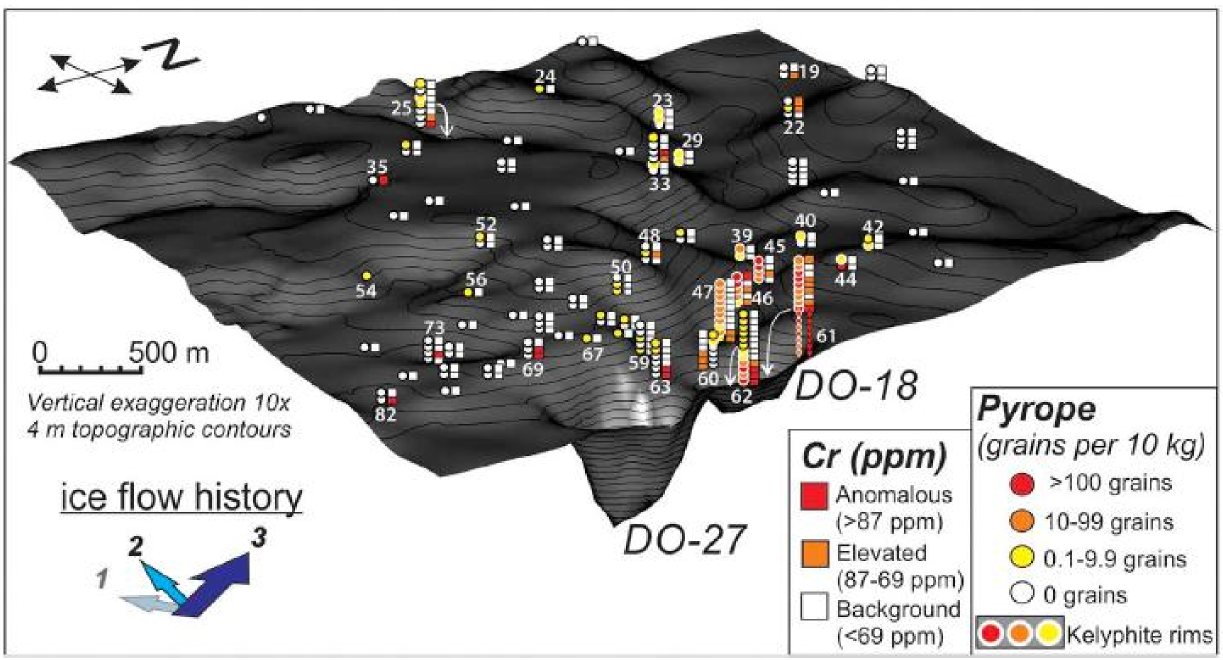

Figure 1.13: Cr concentration (squares) in the till matrix and P-pyrope abundance in the heavy mineral fraction (circles) of till from RC drill hole samples for the area immediately west/northwest of the DO18/27 kimberlite pipes, with the boreholes noted in the text labeled. (Kelley et al., 2019).

(5) Summary

Kimberlite dispersal trains and ice flow history of the Slave Province are variable and complex. KIM dispersal patterns in the Slave Province range from elongate narrow trains (70 km long, 10° fan spread; >100km, 10°) (McClenaghan et al., 2002; Armstrong, 2003) to broader fans and bilobate trains (11.9 km long, >130° fan spread) (Stea et al., 2009) (Table 1.3, Figure 1.14). There is a consensus that dispersal patterns are often the net effect of several phases of ice flow, with the main direction of dispersal reflecting the predominant ice flow phase(s) (McClenaghan et al., 2002; Stea et al., 2009). It is not uncommon for dispersal fans in the Slave Province to have variable KIM contents in till samples down ice of known kimberlites. Multiple explanations for the discrepancy in shape of dispersal fans have been presented (McClenaghan et al., 2002; Armstrong, 2003; Stea et al., 2009) and as such ideas presented in this study are in addition to previous explanations.

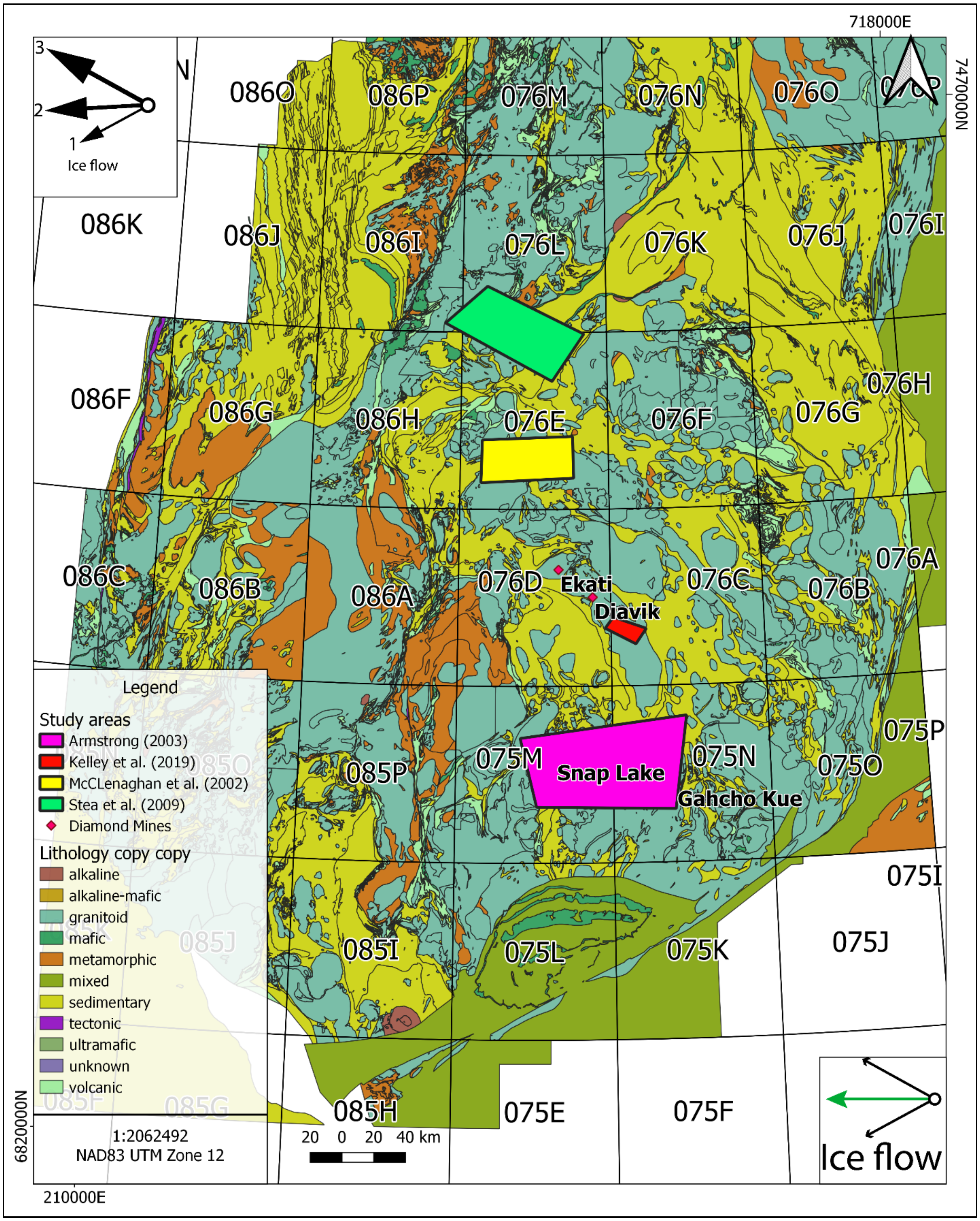

Figure 1.14: Locations of generalized study areas from McClenaghan et al. (2002), Armstrong (2003), Stea et al. (2009), and Kelley et al. (2019). Bedrock geology and data from NWT Open File 2005-001, NWT Geoscience Office (2018); Stubley and Irwin (2019).

Chapter 2: Methods

2.1 Fieldwork

Samples of till in the southern Slave Province, approximately 280 km northeast of Yellowknife, were collected at twenty-one separate sites for this study. Each sample was approximately 10 kg with the coarser (> ~15 cm) clasts removed in the field (Figure 2.1). Samples were collected via helicopter drop off and field traverses during the 2017 field season. The preferred sample medium included felsenmeer terrain, frostboils, and till veneer (McClenaghan and Paulen, 2018). Samples were collected at surface from a hand-dug hole using a shovel and trowel, with material collected in large plastic sampling bags. Two till samples were collected at site 17-DECS-009, as a field duplicate.

Figure 2.1: The > 15 cm clasts of till samples were removed in the field in order to be able to collect favour of a greater volume of till matrix for indicator mineral studies. Site shown in photo is 17-DECS-013.

Several sites within the southern Slave Province NTS map sheets 075M and 075N were selected for sampling based on availability of till, and their location relative to known kimberlites and geophysical anomalies (Figure 2.2, Figure 2.4, Figure 2.5, Figure 2.6). The samples for this study are located within the Munn Lake Property. Twenty-one samples (17-DECS) were collected over a fourteen-day period during July 2017.

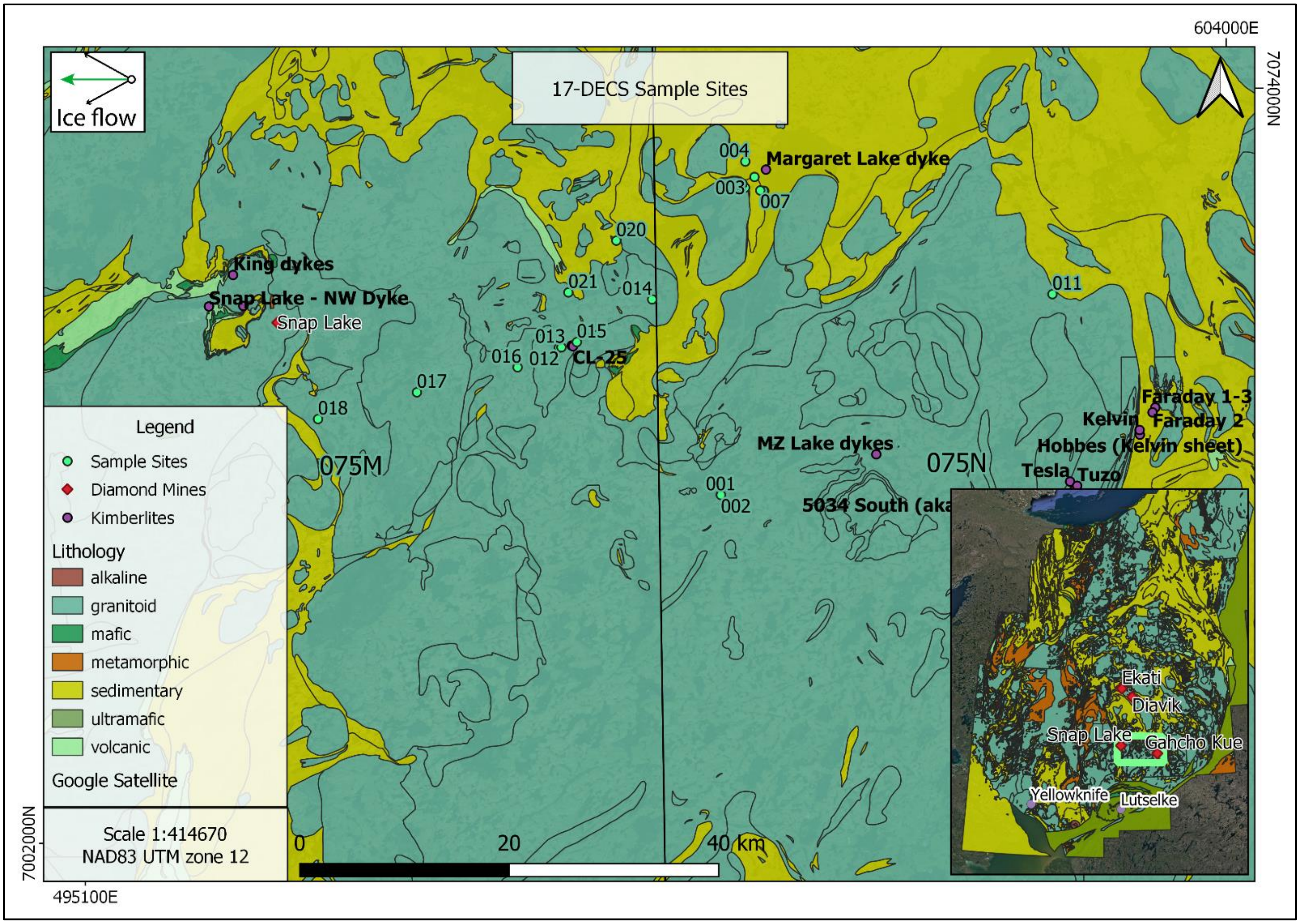

Figure 2.2: Locations of till samples sites in this study in the NTS map sheets 075M and 075N. Bedrock geology from the NWT Open File 2005-001, NWT Geoscience Office (2018). *Samples 005,006, 008, 009, 010, and 019 are in the same cluster as 003, 004, and 007 near the Margaret Lake Dyke. n=21

2.2 Geophysics of the Munn Lake property

An aeromagnetic survey of the central Slave craton area was conducted from February 15th to April 20th, 2017, by EON Geosciences Inc. as part of the Slave Province Surficial Materials and Permafrost study funded by CanNor (Mirza and Elliot, 2017). The survey area is located with the 075N and 075M NTS map sheets, with nominal traverse line spacing of 100 m with east-west direction and control lines spacing of 600 m with north-south direction (Mirza and Elliott, 2017). These maps are useful for interpreting the dispersal of KIMs in the study area, as the interpretation of geophysics may indicate the location of undiscovered kimberlites.

A geophysical survey report was prepared by CGG Canada Services Ltd. (Mirza and Elliot, 2017) in order to aid in interpretation of the data collected in the aeromagnetic survey. Electromagnetic anomalies in this report are based on a near vertical, half plane model. Electromagnetic anomalies are grouped into three general categories in the CGG Canada Services report. The second class of anomalies comprised moderately broad responses that exhibit the characteristics of half-space and do not yield well-defined inflections on the difference channels. Anomalies within this category are labelled “S” or “H” symbol. Some of these anomalies could reflect conductive rock units, zones of deep bedrock weathering, or the weathered tops of kimberlite pipes, all of which can yield “non-discrete” signatures. Till sample sites were selected down ice from “H” and “S” anomalies due to their potential association to kimberlite (Figure 2.3, Figure 2.4, Figure 2.5, Figure 2.6).

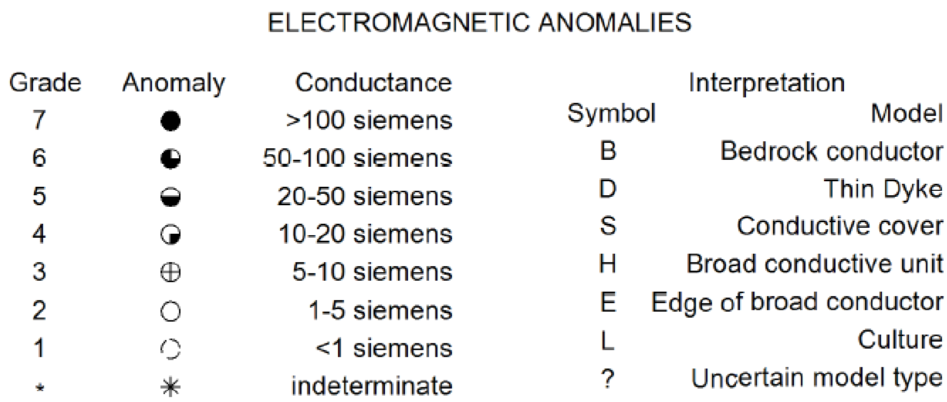

Figure 2.3: Legend for figures 2.4, 2.5, and 2.6.

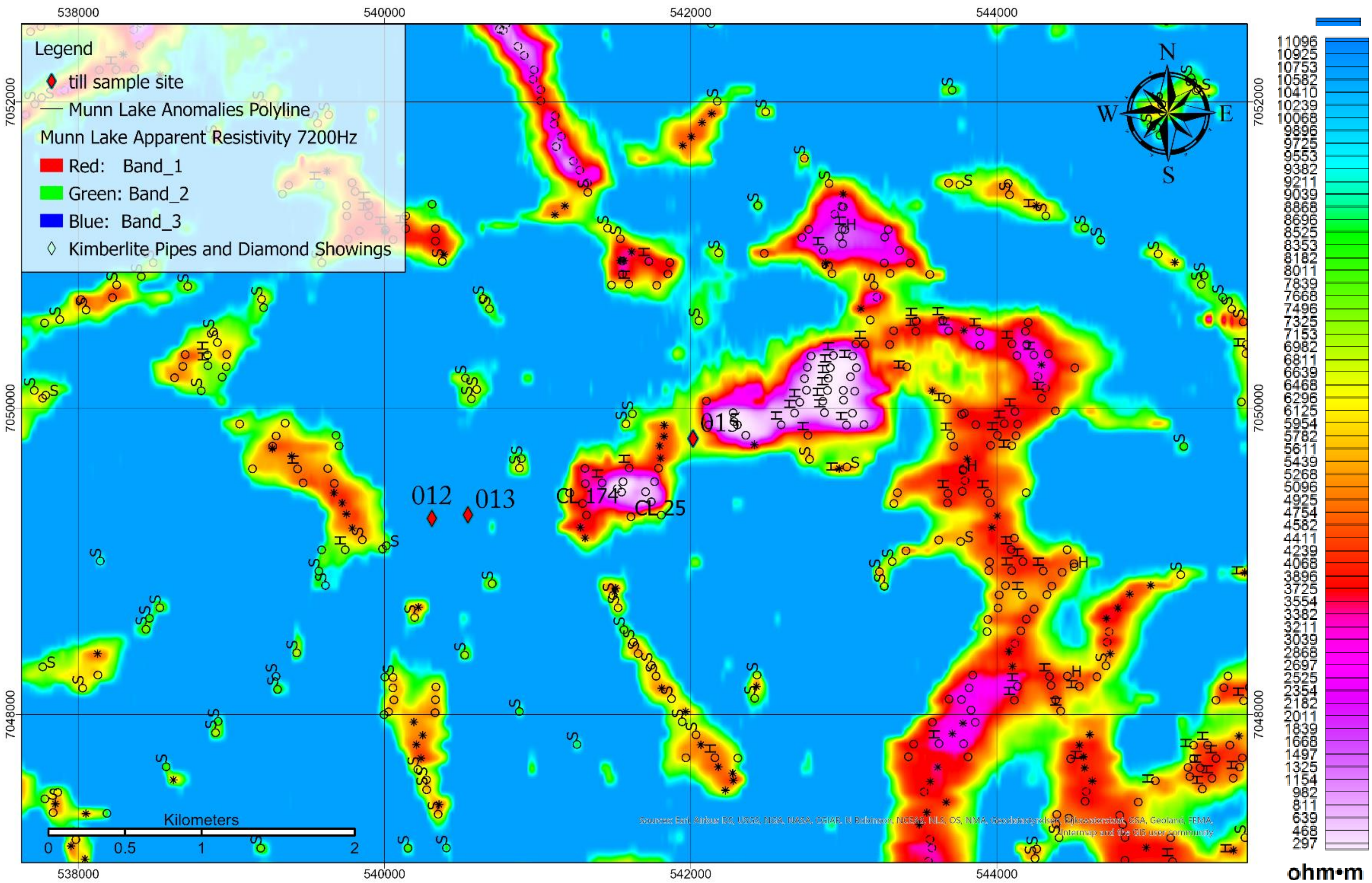

Figure 2.4: Resistivity (7200Hz) map of the Munn Lake Area, with "H" and "S" interpretive symbols, with respect to kimberlites CL-25 and CL-174, and 17-DECS sample locations n=21 (Geophysical data and interpretation from CGG Canada Services Ltd. in Mirza and Elliott, 2017)

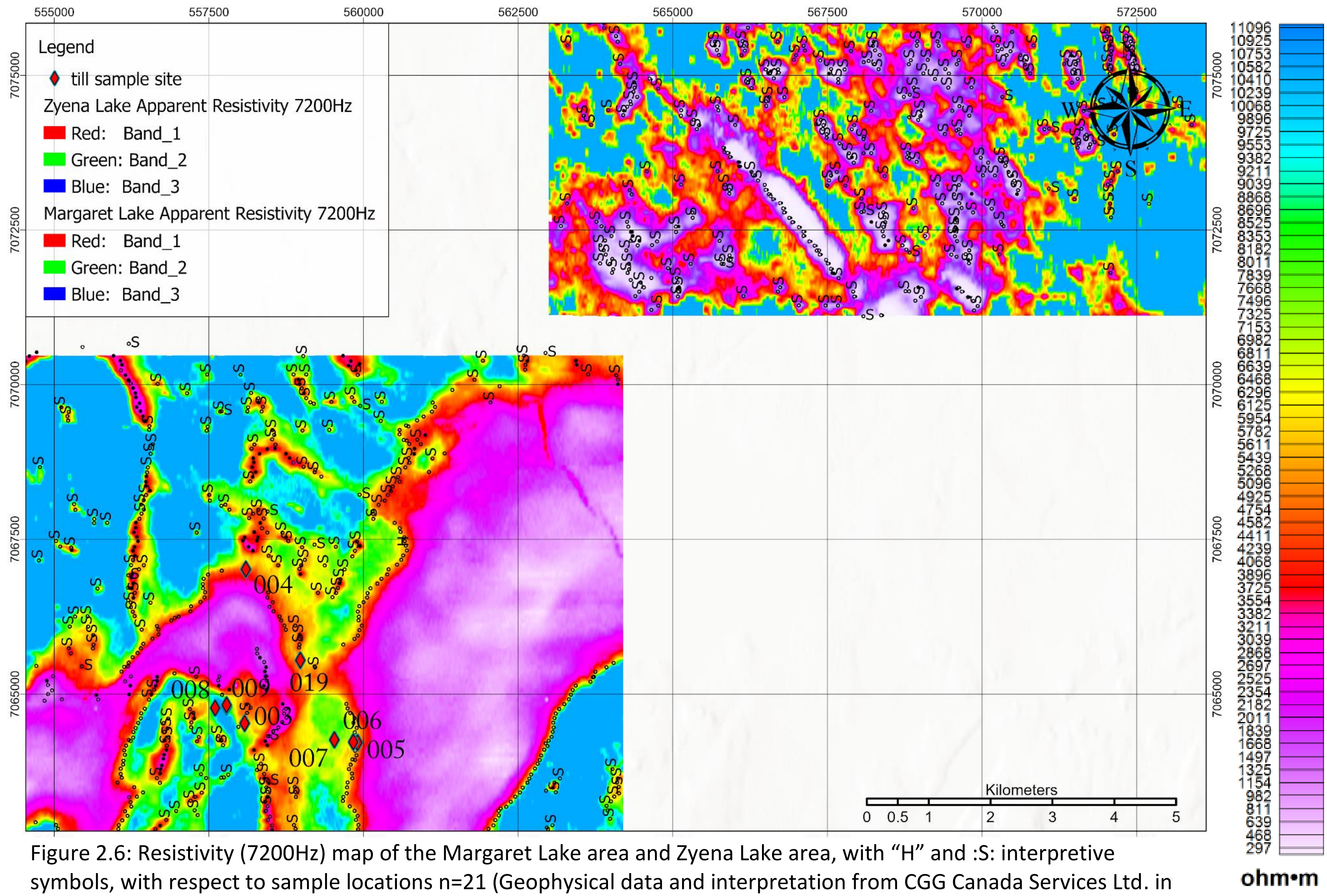

Figure 2.6: Resistivity (7200Hz) map of the Margaret Lake area and Zyena Lake area, with “H” and :S: interpretive symbols, with respect to sample locations n=21 (Geophysical data and interpretation from CGG Canada Services Ltd. in Mirza and Elliott, 2017)

2.3 Northwest Territories Geological Survey database

The NTGS provides publicly accessible databases on the geology of the Northwest Territories and surrounding area. These data include but are not limited to bedrock geology, surficial sediments, kimberlite indicator mineral counts, kimberlite indicator mineral chemistry, kimberlite anomaly drill holes, and kimberlite location data. In this study, data from the Kimberlite indicator mineral chemistry database (KIMC) were used.

The Kimberlite Indicator and Diamond Database (KIDD) contains information about kimberlite samples that were previously compiled from Mineral Assessment Reports for the Northwest Territories and Nunavut. This database contains data for >219,000 surficial sediment samples which include location, date, number of indicator grains and claim holders. The database is the result of continuous data compilation by the NTGS. Previous work using the KIDD has been conducted by Armstrong (2003) to create KIM distribution maps on a reconnaissance scale. Armstrong's (2003) maps were based on data for over 135,000 surficial sediment sample locations and separate the Slave Province into 7 distinct kimberlite regions (**Error! Reference source not found.**). Several KIM trains have been observed by Armstrong (2003) in the southeastern Slave Province.

The KIMC database mineral chemistry data for samples. These data were compiled from Mineral Assessment Reports (2009-2011) for the Northwest Territories and Nunavut. KIMC contains >144,000 records on detailed grain chemistry. Previous work using the KIMC database has been conducted by Armstrong (2001; 2003) to produce sample location maps. The main difference between the KIDD and KIMC database is the content of mineral chemistry in the KIMC database.

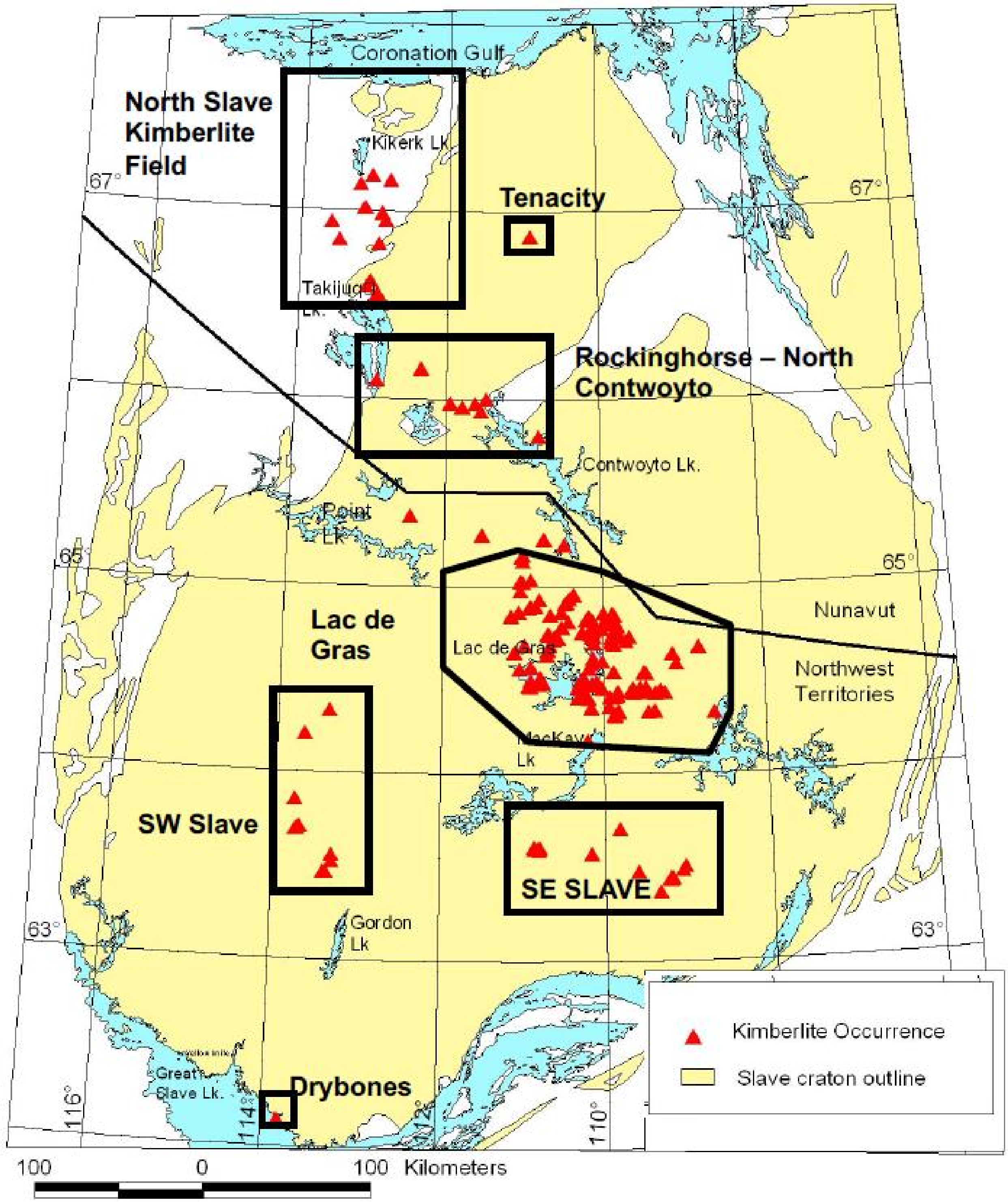

Figure 2.7: Kimberlite regions in the Slave Province as defined by Armstrong (2003).

The KIDD and KIMC databases are a unique and notable dataset for diamond exploration in the Northwest Territories. However, these databases hold unique limitations in terms of use and interpretation. The data contained within KIMC and KIDD are accumulated from a variety of sources with the main source being assessment reports. Although there is a standard for assessment reporting, it does not result in a consistent and directly comparable information. These data which are provided by companies are subject to sampling bias (location of samples, sample sizes, processing methods, and sample media), reporting bias (companies report selective data they deem meaningful or report only data that will not reveal locations of confidential kimberlite discoveries), and potential misidentification of KIMs within the KIDD database (the stereoscopic visual inspection of mineral grains is subjective). With significant variability in sample size, location, media, and processing, it can be difficult to make meaningful comparisons between company datasets and interpretations in terms of the distribution of KIMs using this database. Another limitation of the dataset are the concerns about quality assurance and quality control of the mineral chemistry data collected from various sources. Different analytical instrumentation have different detection limits, different standards used, and different rates of error on a machine and operator basis.

Normalization of KIM counts to a designated sample weight (i.e. 10 kg) would be an ideal practice when working with any KIM count dataset as it creates a reliable base for comparison. Normalizing data to a specific sample weight would help mitigate error in interpretation when sample sizes vary. It is impossible to normalize the mineral chemistry in the KIMC as sample weights are not reported on and sample sites do not necessarily reflect one surficial sediment sample. The database presents chemistry for individual KIM grains with georeferenced data (latitude and longitude) as opposed to a specific sample number. The use of geospatial data instead of sample numbers or identifications creates the possibility that more than one surficial sediment sample is being reported on at the same georeferenced point. What this means is one sample site may represent a >20 kg surficial sediment sample while another represents a <10 kg surficial sediment sample creating a skewed result where the larger sample contains a higher KIM count but has the same abundance of KIMs. As such, in this study surficial sediment samples are used as a synonymous term for inferred sample sites from the KIMC database.

The KIMC database contains chemistry for 145,360 grains, of which 32,964 were defined as grains collected from till, and 101,418 grains (majority) have undefined sample media (Figure 2.8, 2.9). The total number of sample sites defined as till only account for 1,918 sites out of 14,027 sites total (Table 2.1). Data contained in all sample media (defined and undefined) was used to map the distribution of KIMs on the basis of mineral chemistry in the central and southeastern Slave Province. Mineral chemistry data in the KIMC database accounts for 145,360 grains from a total of 14,027 sample sites. Of the 145,360 grains reported in the KIMC database 140,066 are garnet, olivine, ilmenite, picroilmenite, chromite, Cr-diopside, or clinopyroxene (KIM) (Table 2.2) with the remaining minerals being unclassified or other (phlogopite, muscovite…etc.). The available mineral chemistry from the KIMC database was used to classify garnet g-numbers (Grutter et al., 2003) and to confirm mineral identities (ilmenite, picroilmenite, chromite, and Cr-diopside). The KIMC database includes mineral counts from the KIDD. The mineral counts from the KIDD were not used to create maps in this study as this work has been done by Armstrong (2003).

Table 2.1: Number of till defined sample sites and mineral grain counts with mineral chemistry data from the KIMC database.

Slave Province KIMC database till sample sites and grain counts		
Mineral:	Grain count (N):	Till sample sites (n):
Eclogitic Garnet	23901	1322
Pyrope Garnet	1483	124
Olivine	535	59
Ilmenite	2028	193
Chromite	1101	202
Cr-diopside	85	61
Clinopyroxene	2778	722
Picroilmenite	154	42
Total:	32065	1918

Till sample sites total is not the sum of till sample sites per mineral

Table 2.2: Number of sample sites (X,Y matching coordinates) and mineral grain counts with mineral chemistry data from the KIMC database.

Slave Province KIMC database grain counts and sample sites		
Mineral:	Grain count (N):	Sample sites (n):
Eclogitic Garnet	100765	9994
Pyrope Garnet	6490	1128
Olivine	2193	705
Ilmenite	7021	2199
Chromite	7074	2489
Cr-diopside	515	347
Clinopyroxene	15448	6586
Picroilmenite	560	74
Total:	140066	14027

*Sample sites total is not the sum of the sample sites per mineral.

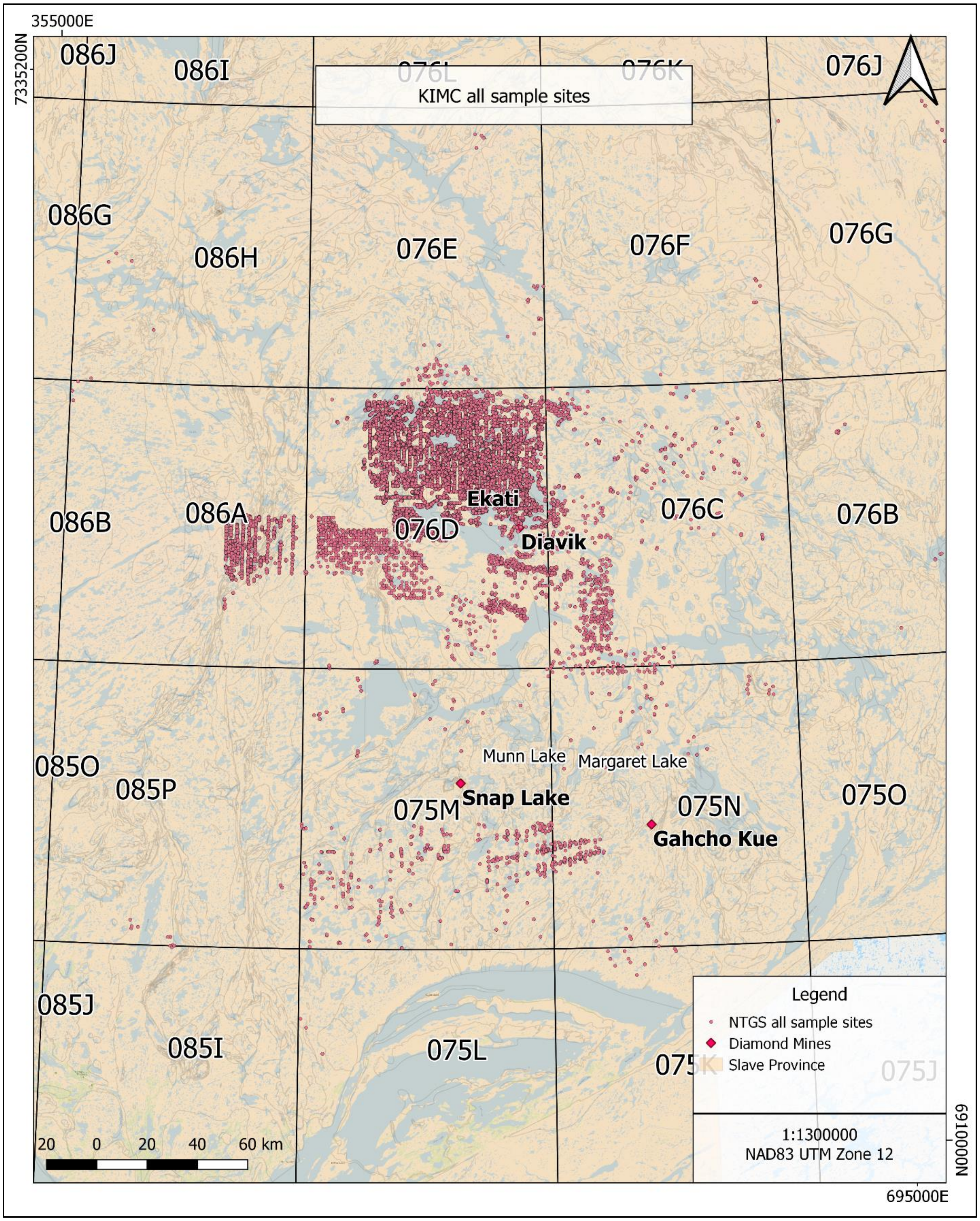

Figure 2.8: Distribution of all KIMC surficial sediment sample locations (surficial data from NWT Open File 2005-001, NWT Geoscience Office, 2018). Total KIMC surficial sediment sample sites n=14,027

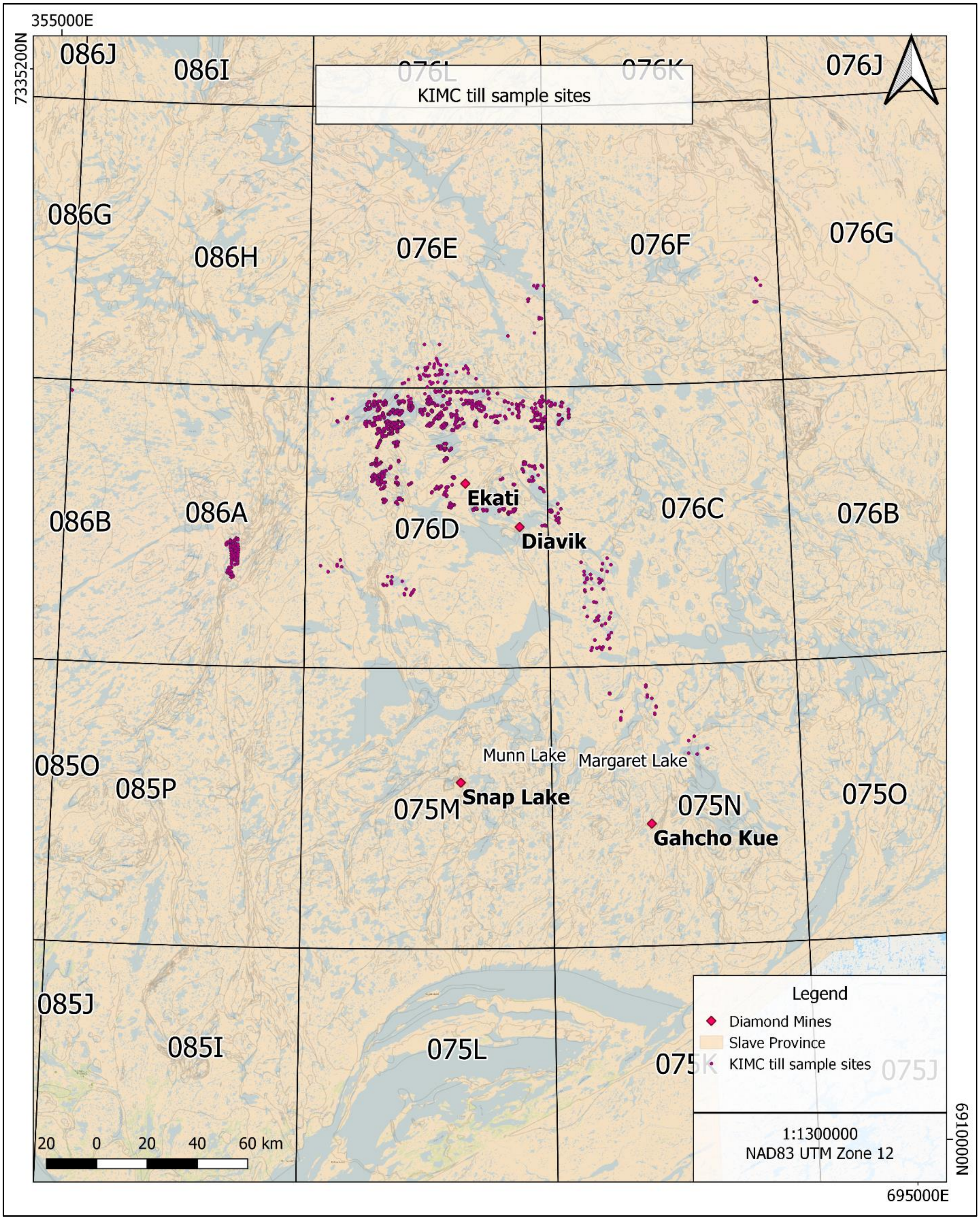

Figure 2.9: Distribution of KIMC database sample locations defined as "till". (surficial data from NWT Open File 2005-001, NWT Geoscience Office, 2018). KIMC till sample sites n=1,918

2.4 NTGS data processing overview

Specific details pertaining to the assessment and classification of individual minerals will be discussed in later sections. This section is intended to be a brief overview to provide the reader with a small frame of reference for how data was categorized. Data from the KIMC database is presented with some of the following information:

- X,Y coordinate
- Object ID
- PK_KIMC (grain ID)
- Grain number
- Total analytical percent
- Miscellaneous data
- Short and long name of mineral analyzed
- KIDD (grain number counts)
- Company
- Size fraction
- Method for HMC
- Comment (can contain material of sample)
- Latitude and longitude
- NTS map sheet
- Territory
- Mineral chemistry data:

SiO_2; TiO_2; Al_2O_3; V_2O_3; Cr_2O_3; Fe_2O_3; FeO; MgO; CaO; MnO; K_2O; Na_2O; P_2O_5; NiO; ZnO; F; Cl; Nb_2O_5; Ca; Na_2OTr; FeOT

The database contains more fields for information than what is mention above, however, the fields above are those which contain data (other fields such as depth and individual elemental data are blank within the database). Samples contained in the KIMC database are all from assessment reports from 2009-2011.

When data from the KIMC database are plotted there are over 145,000 individual data points. In this study the data is reduced based on chemistry into KIMS. All KIMS contain the "Long Name" field in which the mineral with corresponding chemistry is listed. Minerals are subsequently grouped based on the latitude and longitude data using an integration tool in GIS software to create point features with mineral sums (Table 2.3).

Table 2.3: Example of data within the KIMC database. X,Y coordinates highlighted in green show same coordinate information for multiple grains with chemistry. Using an integration geoprocessing tool KIMs are added up to create sum values for specific geospatial points.

X	Y	LONG_NAME	SiO2	TiO2	Al2O3	Cr2O3	FeO	MgO	CaO	MnO	K2O	Na2O	P2O5	NiO	Cl	Na2OTr	FeOT
-106.493	65.81536	Clinopyroxene	53.41	0.11	2.3	0.74	0	14.77	22.81	0.17	0.03	0.52	0	0	0	0	4.88
-106.493	65.81536	Clinopyroxene	53.87	0.17	1.78	0.77	0	15.34	23.12	0.08	0	0.59	0	0	0	0	3.7
-106.493	65.81536	Clinopyroxene	53.93	0.09	2.54	0.61	0	13.99	22.55	0.17	0	1	0	0	0	0	3.78
-106.493	65.81536	Clinopyroxene	53.88	0.15	1.65	1.18	0	14.43	23.08	0.13	0	0.77	0	0	0	0	3.18
-106.493	65.81536	Eclogitic Garnet	0	0.04	99.68	1.54	0	0.03	0.02	0.01	0	0.03	0	0	0	0	0.98
-110.397	64.5443	Eclogitic Garnet	38.1	0.06	21.3	0.02	0	2.21	14.33	1.62	0	0	0	0	0	0.02	23.27
-111.333	64.8287	Eclogitic Garnet	42.08	0.06	20.8	4.03	6.9	19.59	5.46	0.47	0.02	0.45	0	0.08	0.02	0	0

		Clinopyroxene	Eclogitic Garnet
-106.493	65.81536	4	1

Newly derived “sample site” or “inferred sample site” from the integration of identical geospatial reference points.

2.5 Sample processing and indicator mineral separation and selection process

All 21 till samples from the 17-DECS sample series were processed by Overburden Drilling Management Ltd (ODM) in Ottawa, Canada, in order to extract a heavy mineral concentrate (HMC) (specific gravity >2.3) for the examination of kimberlite indicator minerals. In addition, each sample was panned for gold, PGMs, and fine-grained metallic indicator minerals (see Chapter 7:Appendix V). The procedure summarized in Figure 2.10 was designed to extract a high percentage of kimberlite indicator minerals: chrome pyrope garnet, orange garnet (megacrystic and eclogitic), picroilmenite (also referred to as Mg-ilmenite), chrome diopside, and chromite. Heavy mineral concentrates for each sample were sieved into 3 size fractions: 1.0 to 2.0 mm, 0.5 to 1.0 mm, and 0.25 to 0.5 mm. Heavy mineral concentrates were assessed by ODM and kimberlite indicator minerals were visually identified (see Chapter 7:Appendix V).

Selected kimberlite indicator minerals identified by Dana Campbell were prepared at Lakehead University for this study and mounted in a circular epoxy puck for quantitative analysis using scanning electron microscopy and laser ablation mass spectrometry. Grains from the 0.25 mm to 2.0 mm size fractions were selected using an Olympus stereoscope based on their resemblance to known kimberlite indicator minerals (colour and habit) (Figure 2.11).

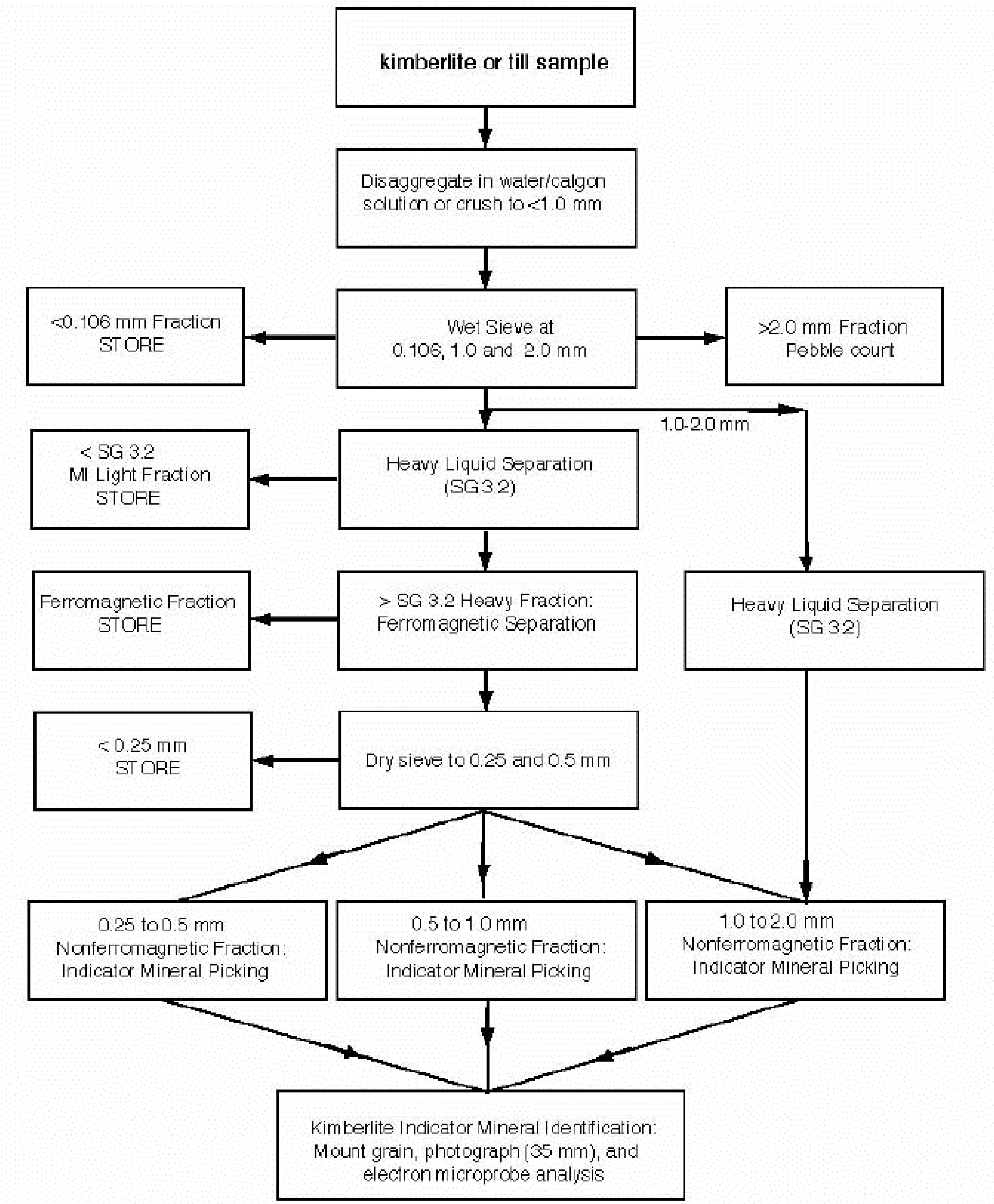

Figure 2.10: Flow chart outlining laboratory procedures used by ODM Ltd. to process till samples and recover kimberlite indicator minerals. (1) Recombined after picking and submitted for geochemical analysis as one sample; (2) Picked only for chrome pyrope and chrome diopside; (3) Picked for chrome pyrope, orange garnet, chrome diopside, picroilmenite, and chromite (McClenaghan et al., 2003).

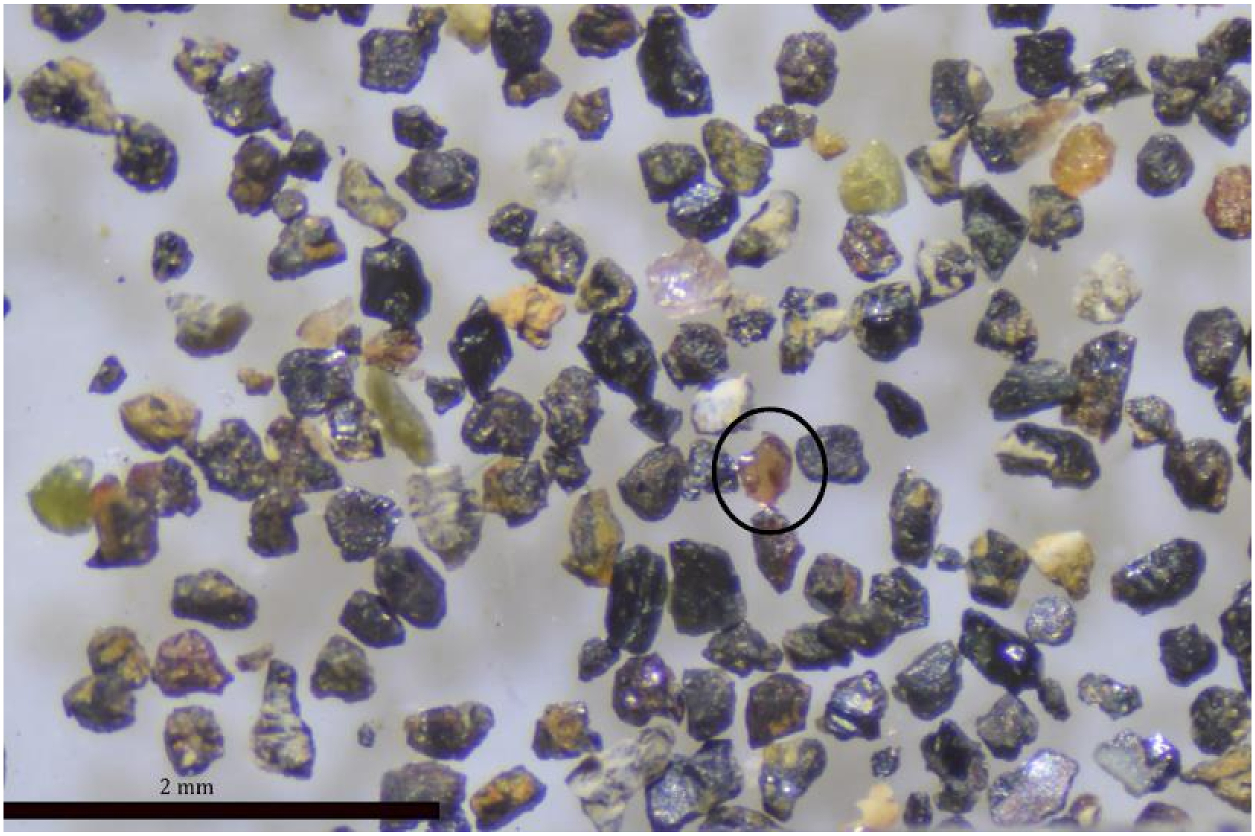

Figure 2.11: Heavy mineral concentrate from till sample 17-DECS-013 as viewed under an Olympus stereoscope with potential G9 garnet circled in black.

2.6 Scanning Electron Microscopy – Energy Dispersive Spectroscopy (SEM-EDX)

A total of 64 epoxy circular mounts containing ~30 grains each were made at Lakehead University. Each mount was photographed using a stereoscope, and carbon-coated for subsequent SEM-EDX quantitative analysis. Over 1000 grains were selected for detailed analysis by standard petrographic methods, and back-scattered (BSE) imagery and energy dispersive X-ray spectrometry using a Hitachi SU-70 scanning electron microscope (SEM) in the Lakehead University Instrumentation Laboratory (LUIL). A Hitachi SU-70 Schottky Field Emission SEM was used to conduct quantitative analyses of the minerals, with a 15mm working distance and an accelerating voltage of 20kV via the Oxford Aztec 80mm/124 eV electron dispersive X-ray spectrometer (EDX) equipped on the SEM. The following well-characterized mineral and synthetic standards were used to monitor the operating conditions and monitor analytical quality control: jadeite (Na, Al); wollastonite (Ca, Si); orthoclase (K); ilmenite (Fe, Ti); periclase (Mg); Mn-hortonolite (Mn); apatite (F, P); barite (Ba and S); $SrTiO_3$ (Sr); Garnet (Cr); and KCl (Cl).

2.7 LA ICP-MS

Each positively identified kimberlitic garnet on the grain mounts subsequently underwent Laser Ablation Inductively Coupled Plasma Mass Spectrometry (LA-ICP-MS) analyses. Garnets from sample sites 17-DECS-006, -008, -013, -016, -017, -018, and -019 and ilmenites from 17-DECS-001, -002, -006, -013, -019, and -021 were analyzed.

The analysis was completed at the University of Manitoba using the Thermo Finnigan Element 2 High Resolution-Inductively Coupled Plasma-Mass Spectrometry (HR-ICP-MS). The HR-ICP-MS is used in combination with a New Wave Research UP-213 nanosecond laser ablation system and a Quantronix Integra-C femtosecond laser ablation system for solid sample micro-analyses. The laser settings included a beam size of 30-55µm, a repetition rate of 5 Hz and fluence of ~4-~6 J/cm^2. The oxide formation rate was 0.2-0.15 %. The glass standards NIST SRM 610 and BCR2G were used as calibration and quality control standards, respectively, with calcium weight percent of garnet as the internal standard. Data were reduced using Iolite Igor pro software.

2.8 Garnet classification

Potential kimberlite garnets recovered in this study are classified based on schemes for mantle-derived garnet by Grütter et al. (2004) and Hardman et al. (2018a). Studies by Hardman et al. (2018a) may provide a more statistically accurate way of differentiating mantle and crustal garnet with a difference of approximately ~7% higher accuracy. Both classification schemes are used in this study because the classification by Grütter et al. (2004) is a widely used method and the classification from Hardman et al. (2018a) is a more recent scheme. These techniques were assessed in terms of their application in the Slave Province.

Garnet is a common mineral inclusion in diamond (Grütter et al., 2004). In general, garnet is a robust mineral that can withstand weathering and glacial erosion and deposition processes and is abundant within kimberlite. These characteristics make it an ideal kimberlite indicator or pathfinder mineral. In contrast to common mantle-derived garnet, the peridotitic (P-type) and eclogitic (E-type) varieties found as inclusions in diamond have distinct compositions (Grütter et al., 2004). The composition of these garnets can be assessed using simple compositional schemes based on bivariate scatterplots to classify and prioritise mantle-derived garnets recovered during exploration programmes (Grütter et al., 2004).

Grütter et al.'s classification scheme is calibrated by design for geotherms intersecting the graphite/diamond transition at temperatures in the 920 to 1000°C range (Grütter et al., 2004). Grains with a strong compositional association with diamond that also plot within the diamond stability field under these conditions are considered "diamond-facies" and are assigned the suffix "D" (Grütter et al., 2004). The four main features of this scheme are (1) reliance only on compositional data obtained from electron microprobe analysis, (2) backward compatibility with previous work, concepts and nomenclature, (3) internal consistency with known diamond associations, and (4) ease and transparency of implementation (Grütter et al., 2004).

Under this scheme garnets are classified as G0, G1, G2, G3, G4, G5, G9, G10, G11, or G12. Of importance and notability in this study are garnets classified as G3, G4, G5 and G10 for their statistical correlation to diamond-bearing kimberlites, suffix "D" applied when specific criteria are met (See Grütter et al., 2004).

Eclogitic G3 garnets represent very important pathfinder minerals for diamond exploration (Grütter et al., 2004). These eclogitic garnets are aluminous and show variations in FeO, MgO and CaO contents. The eclogitic category as defined by Grütter et al. (2004):

Cr_2O_3 [wt.%]: 0 to < 1.0

CaO [wt.%]: ≥6 to < 32.0

MGNUM: ≥0.17 to < 0.86

TiO_2 [wt.%]: < 2.13_2.1*MGNUM

TiO_2 [wt.%]: < 2.0

It is worth noting that these compositional limits for G3 garnets also encompass ranges observed for garnets in alkremite and certain lower crustal garnet granulite xenoliths (Grütter et al., 2004).

Pyroxenitic, websteritic and eclogitic (G4 and G5) are moderate to low-Cr garnets that are significant to kimberlite exploration due to a distinct diamond association (Grütter et al., 2004). Pyroxenitic garnets similar to, but richer in Fe than moderate to low- Cr G9 garnets are termed "G5" garnets in this scheme. The G5 garnet category is characterised by:

TiO_2 [wt.%]: < 2.13_2.1*MGNUM

Cr_2O_3 [wt.%]: ≥1 to < 4.0

CA_INT [wt.%]: ≥ 3.375 to < 5.4

MGNUM: ≥0.3 to < 0.7.

Pyroxenitic garnets with lower Cr than G9 garnets, with compositions overlapping low-Ca eclogitic garnets are termed "G4" garnets (Grütter et al., 2004). This updated G4 category is characterized by:

TiO_2 [wt.%]: < 2.13-2.1*MGNUM

Cr_2O_3 [wt.%]: < 1.0

CaO [wt.%]: ≥2.0 to < 6.0

MGNUM: ≥0.3 to < 0.90

Harzburgitic (G10) garnets are generally considered the "standard" for which diamond potential of exploration projects is often evaluated (Grütter et al., 2004). The association with diamond in terms of G10 garnets is dominantly geochemical and statistical (Grütter et al., 2004). Harzburgitic garnets in the scheme are characterized by:

Cr_2O_3 [wt.%]: ≥1.0 to < 22.0

CA_INT [wt.%]: 0 to < 3.375

MGNUM: ≥0.75 to < 0.95

where MGNUM=(MgO/40.3)/ (MgO/40.3 + FeOt/71.85) [oxides in wt.%]. G10D "diamond-facies" garnets have (in wt.%) (Grütter et al., 2004):

Cr_2O_3 ≥5.0 + 0.94*CaO, or

Cr_2O_3 < 5.0 + 0.94*CaO and MnO < 0.36

This study also uses raw mineral chemistry data of mineral grains from till from the NTGS Data hub (2018) in order to classify G number for over 100,000 garnets in the Slave Province. Garnet was classified using raw geochemical data with pre-existing classifications of P-type and E-type garnets. An excel spread sheet consisting of mineral chemistry data was used to create IF and AND functions to meet the chemical criteria of Grütter et al. (2004) G-number classifications. The excel functions were implemented in the order of G1-G11-G10-G9-G12-G5-G4-G3-G0. There is chemical overlap within classifications which is compensated for by following this order of garnet classification. If the chemical criteria for a classification was met the excel sheet indicated a “positive” identification (Chapter 7:Appendix I), which can only be applied to one G-number. Very large data sets (>110,000 individual mineral grains with chemistry) have not been used (publicly) to map the distribution of different classes of KIMs in the southeastern Slave Province. It is imperative to assess the implications of G-number classification over a regional spectrum, and to determine effective uses of these data. Data sets this large are not often available, and as a result may not be viewed as a useful tool in exploration due to unfamiliarity. Classifying a large data set using a common exploration tool such as G-number classification may provide insight into indicator mineral research on a regional scale.

Chapter 3: Results

3.1 Overview

Although there are several thousand surficial sediment samples that have been collected from the Slave Province for recovery of KIM, most of the KIM chemistry data publicly available are from the central and northern Slave province as previously observed by Armstrong (2003) and McClenaghan et al. (2002). Quantitative analysis of minerals from 17-DECS series samples was conducted in this study in order to classify minerals from till in the southern Slave Province as KIMs, and to differentiate them from visually similar minerals. These data are used to determine whether there are kimberlites in the vicinity, diamond potential, and to determine potential indicator mineral dispersal trains. Lastly, once more is known about the southern Slave Province KIMs, it's possible to assess similarities and differences between the northern and southern region in terms of chemistry and glacial transport. There is a large amount (>145,000) of raw KIM chemistry data publicly available for classification and assessment through the recently released NTGS open data hub (http://datahub-ntgs.opendata.arcgis.com/, 2018). These public raw indicator mineral data were used in this study to 1) classify and identify KIMs from the Slave province, and 2) perform regional interpretations regarding indicator mineral distributions based on chemistry of indicators by area. This information can then be used to interpret glacial transport in the southern Slave Province and make inferences on the kimberlite and diamond potential of the region.

The 17-DECStill samples collected for this study contain a total of 262 KIM grains including chromite, low-Cr Cr-diopside, and garnet (Table 3.1). When assessing KIM contents of a sample, it is important to correct counts by normalizing to a 10 kg sample weight

(McClenaghan et al., 2004). The mineral count data in this study is presented as non-normalized in order to compare results the KIMC database, which reports only non-normalized data Sample weights are often not reported in the KIMC database making the normalization of KIM grain counts impossible. The normalized values of KIMs collected from the 17-DECS series are provided below for external use within larger normalized databases (Table 3.2).

Table 3.1: KIMs identified in the 17-DECS sample series till samples.

Sample site	**Garnet (Total)**	**Cr-diopside**	**Chromite**
17-DECS-002	-	-	-
17-DECS-003	1	1	-
17-DECS-004	-	-	-
17-DECS-013	240	-	4
17-DECS-015	2	-	-
17-DECS-016	9	-	-
17-DECS-017	2	-	-
17-DECS-018	2	-	-
17-DECS-020	1	-	-
Total	**257**	**1**	**4**

*(-) represent no data for that field.

Table 3.2 Abundances of KIMs (<2mm) normalized to 10 kg from 17-DECS sample series till samples collected in the study area and garnets classified using the Grütter et al. (2004) scheme.

KIMs normalized to 10kg											
Sample site	**Garnet (Total)**	**Cr-diopside**	**Chromite**	**G1**	**G3**	**G4**	**G5**	**G9**	**G10**	**G12**	**G0**
17-DECS-003	1	1	-	-	-	-	-	-	-	1	-
17-DECS-013	222	-	4	11	13	1	-	159	9	1	28
17-DECS-015	2	-	-	-	-	-	-	1	-	-	-
17-DECS-016	9	-	-	1	-	-	-	8	-	-	-
17-DECS-017	2	-	-	-	-	-	-	1	-	-	1
17-DECS-018	1	-	-	-	-	-	-	1	-	-	-
17-DECS-020	1	-	-	-	-	-	-	-	-	-	1
Total	**238**	**1**	**4**	**12**	**13**	**1**	**0**	**170**	**9**	**2**	**30**

*(-) represent no data for that field.

In this study, over 250 garnets collected from the 21 till sample sites (17-DECS series samples) were positively identified by their chemical composition by analysis performed using a scanning electron microscope (Chapter 7:Appendix I). A total of ten G10 garnets, fourteen G3 garnets, thirteen G1 garnets, and one G4 garnet were identified (Table 3.2, Table 3.3). Of the ten G10 garnets identified, only one does not meet the criteria for the suffix “D”. Additionally, 33 garnets analyzed were considered to be unclassified or G0, indicating unusual or “polymict” mantle lithologies requiring further investigation (Grütter et al., 2004).

Table 3.3: Abundances of garnets (<2mm) in the 17-DECS till samples collected in the study area and classified using the Grütter et al. (2004) scheme. Abundances are reported for seven till samples that were found to contain kimberlite- and/or diamond-associated garnets.

Sample site	**G1**	**G3**	**G4**	**G5**	**G9**	**G10**	**G12**	**G0**	**Total**
17-DECS-003	-	-	-	-	-	-	1	-	**1**
17-DECS-013	12	14	1	-	172	10	1	30	**240**
17-DECS-015	-	-	-	-	1	-	-	1	**1**
17-DECS-016	1	-	-	-	8	-	-	-	**9**
17-DECS-017	-	-	-	-	1	-	-	1	**2**
17-DECS-018	-	-	-	-	2	-	-	-	**2**
17-DECS-020	-	-	-	-	-	-	-	1	**1**
Total	**13**	**14**	**1**	**-**	**184**	**10**	**2**	**33**	**257**

*(-) represent no data for that field.

Garnets with a high statistical association to diamond (G3, G4, G5 and G10) were only found in till sample 17-DECS-013 (Figure 2.2). Compositional fields for garnets in this study are illustrated using Cr_2O_3 vs CaO contents (Figure 3.1). Compositional overlap has been resolved to create a robust scheme reflecting the needs of diamond explorers, rather than mantle researchers (Grütter et al., 2004). The implementation order of garnet G-number classification is as follows: G1-G11-G10-G9-G12-G5-G4-G3-G0.

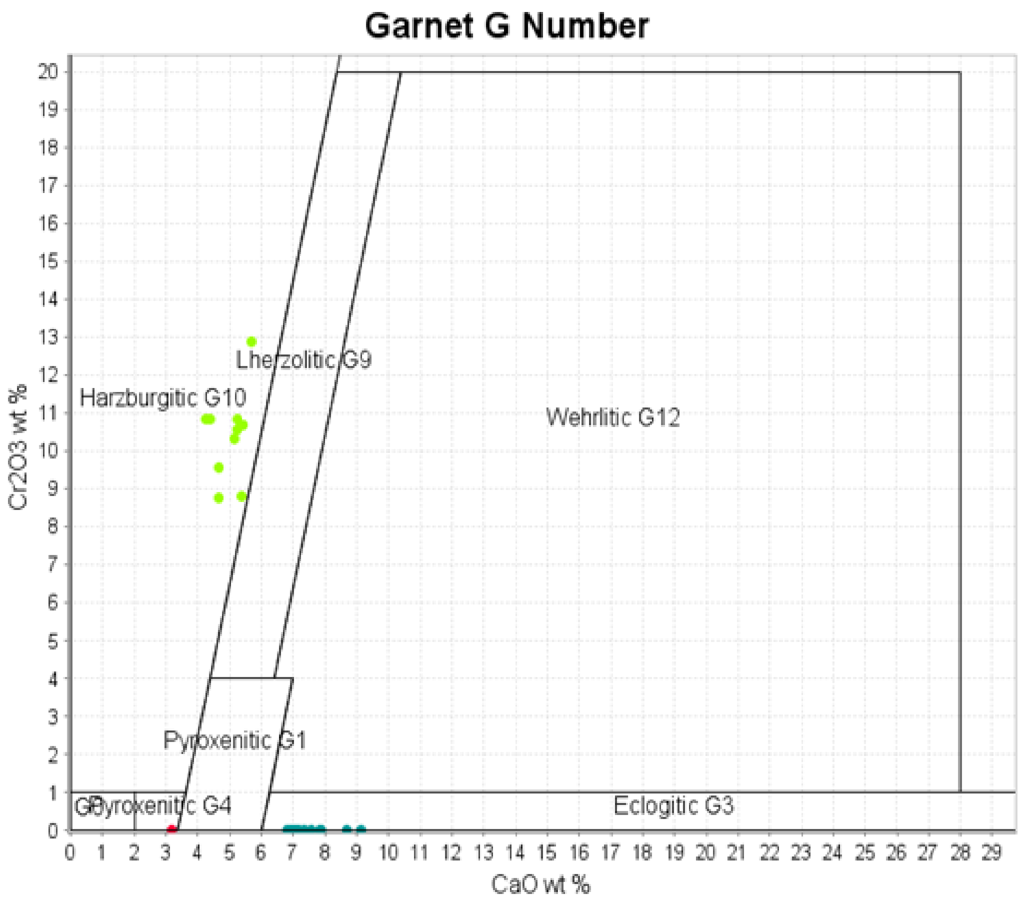

Figure 3.1: Garnet G-number classification of diamond facies garnet from 17-DECS-013 based on Grutter et al. (2004) N=224, n=21

The classification scheme presented by Hardman et al. (2018a) reduced error rates on ten test datasets from ~17.1 to ~10.1% relative to the findings of Schulze (2003). This classification scheme is a graphical depiction of wt%-based ratios of Fe, Mg, Ti and Si. A statistically derived decision boundary is implemented on a bivariate plot of *ln(Mg/Fe) vs ln(Ti/Si)*. Data which plot on the decision boundary are considered ambiguous and cannot be assigned crustal or mantle origins. Data below the decision boundary are considered crustal, and data above the decision boundary are considered mantle derived. Confidence intervals (CI) are used to provide a measure of uncertainty in the classification of single garnets (Hardman et al., 2018a). All garnets collected for this study plot within the mantle field, as such Grütter et al. (2004) will be preferentially referenced due to its wide application in exploration programs (Figure 3.2).

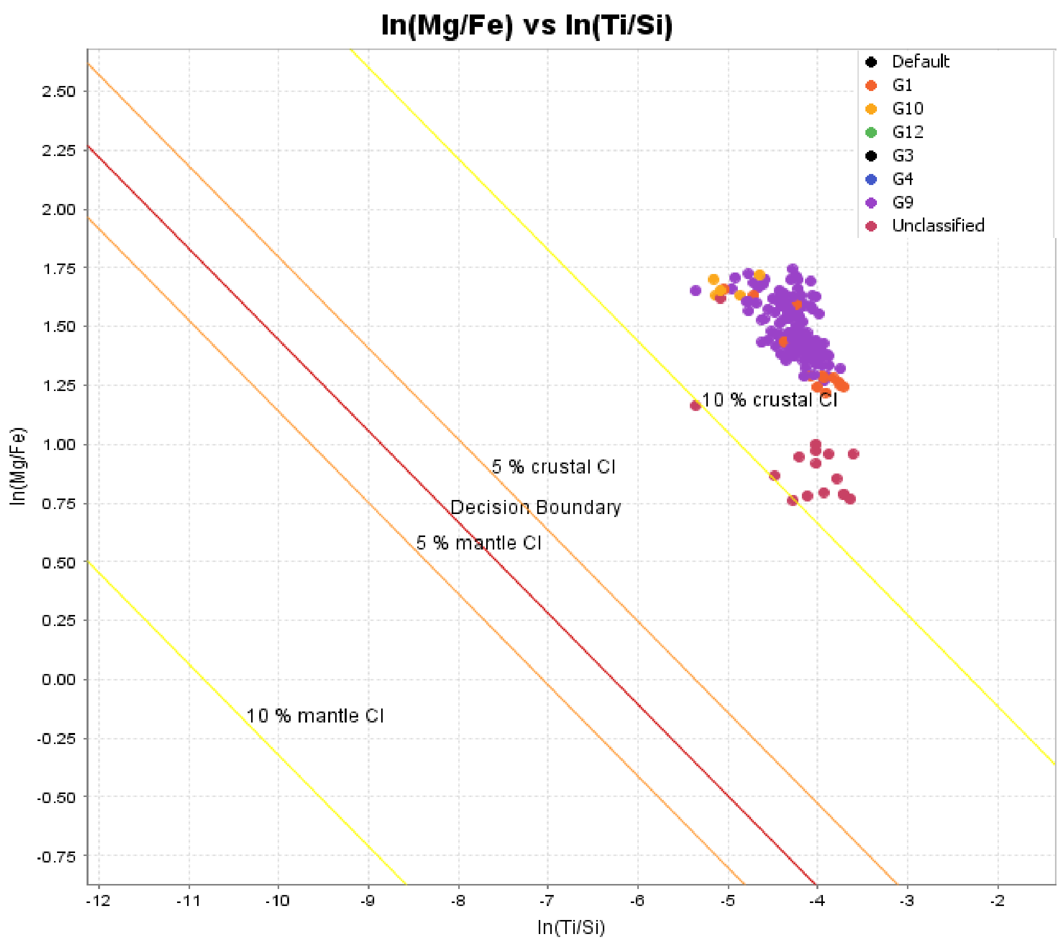

Figure 3.2: Combined classifications from Grutter et al. (2004) (coloured dots) and Hardman et al. (2018a) (sloping lines) for till samples from 17-DECS-013 sample location. 17-DECS-015, -016, -017, and -018 all plot in the mantle field. N=211, n=1

Within the 075M and 075N NTS map sheets, there are a total of 1,412 garnets in the NTGS database, with the dominant G class being G9 garnets (Figure 3.3). There is a total of 14,444 G10 garnets, 42 G5 garnets, 1,236 G4 garnets, and 299 G3 garnets in the NTGS database for the Slave Province. These data are also used to graphically display mantle vs crustal compositions outlined by Hardman et al. (2018a) in order to assess G-number classification in the southern Slave Province in terms of mantle composition (Figure 3.4).

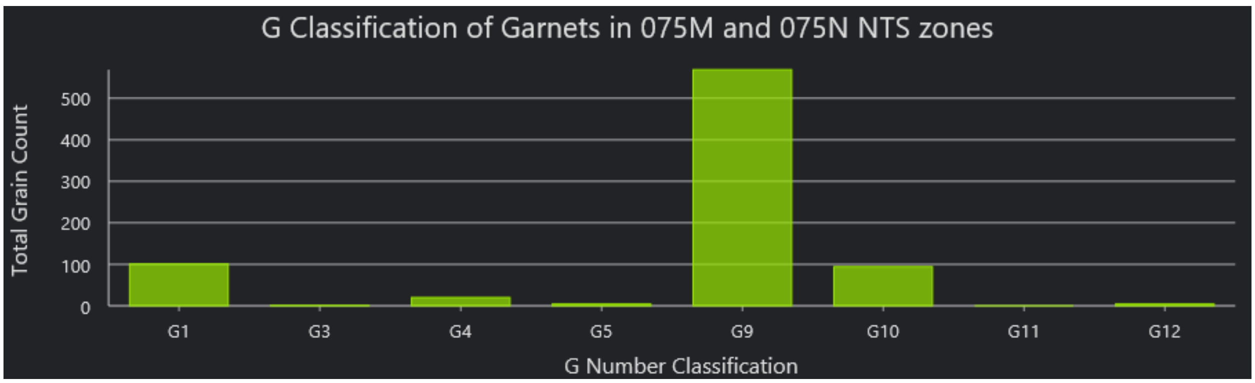

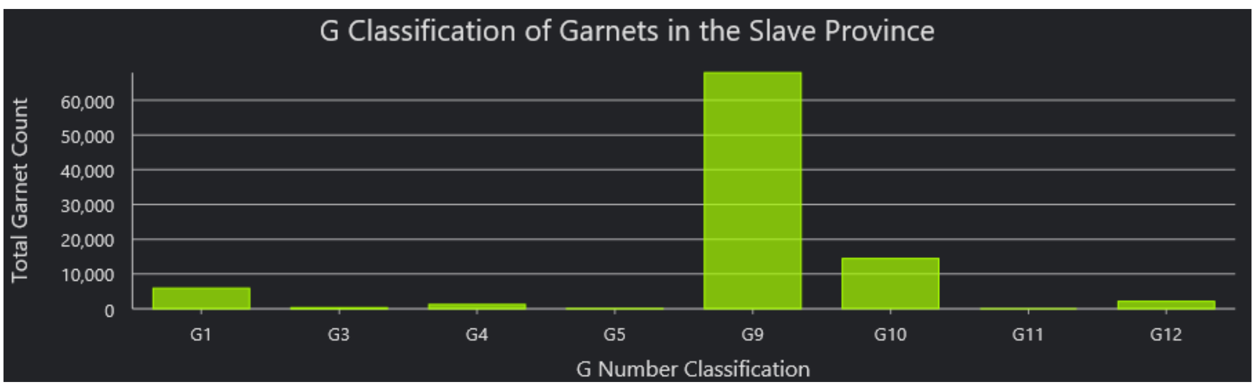

Figure 3.3: Abundance of garnet grains in each G-number category from surficial sediment samples In the NTGS database in NTS 075M and 075M map sheets and listed in the government database(N=1,412) (Top) and Garnet G number classifications from the entire Slave Province (N=91,859) (Bottom).

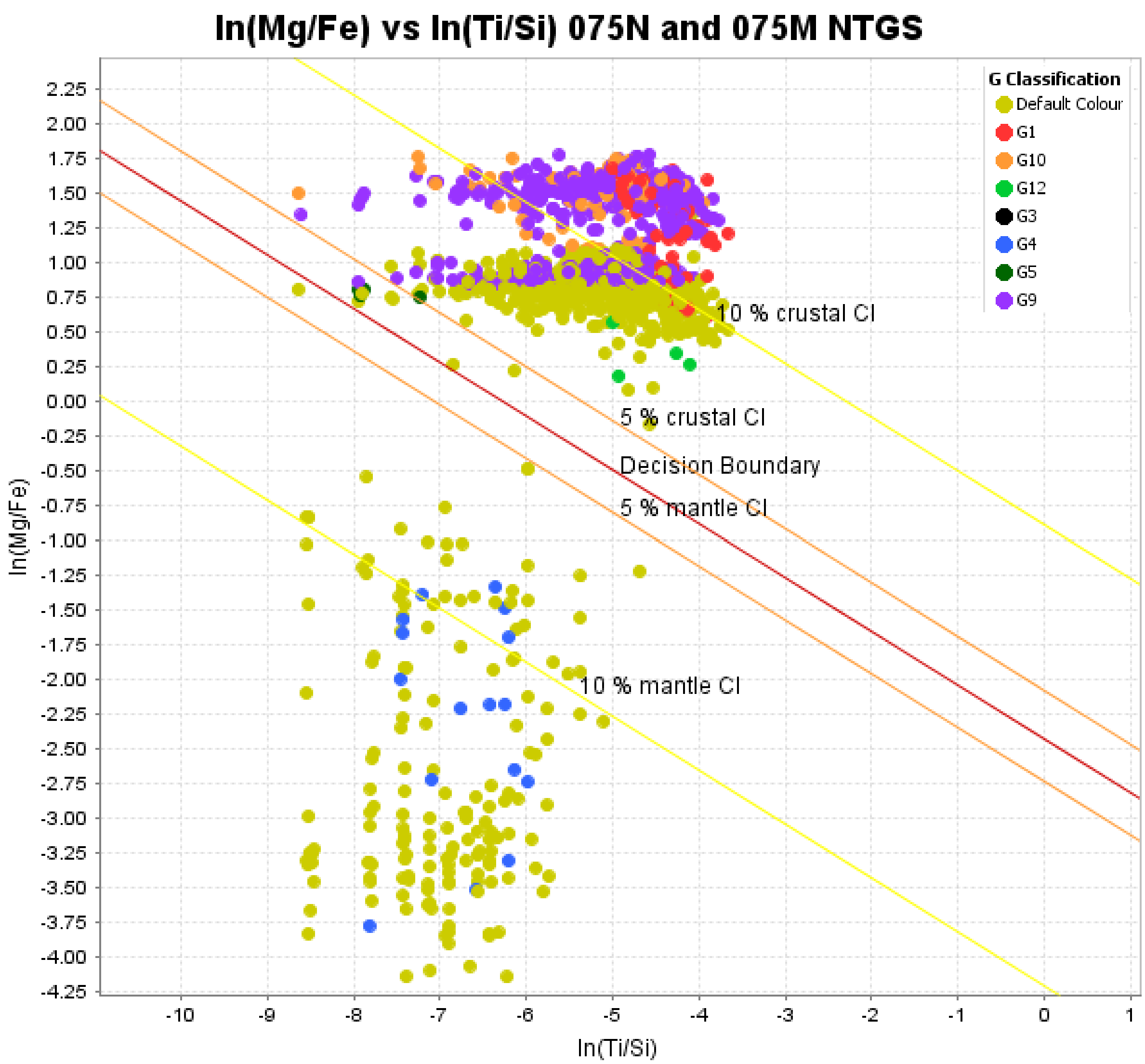

Figure 3.4: G classifications for garnets in the NTGS database from the 075M and 075N NTS map sheets using the scheme of Grutter et al. (2004) (coloured dots) and plotted on the mantle vs crustal discrimination bivariate plot of Hardman et al. (2018a) (sloping lines). “Default Colour” dots represent garnets that are unclassified (G0) by the criteria of Grutter et al. (2004). N=1,412

Low-Cr garnets are present in a variety of host lithologies which form in the mantle and the crust (Hardman et al., 2018b). These crustal rocks form in pressure-temperature conditions that fall outside the diamond stability field and include garnet-granulites, amphibolites, and other plagioclase-bearing metamorphic assemblages formed at high temperatures and pressures in the lower crust (Hardman et al., 2018b). As such, garnets which form at greater depths from within the mantle are more useful in diamond exploration. Trace element systematics for mantle and crustal garnets have proven complex. Existing trace element data of crustal garnets, particularly from metamorphic rocks of cratons, is limited, making comparison to mantle low-Cr garnet trace element data difficult (Hardman et al., 2018b).

Hardman et al. (2018b) has generated a representative database in order to create a trace element statistical analysis for mantle vs crustal garnets. Rare earth element (REE) systematics indicate broad similarities in the shapes of the median chondrite-normalized ($_N$) REE patterns for crustal and mantle garnet groups (Hardman et al., 2018b). Crustal garnets have up to two times higher median $MREE_N$ and $HREE_N$ concentrations than mantle garnets (Hardman et al., 2018b). In addition, the median REE_N pattern for crustal garnets is steeper in the $LREE_N$ with lower La and Nd concentrations as compared to mantle garnet (Hardman et al., 2018b).

There are two distinct trends in the REE_N data from till sample 17-DECS-013 which appear to be trends for mantle and crustal REE (Figure 3.5). Of garnets classified based on Grütter et al. (2004), G10s exhibit a mantle signature and G3 garnets appear to exhibit a crustal signature (Figure 3.6). Rare earth element data for garnets from till sample 17-DECS-016 displays both mantle and crustal patterns (Figure 3.7).

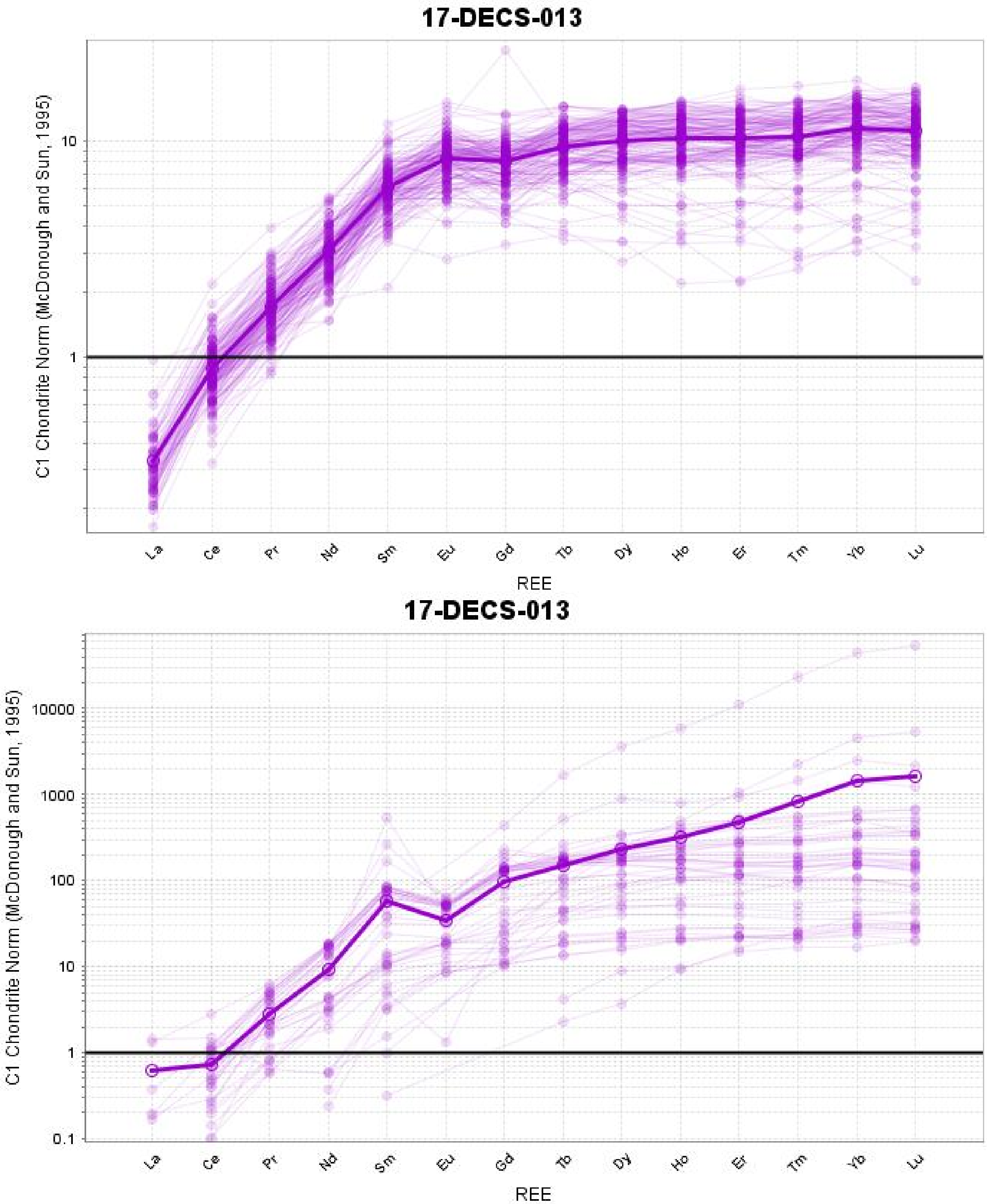

Figure 3.5: Rare earth element data for garnets from till sample 17-DECS-013 for garnets classified as mantle (upper plot) and crustal (lower plot). Mean values shown by thick dark purple line.

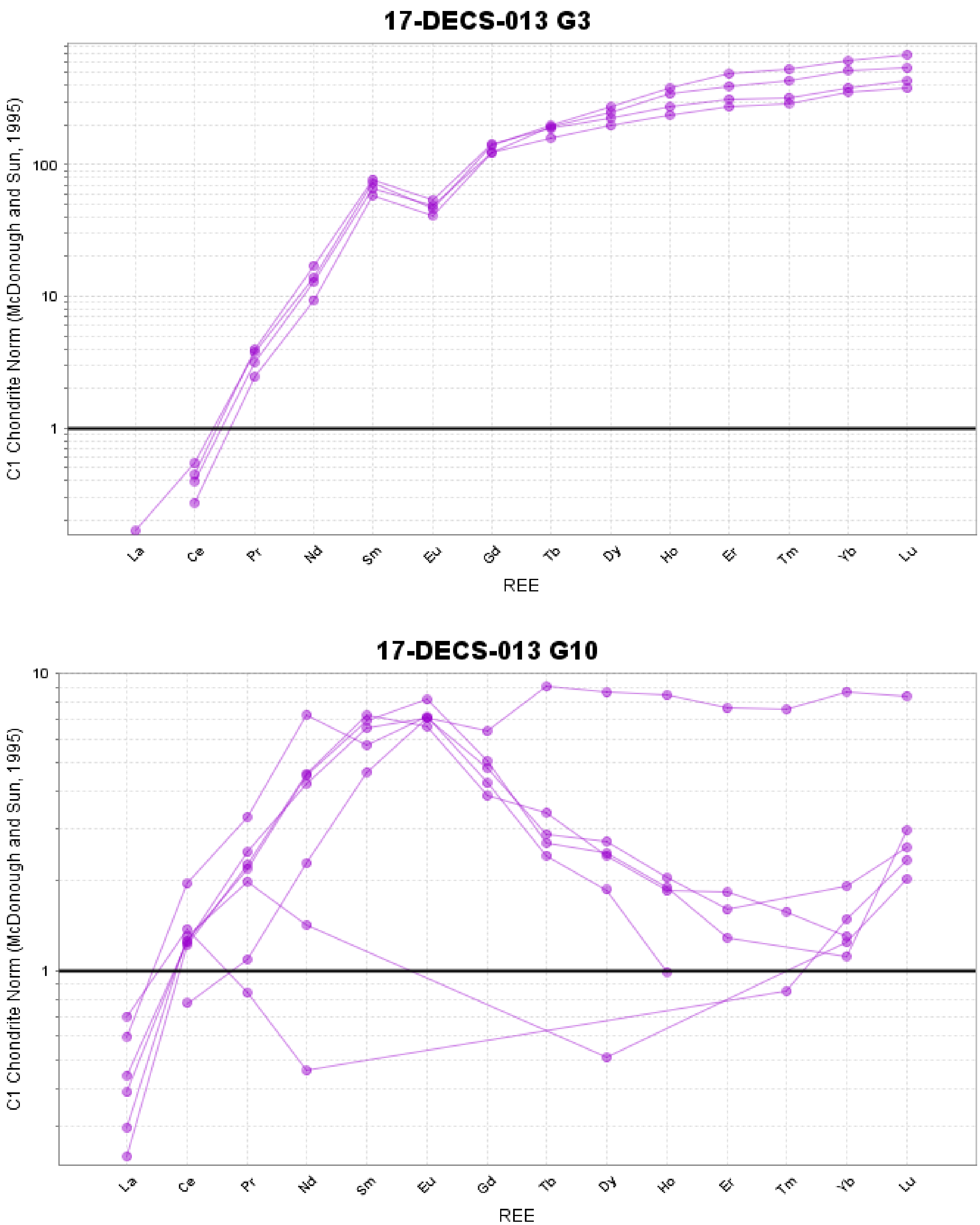

Figure 3.6: Rare earth data for garnets from till sample 17-DECS-013 showing a crustal signature for G3 garnets N=5 (top plot) and mantle signature for G10 garnets N=7(bottom plot).

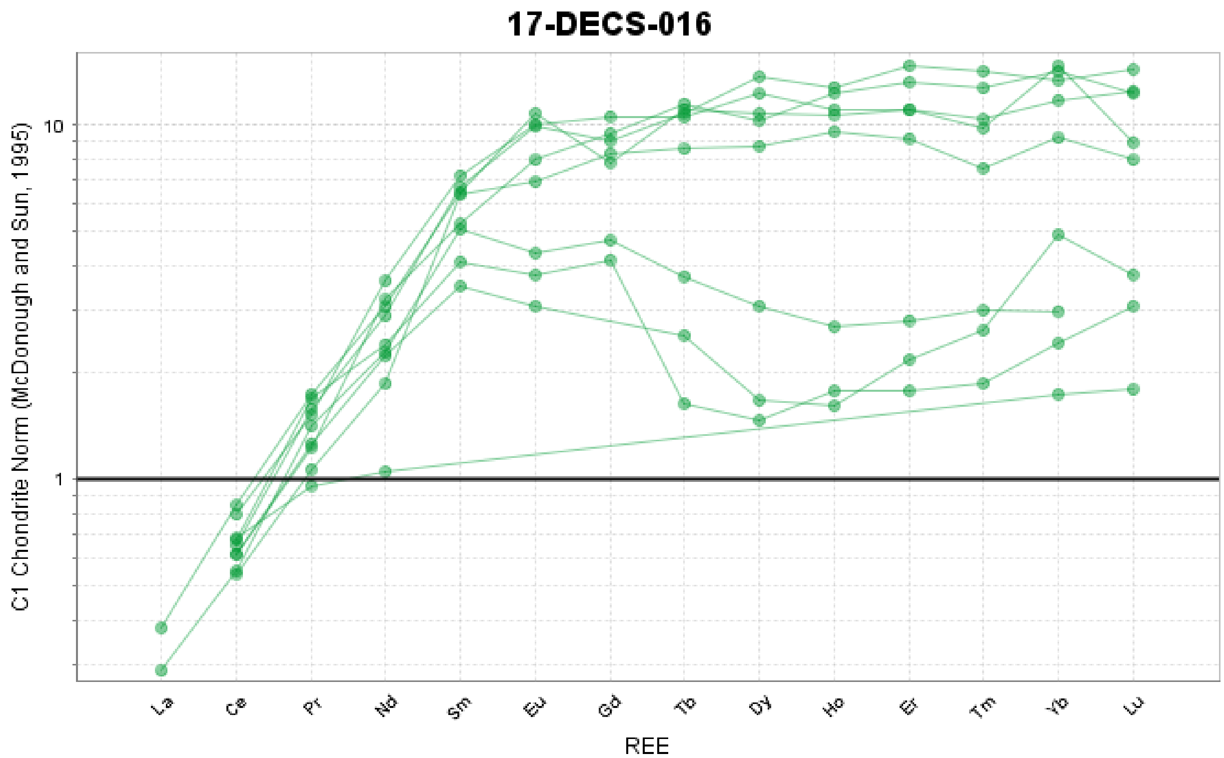

Figure 3.7: Rare earth element data for garnets from till sample 17-DECS-016 showing both crustal and mantle signatures N=8.

3.2 Cr-diopside classification

Pyroxene derived from peridotitic and eclogitic mantle sources can be a KIM and it is a common mineral phase in kimberlite (Nimis, 1998; Quirt, 2004; McClenaghan and Kjarsgaard, 2001, 2007). There are two issues with the use of clinopyroxene as a KIM, the colour criteria used for visual identification can vary and non-kimberlitic Cr-diopside in the sediment sample can create data interpretation problems (Quirt, 2004). Kimberlite is among the few rock types to commonly host very Cr-rich diopsidic clinopyroxene (Quirt, 2004). Grains of Cr-diopside were selected for analysis from the HMC of the 21 till samples based on their pale to emerald green colour. Clinopyroxenes were positively identified (using the SEM) in till samples from sites: 002, 003, 004, and 013. The grains in samples 002, 004, and 013 are not kimberlitic in composition. One Cr-diopside grain in till sample 17-DECS-003 was classified as kimberlitic based on its Na-Ca-Mg content as shown in discrimination diagrams in (Figure 3.8, Figure 3.9). This sample also contained one G12 garnet grain. All potential Cr-diopside grains from the 17-DECS till samples were classified as low-Cr diopsides because they contained <1.5 wt. % Cr_2O_3 (Appendix I). Kimberlites and mantle xenoliths are the only rocks which contain very Cr-rich diopside at concentrations greater than 1.5 wt. % Cr_2O_3 (Deer et al., 1982; Fipke et al., 1989, 1995).

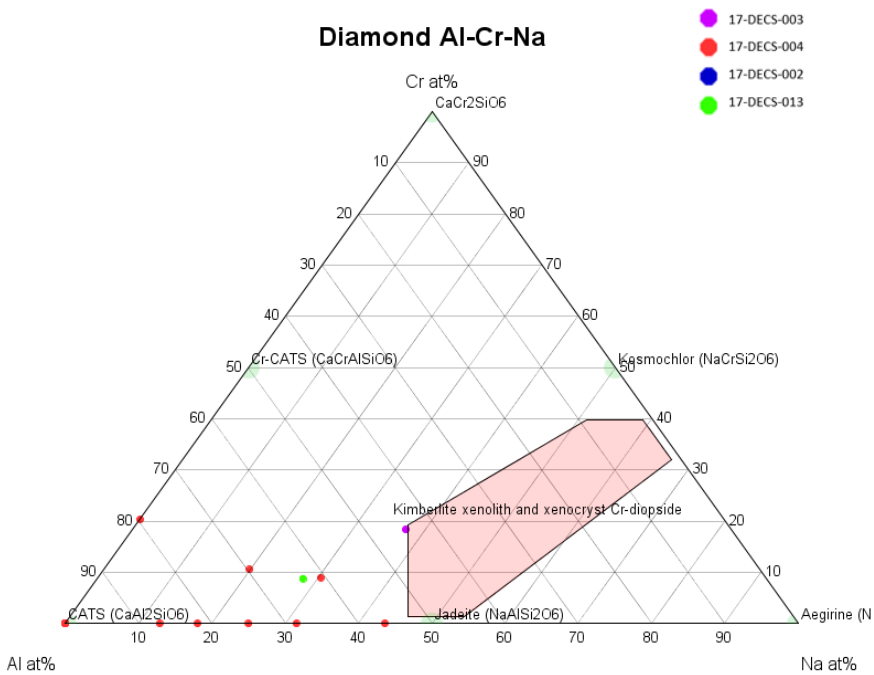

Figure 3.8: Al-Cr-Na ternary cation plot for potential Cr-diopside grains from four till samples (coloured dots) with 85 % Cr-diopside field for kimberlite xenoliths and xenocryst from Morris et al. (2002). N=11, n=4

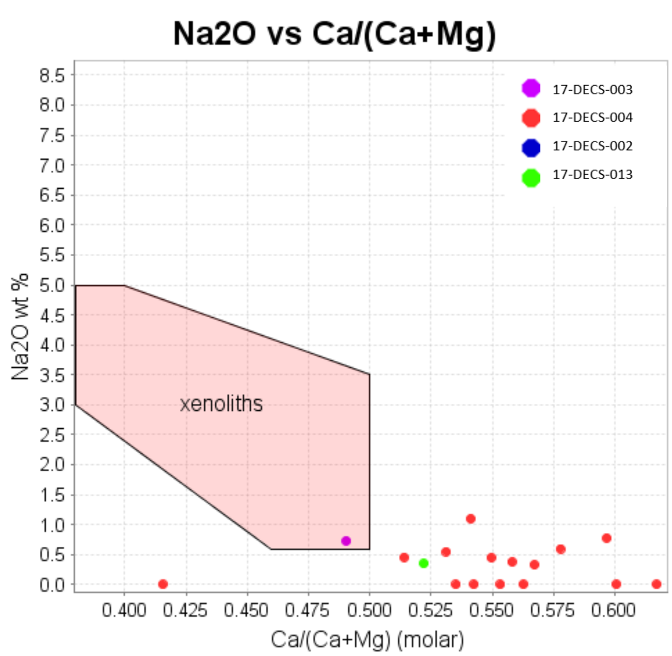

Figure 3.9: Plot of Na_2O versus Ca/(Ca+Mg) for Cr-diopside grains from 4 till samples (coloured dots) in this study. Field for kimberlite xenoliths and xenocrysts from Morris et al. (2002). N=17, n=4

3.3 Ilmenite and chromite

Mg-ilmenite is an important KIM (Fipke et al., 1995; McClenaghan and Kjarsgaard, 2001, 2007; Nowicki et al. 2007). Compositional data for ilmenites derived from potentially diamondiferous sources and non-kimberlitic sources have been compiled in order to identify compositional fields for kimberlitic ilmenite (Wyatt et al., 2004). Commonly used are MgO – TiO2 and MgO-Cr2O3 diagrams (Wyatt et al., 2004) to discriminate kimberlitic from non-kimberlitic ilmenites. However, the use of Mg-ilmenite in diamond exploration is controversial due to the inability to discern host rock lithology (Castillo-Oliver et al., 2017). In this study the ilmenites from the 17-DECS till samples do not chemically correspond with KIM Mg-ilmenite chemistry (Table 3.4).

Table 3.4: Chemistry of potential KIM ilmenite grains from 17-DECS till samples. N=7, n=4

17-DECS-	**013**	**013**	**006**	**006**	**018**	**002**	**002**
TiO_2	55.09	53.68	49.85	53.96	50.47	51.26	50.72
Al_2O_3	0.56	0.71	0	0	0	0	0
FeO Total	33.45	35.93	46.74	44.33	50.33	45.55	47.17
MnO	0	0	0.67	1.27	0.44	2.3	0
MgO	10.65	9.77	0	0	0	0	0.43
Total	99.75	100.09	97.26	99.56	101.24	99.11	98.32
Formula on the basis of 6 oxygen							
Ti	1.947	1.913	1.962	2.041	1.924	1.975	1.967
Al	0.031	0.040	0.000	0.000	0.000	0.000	0.000
Fe^{2+} all ferrous	1.314	1.424	2.046	1.864	2.133	1.951	2.033
Mn	0.000	0.000	0.030	0.054	0.019	0.100	0.000
Mg	0.746	0.690	0.000	0.000	0.000	0.000	0.033
Total	4.038	4.067	4.038	3.959	4.076	4.025	4.033

Chromite xenocrysts are deemed to have formed co-genetically with diamond based on the presence of chromite inclusions in diamond (Gurney, 1984; Harvey et al., 2001). Chromite is thought to be exclusively of peridotitic origin. Chromite with high Cr and moderate to high MgO contents are potential indicators of diamond due to the similarities in composition to chromite included in diamond (Harvey et al., 2001; Nowicki et al., 2007).

Kimberlitic chromite was found only in till sample 17-DECS-013. A total of 4 kimberlitic chromite were identified out of possible 36 grains analysed using the discrimination plot of Grütter and Apter (1998) (Appendix I, Figure 3.10).

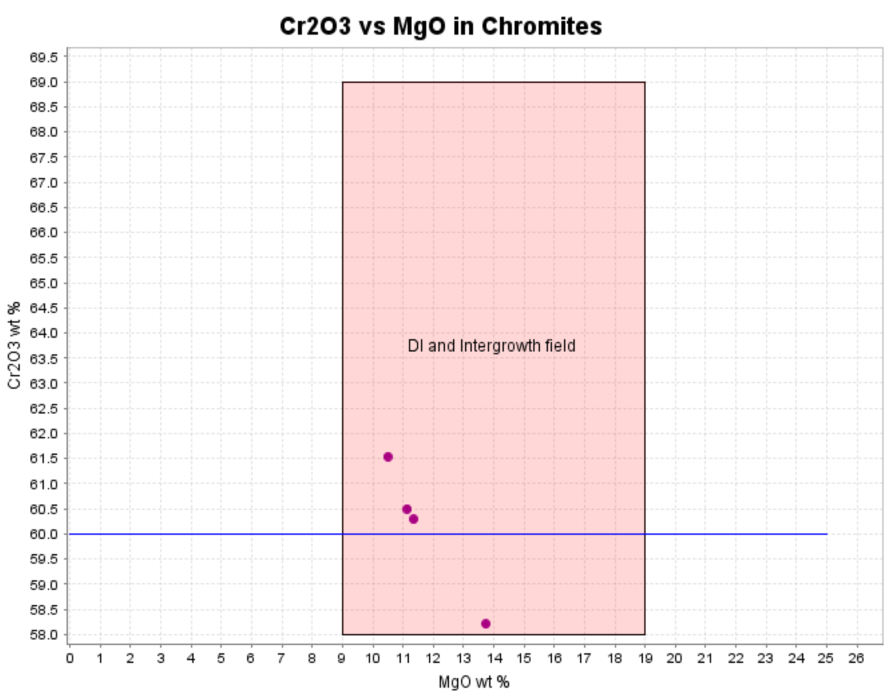

Figure 3.10: Plot of Cr_2O_3 vs MgO wt % for chromite from till sample 17-DECS-013 N=4, n=1 (after Grütter and Apter, 1998).

3.4 Indicator distribution maps

In order to understand the distribution of KIM in glacial sediments across the Slave Province, several maps have been produced using the data for till samples collected in this study and from the NTGS open data hub (http://datahub-ntgs.opendata.arcgis.com/, 2018). Data are plotted based on the different classifications of garnets mentioned previously, and KIMs such as Cr-diopside, chromite, Mg-ilmenite, and olivine from the KIMC database. The visual representation of KIM distributions is intended to aid diamond exploration in the southern Slave Province using the mineral chemistry data available.

It is important to acknowledge the previous work of Armstrong (2003) who has produced numerous maps of the distribution of kimberlite indicator minerals in the Slave Province using the NTGS open data hub. Armstrong (2003) has made maps using KIDD showing distributions of chromite, ilmenite, Cr-diopside, and total indicator minerals as well as maps displaying the variable amounts of data within the KIDD and KIMC databases (Figure 3.11).

Kimberlite glacial dispersal trains down ice of individual kimberlites in the Slave Province are typically elongate, up-ice narrowing features produced by a single phase of ice flow (McClenaghan et al., 2002). Some bilobate and fan-shaped dispersal trains produced by two phases of ice flow have also been reported for the Slave region (Stea et al. 2009). In the southern Slave Province, there are 3 dominant potential dispersal trains which are best observed in the garnet population distribution data. These trains have been previously observed in the maps of Armstrong (2003) using the total indicator mineral counts from the KIDD (2003).

In the northern Slave Province, it is difficult to discern individual kimberlite indicator dispersal trains using all of the raw data from the NTGS (2018) due to the large volume of data that is available, the proximity of kimberlite pipes, and the complex glacial history. Prolific surficial sediment sampling has been conducted within a small region referred to here as the high-density sample area (HDSA) (Figure 3.11, Figure 3.12) such that individual dispersal train overlap. The HDSA of the northern Slave Province is proximal to what is now the Ekati and Diavik mine complexes (Figure 3.11, Figure 3.12).

The high density of KIM-rich kimberlites (Figure 3.11) has generated KIM-rich till over a large area down ice of the Lac de Gras kimberlite cluster. This high-density distribution pattern is further complicated by the three main phases of ice flow that eroded and transported KIM in the local till (McClenaghan et al., 2002; Armstrong, 2003).

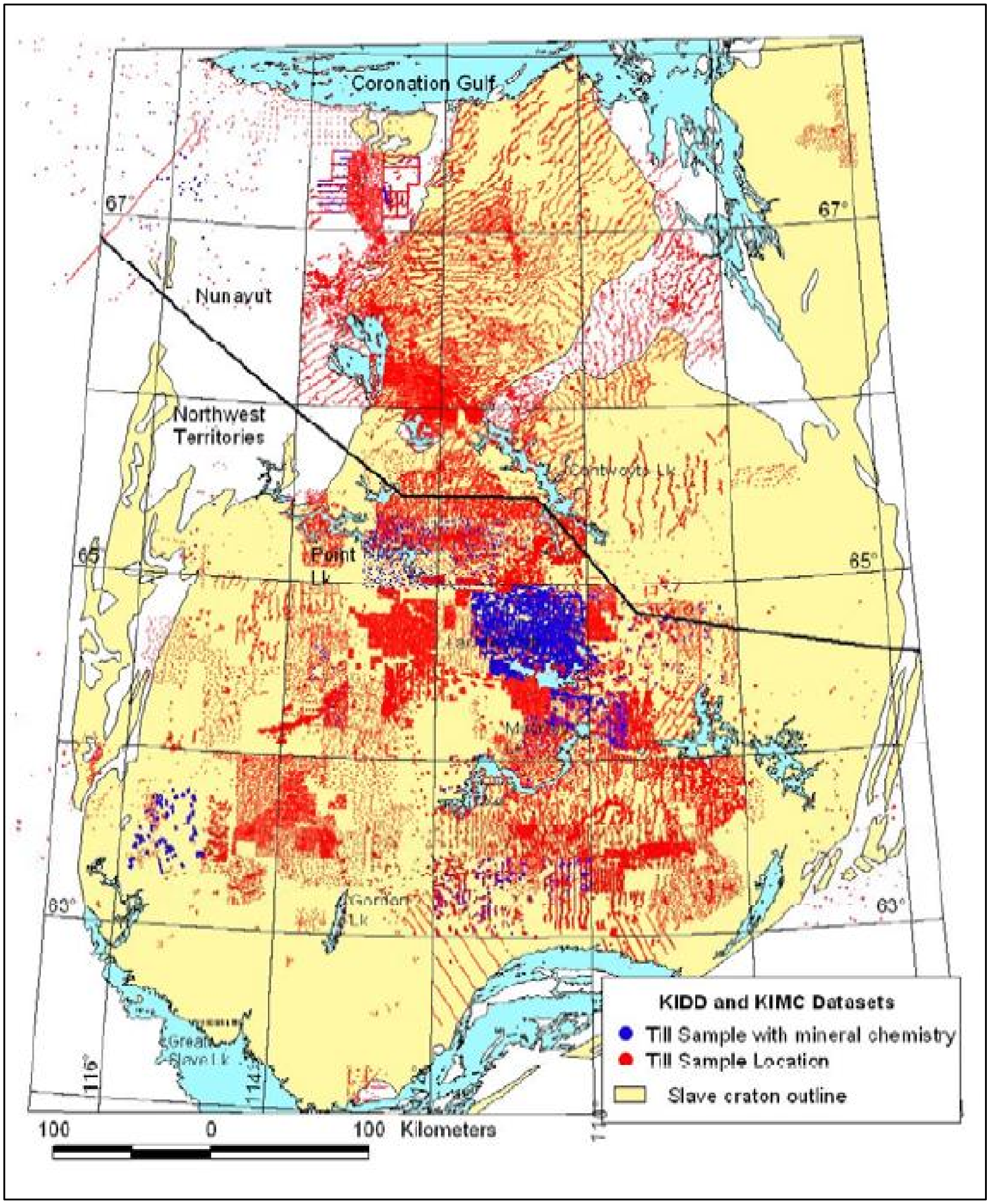

Figure 3.11: KIDD and KIMC datasets sample locations from Armstrong (2003) N=>110,000 KIMS from KIMC and n=>135,000 till sample locations. Till samples with mineral chemistry plotted in blue highlight the discrepancy in mineral chemistry data available by geographic location. The blue area in this map will represents the high density sample area (HDSA) in this study.

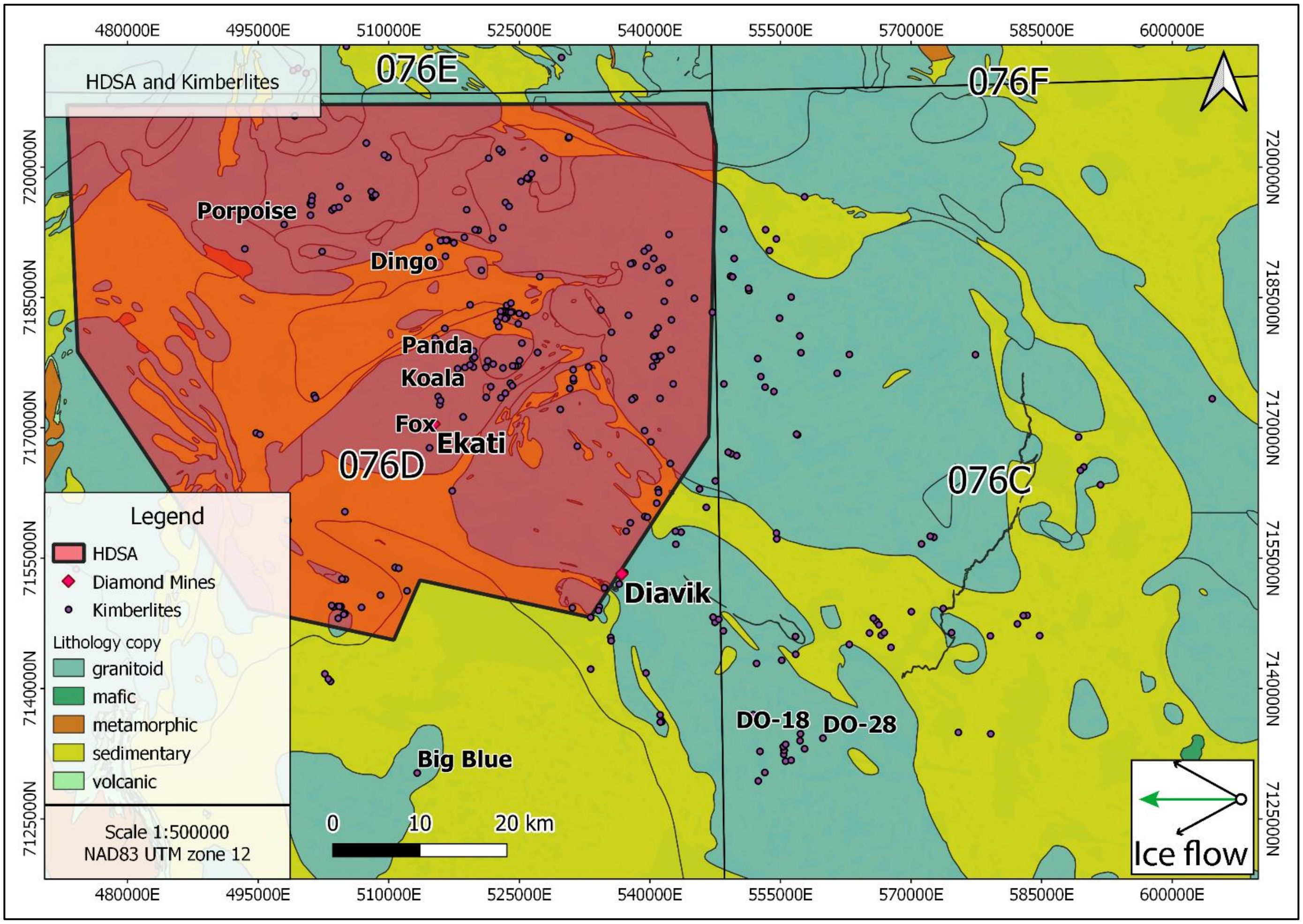

Figure 3.12: High density sample area in the central Slave Province directly up ice (NW) of dense kimberlite clusters of the Lac des Gras kimberlite field. Ice flow direction varies from southwest (oldest), to west, to northwest (youngest) (surficial data from NWT Open File 2005-001, NWT Geoscience Office, 2018; Stubley and Irwin, 2019). Kimberlites in map frame= ~280.

3.4.1 Olivine distribution in surficial sediments

Olivine is present in surficial sediment samples across the northern Slave Province on the borders of the HDSA (Figure 3.13, **Error! Reference source not found.**). The olivine is present (1 to 7 grains) in samples proximal (<5km) to some kimberlites with spikes in concentration (up to 25 grains) more distal (20km) down ice if kimberlites. Kimberlites are densely populated in and around the HDSA and all surficial sediment samples collected are within ~60 km of a known kimberlite.

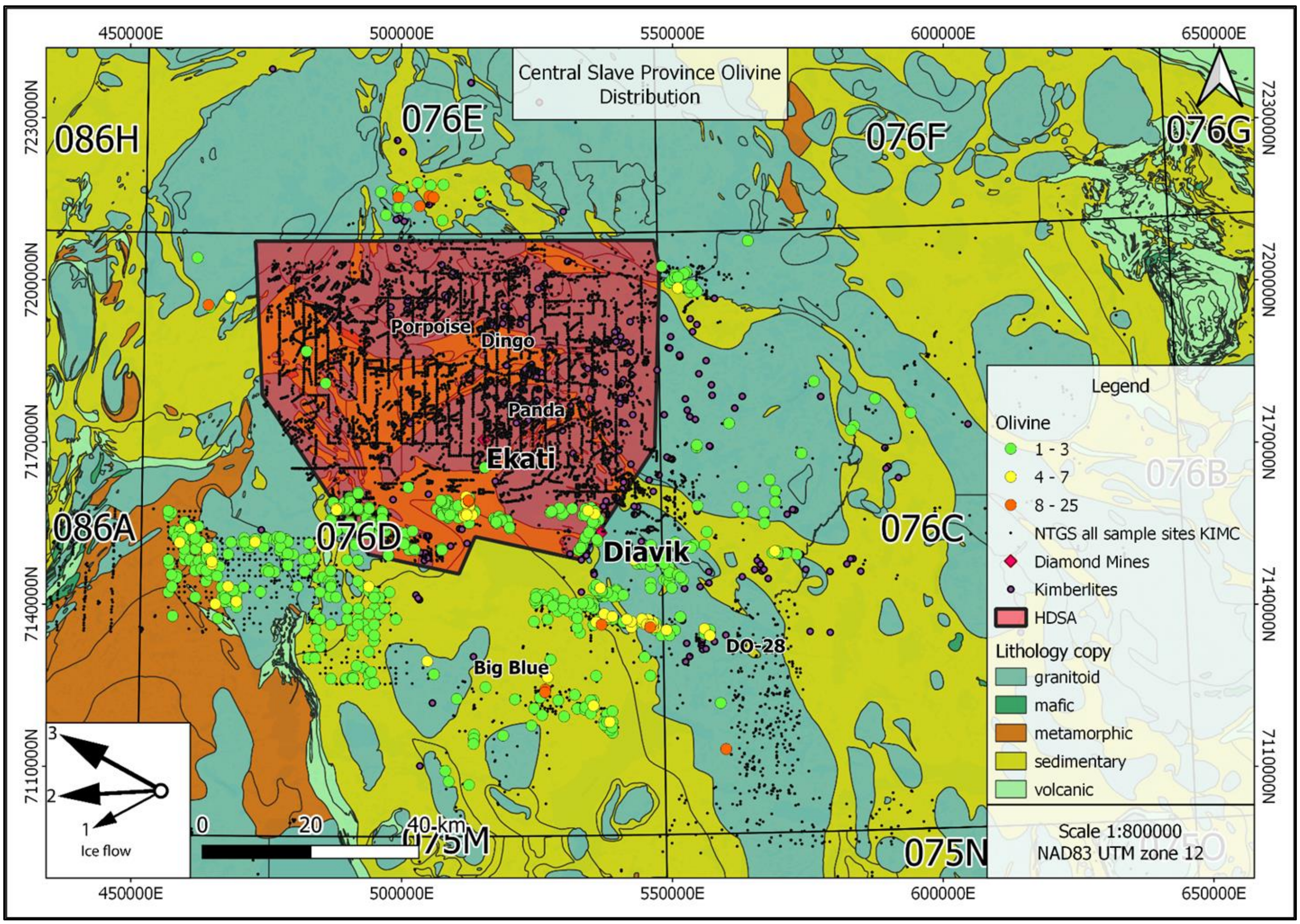

Figure 3.13: Olivine distribution in surficial sediment samples in the northern Slave Province (surficial data from NWT Open File 2005-001, NWT Geoscience Office, 2018). Coloured dots indicate number of grains N=1348, n=632

3.4.2 Chromite, ilmenite and picroilmenite distribution in surficial sediments

In the southern Slave Province chromite and ilmenite are both present in minor amounts (<10 grains per sample) (Figure 3.14, Figure 3.15). In the northern Slave Province, there are similar concentrations of chromite and ilmenite near the southern border of the Lac de Gras kimberlite swarm (Figure 3.16). Concentration of chromite and ilmenite per sample are significantly higher within the HDSA. Chromite values range from 1 to 4 grains per sample to 37 to 112 grains per sample. Ilmenite values vary from 1 to 3 grains per sample up to 312 grains per sample (Figure 3.16, Figure 3.17).

A total of 560 grains from 74 surficial sediment samples classified as picroilmenite from the KIMC database. Of these 560 grains none plot within the central Slave Province (HDSA) or within the southeastern Slave Province and sample area. All grains classified as picroilmenite plot within the 086P NTS map sheet, west to northwest of the Kikerk-1 and Stellaria Kimberlites (Figure 3.18). The highest picroilmenite count for a single sample site based on mineral chemistry is 25 grains.

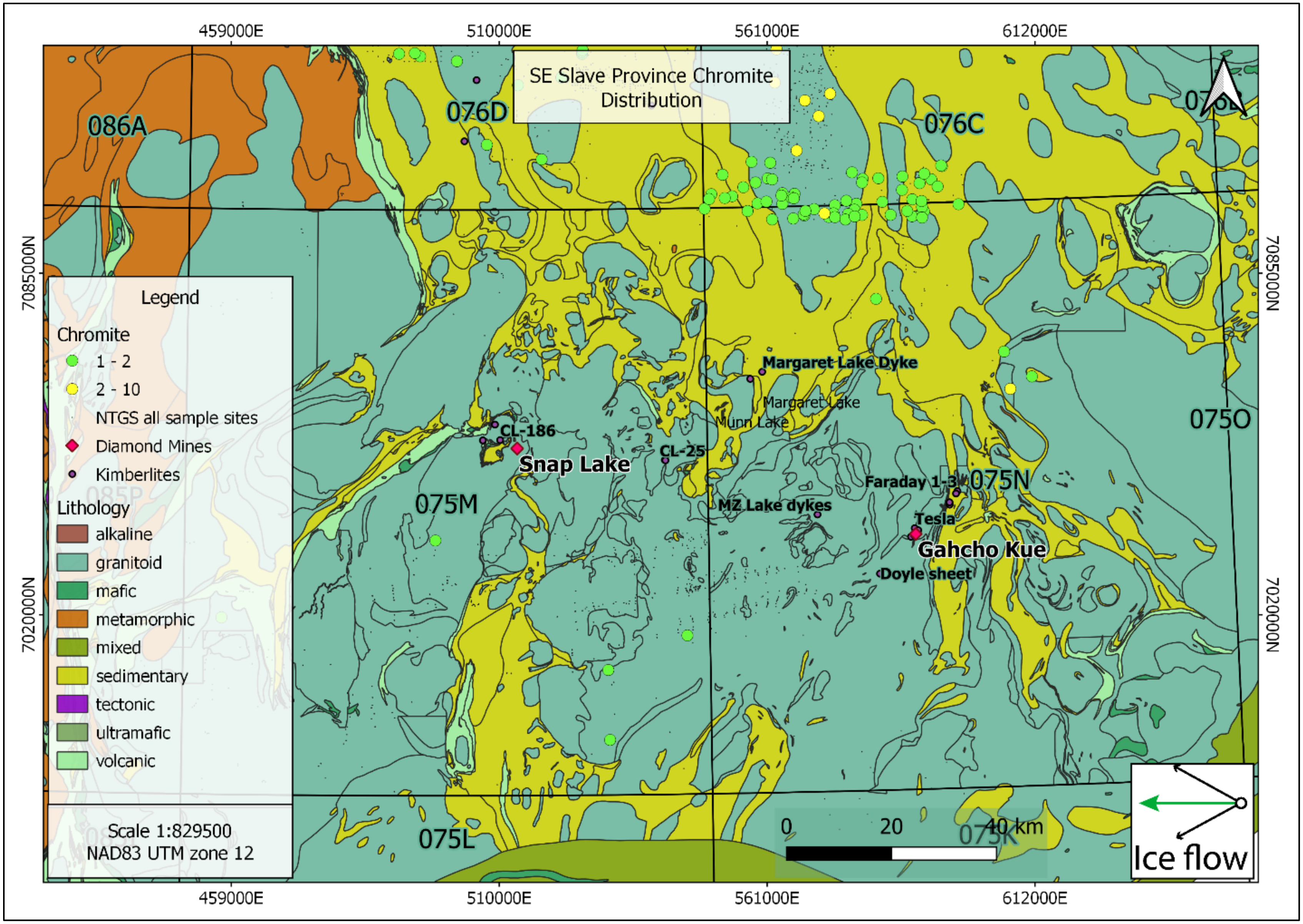

Figure 3.14: Chromite distribution in the southeastern Slave Province based on mineral chemistry from KIMC. (mineral count data and bedrock geology from NWT Open File 2005-001, NWT Geoscience Office, 2018; Stubley and Irwin, 2019). N=5, n=5 (southern samples)

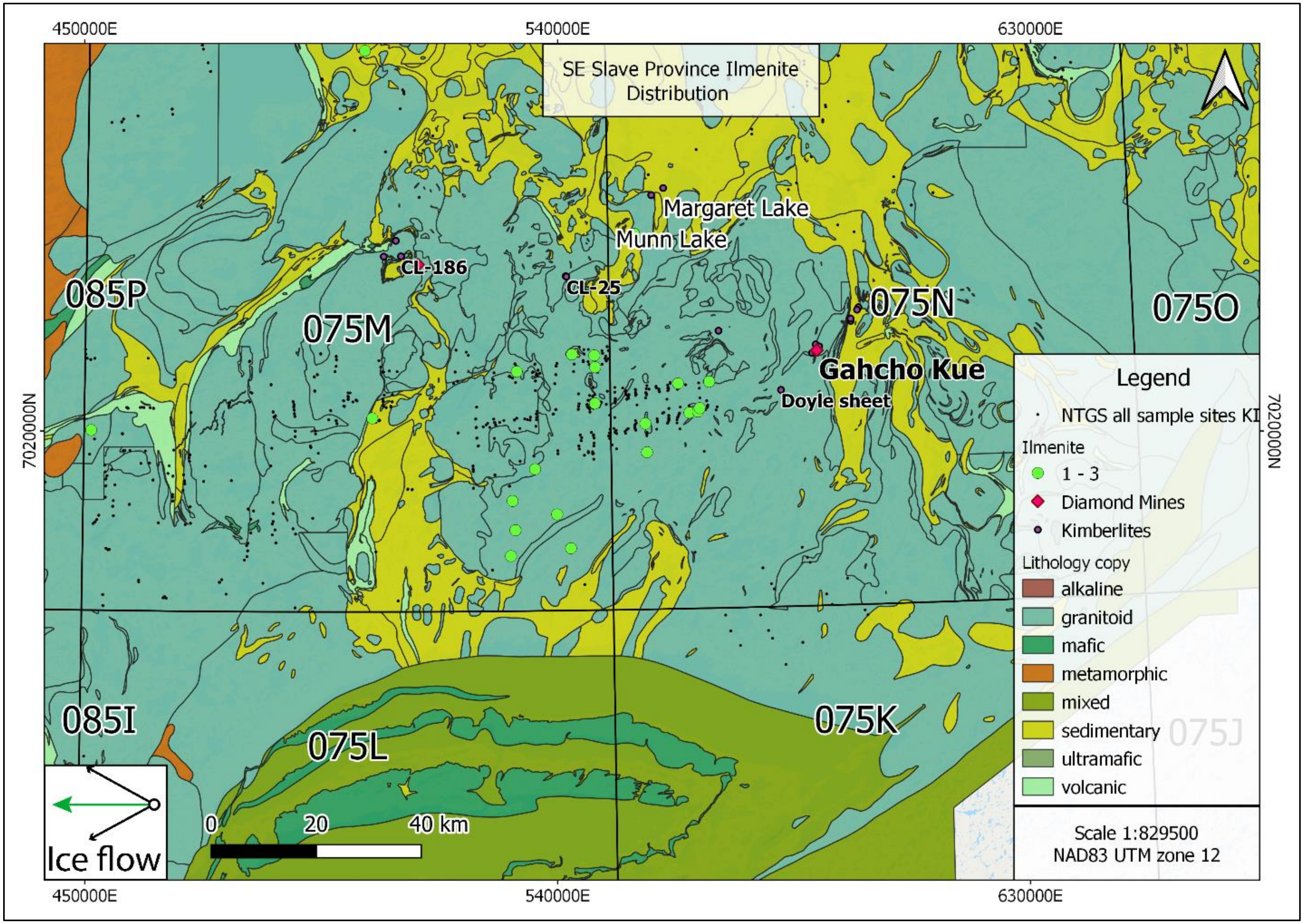

Figure 3.15: Ilmenite distribution in the southeastern Slave Province based on mineral chemistry from KIMC (mineral count data and bedrock geology from NWT Open File 2005-001, NWT Geoscience Office, 2018; Stubley and Irwin, 2019). N=31, n=21

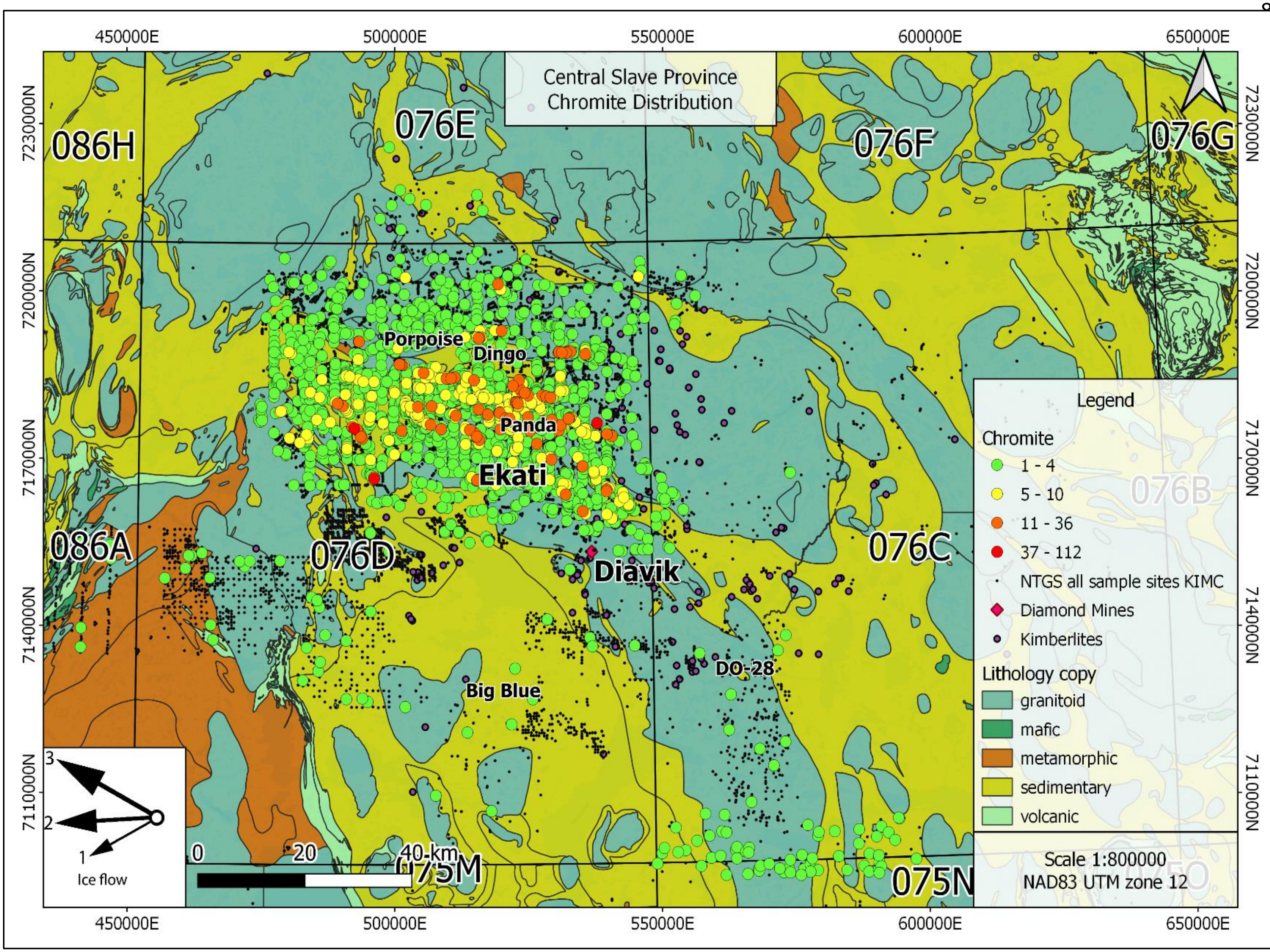

Figure 3.16: Chromite distribution in the central Slave Province based on mineral chemistry from KIMC. (mineral count data and bedrock geology from NWT Open File 2005-001, NWT Geoscience Office, 2018; Stubley and Irwin, 2019). N=5793, n=2031

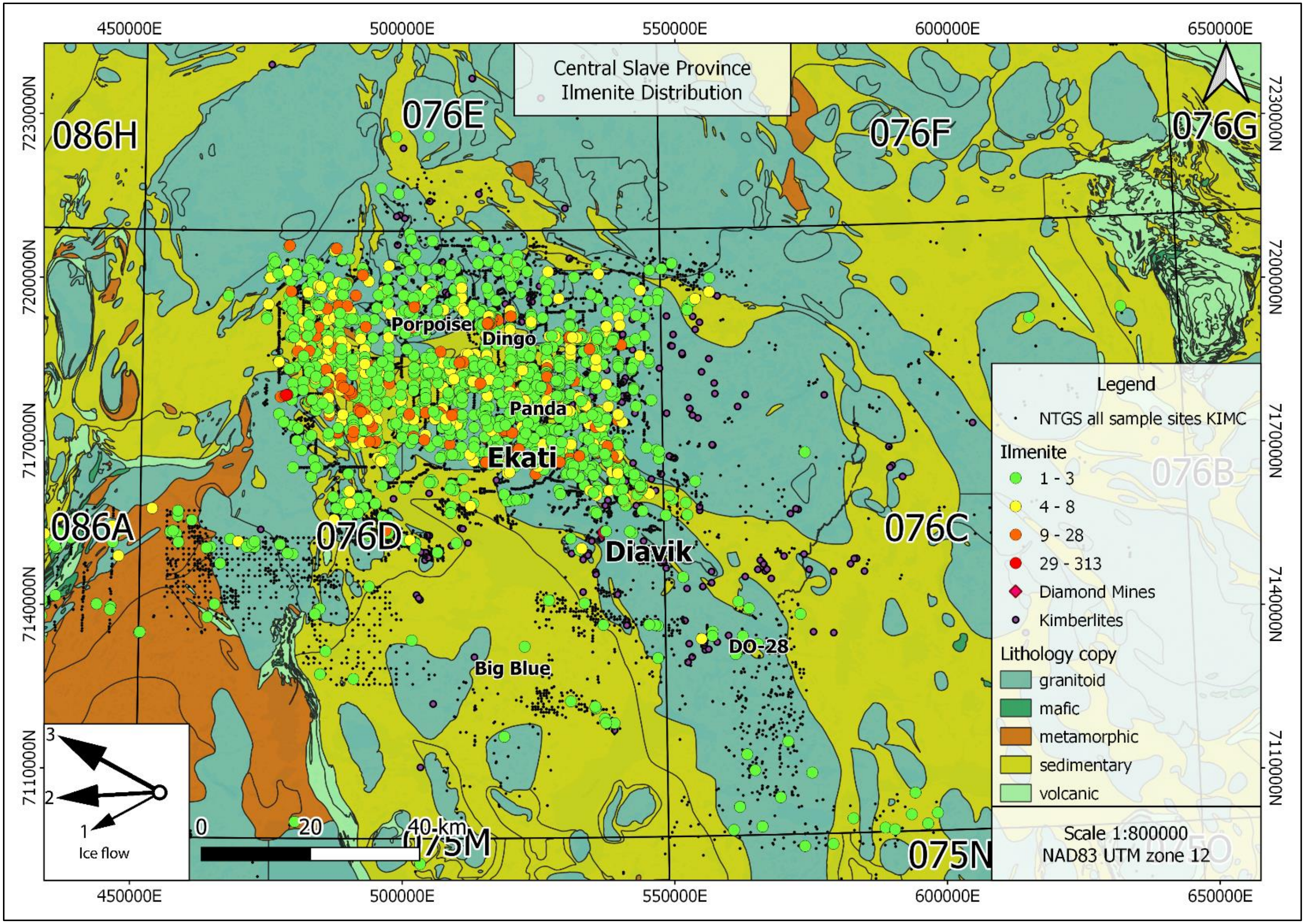

Figure 3.17: Ilmenite distribution in the central Slave Province based on mineral chemistry from KIMC (mineral count data and bedrock geology from NWT Open File 2005-001, NWT Geoscience Office, 2018; Stubley and Irwin, 2019). N=4939, n=1613

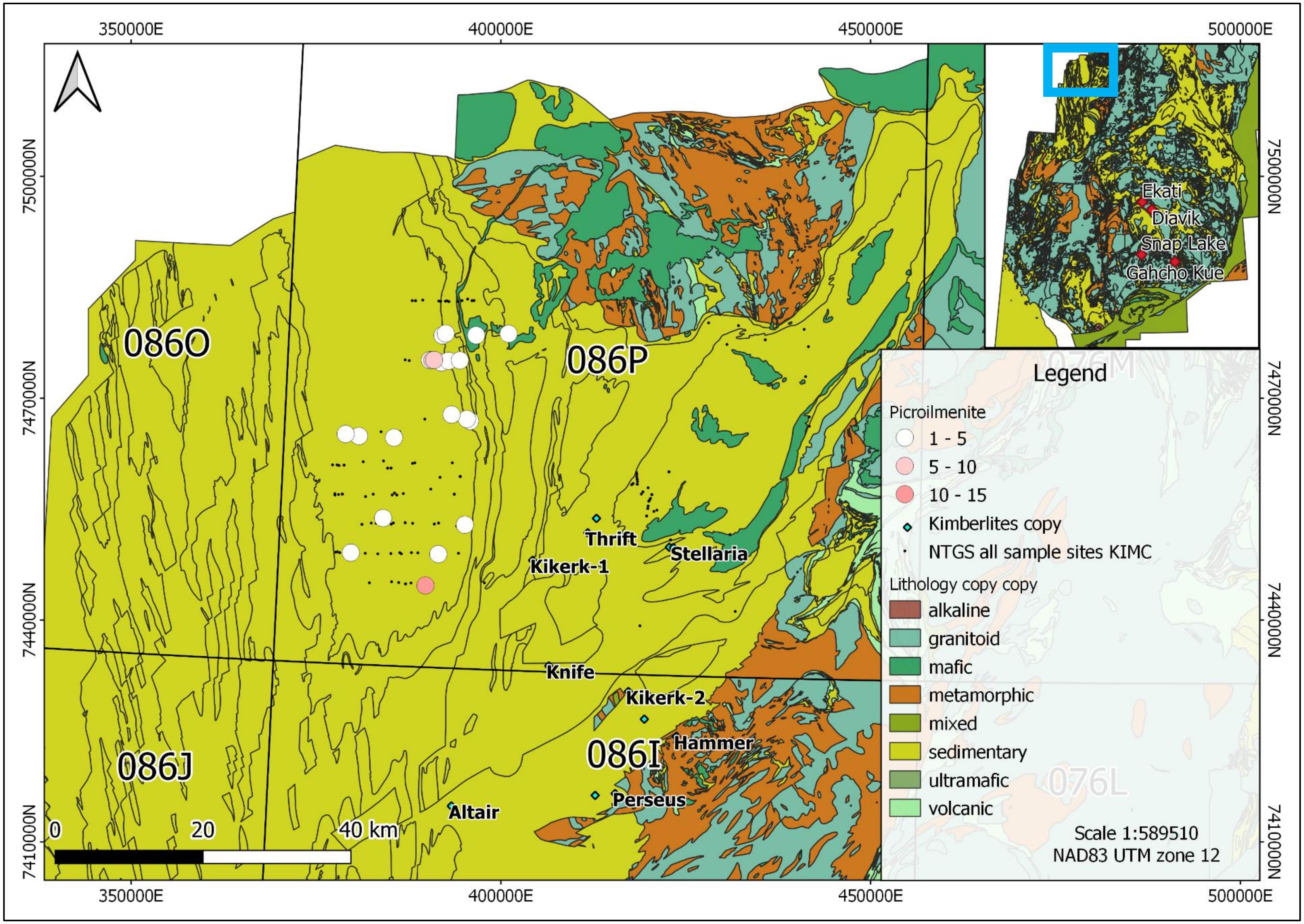

Figure 3.18: Picroilmenite distribution in the northeastern corner of the Slave Province based on mineral chemistry from the KIMC database (mineral count data and bedrock geology from NWT Open File 2005-001, NWT Geoscience Office, 2018; Stubley and Irwin, 2019). N=49, n=21

3.4.3 Cr-diopside distribution in surficial sediment

High-Cr diopside (>1.5 wt. % Cr_2O_3) is sparsely distributed in surficial sediments across the Slave Province (Figure 3.19). There is a notable low concentration of Cr-diopside in the HDSA (0 grains) based on mineral chemistry (Figure 3.19). Cr-diopside is more common in the sediments in the region between the HDSA and the 17-DECS sample area. Similar distribution patterns are seen for high-Cr diopside. High Cr-diopside is found down ice of known kimberlites (Big Blue, Bishop, Adams, and unnamed dykes) with up to 9 grains being recovered from a single surficial sediment sample within 16-60 km (Figure 3.20). The Cr-diopside with no known up-ice kimberlites contains <1.5 wt. % Cr_2O_3.

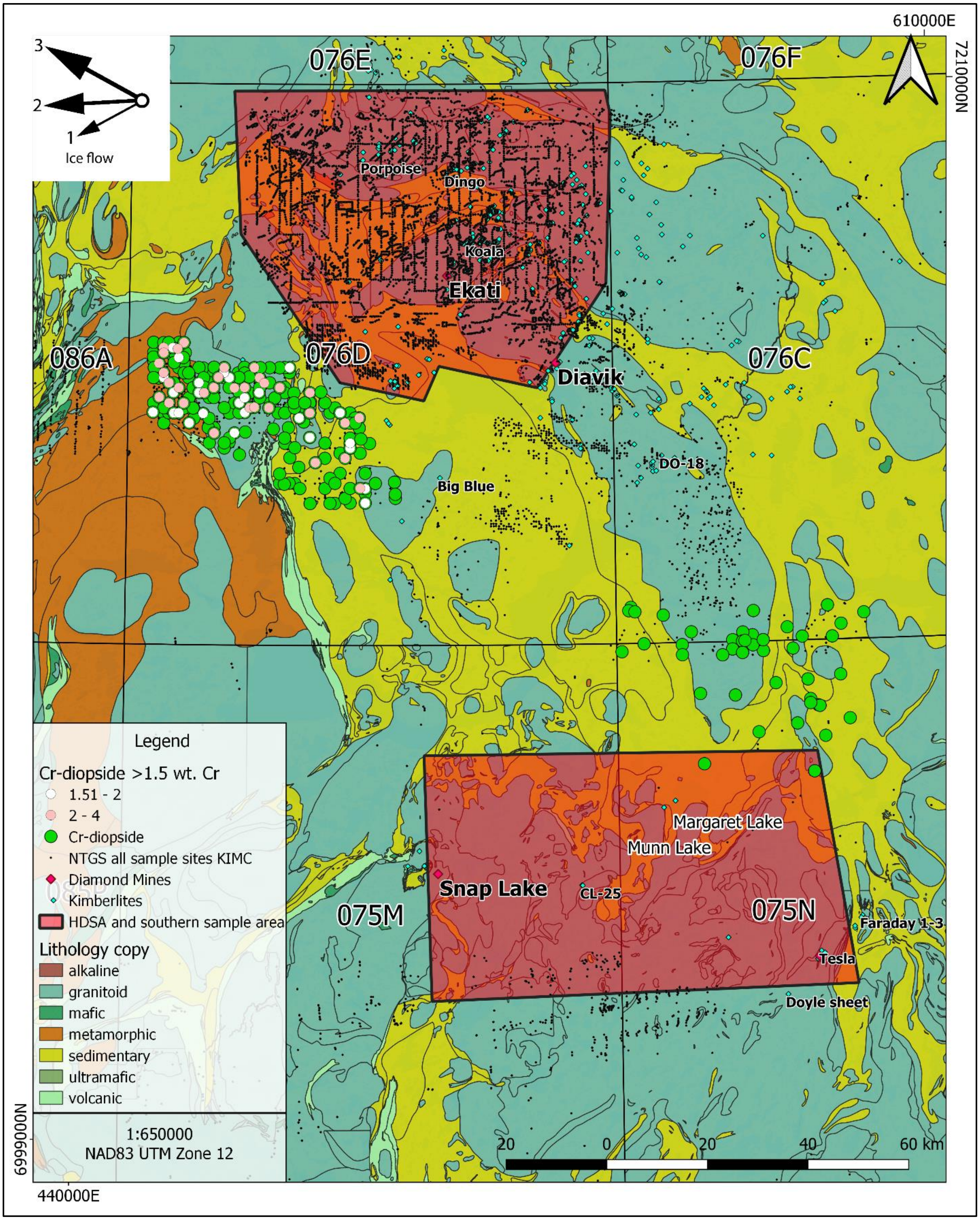

Figure 3.19: High-Cr diopside and Cr-diopside distribution in the Slave Province (mineral count data and bedrock geology from NWT Open File 2005-001, NWT Geoscience Office, 2018; Stubley and Irwin, 2019). N=515, n=347

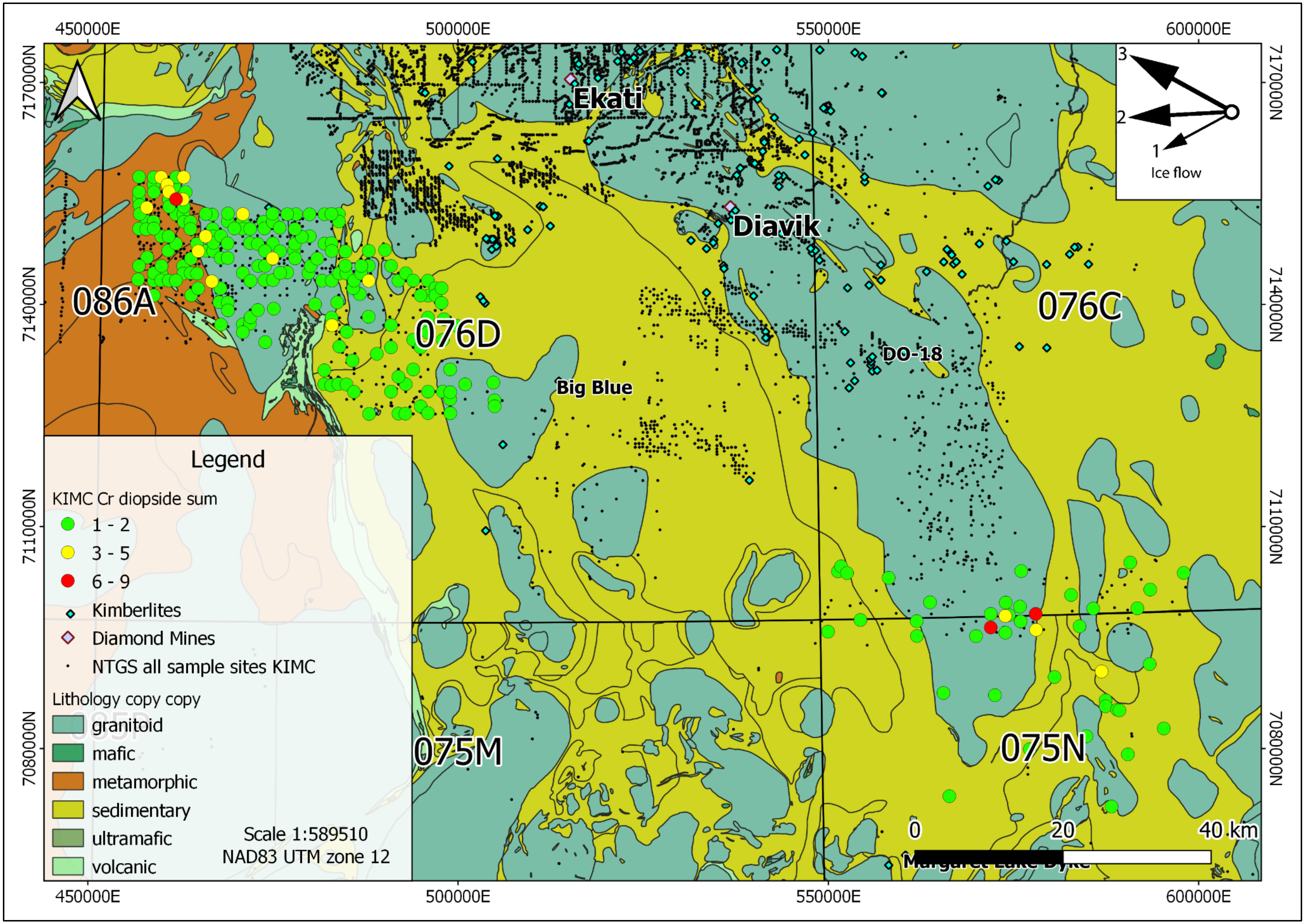

Figure 3.20: Distribution of Cr-diopside grains in surficial sediment samples between the HDSA and southern sample area (mineral count data and bedrock geology from NWT Open File 2005-001, NWT Geoscience Office, 2018; Stubley and Irwin, 2019). N=515, n=347

3.4.4 Garnet distribution in surficial sediments

Garnet is the most abundant KIM found in surficial sediment samples in the Slave Province, ranging from 1 to 738 total garnet grains per sample with a mean content of 9 grains per surficial sediment sample. The 17-DECS sample series contains 257 garnets, including G1, G3, G12, G9 and G10 garnets (17-DECS-003) (Figure 3.21).

G9 and G10 garnets are the most common garnets in the till samples with the exception of unclassified garnets (G0). Garnet is the only KIM from the KIMC database that can be used to identify glacial dispersal trains in the southern Slave Province (Figure 3.22, Figure 3.23, Figure 3.24, Figure 3.25), because of their high abundances in sediment samples and wider areal distribution.

Abundance of G9 garnet in the 17-DECS till sample suite ranges from 0 to 172 grains. The abundance of G9 garnets in the 17-DECS sample series is reflective of G9 concentrations in samples of the northern Slave Province (Figure 3.22, Figure 3.23Figure 3.22). The G9 garnets increase in abundance westward in the southern Slave Province, indicative of dispersal from kimberlites in the east.

The concentration of G10 and G10D garnet in surficial sediments ranges from 1 to 5 grains and is notably lower in the southern Slave Province than the HDSA (1 to 64 grains per site), but similar to other areas in the northern Slave Province (Figure 3.24, Figure 3.25, Figure 3.26, Figure 3.27). The number of G10 and G10D garnets identified in till sample 17-DECS-013 is high at 10 and 9 grains respectively, in the sample area (Figure 3.24, Figure 3.26). The overall pattern of dispersal for the G10 garnets appears to increase in concentration down-ice of known kimberlites.

Concentration of G1 garnets is low (1 to 5 grains per site) in the southern Slave relative to the north (1 to 80 grains per site) (Figure 3.28, Figure 3.29). G1 abundance at 17-DECS-013 is high at 12 grains for the southern Slave. Similar to G9 and G10, G1 garnets increase in concentration down-ice from known kimberlites.

The concentration of eclogitic G3 garnets is low (<4 grains) throughout the region. Sample site 17-DECS-013 is considerably high in G3 concentration (14 grains) relative to the entire Slave Province (Figure 3.30, Figure 3.31).

G4 garnets are less common than most other KIM garnets in the Slave Province and occur in the most till samples in the northern Slave (Figure 3.32, Figure 3.33). Garnets classified as G5 are the least abundant throughout the Slave Province, with their highest (14 locations containing 1-2 grains) occurring in the northern Slave Province (Figure 3.34, Figure 3.35).

G12 garnets are present in relatively high abundances (up to 32 grains in 1 site) in the central Slave Province, with lower abundances of <5 grains per site in the southeastern Slave Province (Figure 3.36, Figure 3.37).

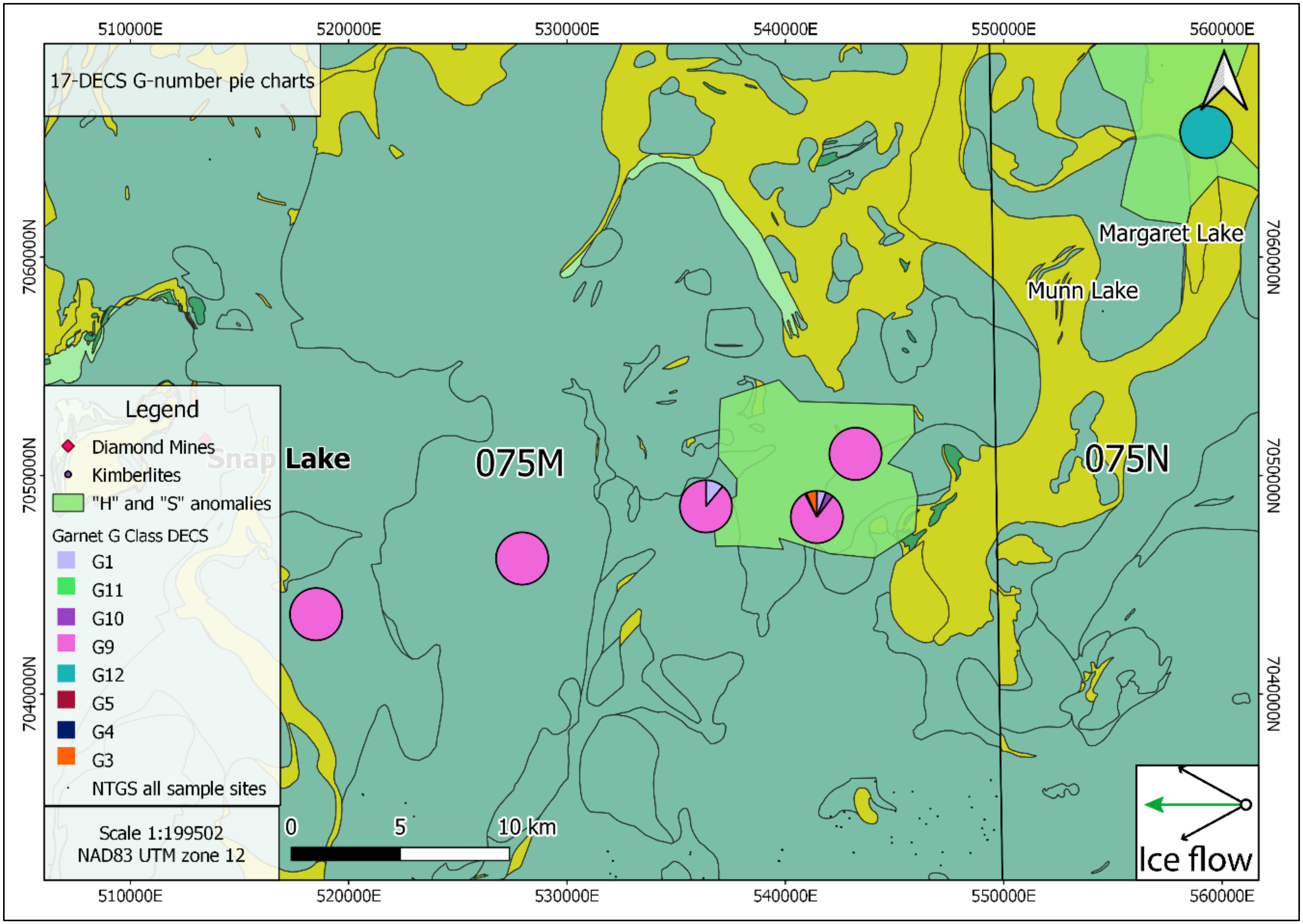

Figure 3.21: Pie plots of the relative abundance of garnet types in the 17-DECS sample suite relative to H and S geophysical anomalies (ice flow data and bedrock geology from NWT Open File 2005-001, NWT Geoscience Office, 2018; Stubley and Irwin, 2019; Geophysical data and interpretation from CGG Canada Services Ltd., 2017; Mirza and Elliott, 2017). 17-DECS garnets N=224, sample sites n=21

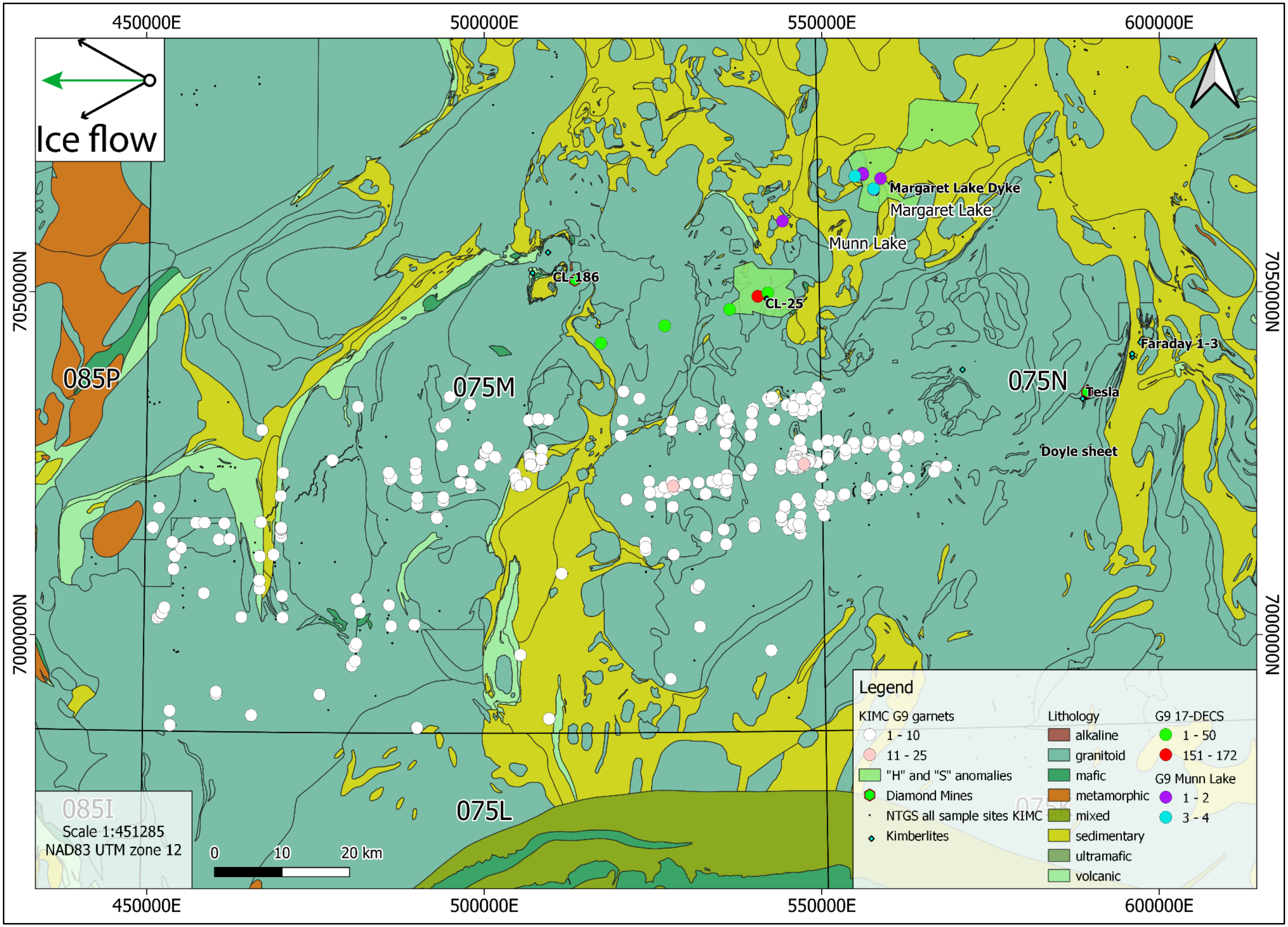

Figure 3.22: G9 garnet distribution in the southeastern Slave Province for 17-DECS (N=184, n=5), Munn Lake (N=13, n=5), and KIMC (N=564, n=354) with respect to “H” and “S” geophysical anomalies. (mineral chemistry data and bedrock geology from NWT Open File 2005-001, NWT Geoscience Office, 2018; Stubley and Irwin, 2019; Geophysical data and interpretation from CGG Canada Services Ltd., 2017; Mirza and Elliott, 2017)

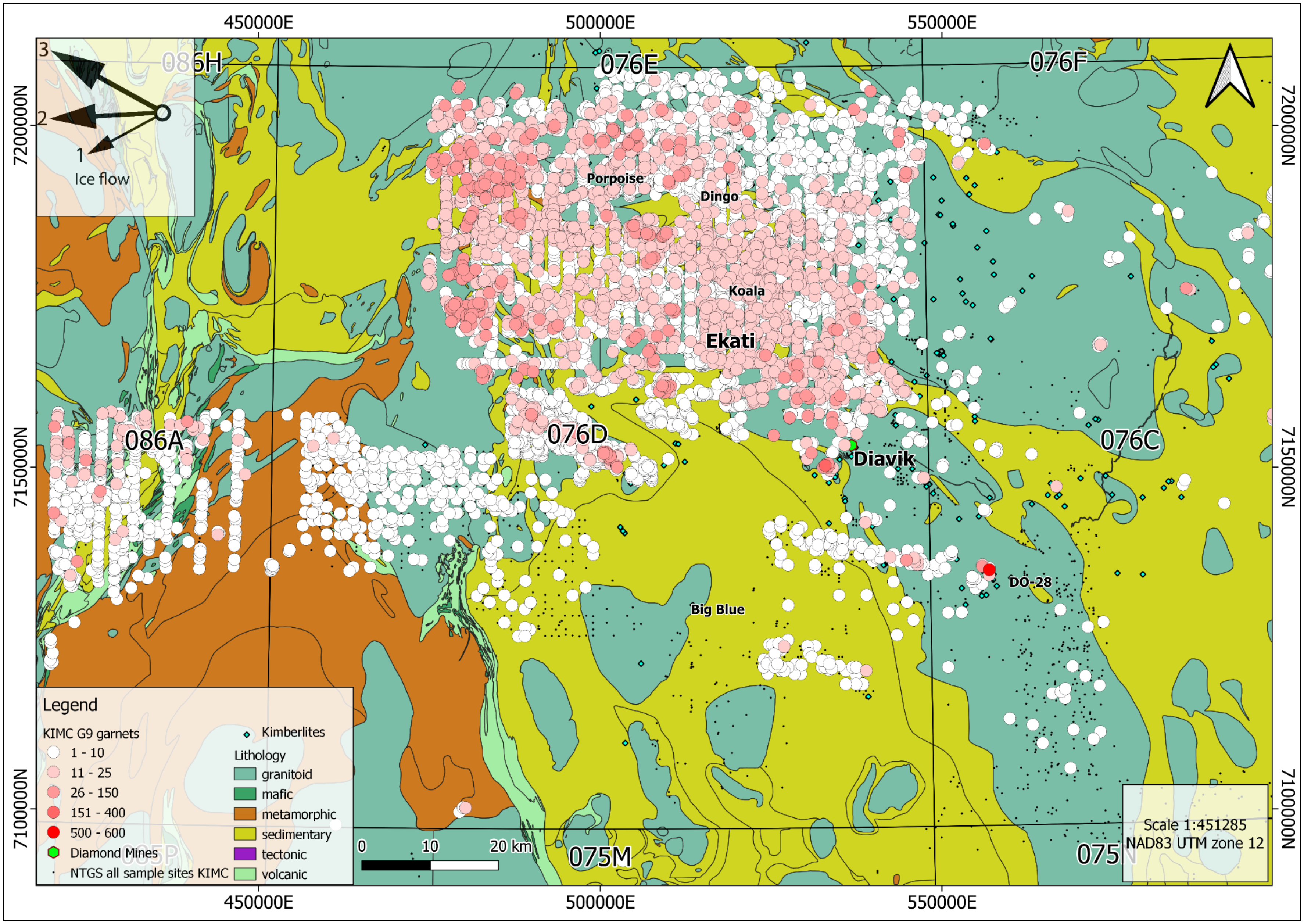

Figure 3.23: G9 garnet distribution in the central Slave Province from KIMC (N= 62,154, n=7897) (mineral chemistry data and bedrock geology from NWT Open File 2005-001, NWT Geoscience Office, 2018; Stubley and Irwin, 2019)

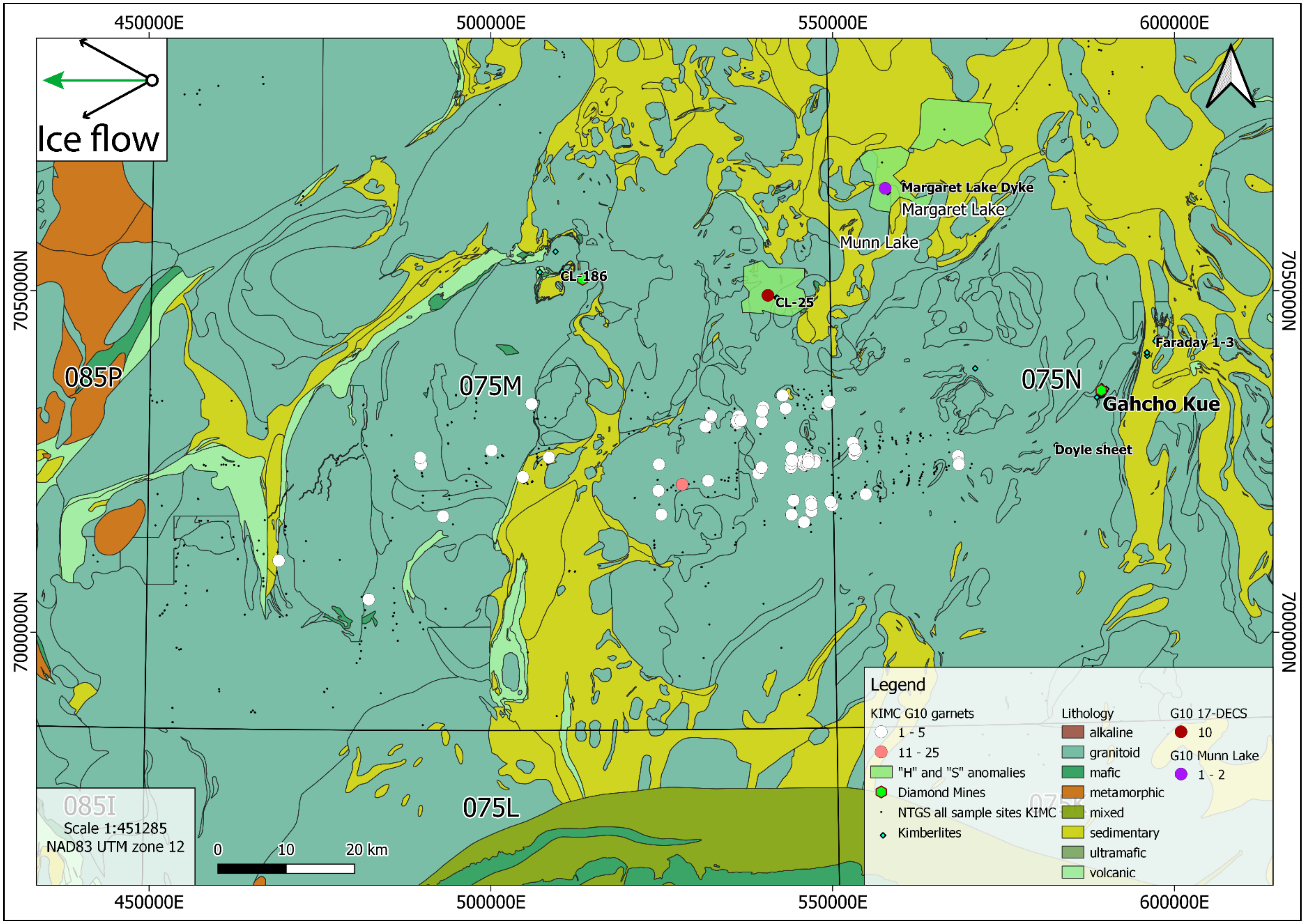

Figure 3.24: G10 garnet distribution in the southeastern Slave Province from 17-DECS (N=10, n=1) and KIMC (N=94, n=61) with respect to “H” and “S” anomalies. (mineral chemistry data and bedrock geology from NWT Open File 2005-001, NWT Geoscience Office, 2018; Stubley and Irwin, 2019; Geophysical data and interpretation from CGG Canada Services Ltd., 2017; Mirza and Elliott, 2017)

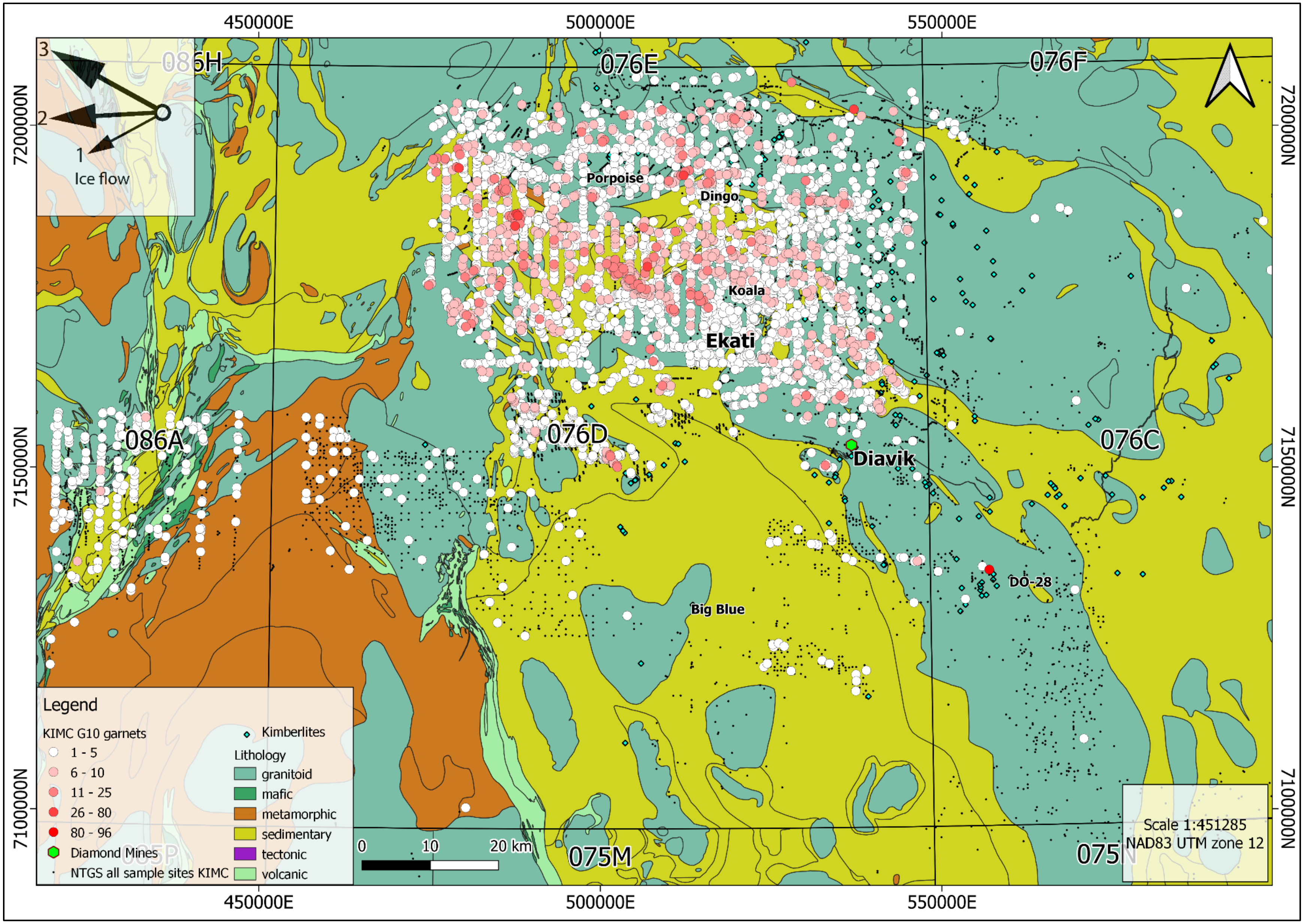

Figure 3.25: G10 garnet distribution in the central Slave Province from KIMC (N=13,932, n=4340) (mineral chemistry data and bedrock geology from NWT Open File 2005-001, NWT Geoscience Office, 2018; Stubley and Irwin, 2019)

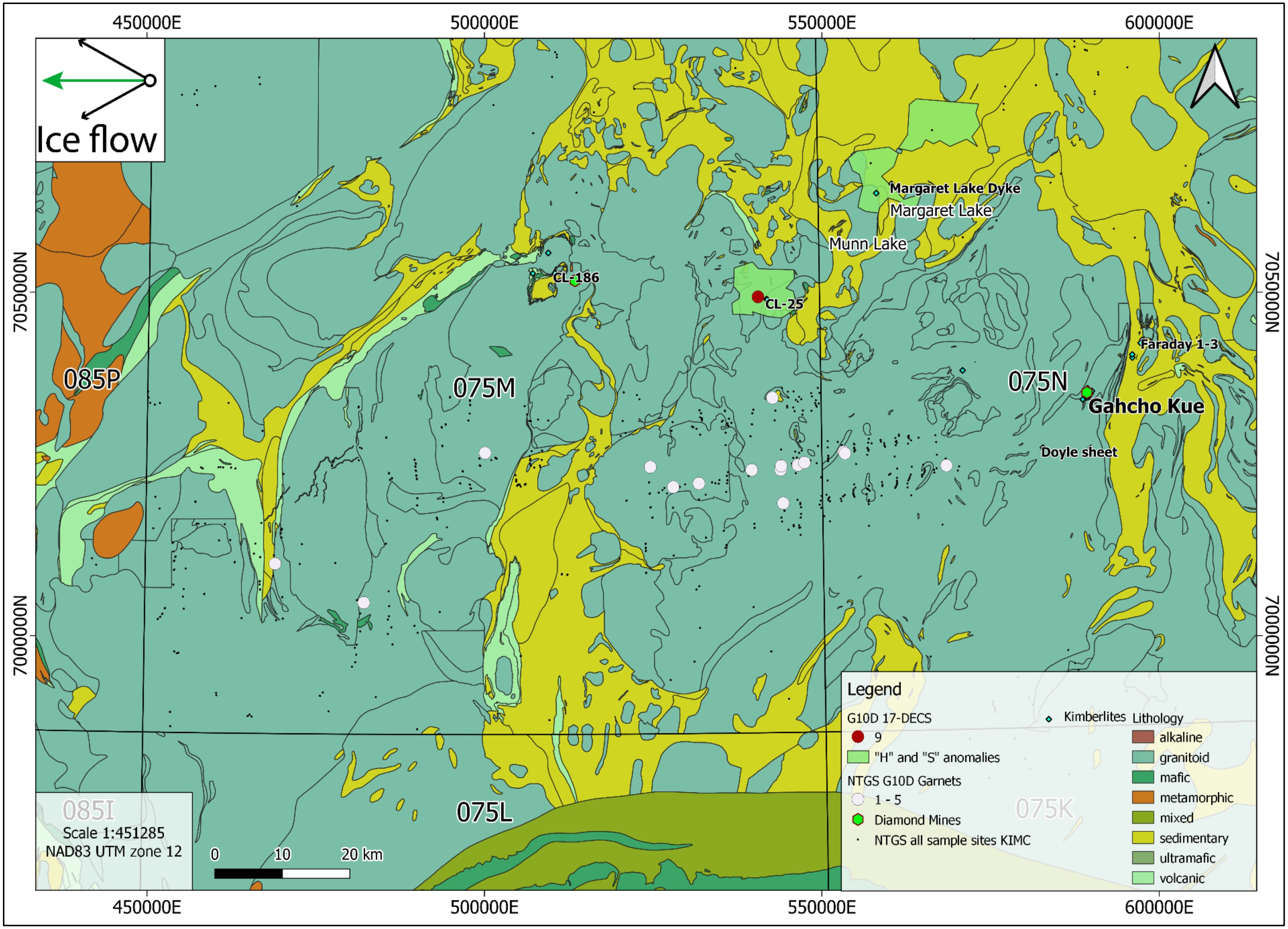

Figure 3.26: G10D garnet distribution in the southeastern Slave Province from 17-DECS (N=9, n=1) and KIMC (N=20, n=15) with respect to “H” and “S” anomalies. (mineral chemistry data and bedrock geology from NWT Open File 2005-001, NWT Geoscience Office, 2018; Stubley and Irwin, 2019; Geophysical data and interpretation from CGG Canada Services Ltd., 2017; Mirza and Elliott,

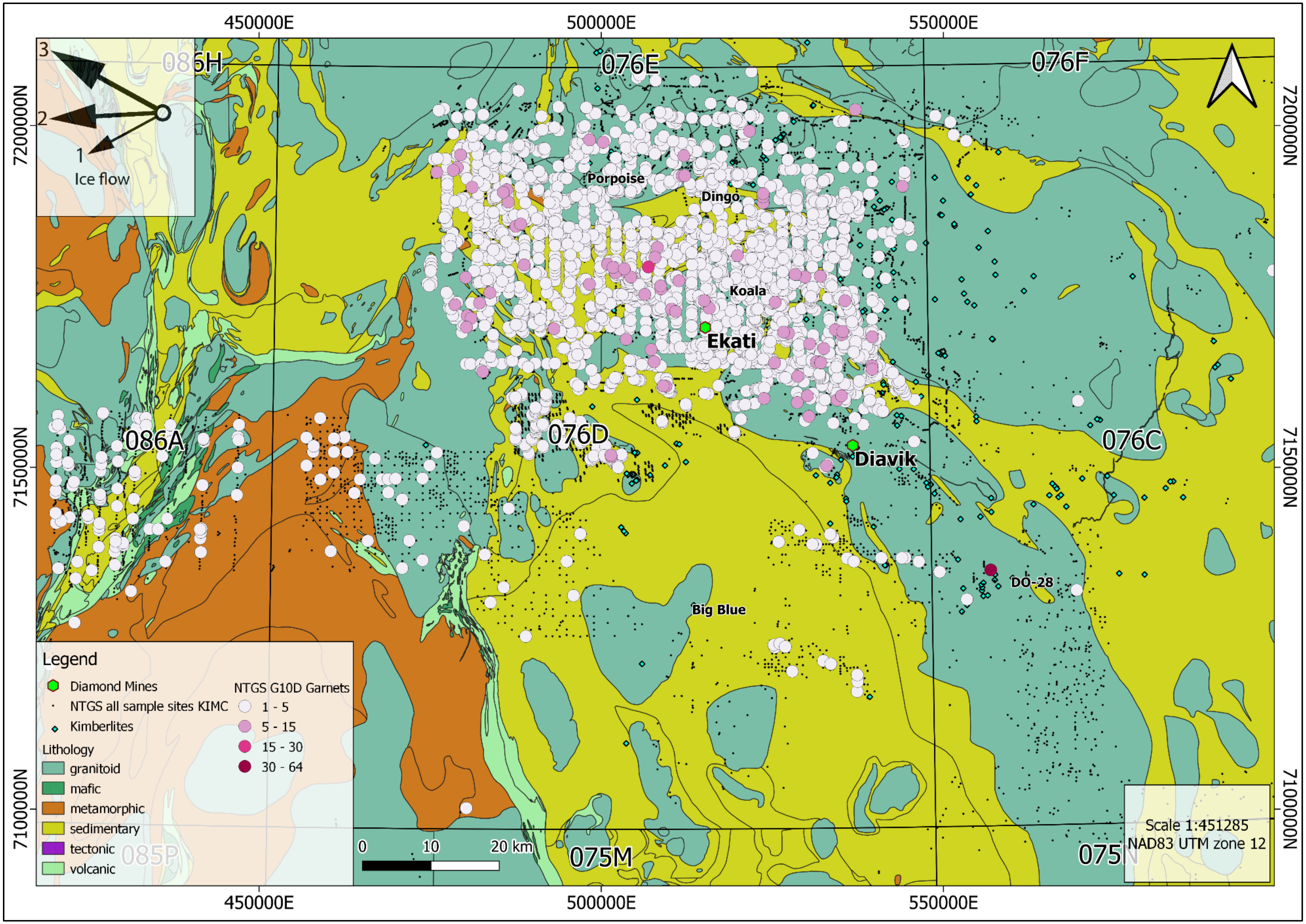

Figure 3.27: G10D garnet distribution in the central Slave Province from KIMC (N= 4861, n=2540) (mineral chemistry data and bedrock geology from NWT Open File 2005-001, NWT Geoscience Office, 2018; Stubley and Irwin, 2019)

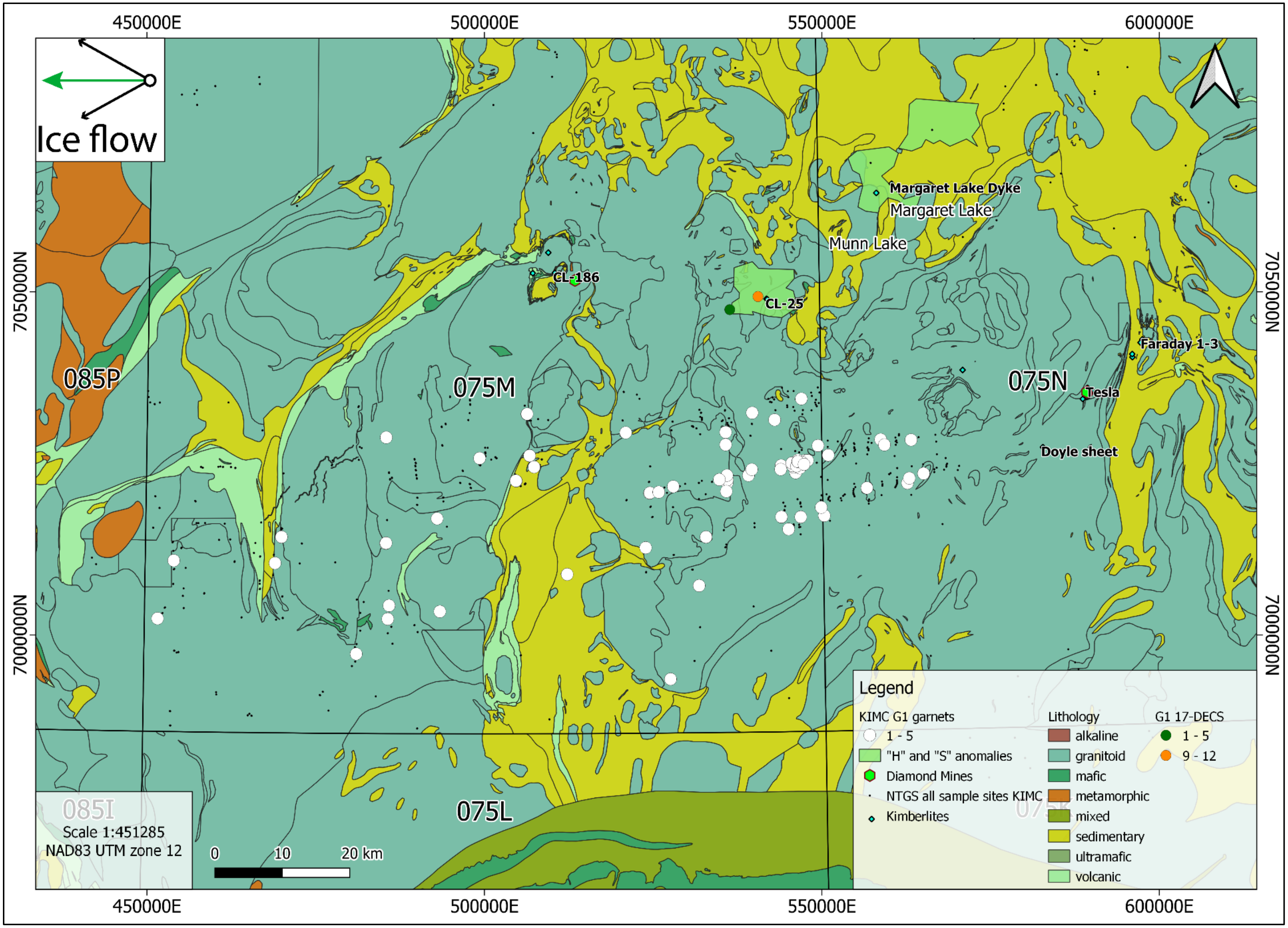

Figure 3.28: G1 garnet distribution in the southeastern Slave Province from 17-DECS (N=13, n=2) and KIMC (N=101, n=81) with respect to “H” and “S” anomalies. (mineral chemistry data and bedrock geology from NWT Open File 2005-001, NWT Geoscience Office, 2018; Stubley and Irwin, 2019; Geophysical data and interpretation from CGG Canada Services Ltd., 2017; Mirza and Elliott, 2017)

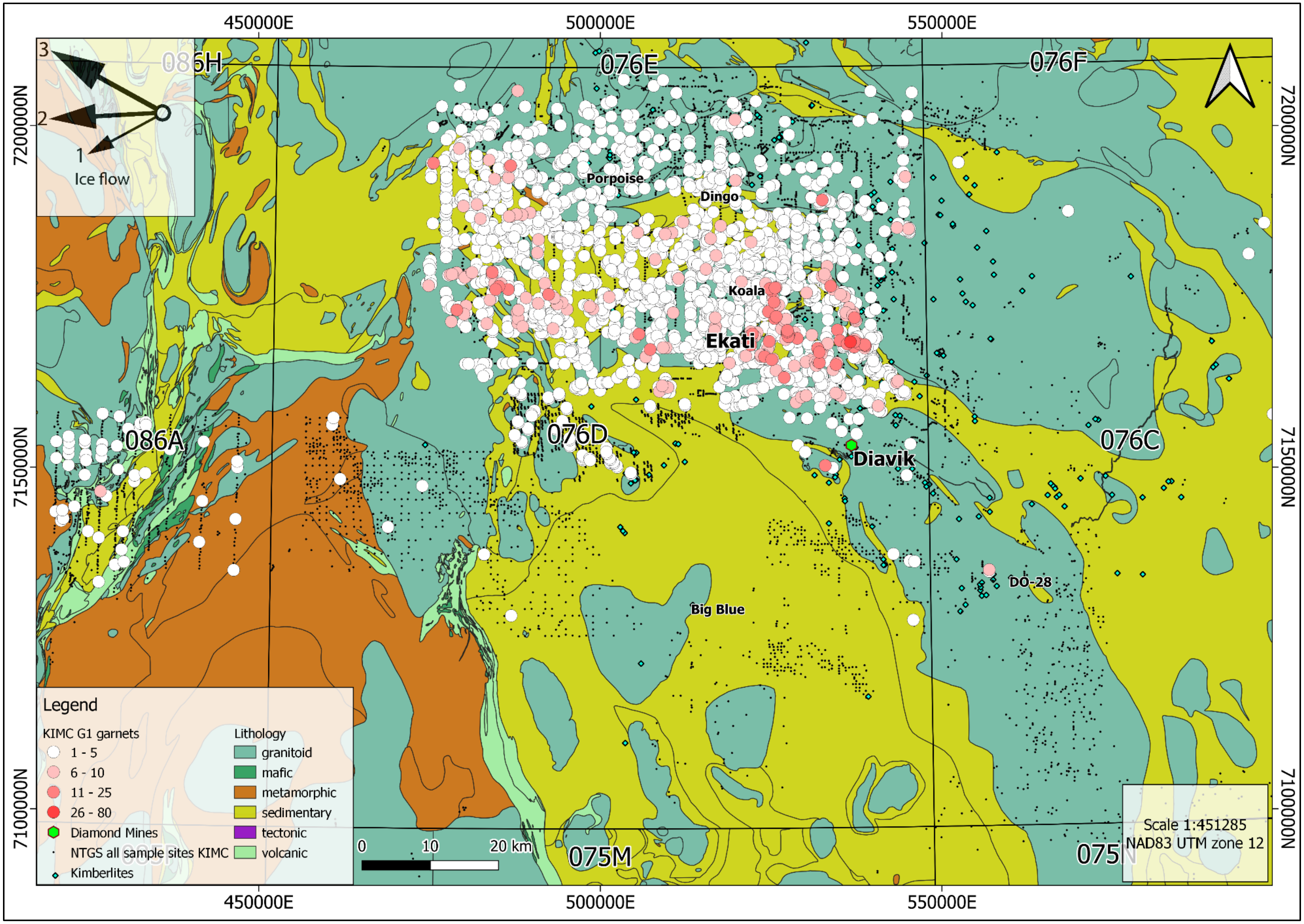

Figure 3.29: G1 garnet distribution in the central Slave Province from KIMC (N=5404, n=2244) (mineral chemistry data and bedrock geology from NWT Open File 2005-001, NWT Geoscience Office, 2018; Stubley and Irwin, 2019)

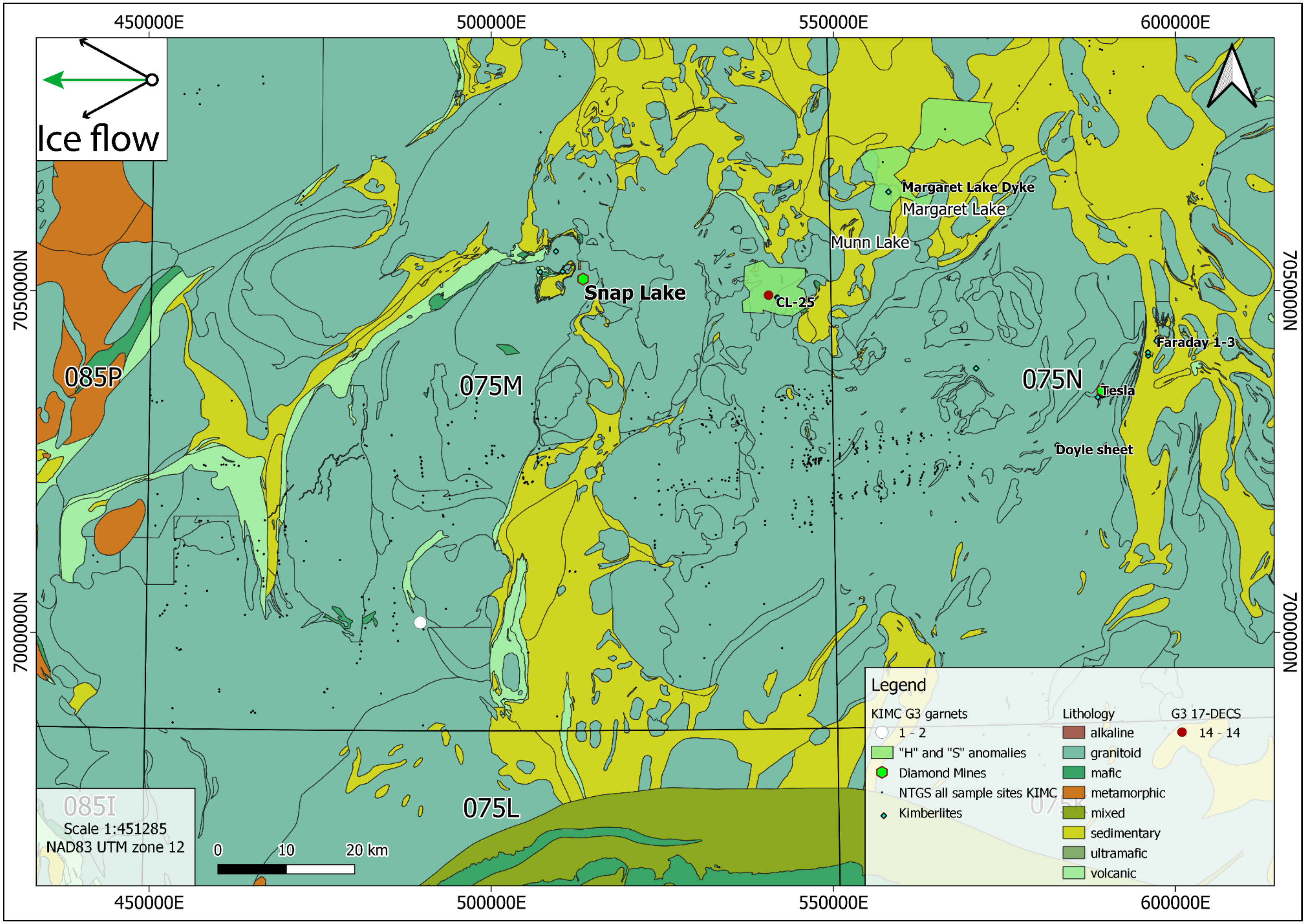

Figure 3.30: G3 garnet distribution in the southeastern Slave Province from 17-DECS (N=14) and KIMC (N=1, n=1) with respect to "H" and "S" anomalies. (mineral chemistry data and bedrock geology from NWT Open File 2005-001, NWT Geoscience Office, 2018; Stubley and Irwin, 2019; Geophysical data and interpretation from CGG Canada Services Ltd., 2017; Mirza and Elliott, 2017)

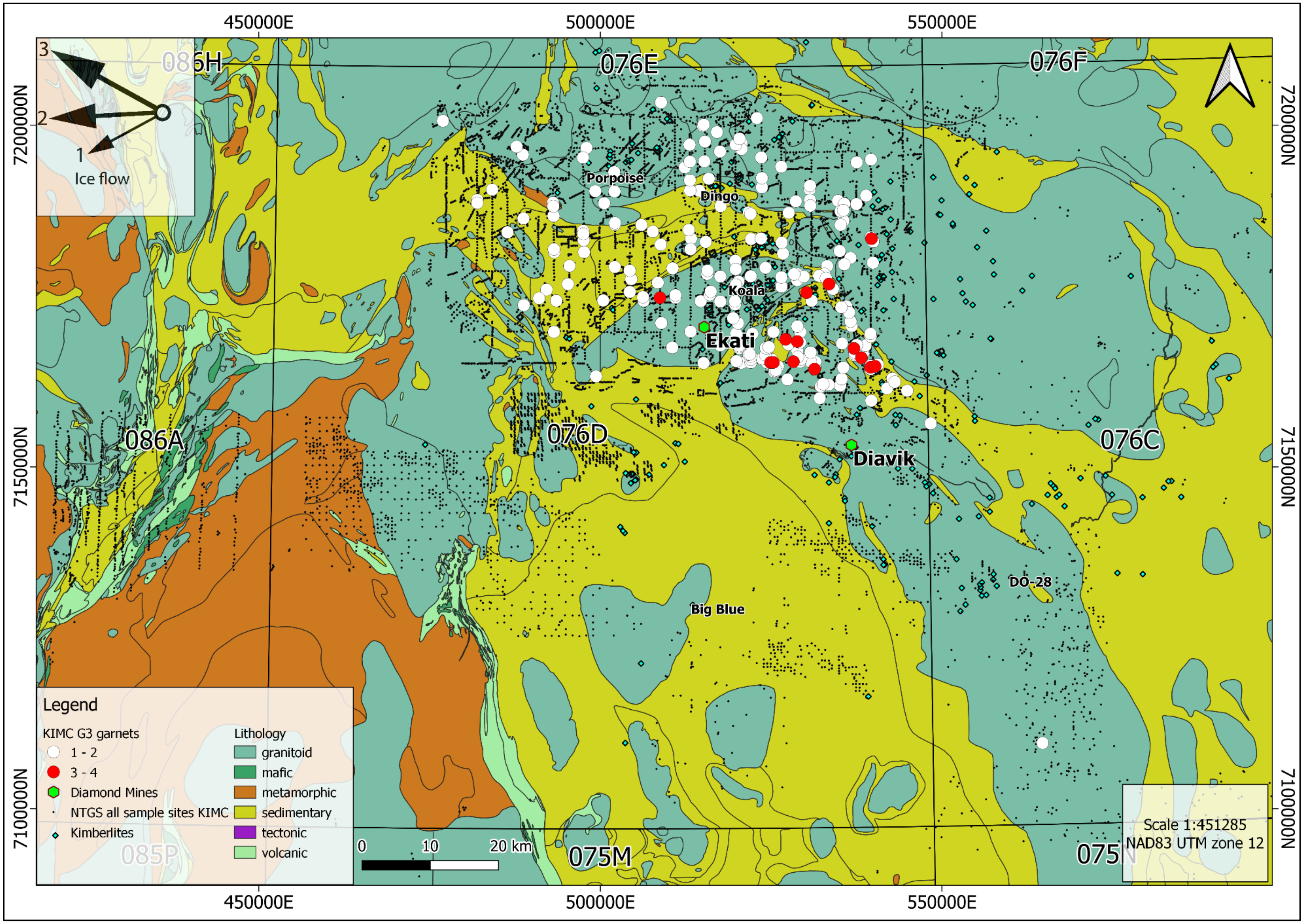

Figure 3.31: G3 garnet distribution in the central Slave Province from KIMC (N= 280, n=224) (mineral chemistry data and bedrock geology from NWT Open File 2005-001, NWT Geoscience Office, 2018; Stubley and Irwin, 2019)

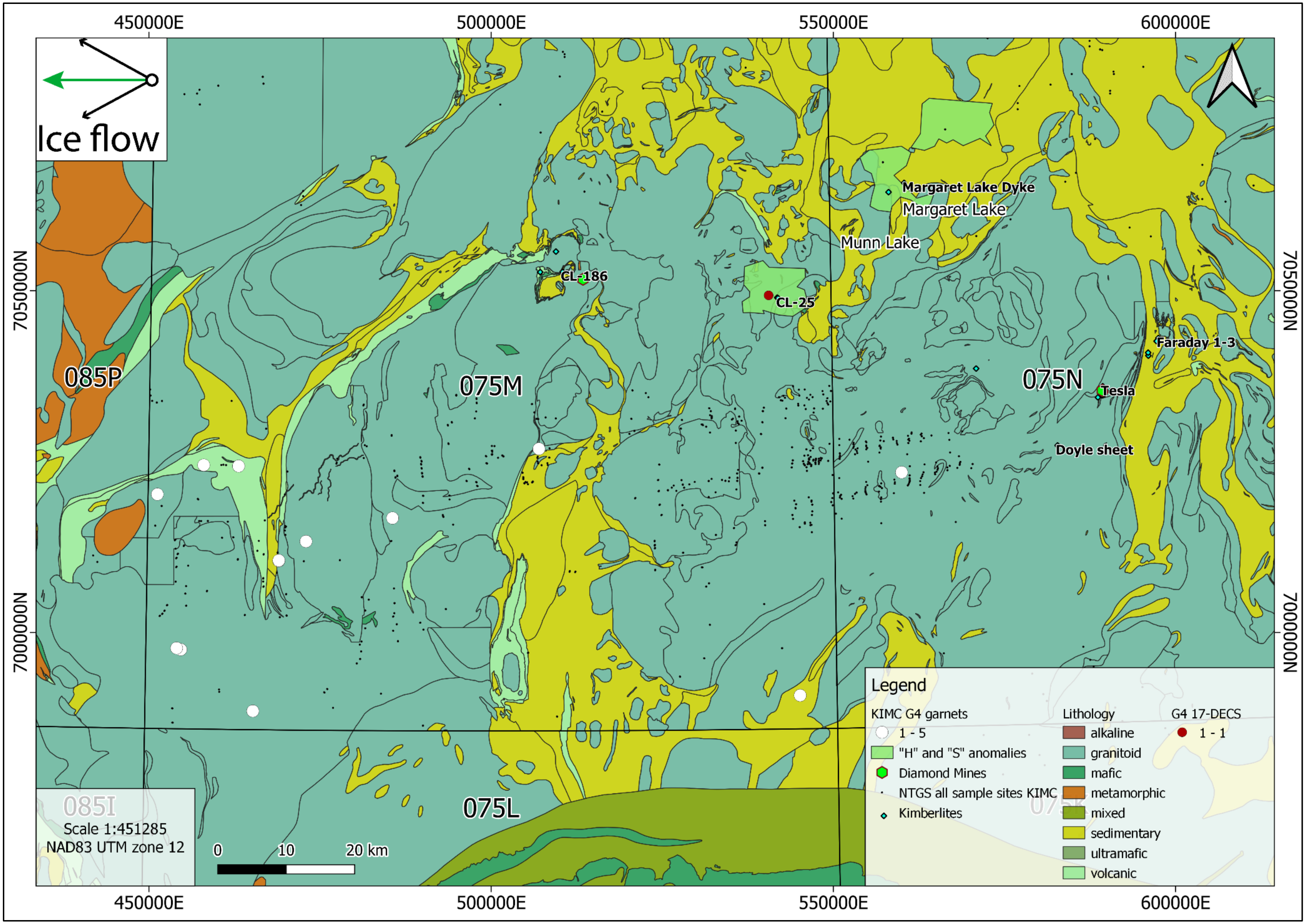

Figure 3.32: G4 garnet distribution in the southeastern Slave Province from 17-DECS (N=1, n=1) and KIMC (N=15 n=17) with respect to "H" and "S" anomalies. (mineral chemistry data and bedrock geology from NWT Open File 2005-001, NWT Geoscience Office, 2018; Stubley and Irwin, 2019; Geophysical data and interpretation from CGG Canada Services Ltd., 2017; Mirza and Elliott, 2017)

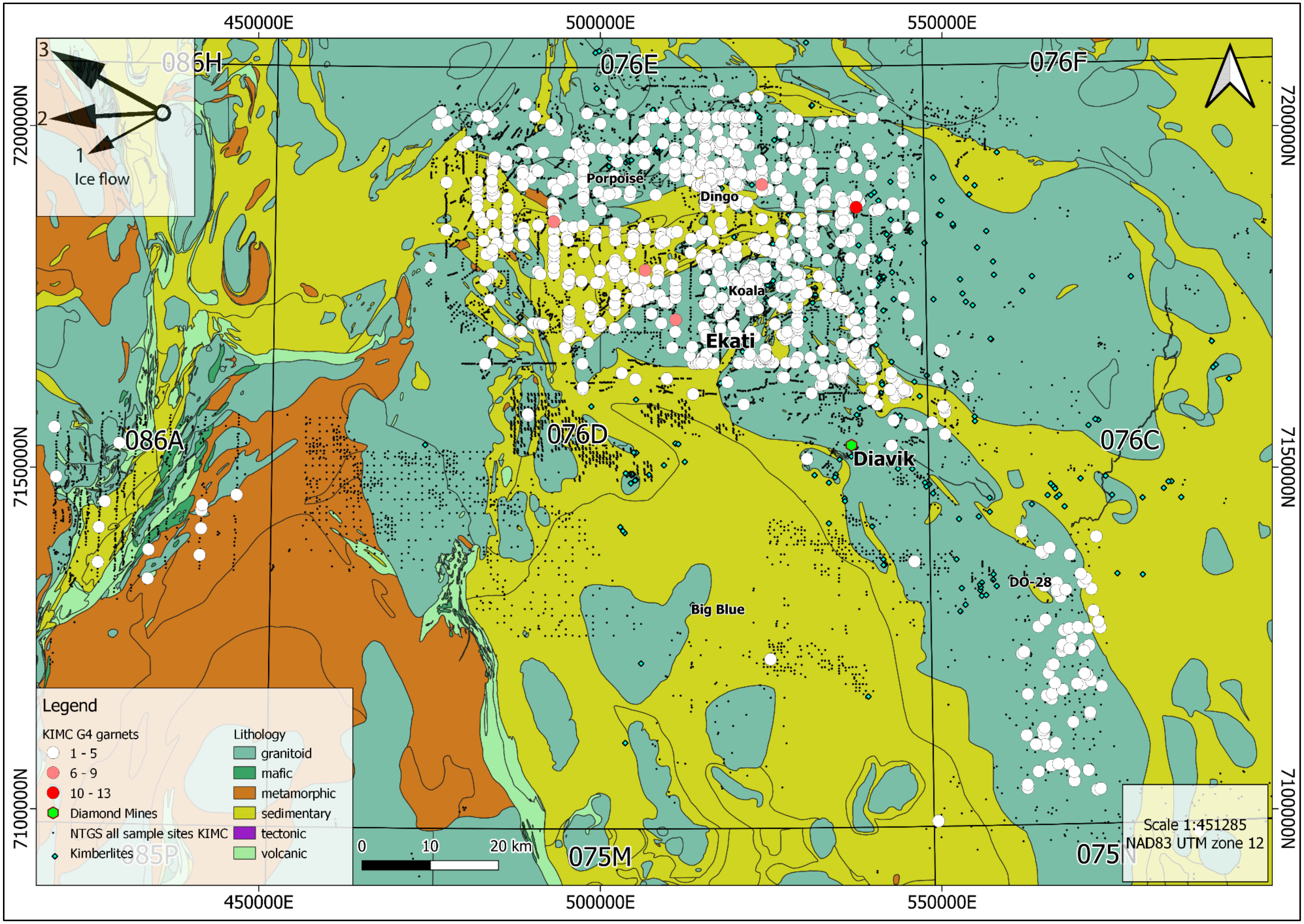

Figure 3.33: G4 garnet distribution in the central Slave Province from KIMC (N= 1128, n=826) (mineral chemistry data and bedrock geology from NWT Open File 2005-001, NWT Geoscience Office, 2018; Stubley and Irwin, 2019)

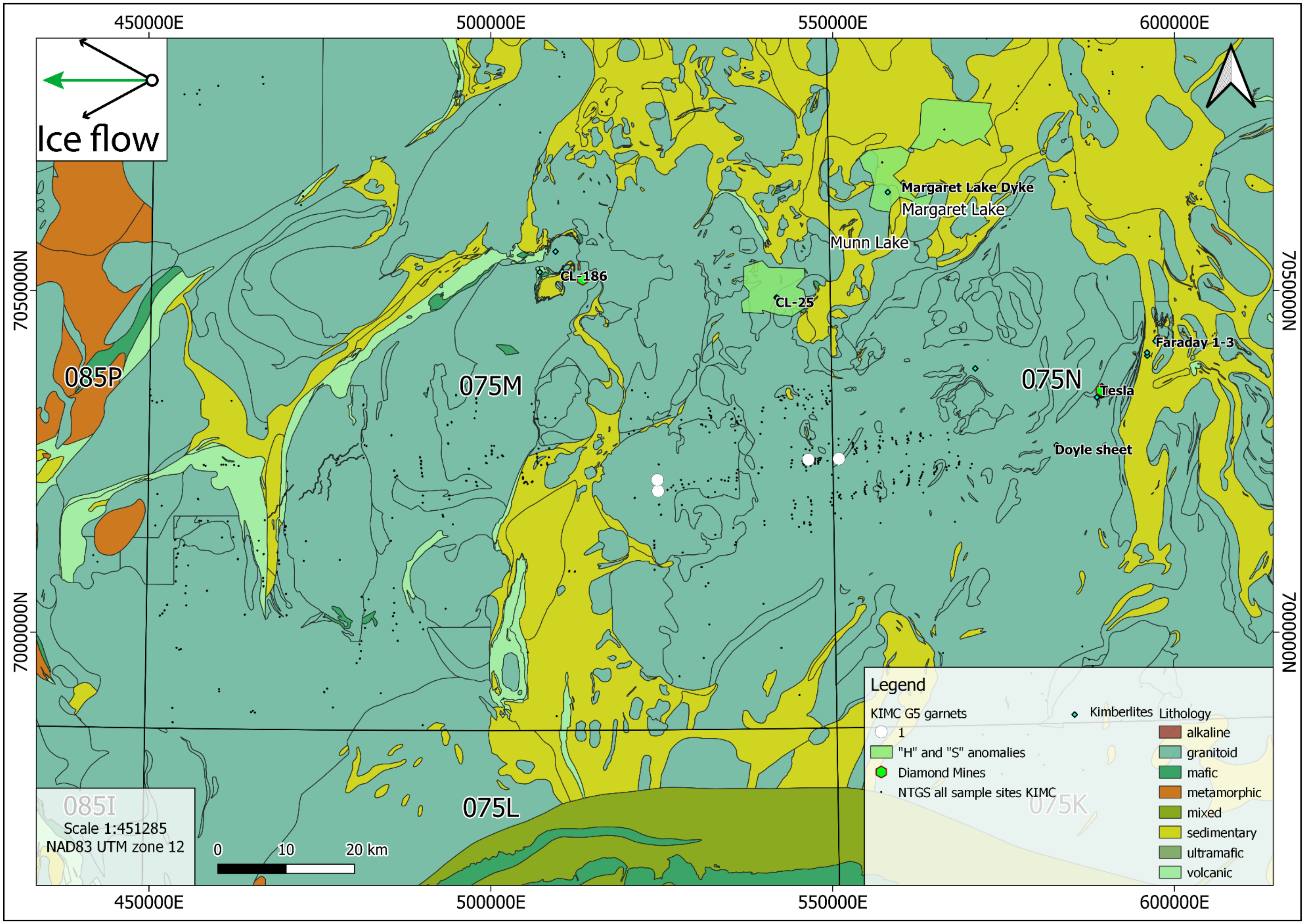

Figure 3.34: G5 garnet distribution in the southeastern Slave Province from KIMC (N=4, n=4) with respect to “H” and “S” anomalies. (mineral chemistry data and bedrock geology from NWT Open File 2005-001, NWT Geoscience Office, 2018; Stubley and Irwin, 2019; Geophysical data and interpretation from CGG Canada Services Ltd., 2017; Mirza and Elliott, 2017)

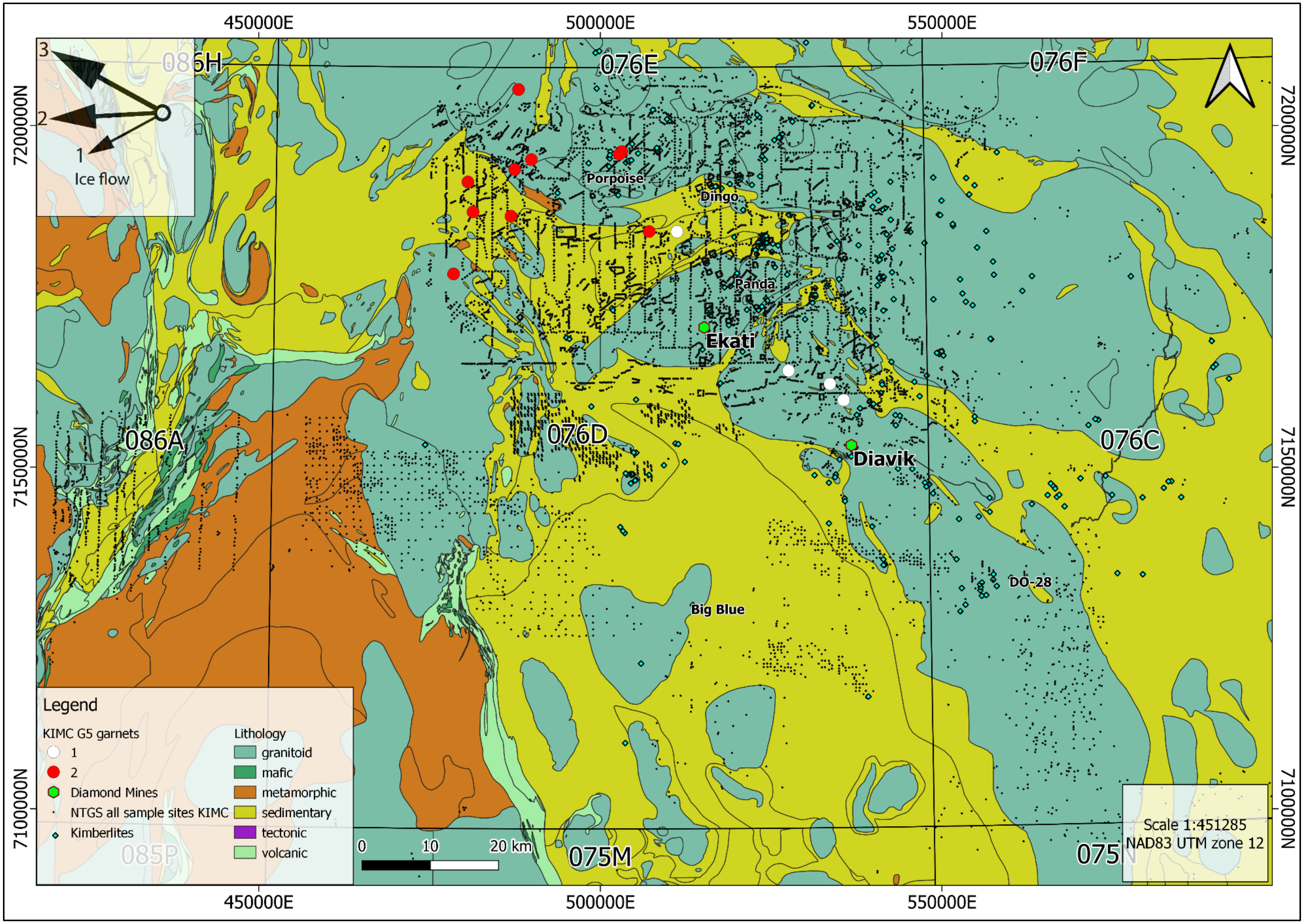

Figure 3.35: G5 garnet distribution in the central Slave Province from KIMC (N= 34, n=15) (mineral chemistry data and bedrock geology from NWT Open File 2005-001, NWT Geoscience Office, 2018; Stubley and Irwin, 2019)

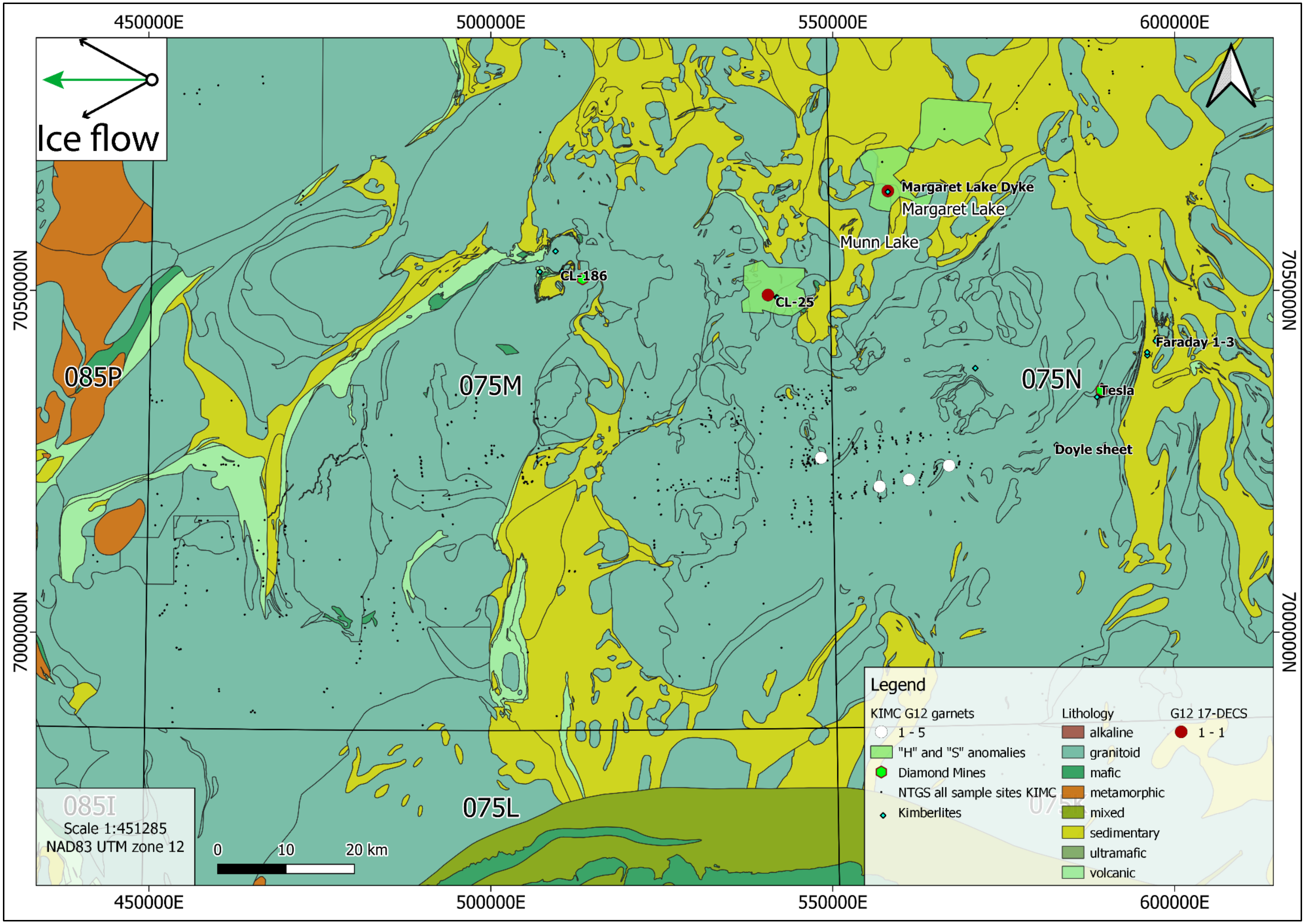

Figure 3.36: G12 garnet distribution in the southeastern Slave Province from 17-DECS (N=2, n=2) and KIMC (N=4, n=4) with respect to “H” and “S” anomalies. (mineral chemistry data and bedrock geology from NWT Open File 2005-001, NWT Geoscience Office, 2018; Stubley and Irwin, 2019; Geophysical data and interpretation from CGG Canada Services Ltd., 2017; Mirza and Elliott, 2017)

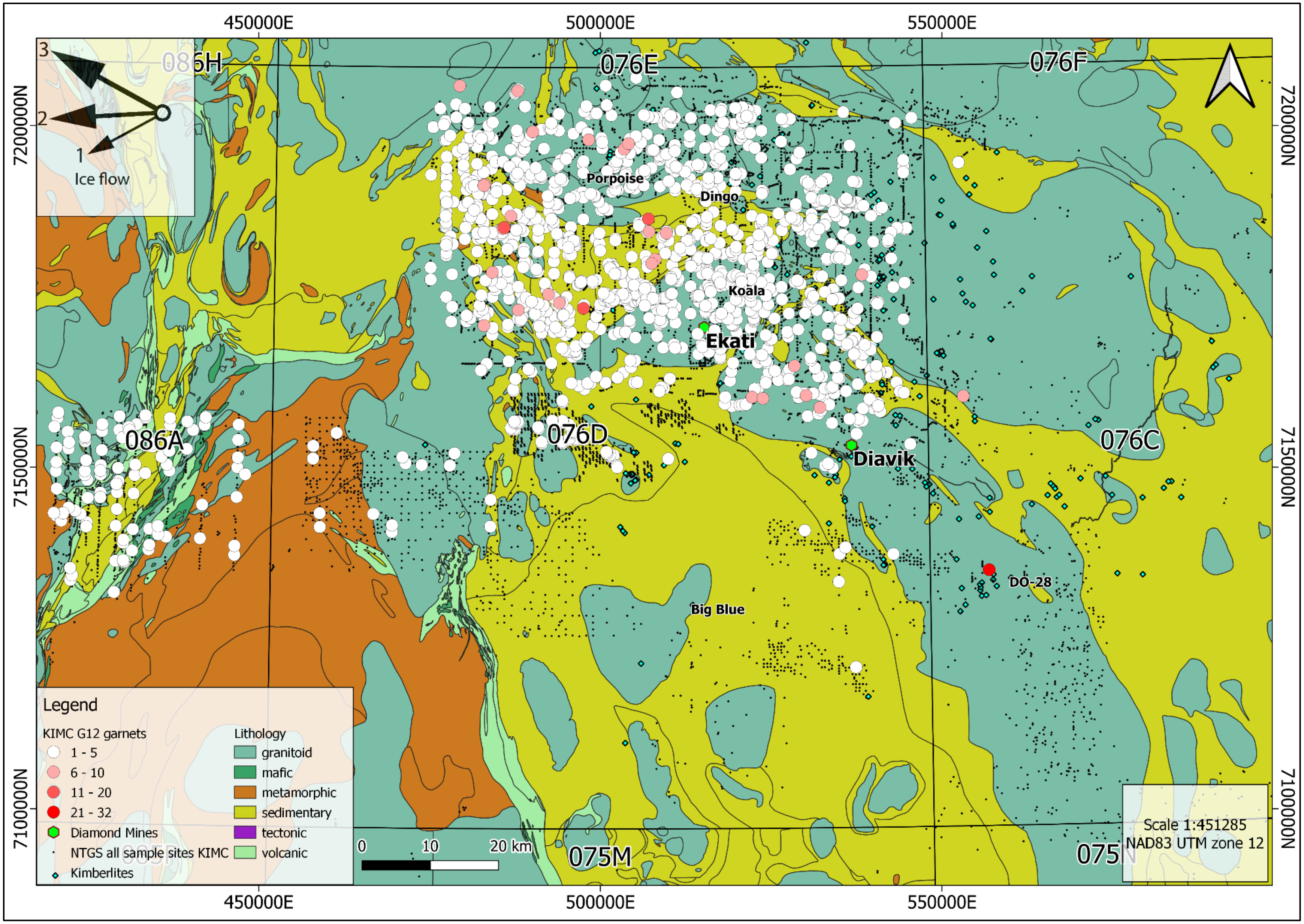

Figure 3.37: G12 garnet distribution in the central Slave Province from KIMC (N= 2040, n=1255) (mineral chemistry data and bedrock geology from NWT Open File 2005-001, NWT Geoscience Office, 2018; Stubley and Irwin, 2019)

Sodium content of garnet can be an exploration tool for diamonds, as the garnets in most diamond-bearing eclogites contain >0.07 wt. % Na_2O (Sobolev and Lavrent'ev, 1971; McCandless and Gurney, 1989; Schulze, 2003; Grütter et al., 2004). Eclogitic garnet according to the classification scheme of Grütter et al. (2004) is a G3 garnet. However, Grütter et al. (2004) have proposed the use of Na_2O content in the classification of G3, G4, and G5 garnets to indicate diamond-facies websteritic, pyroxenitic and eclogitic garnet compositions. In this study, we use Grütter et al.'s (2004) classification for G3, G4, and G5 garnets in order to create regional maps displaying the distribution of "diamond-facies" eclogitic, pyroxenitic and websteritic garnets (Figure 3.38).

Garnet classified as G3 and G4 from the 17-DECS sample suite contained 0 wt. % (Na contents were below detection limit) Na_2O. Garnet classified as G3, G4, and G5 from the NTGS dataset were found to contain little (0.07 wt. %) to no (0 wt.%/LOD) Na_2O in the southern Slave Province, and as a result not meeting the diamond-facies criteria. In the northern Slave Province G3, G4, and G5 garnets were found to contain between 0.07 wt. % and 2.14 wt. % Na_2O (Figure 3.38).

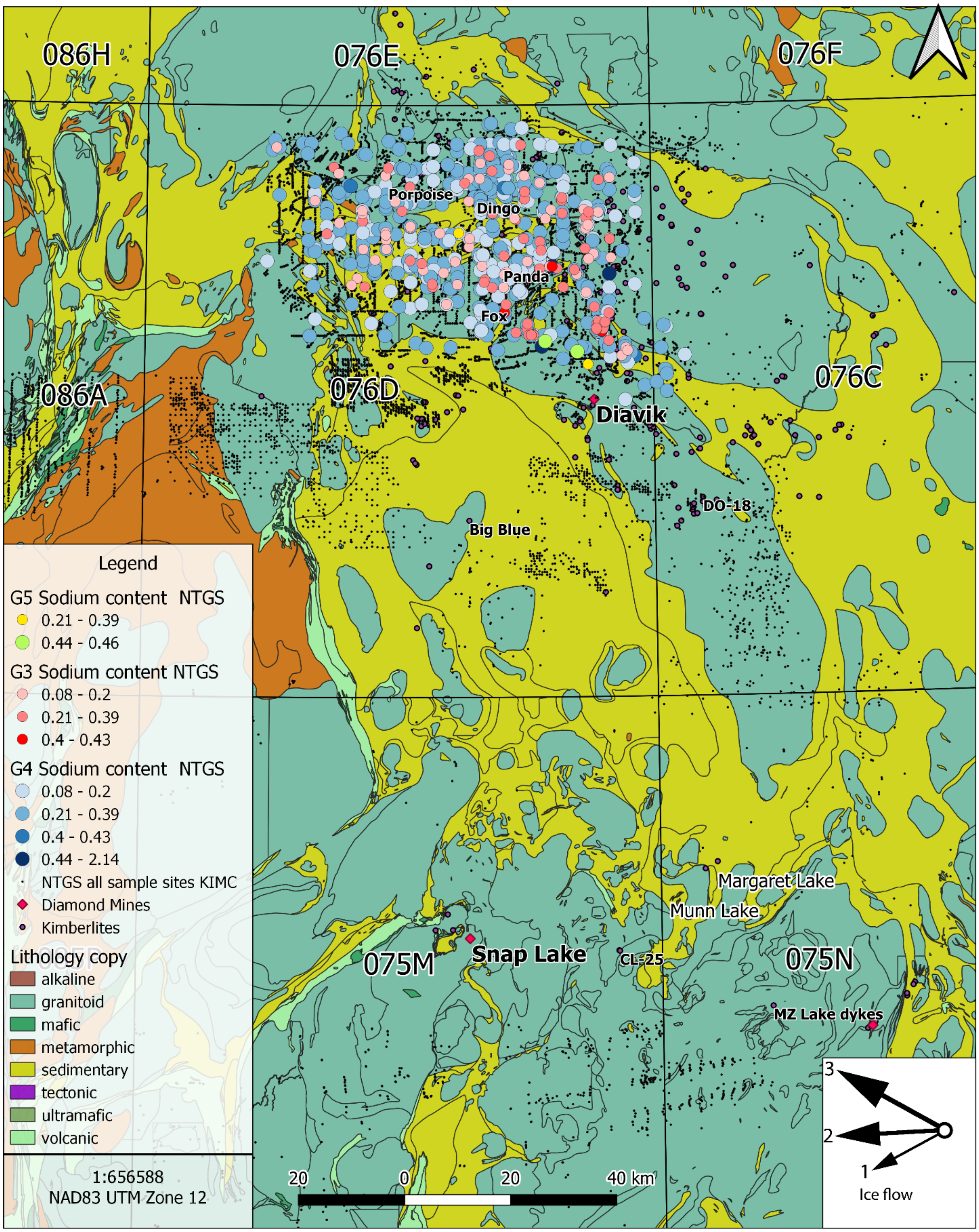

Figure 3.38: Na_2O wt % content of G3, G4 and G5 garnets in surficial sediments in the Slave Province. Higher concentrations are maximum Na_2O wt % of samples analyzed. (surficial data from NWT Open File 2005-001, NWT Geoscience Office, 2018).

3.5 KIM Size and grain shape in 17-DECS samples

KIMs were most abundant in the 0.25-0.50 mm HMC fraction (A) of till sample 17-DECS-013, as compared to the 0.5-1.0 mm and 1-2 mm HMC fractions. Garnets in till sample 17-DECS-013 were fragmented and displayed well preserved surface textures. No kelyphitic rims were observed on any garnet grains. Chromite recovered from 17-DECS-013 is generally euhedral to subhedral and octahedral in shape (Figure 3.39). Garnet recovered from sample 17-DECS-013 is fragmented and anhedral but has well preserved surface textures such as orange peel texture (McClenaghan and Kjarsgaard, 2007) on G9, G10 and G3 garnets. Some G9 garnets display sculpting features similar to those reported by Nowicki et al., (2007, see their Figure 3C) that they concluded were the product of crystallographically-controlled grain dissolution (Figure 3.39).

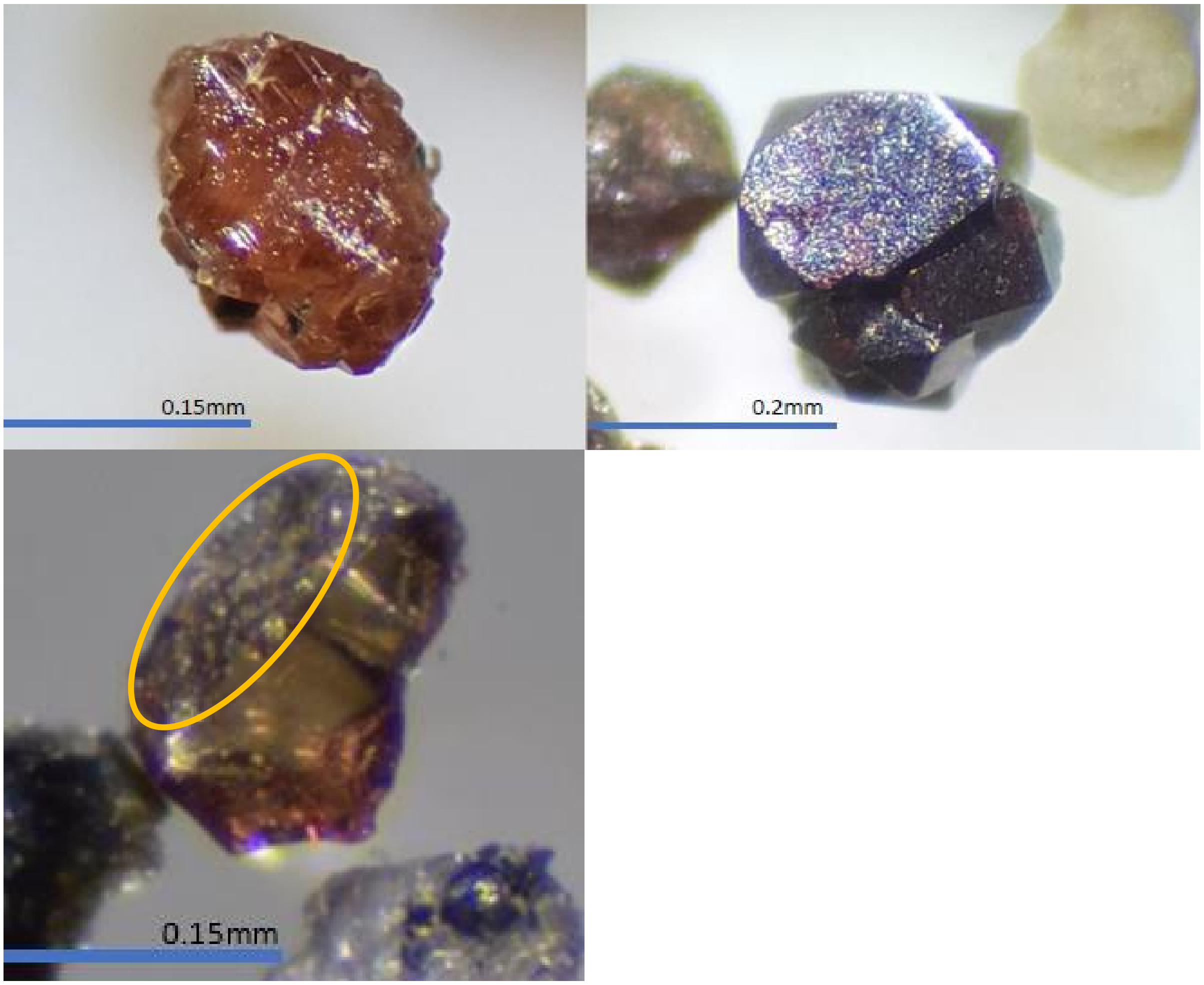

Figure 3.39: (Top left) Orange garnet with “sculpted” surface believed to be a product of crystallographically controlled dissolution in kimberlite. (Top right) Euhedral octahedral chromite. (Bottom left) Orange garnet with conchoidal fracture and sub-kelyphite orange-peel texture (circle). Grains from till sample17-DECS-013.

Chapter 4: Discussion

There is significant spatial variability in the amount of data collected from the north and south regions of the Slave Province, but there is also variability in which indicator minerals are present in surficial sediments and in their relative abundances. The variability in KIM abundances and presence could be a product of said sampling disparity, however, other possibilities will be discussed. Addressing this disparity in data is intended to create useful insight into exploration in the southern Slave Province regarding kimberlite potential. It is important to recall the KIM counts for each sample site have not been normalized to a 10 kg sample, and that each sample site is inferred as 1 sample due to identical coordinates. These samples are also subject to biases that result from the data that each exploration company chooses to report. There is no ideal way to standardize these data into more meaningful results and interpretations are therefore to be taken with moderate skepticism. This study is an assessment of the value of and geological insights that can be gained from KIM chemistry data for the region, and whether or not the currently available KIM chemistry provides insights that are similar to previous findings reported for KIMs in the Slave Province.

Data used in this study is part of a NTGS regional compilation KIMC dataset. Additional data used in this study were obtained from till samples collected during the 2017 field program for the 17-DECS sample series. The confirmed KIM grains from these till samples were analyzed using the LA-ICP MS. Larger quantities of data were obtained from the NTGS open data hub which has compiled a large set of kimberlite and mineral deposit related data of the Northwest Territories. Data used from the KIMC database in the NTGS open data hub included a large regional database of over 100,000 indicator minerals with chemistry from over 14,000 inferred sample sites. Data from the NTGS and 2017 field study were used to assess garnet chemistry and G-number classification in order to compose regional maps of garnet distributions, in addition to regional maps produced using chromite, ilmenite, and olivine data from the NTGS. These maps provide insight to the nature of indicator mineral distribution and quantity in the Slave Province.

4.1 Garnet

Garnet is the most abundant kimberlite indicator mineral recovered from exploration surficial sediment sampling in the Slave Province. The high concentration of KIM garnet in sediment samples is a reflection of the high abundance of garnet in the local kimberlites, its ability to survive long distances of glacial transport, and its distinct visual characteristics (colour, surface features) that make grain identification in HMC straightforward. The physically robust nature of garnet in comparison to Cr-diopside and olivine (but not ilmenite or chromite) makes garnet an ideal mineral for tracing kimberlite glacial dispersal.

A general trend in modern diamond exploration is differentiating garnet as eclogitic or peridotitic, based on the chemical characteristics of garnets that occur as inclusions in diamond. In this study, the classification scheme of Grütter et al. (2004) was used to avoid vagueness associated with the eclogitic or peridotitic garnet classifications.

4.1.1 Garnet classification

Recently, Hardman et al. (2018a) presented a new classification scheme for mantle-derived garnets with a reduced error rate as compared to Schulze (2003). In this study,chemical data for over 100,000 garnet grains were processed using the classifications of both Grütter et al. (2004) and Hardman et al. (2018a). Hardman et al. (2018a) advises using the classes of Grütter et al. (2004) for classification of G3 and G4 garnets. Eclogitic G3 garnets and eclogitic, pyroxenitic, and websteritic G4 garnets are reliable kimberlite indicators, however, when plotted on the biplot of Hardman et al. (2018a), they plot within 10% confidence interval of crustal garnet rendering them obsolete (Chapter 7:Appendix III). Garnets classified as G1, G9, G10, and G12 assessed using the discrimination plot of Hardman et al. (2018a), plot within the mantle field and the 10% confidence interval for crustal garnet (Chapter 7:Appendix III). Using the classification of Grütter et al. (2004), G1, G9, G10, and G12 garnets are considered to be of mantle origin. However in the classification of Grütter et al. (2004), their association to diamond and kimberlite is indicated, whereas in the classification of Hardman et al. (2018a) there is no distinction between mantle sources. The classification of mantle vs crustal garnets presented by Hardman et al. (2018a) is accurate, however its usefulness in diamond exploration is limited, and has the potential to create overconfidence when used exclusively. The classification scheme of Grütter et al. (2004) addresses the multivariate nature of the classification problem and the diversity of chemical, physical and lithological environments in which mantle garnets and diamond occur.

Garnets plotted on the Hardman et al. (2018a) biplot as G-number classified grains (Grütter et al., 2004) are grouped based on NTS map sheet locations (Appendix III). This helps further visualize the distribution of mantle vs. crustal garnets in the Slave Province with respect to both classification schemes. The 076D map sheet is host to Diavik and Ekati, and the HDSA, resulting in a dense data population accounting for over 90% of NTGS garnet data (Table 4.1).

Table 4.1: Total garnet percent totals of each map sheet.

075N/M		076C		076D		086A	
Total Garnets	Percent of Total	Total Garnets	Percent of Total	Total Garnets	Percent of Total	Total Garnets	Percent of Total
1575	1.57%	2322	2.31%	92029	91.73%	4396	4.38%
Total Garnets for map sheets listed: 100,322							

It is worth noting that samples collected for this study that were left unclassified by Grütter et al. (2004) plot within the mantle field of the discrimination biplot of Hardman et al. (2018a). However, the classification of garnets as mantle origin has no implications for exploration other than the possible indication the region has mantle source rock.

4.1.2 Garnet G-number distribution

Of significance to diamond exploration are Harzburgitic G10 garnets. These garnets are often considered to be the standard for which diamond potential is determined (Grütter et al., 2004). There is an implied association of graphite and diamond with low-Ca G10 garnet compositions, making the use of Cr-saturation and MnO content imperative for assessing their diamond association (Grütter et al., 2004). Garnets which meet more specified criteria for diamond-facies are suffixed by “D”. Concentrations of G10D garnets are lower in the southern Slave Province than in the north, likely a result of the contrast in sample density (Figure 4.1, Figure 4.2). The concentration of G10D garnets at the sample location 17-DECS-013 is high compared to other 17-DECS samples and other surficial sediment samples in the NTGS database in the southern Slave Province.

Lherzolitic G9 garnets are the most common garnets recovered in surficial sediments in the Slave Province. The statistical association of G9 garnets and diamond is weak according to Grütter et al, given their high abundance as xenocrysts in diamondiferous kimberlites (Grütter et al., 2004). G9 garnets in the southern Slave Province appear to contribute to a possible kimberlite indicator mineral dispersal train (Figure 4.3, Figure 4.5). The abundance of G9 garnet in the southern Slave Province is lower than that of the northern Slave Province. The distribution of G9 garnets appears to follow a westward ice-flow direction, supporting the interpretation of the most recent glacial advance in the southern Slave Province being west. However, the distribution of these G9 garnets follow the sample site location pattern creating a biased view of the distribution. Although these G9 garnets appear to follow a westward ice flow direction, this is the product of sampling bias.

Low-Cr megacryst G1 garnets may occur in high relative abundance in certain kimberlites, but they also occur in other mantle-derived magmatic rocks such as alnöites, and in certain alkali basalts (Grütter et al., 2004). Garnets that are classified as G1 using the scheme of Grütter et al. (2004) have no established association to diamond. Low-Cr megacryst garnets are more common in the southern Slave Province surficial sediments (>100 grains) relative to the abundance of other garnets present excluding G9 garnet. This abundance pattern could potentially reflect mantle composition during kimberlite ascent, further investigations would require comparison to garnets in kimberlites in the southern Slave Province.

Eclogitic G3 garnets are considered extremely important pathfinder minerals for diamond (Grütter et al., 2004). The concentration of G3 garnets in surficial sediments throughout the Slave Province is low (<295 grains between the central and southeastern Slave

Province, Table 4.2). This low abundance in sediment samples could be reflective of the G3 garnet content of the source kimberlites (ie., mantle composition during magma ascent), or a result of the garnet visual selection process during sediment sample picking. G3 garnets are generally orange-pink and resemble many non-kimberlitic garnets such as crustal almandine and therefore have the potential to be overlooked compared to orange-purple G9 and G10 garnets. Sample 17-DECS-013 has a high concentration of G3 garnets (14 grains) in comparison to the central Slave Province KIMC dataset (<5 grains per site) (Figure 4.1, Figure 4.2). This higher abundance could be reflective of variability in mantle composition and diamond potential of the southern Slave province or the improved ability to visually identify these orange-pink garnets as compared to 10 to 20 years ago when most of the surficial sediments samples in the database were examined.

Pyroxenitic, websteritic and eclogitic G5 and G4 garnets are the second least abundant garnet in the surficial sediment samples across the Slave Province. G5 garnets occur in sediment samples in four separate locations in the southern Slave Province. G4 garnets occur in fifteen locations as 1 to 2 grains in surficial sediment samples in the southern Slave Province (Table 4.2). These garnets are considered important in diamond exploration due to their known association with diamond (garnet inclusions in diamond) (Grütter et al., 2004). The presence of G4 and G5 garnets in surficial sediment samples could indicate a high diamond potential in the southern Slave Province.

The high density of garnets in the northern Slave Province reflects sample distribution, abundance of garnets in source kimberlites and glacial dispersal. There is also the potential that sample concentration per site is a product of sample overlap as data processing groups grain counts based on identical latitude and longitude and not necessarily one specific sample. However, the potential for till in the northern Slave Province to contain higher concentrations of indicator minerals is likely. The HDSA is located up-ice of several known and economic kimberlite in the youngest interpreted ice-flow direction (NW). Variations in garnet population is reflective of kimberlite or host rock concentrations. The contrast in garnet abundance between the north and south Slave Province is likely a function of the following factors: till sample density, kimberlite density, kimberlite mineralogy and relative KIM abundance.

Table 4.2: Comparison of the abundance of the different garnet types in terms of sample sites and grain counts in the central and southeastern Slave Province (zones as defined by Armstrong, 2003, **Error! Reference source not found.**) as identified in this study.

	KIMC grain counts			
	Central Slave Province		Southeastern Slave Province	
Garnet	**Sample sites (n)**	**Grains (N)**	**Sample Sites (n)**	**Grains (N)**
G1	2244	5404	81	101
G3	224	280	1	1
G4	826	1128	15	17
G5	15	34	4	4
G9	7897	62154	354	564
G10	4340	13932	62	94
G10D	2541	4861	15	20
G12	1255	2040	4	4

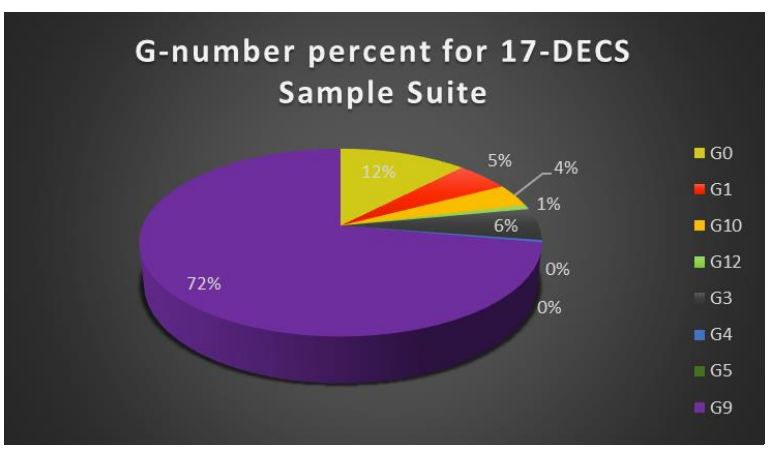

Figure 4.1: Pie plot of the relative abundances of the different garnet types in the twenty one 17-DECS till

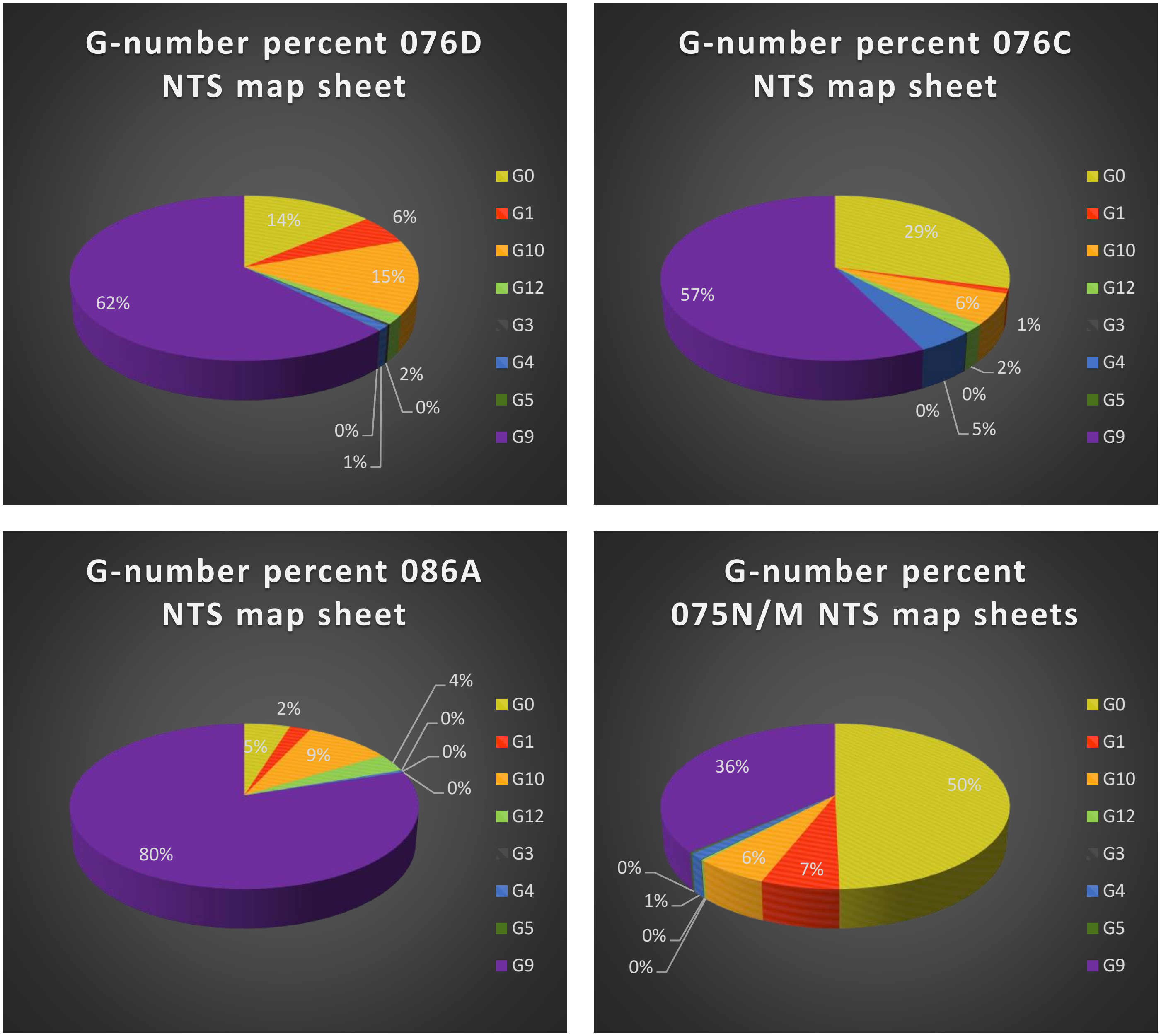

Figure 4.2: Pie plots of the relative abundances of the different garnet types in the surficial sediment samples in the NTGS database based on NTS map sheet.

4.1.3 Garnet dispersal trains

Armstrong (2003) identified several kimberlite dispersal trains trending southwest in the southern Slave Province region (Figure 4.3). It is important to note that sample distribution and mineral count data for these trains were plotted as is, using the data that was available in the NTGS dataset in 2003. G9 garnet data for surficial sediments examined in this study (Figure 3.23) plot in the middle sections of the known Kennady, Doyle, and a third unnamed dispersal train identified by Armstrong (2003) (Fig. 4.3, Figure 4.5). Note his Kennady dispersal train originates at Kennady Lake, and what is now known as the Gahcho Kué mine. G1 (Figure 3.29) and G10D (Figure 3.25) also help define the mid sections of the known dispersal trains.

Each of the 3 dispersal trains displays an increase of garnet concentration with increasing distance down-ice (west-southwest) from known kimberlites up-ice. This increase down ice can be typical of KIM glacial dispersal trains as a result of aggradational-decay (McClenaghan and Paulen, 2018). Samples used in this study are located at a minimum distance of 7 km down-ice from known kimberlite sources (e.g. the Doyle Sill). It appears that the 3 sample grids first report by Armstrong (2003) were planned to test the down-ice dispersal patterns of geophysical anomalies that were subsequently discovered to be kimberlites. There is no mineral chemistry data publicly available for sediment samples up-ice of known kimberlites in the southern Slave Province.

For the NTGS dataset, samples are local to distal (>15 km) from known kimberlites. Few to no samples with publicly available mineral chemistry are up ice of known kimberlite or anomalies. For these reasons, it is difficult to discern meaningful indicator dispersal interpretations in terms of KIM origins for the NTGS dataset.

Ice-flow history in the southern Slave Province is relatively simple with dominantly westward to WSW ice flow (Armstrong, 2003; Knight, 2018) (Figure 1.10), making predictions of indicator mineral dispersal potentially simpler than in the North Slave. Samples collected from the Ranch Lake kimberlite showed the dispersal train to be as wide as ~ 2 km at 20 km down-ice (McClenaghan et al., 2002). Widths of indicator mineral trains in the southern Slave Province are as wide as 3 km, with no well-defined boundaries due to the end of sample locations laterally. Increase in KIM concentration in the Ranch Lake dispersal train occurs over a distance of ~4 km from the kimberlite source (McClenaghan et al., 2002), while an increase in KIM concentration in the three dispersal trains discussed here are up to 8 km from source, but discontinuous in nature. It is difficult to discern whether this increase in indicator abundance down ice is a product of KIM being incorporated into till from undiscovered kimberlites within the sample area or a product of different glacial processes in the north and south regions.

The presence of kimberlite within or proximal to the sample areas could account for indicator mineral recharge over a longer distance (i.e. the recharge of indicator minerals is discontinuous as a result of separate kimberlites, creating a long “pseudo-dispersal train” composed of multiple dispersal trains). Frost boils in till in the southern Slave Province is active to depths approximately 20 cm deeper than in the northern Slave Province, which also has the potential to account for higher abundances of indicator minerals over greater distances. However, it is important to note the greatest control on KIM abundance in till is the mineral content of the source.

Frostboils are a product of cryoturbation and bring materials from depth to surface through hydrostatic pressure and are a popular sample medium in permafrost terrain. Frostboils are only active in the active layer of till. Till in the southern Slave Province is active to greater depths than in the northern Slave Province, creating the possibility that indicator minerals are sampled from greater depths and brought to the surface closer to host deposits (Figure 4.4). This could indicate samples may be collected from frostboils more proximal to anomalies, however, it could also mean greater sample dilution in indicator mineral concentration from dispersal trains at surface in the southern Slave Province. These dilution and enrichment effects are not mutually exclusive but hold a small potential for indicator minerals to be recovered more proximal to deposit. This would have significantly lower control than the overall mineral content of source lithologies.

.

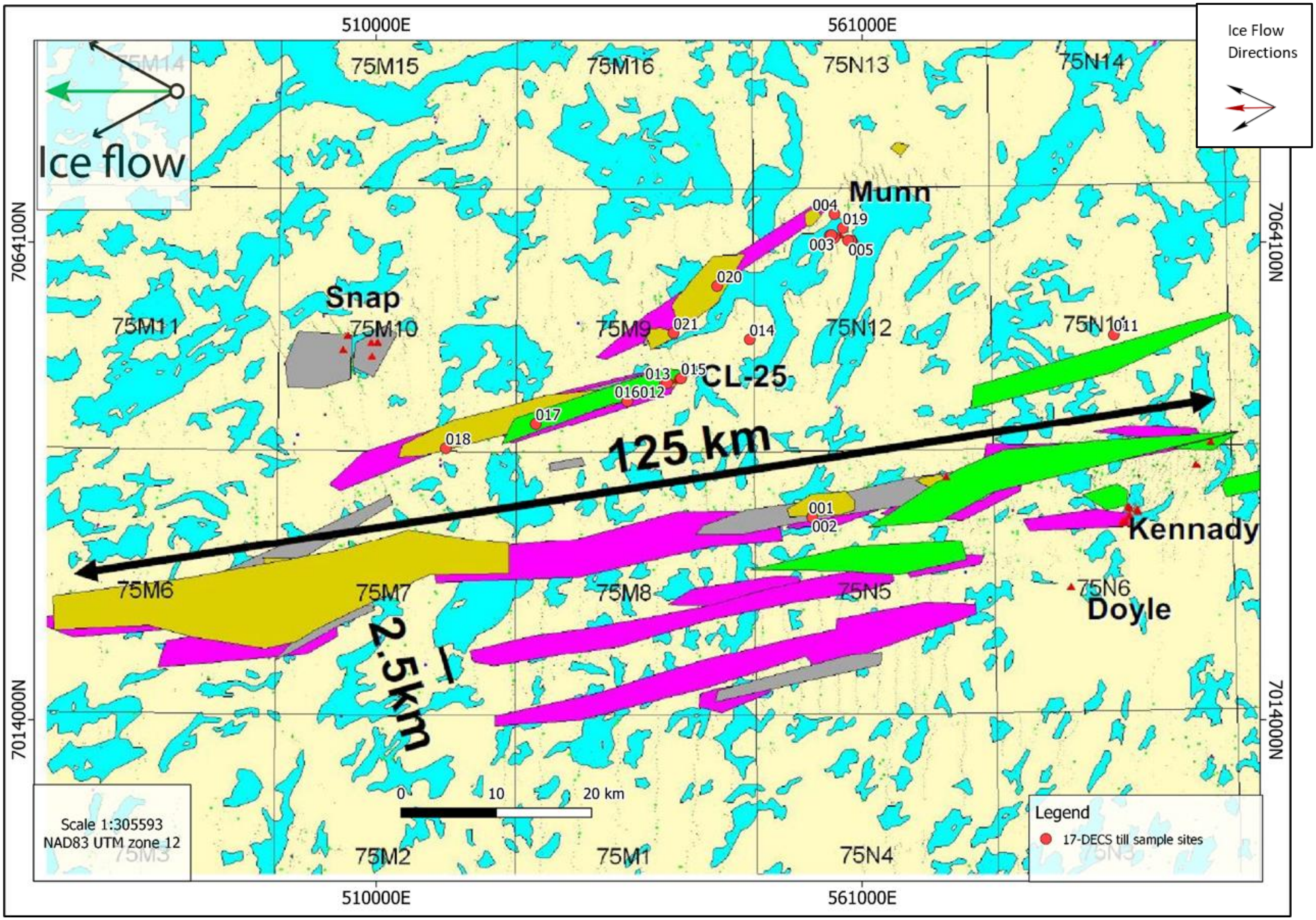

Figure 4.3: Distribution of surficial sediment samples that contain KIM in the southern Slave Province identified by Armstrong (2003) using the KIMC database. PColored polygons ourline the areas in which a particular KIM species was found in the surficial sediment sample. Green= Cr-diopside, grey = spinel, pink = garnet, yellow = ilmenite. Red triangle indicates kimberlite location.

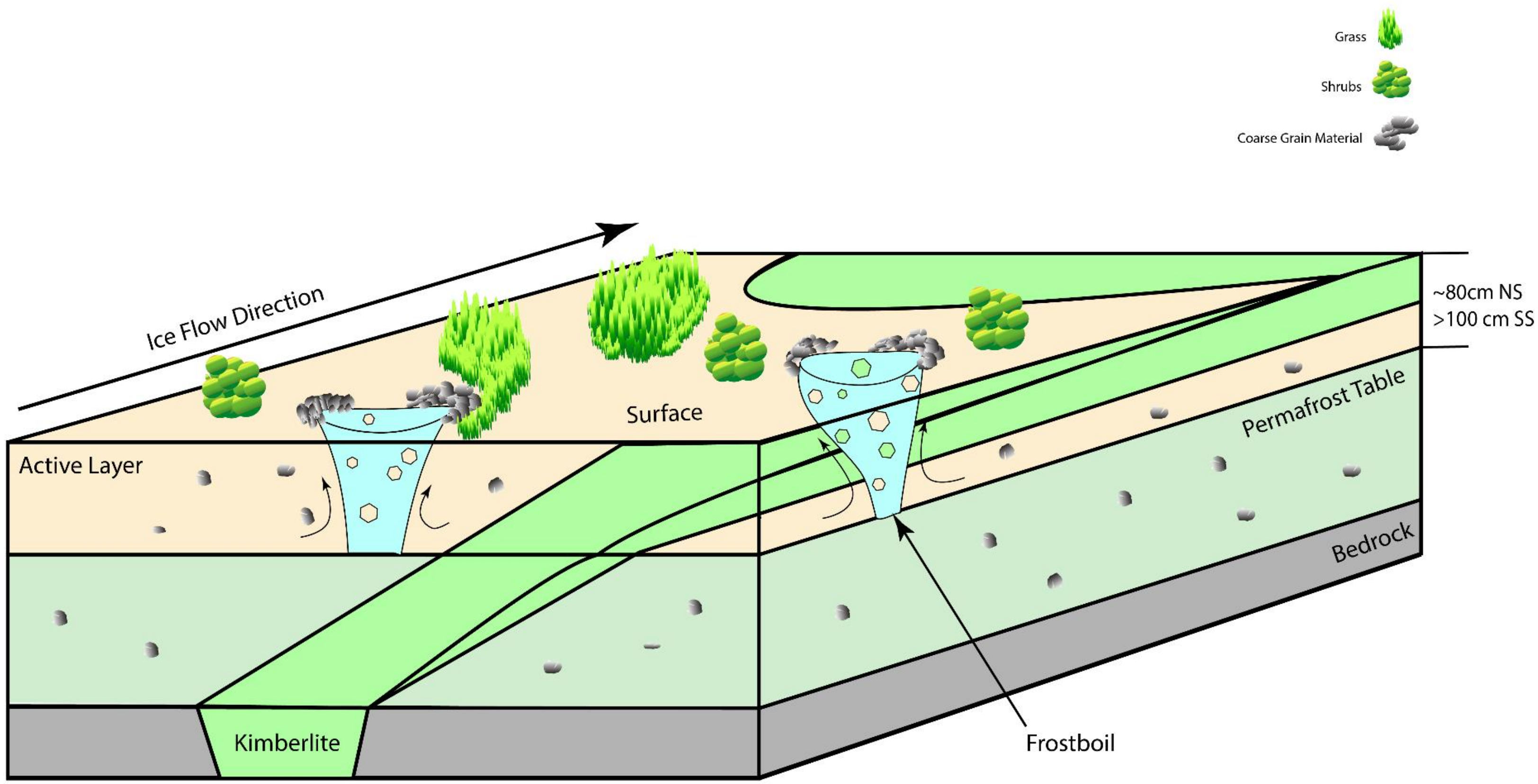

Figure 4.4: Simplified cross section of mineral dispersal and the potential effects of frostboils on sample proximity. 80 cm NS (northern Slave) and 100 cm SS (southern Slave). Frostboils sample dispersal materials from dispersal trains not exposed at surface. *not to scale

4.1.1 17-DECS-013

Till sample 17-DECS-013 has a high garnet concentration (257 grains) with respect to the nearby surficial sediment sample sites in the regional dataset across the southern Slave Province (Table 3.1, Table 4.2). Striation data in the immediate area of sample 17-DECS-013 indicates a dominant westward ice-flow direction (Knight, 2018). Directly up-ice (east northeast) are kimberlites CL-25 and CL-174 and the “H” and “S” geophysical anomalies (these anomalies potentially represent the CL-25 and CL-174 kimberlites) (Mirza and Elliott, 2017).

Weathered and eroded kimberlites in glaciated terrain tend to be topographic lows with respect to the surrounding bedrock (McClenaghan and Kjarsgaard, 2001, 2007). Indicator minerals in till immediately down ice of kimberlite will be at the base of the till unit, at the till-bedrock interface. Further down ice as the KIM dispersal train rises above the bedrock surface, KIM counts in surface till may be higher as reflected in Stanley’s (2009) dispersal model.

Sample 17-DECS-013 is situated on the stoss slope of a topographic high within a WSW trending dispersal train first identified by Armstrong (2003) (Figure 4.3, Figure 4.5). The sample was collected from a relict frostboil that has been subjected to moderate to high amounts of oxidation (Chapter 7:Appendix IV). The closest sample to 17-DECS-013 is 17-DECS-012, 236 m to the WSW (down-ice). Sample 17-DECS-012 contains no KIMs. Other proximal samples include up-ice 17-DECS-015, and down-ice 17-DECS-016. Sample 17-DECS-015 contains a background of one G9 garnet. Down-ice, sample 17-DECS-016 contains nine G9 garnets and one G1 garnet. Samples 17-DECS-017 and -018 further down ice (WSW) contain one G9 and two G9s, respectively (Figure 4.6).

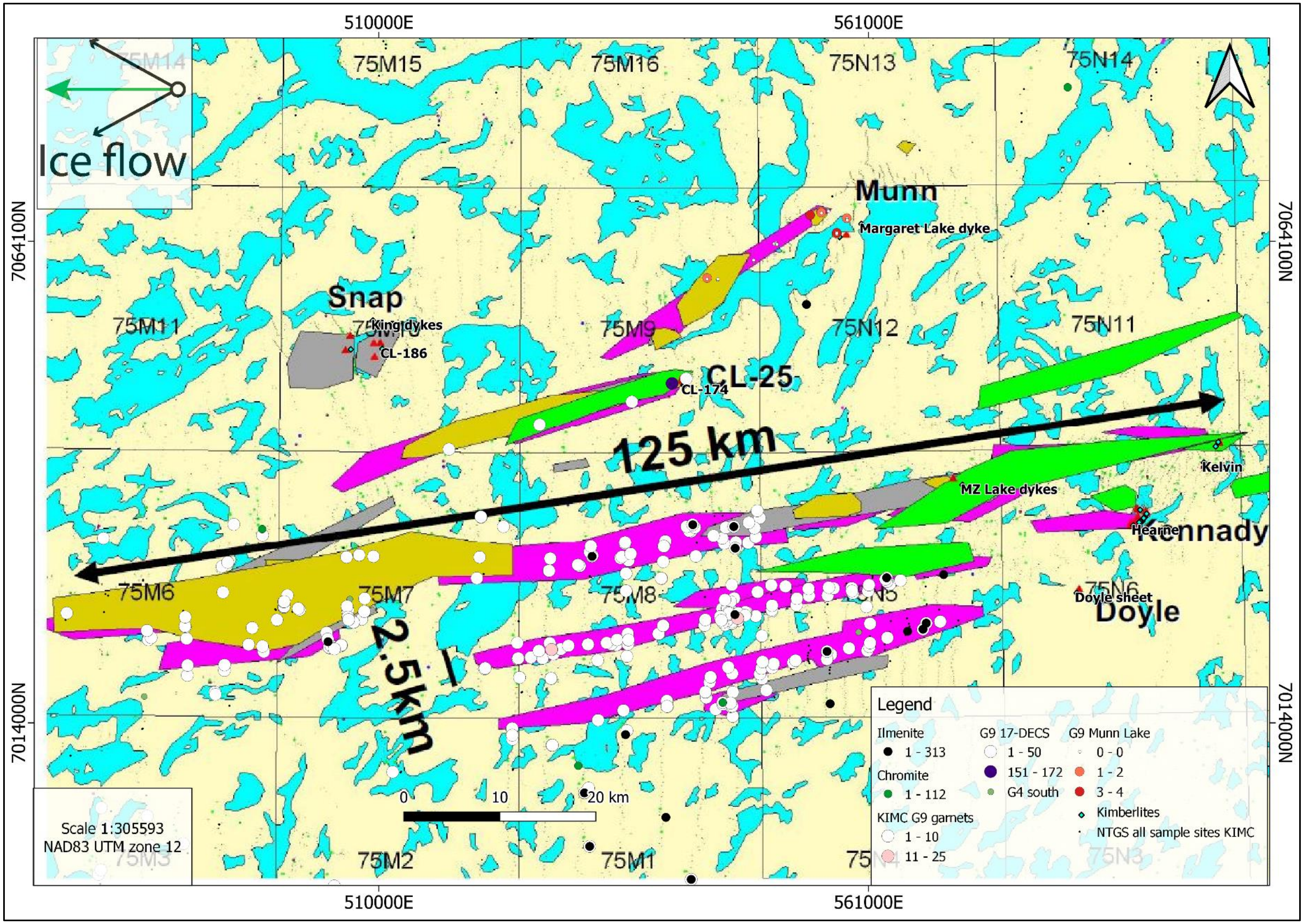

Figure 4.5: G9 garnet distribution from KIMC database surficial sample sites superimposed on the kimberlite dispersal trains mapped by Armstrong (2003)

Possible explanations for the high concentration of garnet in 17-DECS-013 could be the depth of frostboil sampling in the active layer and overall depth of till proximal to kimberlite, or the location of the sample site on the stoss slope of a topographic high (ridge), or both. It is also possible this spike in concentration is the product of unidentified kimberlites up-ice of 17-DECS-013, CL-25, and CL-174. It is also worth noting that KIM-rich and KIM-poor till can exist within the same area of a dispersal train (McClenaghan et al., 200). McClenaghan et al. (2004) have shown KIMs may be distributed in clots, blobs, and ribbons within KIM-poor till down ice of Kimberlite. The high concentration of sample 17-DECS-013 may reflect a blob of KIM-rich debris.

Other till samples collected in the southern Slave Province have been distal to known kimberlites (minimum sample distance is 7 km) with sample medium being unknown outside of 17-DECS suite, making the application of this theory challenging. It is possible that the depth of the active layer in the southern Slave Province could produce higher KIM concentrations more proximal to deposits when samples are collected from basal till and till veneer as mentioned in section 4.1.3. Frostboils, while they may bring buried material to surface, at the same time may remove material currently exposed at surface to a certain degree (Figure 4.7). It may be beneficial to sample frostboils proximal to deposits and frostboils and other medium more distal to deposits.

The significance of the sample location on the stoss side of a topographic high is the potential for accumulation of lodgement till from the subglacial environment. Indicator grains identified in sample 17-DECS-013 were dominantly fractured with well-preserved textural attributes. Fracturing of garnet is not uncommon in kimberlite (ie the source rock) and is generally not a product of subsequent glacial transport. The preservation of textures and lack of rounded and abraded garnet grains in till is possible evidence that the KIMs in the till sample were not transported over long (>5 km) distances, supporting the idea the material was sourced from a near by host. If sample locations proximal to a kimberlite contain high KIM counts, it may help determine the location of the kimberlite and ultimately its diamond potential. In order to assess this potential, survey grids should be planned with till samples collected up-ice and overlying, as well as down ice of known kimberlites and/or geophysical anomalies.

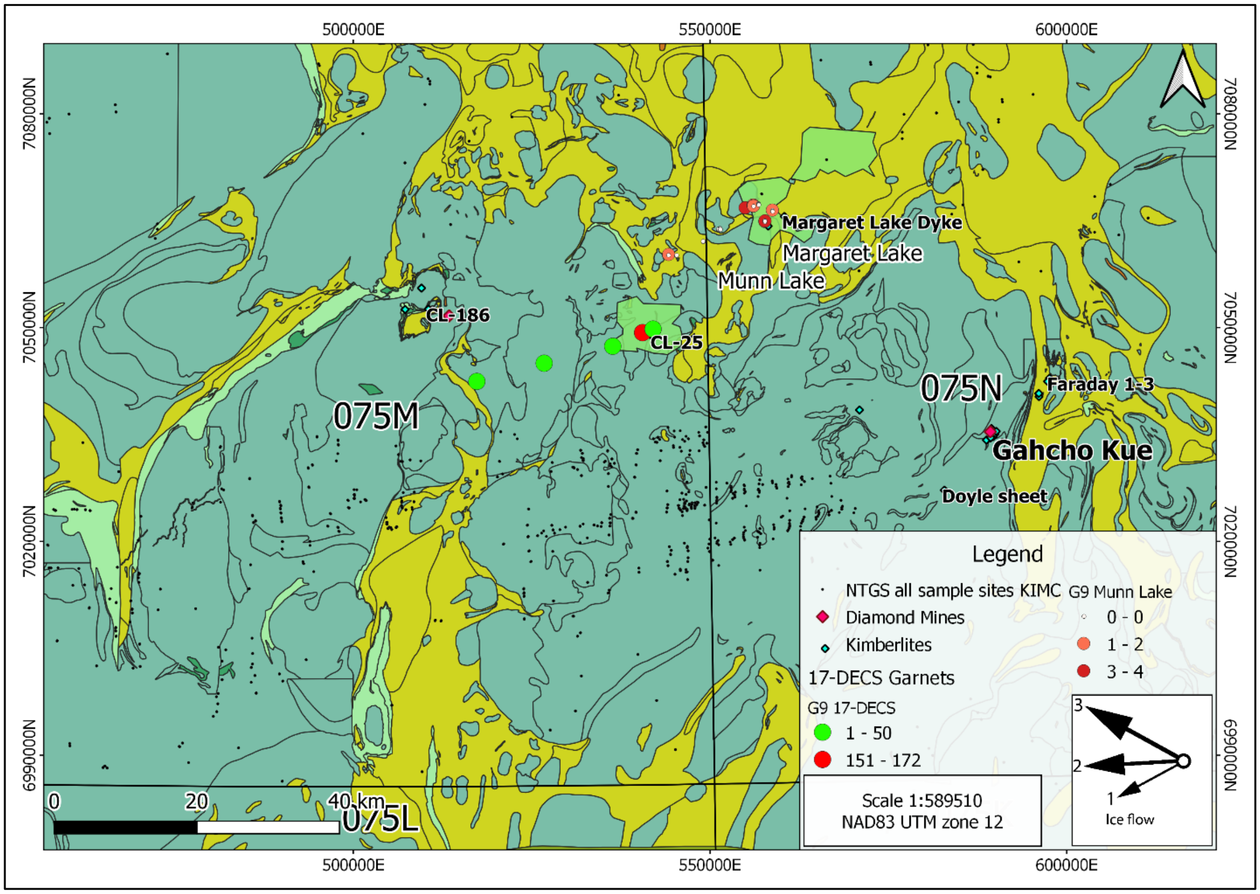

Figure 4.6: Concentration of G9 garnets of 17-DECS and Munn Lake (Miller, 2016) with respect to known kimberlite and "S" and "H" geophysical anomaly area outlines (surficial data from NWT Open File 2005-001, NWT Geoscience Office, 2018; Geophysical data and interpretation from CGG Canada Services Ltd., 2017; Mirza and Elliott, 2017)

Field samples collected during the 2015 season for the Munn Lake Property (Miller, 2016) have high G9 concentrations proximal to geophysical anomalies (Figure 4.6). This close association could represent the incorporation and dilution effects of active layer thickness and frostboil depth sampling in the southern Slave Province, in addition to being a direct reflection kimberlite KIM content. Further work on the property should include sample grids down-ice from the geophysical anomalies. More specifically sample grids should be conducted down-ice and proximal to the northern-most geophysical anomaly identified in this study in order to assess the diamond potential as well as distribution of indicator minerals.

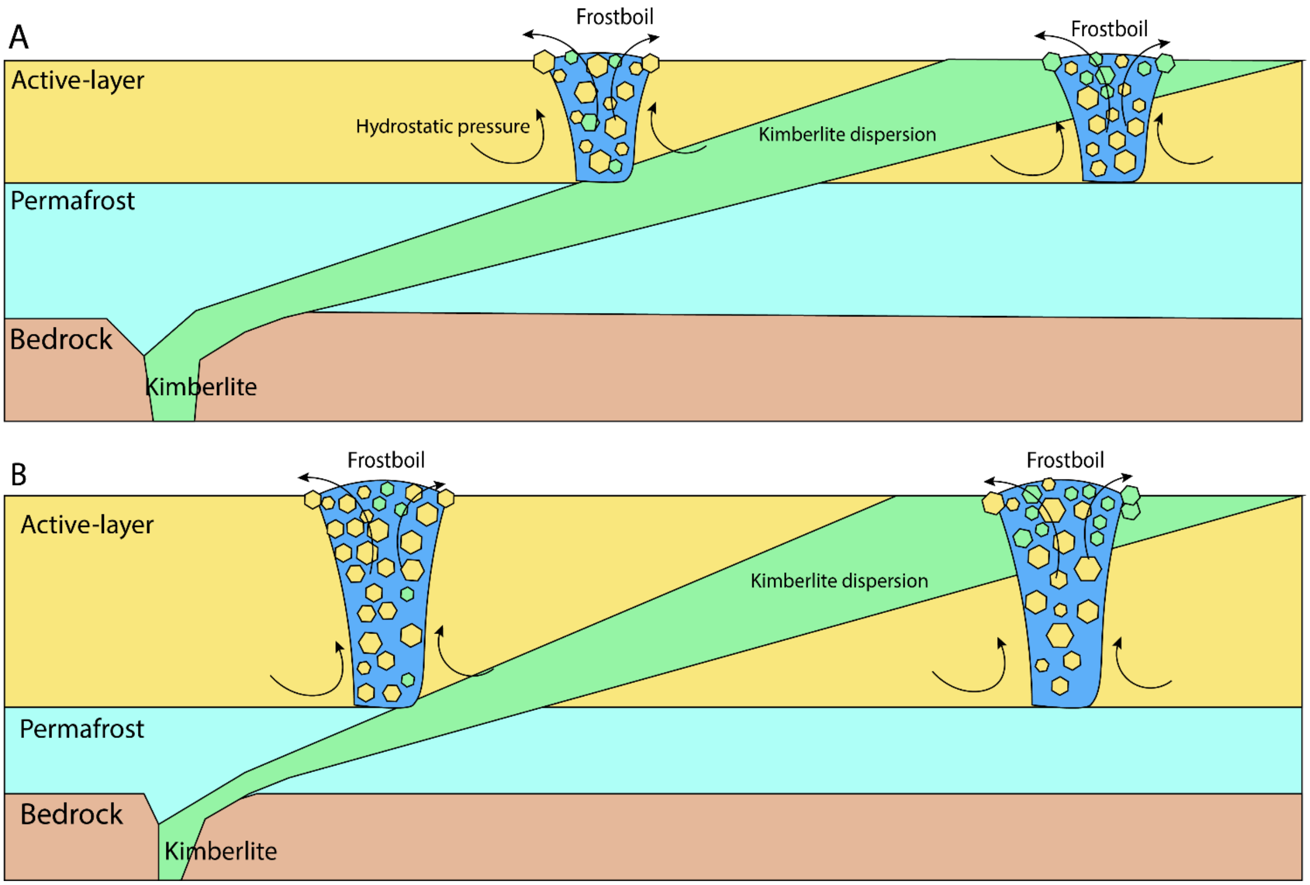

Figure 4.7: (A) The potential dilution and incorporation effects of frostboils in shallower active-layer areas. Frostboil sampling the dispersal train more distal to kimberlite. Frostboil incorporating less till into dispersal train surface exposure. (B) The potential effects of frostboil dilution and incorporation in a deeper active layer areas. First frostboil sampling dispersal train more proximal to kimberlite than in shallow active layer. More active layer dilution of dispersal train at surface. *not to scale.

4.1.2 Na_2O content of garnet

The dominant control on Na content in eclogitic garnet are the conditions under which the garnet forms (Hardman et al., 2018a). With increasing depth in the mantle, Na increasingly partitions into eclogitic garnet with increasing pressure (Hardman et al., 2018a). Eclogitic garnet inclusions in diamond have may have Na_2O concentrations higher than 0.07 wt. % (Grütter et al., 2004). The discrimination of diamond-facies garnet using this Na_2O wt. % threshold is not absolute. However, it is used by Grütter et al. (2004) to establish G3, G4 and G5 garnets with a high association to diamond, suffix "D". In the southern Slave Province, G3, G4, and G5 garnets have concentrations of <0.07 wt. % Na_2O exclusively. In the northern Slave Province G3, G4, and G5 garnets have Na_2O concentrations of up to 2.14 wt. % (Equivalent of Group I eclogites, Schulze, 2003). Based on the distinction made by Grütter et al. (2004), this difference in Na_2O content could indicate a higher diamond potential of the northern Slave Province, and lower diamond potential of the southern Slave Province.

4.1.3 Trace elements in garnet

In addition to SEM-EDX quantitative mineral analysis, garnets from this study were analyzed for trace elements. REE_N (chondrite normalized (N) rare earth element) data was assessed using the classification of Hardman et al. (2018b). There are two distinct trends in the REE_N data from 17-DECS-013 which appear to be trends for mantle and crustal REE. G10 garnets appear to have to a mantle signature as indicated by the REE_N pattern seen in Figure 3.6 based on criteria from Hardman et al. (2018b).

G3 garnets displayed a crustal signature as indicated by the REE_N pattern seen in Figure 3.6 based on criteria from Hardman et al. (2018b).

G9 garnets did not exclusively fit one category. The G10 garnets from 17-DECS-013 were classified as diamond-facies “G10D” (all but 1), indicating a mantle origin in agreement with the REE_N data. The G3 garnets from the 17-DECS suite were not given a diamond-facies classification, which is consistent with the REE_N data. Trace element work is unpopular in exploration due to the time consuming and expensive nature of the work. Trace element data in this study did not provide extra insight in terms of diamond potential of the southern Slave Province other than confirming G3 garnets analyzed are not of deep mantle origin.

4.2 Olivine

Olivine represents a more controversial kimberlite indicator mineral. It is difficult to discern kimberlitic and non-kimberlitic olivine based on composition, as olivine can be found as phenocrysts in a variety of ultrabasic and basic rocks with a more primitive mineral chemistry (McClenaghan and Kjarsgaard, 2001; Averill, 2009). Olivine is present in inferred sample sites in the northern Slave Province in significant quantities. and absent from any till samples in the southern Slave Province. The kimberlite in the northern and southern Slave do show differences in kimberlite facies (northern Slave Province Lac des Gras kimberlites of Ekati are dominantly volcaniclastic kimberlite (VK) (Nowicki et al., 2004), southern Slave Province kimberlites of Gahcho Kué are dominantly hypabyssal kimberlite (HK) and tuffisitic kimberlite breccia (TKB) (Caro et al., 2004)), however, kimberlites in the north and south have been shown to both contain olivine (Nowicki et al., 2004; Caro et al., 2004). This presents the question, what could cause the difference in olivine concentration in till in the Slave Province? There are several possibilities that could potentially explain this variation:

i) The northern Slave Province is densely sampled in comparison to the south. The density of sample collection and analysis may have enabled a higher yield of olivine over the years.

It is intuitive that a more densely sampled area is more probable to yield some anomalous results. It is possible that with the amount of sampling in the northern Slave Province, and the close proximity of sampling, that there would be a higher yield of olivine if it is present in till. However, within the HDSA there is still a discrepancy in the concentration of olivine. If the olivine concentration were higher due to sample density this would be visible in the HDSA, however the HDSA has a lower concentration of olivine than the surrounding area (Figure 3.13), making this explanation not likely to be the case.

ii) The kimberlites of the northern Slave Province could potentially have a higher olivine content relative to kimberlites in the south Slave.

If the kimberlites of the northern Slave Province had a higher olivine content, this would also likely increase the amount of olivine yielded in the HDSA from till, making this explanation less likely. Studies by Caro et al. (2004) and Moss et al. (2008) have shown variable concentrations within individual kimberlite pipes from Gahcho Kué and Diavik, respectively, with similar overall olivine concentrations per pipe.

iii) The olivine could be sourced from a host other than kimberlite, reflecting a variation in bedrock lithology in the northern Slave Province, and may not be representative of kimberlite.

The immediate up-ice lithology of the HDSA is predominantly metasedimentary units with minor pyroxenitic, gabbroic, and diabase units. It is possible there are smaller, undiscovered lithologies up-ice of the till samples olivine present.

iv) The complex nature of glacial movement in the northern Slave Province may affect olivine differently than other indicator minerals such as garnet.

Olivine is a kimberlite indicator mineral known for its inability to travel well in a basal glacial environment. It is possible that the complex glacial history of the northern Slave Province may have resulted in the degradation of olivine in till. This would result in olivine being less prominent in the courser size fraction of till sampled for traditional indicator minerals. The northern Slave Province is believed to have experienced at least three different prominent directions of ice-flow (Figure 1.10). The ice-flow history of the northern Slave province may account for the low concentration of olivine, but it does not account for the presence of olivine between the HDSA and the southern Slave Province.

It is apparent that the olivine in the northern Slave Province is in higher concentrations than in the south. It is particularly noteworthy that within the HDSA there is little olivine in comparison to its immediate surroundings. This might suggest that the olivine in the northern Slave Province is not a product of kimberlite dispersal, but the dispersal of a different host lithology. For this reason, olivine should not be used as a sole indicator of the presence of kimberlite, but as an accessory indicator mineral with less emphasis to more prominent indicators.

4.3 Cr-Diopside

The discrimination of kimberlitic and non-kimberlitic Cr-diopside is less than ideal. Cr-diopside can form as phenocrysts in a variety of ultrabasic and basic rocks, much like olivine, and may have primitive mineral chemistry (McClenaghan and Kjarsgaard, 2001). Kimberlites and mantle xenoliths are the only rocks which contain very Cr-rich diopside with concentrations >1.5 wt. % Cr_2O_3 (McClenaghan and Kjarsgaard, 2001). However, Cr-diopside in kimberlite may also have lower concentrations of Cr, resulting in the need for better discrimination of Cr-diopside with <1.5 Wt. % Cr_2O_3 (McClenaghan and Kjarsgaard, 2001).

The distribution of Cr-diopside in inferred sample sites across the Slave Province is comparable to the distribution of olivine (Figure 4.8). The distribution of Cr-diopside is subject to the same potential explanations as the olivine distribution. The distribution of Cr-diopside and olivine seem to support the notion that these indicator minerals could potentially be sourced from a non-kimberlitic host rock, as they can both be minerals produced by other basic and ultrabasic rocks (McClenaghan and Kjarsgaard, 2001). The presence of Cr-diopside and olivine would be expected to be most abundant in the youngest ice-flow direction (NW within the HDSA (Kelley et al., 2019)), as they are typically less resistant to glacial dispersion than other indicator minerals. The lack of Cr-diopside and olivine in the HDSA may serve as an indication of their unreliability as KIMs.

This trend of Olivine and high-Cr Cr-diopside could also potentially indicate a higher abundance of these KIMs in the Big Blue and surrounding kimberlites, including kimberlites just south of the HDSA (Figure 4.8).

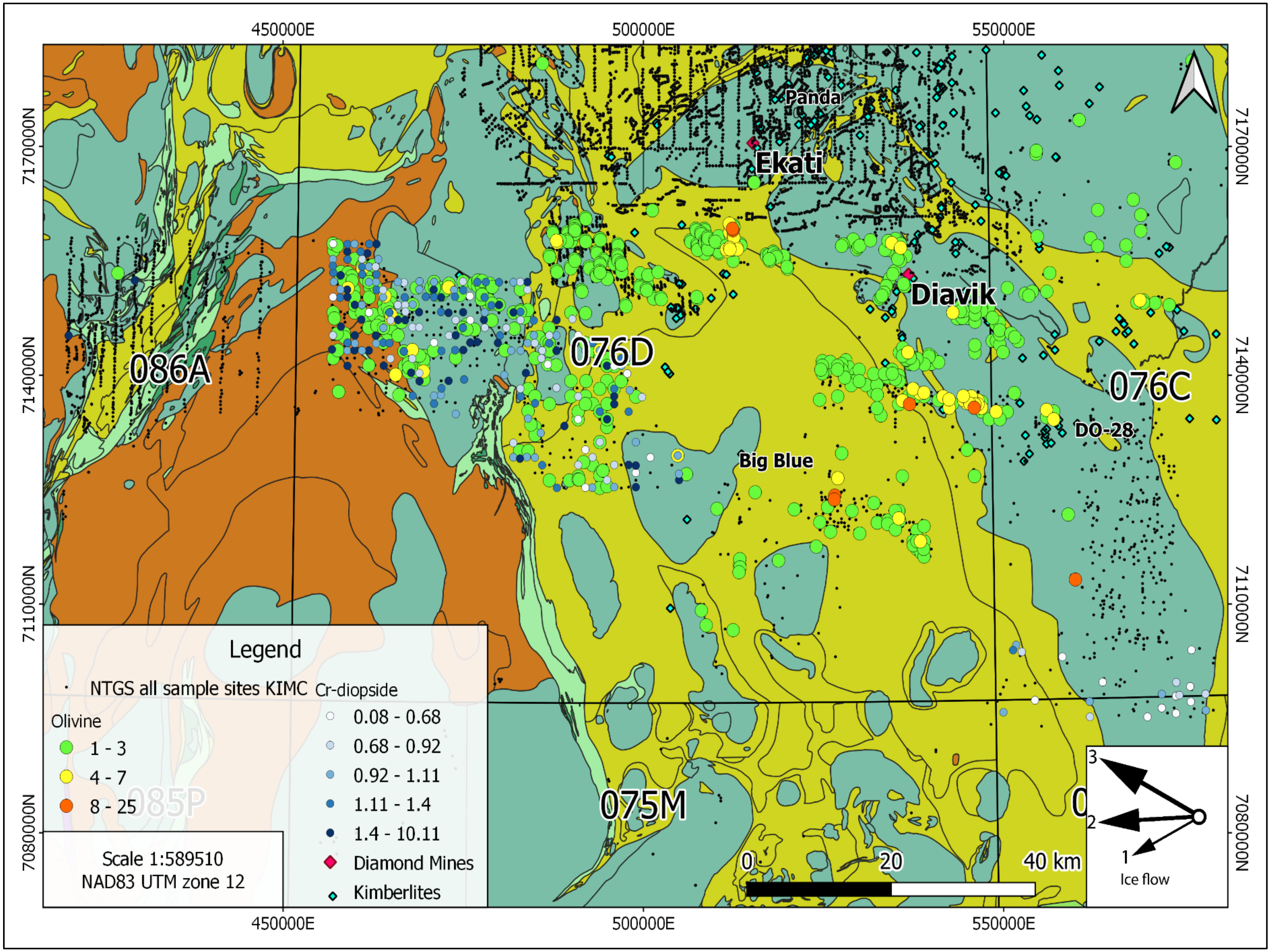

Figure 4.8: Olivine and high-Cr Cr-diopside distribution in the central Slave Province with respect to known kimberlites (Surficial data from NWT Open File 2005-001, NWT Geoscience Office, 2018).

4.4 Ilmenite and chromite

Ilmenite and chromite are both prominent indicator minerals in surficial sediments the northern Slave Province within the HDSA, and present in the southern Slave Province. Along the borders of the HDSA concentrations of chromite and ilmenite are mostly consistent with the concentrations throughout the Slave Province. The chromite and ilmenite distributions in the southern Slave Province are less suitable for indicator mineral train identifying potential dispersal trains on their own but can be used as part of the KIM suite . Both ilmenite and chromite contribute to the identification of three potential indicator mineral trains in the southern Slave Province.

The difference in concentration of chromite and ilmenite between the Slave Province and the HDSA of the Slave Province is significant. Previously, this discrepancy has been observed within the KIDD and explained as a product of the differences in kimberlites ages their relative abundances of KIM (Armstrong, 2003). The kimberlites in the area of the HDSA are 47-72 Ma with kimberlites in the southeastern Slave Province being ~540 Ma (Armstrong, 2003; Heaman 2003). Armstrong (2003) reported that kimberlites in the younger central Slave Province kimberlite field (Lac de Gras field) sheds a larger number of indicators which are dominated by clinopyroxene and garnet. Armstrong (2003) has also stated that kimberlite in the southeastern Slave Province field are dominated by garnet, clinopyroxene, and ilmenite.

The variation of KIM contents in kimberlites in different parts of the Slave Province is also observable in the KIM chemistry from the KIMC database. Along with Armstrong's (2003) initial findings, this is likely the result of the much higher surficial sediment sample density in the HSDA as compared to the south Slave (I.e. the overlap of geospatial data). Another contributing factor could also be the challenge in visually differentiating between chromite and ilmenite in samples (all fragmented black minerals). Based on mineral chemistry data with georeferenced points, ilmenite and chromite are less prevalent in the southern Slave Province than the north. Their use in exploration has always been somewhat limited due to a lack of clear chemical constraints and specific diamond associations.

4.5 Recommendations

The southern Slave Province has been a subject of analysis over recent years as not much is known in comparison to the northern Slave in terms of KIM chemistry. The findings of this study show the variations in distribution and abundance of KIM with mineral chemistry data in the Slave Province. These findings may show which indicator minerals are most abundundant and thus, best suited for diamond exploration in the southern Slave Province by using regional mineral chemistry data to assess glacial dispersal and KIM concentrations. This study has shown garnet to be a particularly useful KIM in the southern Slave Province in contrast to other indicator minerals. Garnets have been shown to be best suited for exploration using the classifications of Grütter et al. (2004). Low sodium content has been observed in G3 garnets of the southern Slave Province, potentially indicating a lower diamond potential than in the northern Slave Province. This G3 classification, however, requires further research into the relationship between sodium content of garnet and diamond facies kimberlites. The large data set analyzed could provide insight into regional variation in kimberlite indicator mineral distribution not visible at a smaller scale. Uncertainty in using large databases such as the one provided by the NTGS include not knowing the sample medium, sample size, the quality control measures or the details of various methods used during sampling, sample processing to recover heavy minerals, KIM identification, and mineral chemistry analysis. Knowing sample size, sample processing methods and quality control measures would help reduce large scale error, and knowledge of sample medium may help determine variability in glacial transport mechanisms and permafrost effect on the collection of indicator minerals. Additional research that is worthwhile to conduct includes more sample collection in the southern Slave Province as well as the assessment of indicator minerals such as Cr-diopside and olivine with respect to kimberlites and other potential non-kimberlite source rocks of the Slave Province. The significant abundance of diamond and kimberlite- associated garnets in surficial sediments in the southern Slave Province indicate a high potential for diamondiferous kimberlites in the region. There are several geophysical anomalies which require further investigation, particularly the anomalies directly up-ice from sample 17-DECS-013 (Figure 3.21) which contained the most KIM of any of the samples collected in this study. Additional till samples down ice of geophysical anomalies may provide useful insights into the nature of the local bedrock and the presence of kimberlites.

Chapter 5: Conclusions

This study assessed the diamond potential and indicator mineral distribution of the southern Slave Province. Field sampling was conducted within the 075M and 075N NTS map zones, with materials being collected from frostboils and relict frostboils down-ice of known kimberlites and geophysical anomalies.

Kimberlite indicator minerals recovered from heavy mineral concentrates were dominated by garnets, more specifically G9 garnets. In addition, a total of 100,322 garnets from the NTGS database were classified and 255 garnets from the 17-DECS sample suite. Striation and geomorphological features were used by Knight (2018) to make interpretations of ice-flow direction. There are multiple directions of flow indicated by striation data within the southern Slave Province (Figure 1.10), with the most recent ice-flow direction being interpreted as approximately 270°. The most recent ice-flow direction of the northern Slave Province is interpreted to be approximately 300°, with the most dominant transport direction interpreted as westward (Ward et al., 1997). It is visually apparent that the most recent ice-flow direction in the northern Slave Province has influenced the distribution of indicator minerals. For instance, G10 garnets increase in concentration in a down-ice direction ~300° of known kimberlites in the northern Slave Province (Figure 3.25). In addition, the complex nature of glacial ice-flow directions of the northern Slave Province create a smearing effect, that is, where indicator minerals are fanned out as a product of multiple glacial advances (i.e. kimberlite dispersal trains are redistributed). The relatively simple ice flow history of the southern Slave Province creates a simpler distribution pattern of indicator minerals directly west of kimberlites, making mapping indicator minerals distribution in the area easier.

Garnet is the most useful indicator mineral found in the southern Slave Province, due to its robust nature, high concentrations in till, and its unique properties making grain visual grain identification in till HMC simple. Garnet G-number classifications from Grütter et al. (2004) were most useful in application than other methods used in this study. The Grütter et al. (2004) classification proved a useful comparative tool in assessing distribution patterns in the north and south Slave Province. It also provided a useful base for determining diamond potential of the southern Slave Province. Garnets with a high statistical association to diamond (G10D) were present in high amounts at several sites in the southern Slave Province. Other garnets with high statistical association such as G3D garnets with high Na content were absent in the southern Slave Province, and in relative low abundance in the northern Slave. Most classifications of Grütter et al. (2004) are indicative of some inherent association to kimberlite, and therefore it is useful to use each classification to assess distribution patterns.

There is a significant variation in the amount of garnet in the northern and southern Slave Provinces. This variability is a function of kimberlite mineralogy (Armstrong, 2003) as well as the product of sample density. In the northern Slave Province, there have been prolific sample grids conducted over several years in the Lac des Gras kimberlite field. The lower concentration of garnets in the southern Slave Province is not reflective of the regions diamond potential.

Overall, the garnets present are indicative of potentially diamond bearing kimberlites in the region. Garnets in the southern Slave Province could potentially be used solely as kimberlite indicator minerals when all classifications of Grütter et al. (2004) are used. The trace element classifications and quantitative mineral chemistry classifications of Hardman et al. (2018b) did not provide additional insight on garnet and diamond potential in this study and is costly and time consuming making it an inefficient exploration tool.

Olivine and Cr-diopside both followed similar distribution patterns throughout the Slave Province. Olivine was absent from every sample taken in the southern Slave Province, rendering it an ineffective exploration tool in the area. Cr-diopside was rare in the southern Slave Province with compositions not always indicative of kimberlite. The use of Cr-diopside in the southern Slave Province is possible in conjunction with other indicators and garnet but means very little on its own. Both Cr-diopside and olivine appear to likely represent a lithology in the Slave Province other than kimberlite. The commonality of olivine and Cr-diopside in other ultrabasic and basic lithologies indicate a source of contamination when conducting indicator mineral dispersal mapping. Cr-diopside and olivine chemistry should be subject to more research in terms of its association to kimberlite. Without clear, reproducible chemical constraints these minerals cannot be relied on solely as kimberlite indicators.

Ilmenite and chromite are both present in drastically higher concentrations in the northern Slave Province than in the south. Chromite and ilmenite are both black minerals which can be difficult to distinguish in sizes smaller than 0.5 mm diameter. This may result in difficulty selecting chromite and ilmenite from heavy mineral concentrates with different black minerals present, or with lower starting abundances. The difference in concentration of chromite and ilmenite from the north and south are a function of kimberlite mineralogy (Armstrong, 2003) and likely a product of sample density. Prolific sample grids in the northern Slave Province could result inferred sample site overlap causing grains to be selected from >20 kg samples in close proximity as opposed to standard ~10 kg samples at spacing >100 m. Samples containing ilmenite and chromite can be used in conjunction with garnet when mapping kimberlite dispersal trains. Ilmenite is often regarded as a controversial indicator mineral due to the irreproducibility of mantle and crustal chemical signatures.

Indicator mineral dispersal in the southern Slave Province appears to be relatively straightforward. The most recent and dominant ice-flow direction is interpreted to be westward (Figure 1.10). Samples taken down-ice of known kimberlites contain kimberlite indicator minerals in varying amounts. It is evident samples have not been collected proximal to most deposits in the southern Slave Province. The only sample collected proximal to a known kimberlite was part of 17-DECS sample suite. Samples proximal to kimberlites CL-25 and CL-174 contained the highest abundance of garnet in the southern Slave Province. It is possible that samples in the southern Slave Province can be collected closer to deposits due to differences in glacial deposits and the active layer thickness. Till thickness is variable (generally <10 m) throughout the Slave Province based on the mechanism of glacial deposition. The depth to which frostboils have the potential to sample layers of till is also variable in the Slave Province, with active layer depths of greater than 100 cm in the southern Slave Province and depths often less than 80 cm in the northern Slave Province. In theory, the greater the active layer depth, the deeper the till source, the more proximal a sample can be collected to its kimberlite source (Figure 4.4, Figure 4.7). This could indicate higher concentrations of indicator minerals proximal to host deposits in the southern Slave Province and depletion in concentration with distance from hosts due to dilution effects (Figure 4.7).

On the Munn Lake property, sample 17-DECS-013 has high KIM garnet content (>200 grains) proximal to the CL-174 and CL-25 kimberlites as compared to the southeastern Slave

Province KIMC database samples. Till samples collected during the 2015 Munn Lake field season and reported by Miller (2016), also contains G9 garnets proximal to a geophysical anomaly (>3 grains). It is unknown in this region whether kimberlite indicator mineral concentrations are highest proximal or distal to kimberlite sources. The data assessed in this study is indicative of proximal sample locations having high concentrations of garnet indicators. More sample grids down-ice of known kimberlites and geophysical anomalies in the southern Slave Province are required to obtain a baseline for this hypothesis. In theory, if samples are collected from till veneer (<2 m thick) proximal to deposits with an active layer thickness of > 100 cm, there will be a spike in KIM concentration proximal to the deposit where the dispersal train is narrow. This would appear to be the case for the Munn Lake property location and 17-DECS-013 sample. Sample 17-DECS-013 may indicate a high diamond potential for the CL-25 and CL-174 kimberlites. More extensive sampling may be required prior to further exploration efforts.

Chapter 6: References

Armstrong, J.P. 2003a. Diamond discovery in the Slave Craton: compilations of exploration data as tools for future discovery; 8th International Kimberlite Conference, Long Abstract, https://ikcabstracts.com/index.php/ikc/article/view/3117/3117

Armstrong, J.P., 2003b. Regional distribution and chemistry of kimberlite indicator minerals: Slave Craton. In: Extended Abstracts + oral presentation, Indicator mineral methods in mineral exploration. Short Course Notes, Prospectors and Developers Association of Canada. March 2003.

Armstrong, J.P. and Chatman, J. 2001. Kimberlite indicator and diamond database; Department of Indian and Northern Affairs, Northwest Territories Geology Division, EGS Report 2001-01.

Armstrong, J.P. and Kjarsgaard, B.A., 2003. Geological setting of kimberlites. *In* the Archean Slave Province; VIIIth International Kimberlite Conference, Slave Province and Northern Alberta Field Trip Guide Book, p. 31 -38.

Aylsworth, J. M. and Shilts, W. W. 1989. Glacial features around the Keewatin ice divide: districts of Mackenzie and Keewatin. Geological Survey of Canada, Paper 88-24, p. 1-21 and map 24-1987, 1: 1000000.

Averill, S.A. & McClenaghan, M.B. 1994. Distribution and character of kimberlite indicator mineral in glacial sediments, C14 and Diamond Lake kimberlite pipes, Kirkland Lake, Ontario. Geological Survey of Canada, Open File 2819.

Clark, P.U., Dyke, A.S., Shakun, J.D., Carlson, A.E., Clark, J., Wohlfarth, B., Mitrovica, J.X., Hostetler, S.W., McCabe, A.M. 2009. The Last Glacial Maximum. Science 325, 710e714.

Caro, G., Kopylova, M., and Creaser, R. 2004. The hypabyssal 5034 kimberlite of the Gahcho Kué cluster, southeastern Slave craton, Northwest Territories, Canada: a granite-contaminated Group-I kimberlite. The Canadian Mineralogist, *42* (1), p183-207. doi: 10.2113/gscanmin.42.1.183

Castillo-Oliver, M., Melgarejo, J.C., Galí, S., Pervov, V., Olimpio Gonçalves, A., Griffin, W.L., Pearson, N.J., O'Reilly, S.Y. 2017. Use and misuse of Mg- and Mn-rich ilmenite in diamond exploration: A petrographic and trace element approach, Lithos 292–293, 348-363, ISSN 0024-4937.

Dredge, L.A., Kerr, D.E., Wolfe, S.A. 1999. Surficial materials and related ground ice conditions, Slave Province, NWT, Canada. Canadian Journal of Earth Sciences 36, 1227-1238.

Fulop, A., Kopylova, M., Kurszlaukis, S., Hilchie, L., Ellemers, P., and Squibb, C. (2018). Petrography of Snap Lake Kimberlite Dyke (Northwest Territories, Canada) and its Interaction with Country Rock Granitoids. Journal Of Petrology, 59(12), 2493-2518. doi: 10.1093/petrology/egy025

Gernon, T. M., Field, M. and Sparks, R. S. J. 2012. Geology of the Snap Lake kimberlite intrusion, Northwest Territories, Canada: field observations and their interpretation. Journal of the Geological Society 169, 1–16.

Gowan, E.J. 2013. An assessment of the minimum timing of ice-free conditions of the western Laurentide Ice Sheet Quat. Sci. Rev., 75 (2013), pp. 100-113, 10.1016/j.quascirev.2013.06.001.

Grütter, H.S., Apter, D.B. 1998. Kimberlite- and lamproite-borne chromite phenocrysts with ‘‘diamond inclusion’’-type chemistries. 7^{th} International Kimberlite Conference Extended Abstracts, Cape Town, pp. 280 – 282.

Grütter, H.S., Gurney, J.J., Menzies, A.H., Winter, F. 2004. An updated classification scheme for mantle-derived garnet, for use by diamond explorers. Lithos 77 (1–4), 841–857.

Gurney, J.J. 1984. A correlation between garnets and diamond in kimberlites; in Glover, J.E. and Harris, P.G. (eds.), Kimberlite Occurrences and Origin: A Basis for Conceptual Models in Exploration, Univ. West. Austr., Publ. 8, p143-166.

Harvey, S.E., Kjarsgaard, B.A., and Kelley, L.I. 2001. Kimberlites of central Saskatchewan: Compilation and significance of indicator mineral geochemistry with respect to diamond potential; *in* Summary of Investigations 2001, Volume 2, Saskatchewan Geological Survey, Sask. Energy Mines, Misc. Rep. 2001-4.2.

Hardman, M., Pearson, D., Stachel, T., & Sweeney, R. 2018a. Statistical approaches to the discrimination of crust- and mantle-derived low-Cr garnet – Major-element-based methods and their application in diamond exploration. Journal of Geochemical Exploration 186, 24-35. doi: 10.1016/j.gexplo.2017.11.012

Hardman, M., Pearson, D., Stachel, T., & Sweeney, R. 2018b. Statistical approaches to the discrimination of mantle- and crust-derived low-Cr garnets using major and trace element data. Mineralogy and Petrology, 112(S2), 697-706. doi: 10.1007/s00710-018-0622-7

Henderson, K.B. 1970. Stratigraphy of the Archean Yellowknife Supergroup, Yellowknife Bay-Properous Lake area, District of Mackenzie; Geological Survey of Canada, Paper 70-26, 12p.

Isachsen, C., & Bowring, S. (1994). Evolution of the Slave craton. Geology, 22(10), 917. doi: 10.1130/0091-7613(1994)022<0917:eotsc>2.3.co;2

Kelley, S., Ross, M., Elliott, B., Normandeau, P. 2019. Effect of shifting ice flow and basal topography in shaping three-dimensional dispersal patterns, Lac de Gras region, Northwest Territories, Canada. Journal of Geochemical Exploration, 199, 105-127. doi: 10.1016/j.gexplo.2019.01.012.

Kerr, D.E., Kjarsgaard, I.M., Dredge, L.A., Ward, B.C. and Stirling, J.A.R. 1996. Distribution and composition of kimberlite indicator minerals, Napaktulik Lake map area, Northwest Territories (86I). Geological Survey of Canada, Open File 3355, 34 p.

Kerr, D; Budkewitsch, P; Bryan, D; Knight, R; Kjarsgaard, B. 2002. Surficial geology, spectral-reflectance characteristics, and their influence on hyperspectral imaging as a drift-prospecting technique for kimberlite in the Diavik diamond mine area, Northwest Territories; Geological Survey of Canada, Current Research (Online) no. 2002-C4, 2002, 10 pages, https://doi.org/10.4095/213167.

Kerr, D.E., Knight, R.D. 2007. Overburden thickness models: examples from the Slave Province, Northwest Territories, NTS Maps 76C, D, E, M, O, 77A, 86A, H, I, O, and P, Geological Survey of Canada, Open File 5522, 10 p.

Kjarsgaard, B.A., Levinson, A.A., 2002. Diamonds in Canada. Gems and Gemology 2002, 208–238 (Fall).

Knight, J., 2018. An interpretation of the deglaciation history of the southern Slave Province using 1:50 000 surficial geology maps; Northwest Territories Geological Survey, NWT Open Report 2017-018, 70 pages, digital data, and appendices.

McCandless, T.E., Gurney, J.J. 1989. Sodium in garnet and potassium in clinopyroxene: criteria for classifying mantle eclogites. In: Ross, J. (Ed.), Kimberlites and Related Rocks. Geological Society of Australia Special Publication, vol. 14/2, pp. 827– 832.

McClenaghan, M.B., Kjarsgaard, B.A. 2001. Indicator mineral and geochemical methods for diamond exploration in glaciated terrain in Canada. In: McClenaghan, M.B., Bobrowsky, P.T., Hall, G.E.M., Cook, S.J. (Eds.), Drift Exploration in Glaciated Terrain. Geological Society of London, London, pp. 83-123, Special Publication 185.

McClenaghan, M.B., Ward, B.C., Kjarsgaard, I.M., Kjarsgaard, B.A., Kerr, D.E., Dredge, L.A. 2002. Indicator mineral and till geochemical dispersal patterns associated with the Ranch Lake kimberlite, Lac de Gras region, NWT, Canada. Geochem. Explor., Environ., Anal. 2, 299–319.

McClenaghan, M., Kjarsgaard, I., and Kjarsgaard, B. 2003. Mineralogy of the McLean kimberlite and associated glacial sediments, Lake Timiskaming, Ontario. Geological Survey of Canada, Open File 1762, doi: 10.4095/214410

McClenaghan, M., Kjarsgaard, I., and Kjarsgaard, B. 2004. Kimberlite Indicator Mineral Chemistry and Till Geochemistry around the Seed and Triple B Kimberlites, Lake Timiskaming, Ontario; Geological Survey of Canada, Open File 4822, 27 p., 1 CD-ROM.

McClenaghan, M.B., and Kjarsgaard, B. A. 2007. Indicator Mineral and Surficial Geochemical Exploration Methods for Kimberlite in Glaciated Terrain; Examples from Canada. In W.D. Goodfellow (Ed.), Mineral Deposits of Canada, A Synthesis of Major Deposit-types, District Metallogeny, the Evolution of Geological Provinces, and Exploration Methods, Special Publication No. 5, 983-1006.

McClenaghan, M.B., Paulen R.C. 2018. Chapter 20 - application of till mineralogy and geochemistry to mineral exploration J. Menzies, Jaap J.M. van der Meer (Eds.), Past Glacial Environments (Second edition), Elsevier (2018), pp. 689-751.

McMartin, I., Campbell, J.E 2009. Near surface till sampling protocols in shield terrain, with examples from western and northern Canada. In: Paulen, R.C., McMartin, I. (eds.), Application of Till and Stream Sediment Heavy Mineral and Geochemical Methods to Mineral Exploration in

Miller, W. 2016. 2015-2016 Geological evaluation report on the Munn Lake property, Northwest Territories. Saville Resources Inc. 1450 – 789 West Pender Street Vancouver, BC V6C 1H2 Canada.

Mirza, A.M., and Elliott, B. 2017. Airborne electromagnetic and horizontal-gradient magnetic survey of the central Slave craton area, Northwest Territories, parts of NTS 75M, N, and 76D; Northwest Territories Geological Survey. NWT Open Report 2017-015, 121 pages with 54 maps and digital data.

Morris, T.F., Sage, R.P., Ayer, J.A., and Crabtree, D.C. 2002. A study of clinopyroxene composition: Implications for kimberlite exploration; Geochem. Explor. Analy., v2, no4, p321-331.

Moss, S., Russell, J., Brett, R., and Andrews, G. (2009). Spatial and temporal evolution of kimberlite magma at A154N, Diavik, Northwest Territories, Canada. Lithos, 112, 541-552. doi: 10.1016/j.lithos.2009.03.025Western and Northern Canada. Geological Association of Canada, Canada, pp. 75-95, Short Course Notes 18.

Nixon, F.M. 2000. Thaw-depth monitoring. In: The physical environment of the Mackenzie Valley, Northwest Territories: a baseline for the assessment of environmental change. L.D. Dyke and G.R. Brooks, Eds. Geological Survey of Canada, Natural Resources Canada, Bulletin 547, pp. 119-126.

Nowicki, T., Crawford, B., Dyck, D., Carlson, J., McElroy, R., Oshust, P., & Helmstaedt, H. 2004. The geology of kimberlite pipes of the Ekati property, Northwest Territories, Canada. Lithos, *76*(1-4), 1-27. doi: 10.1016/j.lithos.2004.03.020

Padgham, W. and Atkinson, D. 1991. Mineral deposits of the Slave Province; Geological Survey of Canada, Open File 2168.

Padgham, W.A., and Fyson, W.K. 1992. The Slave Province: A distinct Archean craton. Canadian Journal of Earth Sciences, 29: 2072-2086.

Quirt, D.H. 2004. Cr-diopside (clinopyroxene) as a kimberlite indicator mineral for diamond exploration in glaciated terrains; *in* Summary of Investigations 2004, Volume 2, Saskatchewan Geological Survey, Sask. Industry Resources, Misc. Rep. 2004- 4.2, CD-ROM, Paper A-10, 14p.

Rampton, V.N. and Sharpe, D.R. 2014. Detailed surficial mapping in selected areas of the southern Slave Province, Northwest Territories; Geological Survey of Canada, Open File 7562, 31 pp. doi:10.4095/293879

Rio Tinto. 2015. Diavik Ore Reserves. Rio Tinto. Confidential report? On the web?

Shilts, W.W. 1978. Nature and genesis of mudboils, central Keewatin, Canada. Can. J. Earth Sci. 15, 1053-1068.

Schulze, D.J., 2003. A classification scheme for mantle-derived garnets in kimberlite: a tool for investigating the mantle and exploring for diamonds. Lithos 71, 195–213.

Sobolev, N.V., Lavrent'ev, Y.G. 1971. Isomorphic sodium admixture in garnets formed at high pressures. Contrib. Mineral. Petrol. 31, 1 – 12.

Stanley, C.R. 2009. Geochemical, mineralogical, and lithological dispersal models in glacial till: physical process constraints and application in mineral exploration. In: Paulen, R.C., McMartin, I. (Eds.), Application of Till and Stream Sediment Heavy Mineral and Geochemical Methods to Mineral Exploration in Western and Northern Canada. Geological Association of Canada, Canada, , Short Course Notes 18, pp. 35_48

Stubley, M.P. and Irwin, D., 2019. Bedrock Geology of the Slave Craton, Northwest Territories and Nunavut; Northwest Territories Geological Survey, NWT Open File 2019-01, ESRI® and Adobe® digital files.

Ward, B.C., Dredge, L.A., Kerr, D.E. 1997. Surficial Geology, Lac de Gras, District of Mackenzie, Northwest Territories. In: Geological Survey of Canada, Map 1870A.

Wyatt, B.A., Baumgartner, M., Anckar, E., Grütter, H. 2004 Compositional classification of "kimberlitic" and "non-kimberlitic" ilmenite, Lithos, Volume 77, Issues 1–4, Pages 819 840, ISSN 0024-4937.

Chapter 7: Appendices

Appendix I SEM Results

Sample Nomenclature: G-000-g X,Y					
G		000	g		X,Y
Size/Amperage		Sample Number	Indicator mineral picked		coordinate on the circular grain mount
A	> 1.0 A (0.25-0.5 mm)	001-021	Orange Garnet	o	
B	0.8-1.0 A (0.25-0.5 mm)	001-022	Purple Garnet	p	
C	0.6-0.8 A (0.25-0.5 mm)	001-023	Ilmenite	i	
D	<0.6 A (0.25-0.5 mm)	001-024	Chromite	c	
E	0.5-1.0 mm	001-025	Cr-diopside	do	
F	1.0-2.0 mm	001-026	Olivine	f	

Table 7.7.1: KIM grains per sample site of the 17-DECS sample suite with bulk sample weights.

Sample site	Garnet (Total)	Cr-diopside	Chromite	G1	G3	G4	G5	G9	G10	G12	G0	Bulk weight (kg)
17-DECS-003	1	1	0	0	0	0	0	0	0	1	0	13.2
17-DECS-004	0	0	0	0	0	0	0	0	0	0	0	11.1
17-DECS-013	240	0	4	12	14	1	0	172	10	1	30	10.8
17-DECS-015	2	0	0	0	0	0	0	1	0	0	0	10.5
17-DECS-016	9	0	0	1	0	0	0	8	0	0	0	9.6
17-DECS-017	2	0	0	0	0	0	0	1	0	0	1	12.5
17-DECS-018	2	0	0	0	0	0	0	2	0	0	0	13.6
17-DECS-020	1	0	0	0	0	0	0	0	0	0	1	12.3

Table 7.7.2: KIM grains per till sample site of the 17-DECS sample suite normalized to 10kg sample weight.

	KIMs normalized to 10kg										
Sample site	**Garnet (Total)**	**Cr-diopside**	**Chromite**	**G1**	**G3**	**G4**	**G5**	**G9**	**G10**	**G12**	**G0**
17-DECS-003	1	1	0	0	0	0	0	0	0	1	0
17-DECS-004	0	0	0	0	0	0	0	0	0	0	0
17-DECS-013	222	0	4	11	13	1	0	159	9	1	28
17-DECS-015	2	0	0	0	0	0	0	1	0	0	0
17-DECS-016	9	0	0	1	0	0	0	8	0	0	0
17-DECS-017	2	0	0	0	0	0	0	1	0	0	1
17-DECS-018	1	0	0	0	0	0	0	1	0	0	0
17-DECS-020	1	0	0	0	0	0	0	0	0	0	1

Table 7.7.3: Chemical compositions (wt. % oxides) of individual garnet grains collected using SEM. (*n.d. not detected).

Sample Site	Al_2O_3	CaO	Cr_2O_3	FeO	MgO	MnO	Na_2O	Sc_2O_3	SiO_2	TiO_2	Total
17-DECS-016	17.43	5.71	5.33	8	21.34	n.d.	n.d.	n.d.	42.13	0.64	100.58
17-DECS-016	17.63	5.95	5.03	8.36	20.41	0.37	n.d.	n.d.	40.76	0.88	99.39
17-DECS-016	18.3	5.76	5.57	7.25	21.03	0.37	n.d.	n.d.	42.25	n.d.	100.53
17-DECS-016	18.25	5.58	4.27	8.89	20.23	0.38	n.d.	n.d.	41.46	0.79	99.85
17-DECS-016	16.9	5.82	6.72	6.98	20.68	0.46	n.d.	n.d.	41.32	0.52	99.4

Sample Site	Al_2O_3	CaO	Cr_2O_3	FeO	MgO	MnO	Na_2O	Sc_2O_3	SiO_2	TiO_2	Total
17-DECS-016	16.71	6.5	5.66	9.69	19.26	0.42	n.d.	n.d.	40.49	1.05	99.78
17-DECS-016	19.08	5.43	4.97	7.2	21.57	0.32	n.d.	n.d.	42.1	n.d.	100.67
17-DECS-016	16.48	5.81	9.13	8.12	19.26	0.57	n.d.	n.d.	40.88	n.d.	100.25
17-DECS-016	18.45	5.9	3.31	9.93	19.47	0.32	n.d.	n.d.	40.77	1.28	99.43
17-DECS-013	17.43	5.61	6.44	7.58	20.89	0.32	n.d.	n.d.	41.66	0.73	100.66
17-DECS-013	18.32	5.42	4.28	9.12	19.57	42.08	n.d.	n.d.	n.d.	1.1	99.89
17-DECS-013	14.91	5.96	9.43	6.5	20.8	0.34	n.d.	n.d.	41.38	0.76	100.08
17-DECS-013	17.18	5.85	5.9	8.15	20.56	n.d.	n.d.	n.d.	41.93	0.8	100.37
17-DECS-013	17.85	5.8	5.16	8.31	20.16	0.47	n.d.	n.d.	41.69	0.81	100.25
17-DECS-013	18.06	5.61	5.28	8.4	19.65	0.32	n.d.	n.d.	42.14	0.71	100.17
17-DECS-013	19.17	6.54	6.37	6.59	19.3	0.34	n.d.	n.d.	41.72	n.d.	100.03
17-DECS-013	18.08	5.62	4.73	8.97	20.04	n.d.	n.d.	n.d.	42.31	1.02	100.77
17-DECS-013	17.9	5.72	5.45	8.51	19.95	0.44	n.d.	n.d.	42.02	0.74	100.73
17-DECS-013	17.3	5.52	6.18	7.51	20.79	0.36	n.d.	n.d.	42.08	0.86	100.6

Sample Site	Al_2O_3	CaO	Cr_2O_3	FeO	MgO	MnO	Na_2O	Sc_2O_3	SiO_2	TiO_2	Total
17-DECS-013	17.21	4.65	8.75	7.24	20.02	0.51	n.d.	n.d.	41.43	n.d.	99.81
17-DECS-013	17.47	5.96	6.32	8.09	19.87	0.32	n.d.	n.d.	41.21	0.6	99.84
17-DECS-013	18.2	5.6	4.43	8.77	20.52	0.3	n.d.	n.d.	42.64	0.86	101.32
17-DECS-013	17.81	5.83	5.17	8.17	19.59	0.34	n.d.	n.d.	41.54	0.66	99.11
17-DECS-013	15.43	4.67	9.56	6.97	21.43	n.d.	n.d.	n.d.	41.84	0.32	100.22
17-DECS-013	18.05	5.67	4.88	8.63	20.04	0.37	n.d.	n.d.	41.64	1	100.28
17-DECS-013	17.8	5.68	4.9	8.7	20.14	n.d.	n.d.	n.d.	42.1	0.96	100.28
17-DECS-013	17.87	5.66	5.04	8.84	19.68	n.d.	n.d.	n.d.	41.71	0.88	99.68
17-DECS-013	17.92	5.29	4.61	8.97	19.93	n.d.	n.d.	n.d.	41.77	1.07	99.56
17-DECS-013	18.15	5.75	5.68	8.14	19.9	n.d.	n.d.	n.d.	42.1	0.83	100.55
17-DECS-013	17.1	5.69	6.18	7.39	20.5	n.d.	n.d.	n.d.	41.95	0.68	99.49
17-DECS-013	17.45	5.82	4.43	9.58	19.43	0.44	n.d.	n.d.	41.49	1.13	99.77
17-DECS-013	16.77	5.71	6.2	7.49	20.52	0.35	n.d.	n.d.	41.58	0.94	99.56
17-DECS-013	17.93	5.84	5.53	8.39	19.88	0.37	n.d.	n.d.	42.06	0.68	100.68

Sample Site	Al_2O_3	CaO	Cr_2O_3	FeO	MgO	MnO	Na_2O	Sc_2O_3	SiO_2	TiO_2	Total
17-DECS-013	17.26	5.62	6.06	7.54	20.85	n.d.	n.d.	n.d.	42.18	0.78	100.29
17-DECS-013	18.09	5.75	5.46	8.68	20.04	0.38	n.d.	n.d.	41.84	0.64	100.88
17-DECS-013	17.38	5.72	7.04	6.81	20.11	0.31	n.d.	n.d.	41.8	0.39	99.56
17-DECS-013	13.99	6.5	10.18	6.96	19.88	n.d.	n.d.	n.d.	40.94	0.98	99.43
17-DECS-013	17.54	5.67	5.09	8.77	19.78	0.47	n.d.	n.d.	41.63	0.78	99.73
17-DECS-013	17.87	5.85	5.54	8.2	20.04	0.42	n.d.	n.d.	42.23	0.76	100.91
17-DECS-013	19.16	5.01	2.5	8.53	20.67	0.36	n.d.	n.d.	41.94	0.84	99.01
17-DECS-013	17.51	5.71	6.24	7.42	20.66	0.32	n.d.	n.d.	41.59	0.78	100.23
17-DECS-013	17.52	5.71	4.99	8.56	19.66	n.d.	n.d.	n.d.	41.63	0.89	98.96
17-DECS-013	17.75	5.7	4.79	8.73	19.82	0.42	n.d.	n.d.	41.63	1.02	99.86
17-DECS-013	17.85	5.62	4.63	9	19.62	0.37	n.d.	n.d.	41.45	0.89	99.43
17-DECS-013	18.01	5.65	4.93	8.63	19.89	0.42	n.d.	n.d.	41.49	0.73	99.75
17-DECS-013	17.82	5.84	5.44	8.39	19.74	0.42	n.d.	n.d.	41.42	0.67	99.74
17-DECS-013	17.98	5.88	5.41	8.26	20.02	n.d.	n.d.	n.d.	41.57	0.67	99.79

Sample Site	Al_2O_3	CaO	Cr_2O_3	FeO	MgO	MnO	Na_2O	Sc_2O_3	SiO_2	TiO_2	Total
17-DECS-013	17.09	5.51	6.12	7.34	20.65	0.38	n.d.	n.d.	41.53	0.69	99.31
17-DECS-013	17.93	5.9	5.35	8.41	19.89	0.38	n.d.	n.d.	41.35	0.81	100.02
17-DECS-013	16.03	6.46	7.75	7.93	19.23	0.45	n.d.	n.d.	40.89	0.8	99.54
17-DECS-013	14.4	5.44	10.69	7.25	20.76	n.d.	n.d.	n.d.	40.75	0.32	99.61
17-DECS-013	14.98	5.93	9.37	7.46	20.15	n.d.	n.d.	n.d.	40.72	0.94	99.55
17-DECS-013	16.47	5.72	8.28	6.71	21.05	n.d.	n.d.	n.d.	41.75	0.47	100.45
17-DECS-013	17.86	5.64	4.85	8.66	19.68	0.37	n.d.	n.d.	41.16	0.9	99.12
17-DECS-013	14.36	5.26	10.83	7.09	20.53	n.d.	n.d.	n.d.	40.95	n.d.	99.02
17-DECS-013	17.89	5.6	4.81	8.72	20.14	0.3	n.d.	n.d.	40.83	1.02	99.31
17-DECS-013	17.5	5.77	5.61	7.44	20.95	0.36	n.d.	n.d.	42.04	0.83	100.5
17-DECS-013	14.84	4.25	10.85	6.5	21.25	0.42	n.d.	n.d.	41.11	0	99.22
17-DECS-013	17.59	5.68	5.94	7.44	21.31	0.34	n.d.	n.d.	41.28	0.67	100.25
17-DECS-013	17.45	6.35	7.16	6.84	20.15	0.41	n.d.	n.d.	41	n.d.	99.36
17-DECS-013	18.65	5.16	5.25	7.03	21.28	n.d.	n.d.	n.d.	42	0.5	99.87

Sample Site	Al_2O_3	CaO	Cr_2O_3	FeO	MgO	MnO	Na_2O	Sc_2O_3	SiO_2	TiO_2	Total
17-DECS-013	17.03	5.82	7.3	7.54	20.2	n.d.	n.d.	n.d.	41.58	0.47	99.94
17-DECS-013	15.68	6.22	8.34	7.48	19.88	0.45	n.d.	n.d.	40.72	0.8	99.57
17-DECS-013	13.32	5.7	12.88	6.92	20.89	n.d.	n.d.	n.d.	41.04	n.d.	100.75
17-DECS-013	14.49	5.22	10.55	7.26	20.78	0.38	n.d.	n.d.	40.86	0.42	99.96
17-DECS-013	19.77	6.61	5.14	7.61	18.97	0.58	n.d.	n.d.	41.3	n.d.	99.98
17-DECS-013	17.55	5.87	5.48	8.33	19.7	0.4	n.d.	n.d.	41.27	0.98	99.58
17-DECS-013	17.93	5.72	4.87	8.92	20.1	0.42	n.d.	n.d.	41.57	1.05	100.58
17-DECS-013	14.76	6.04	9.42	6.82	20.78	0.4	n.d.	n.d.	41.03	0.92	100.17
17-DECS-013	14.84	6.72	9.55	7.03	20.11	0.43	n.d.	n.d.	40.96	0.94	100.58
17-DECS-013	20.61	10	0.3	11.8	14.61	0.6	n.d.	n.d.	40.38	1.05	99.32
17-DECS-013	20.85	7.75	0.53	11.5	16.69	0.53	n.d.	n.d.	40.79	1.12	99.71
17-DECS-013	20.04	9.97	0.33	11.9	14.6	0.48	n.d.	n.d.	40.49	1.32	99.08
17-DECS-013	17.9	5.62	4.7	8.6	20	n.d.	n.d.	n.d.	41.2	0.96	98.98
17-DECS-013	19.54	4.74	2.66	9.8	19.77	0.56	n.d.	n.d.	41.16	1.19	99.42

Sample Site	Al_2O_3	CaO	Cr_2O_3	FeO	MgO	MnO	Na_2O	Sc_2O_3	SiO_2	TiO_2	Total
17-DECS-013	19.74	11.41	0.29	11.3	13.93	0.53	n.d.	n.d.	39.87	1.3	98.41
17-DECS-013	22.31	4.55	0.6	10.6	19.06	0.31	n.d.	n.d.	41.61	0.26	99.31
17-DECS-013	19.28	5.25	2.9	9.73	19.81	0.43	n.d.	n.d.	41.25	1.05	99.7
17-DECS-013	21.8	5.25	0.33	7.51	21.25	0.31	n.d.	n.d.	42.25	0.35	99.05
17-DECS-013	18.2	5.66	3.24	9.96	19.38	0.46	n.d.	n.d.	40.91	1.33	99.14
17-DECS-013	20.82	6.58	0.73	11.6	17.14	0.58	n.d.	n.d.	40.6	0.97	99
17-DECS-013	19.2	5.01	2.93	9.71	19.23	0.57	n.d.	n.d.	41.13	1.27	99.05
17-DECS-013	18.13	5.54	4.12	8.87	19.65	0.43	n.d.	n.d.	41.23	1.13	99.1
17-DECS-013	22.96	12.86	n.d.	9.57	13.58	0.37	n.d.	n.d.	40.72	n.d.	100.06
17-DECS-013	22.6	9.12	n.d.	12.2	14.75	n.d.	n.d.	n.d.	40.44	n.d.	99.08
17-DECS-013	20.61	8.05	0.47	11.8	16.47	0.49	n.d.	n.d.	40.86	0.98	99.69
17-DECS-013	20.29	9.21	0.31	11.8	15.45	0.43	n.d.	n.d.	40.43	1.21	99.08
17-DECS-013	16.87	35.45	n.d.	7.31	n.d.	1	n.d.	n.d.	37.62	n.d.	98.25
17-DECS-013	18.89	6.01	3.3	9.88	18.74	0.41	n.d.	n.d.	41.09	1.1	99.42

Sample Site	Al_2O_3	CaO	Cr_2O_3	FeO	MgO	MnO	Na_2O	Sc_2O_3	SiO_2	TiO_2	Total
17-DECS-003	16.31	8.39	9.2	8.32	18.19	0.31	n.d.	n.d.	39.06	n.d.	99.78
17-DECS-015	17.57	5.65	4.51	9.36	21.45	0.37	n.d.	n.d.	40.6	0.85	100.36
17-DECS-015	21.39	1.26	n.d.	30.6	9.92	0.63	n.d.	n.d.	37.83	n.d.	101.63
17-DECS-017	17.62	5.59	5.23	8.27	22.25	n.d.	n.d.	n.d.	40.88	0.71	100.55
17-DECS-017	0.5	n.d.	1.54	42.1	9.63	n.d.	n.d.	n.d.	n.d.	47.07	100.83
17-DECS-020	21.05	35.5	n.d.	3.95	n.d.	0.79	n.d.	n.d.	38.64	n.d.	99.93
17-DECS-018	17.97	5.46	5.85	8.15	21.94	0.38	n.d.	n.d.	40.96	n.d.	100.71
17-DECS-018	17.05	5.77	5.17	9.19	21.83	0.3	n.d.	n.d.	40.7	0.72	100.73
17-DECS-013	17.96	5.61	4.61	9.31	19.62	n.d.	n.d.	n.d.	41.21	0.88	99.2
17-DECS-013	18.17	5.65	5.84	6.93	21.12	0.39	n.d.	n.d.	41.19	n.d.	99.29
17-DECS-013	17.06	5.86	5.8	7.9	20.63	0.28	n.d.	n.d.	40.75	0.81	99.09
17-DECS-013	17.68	5.64	5.36	7.95	20.93	n.d.	n.d.	n.d.	41.26	0.73	99.55
17-DECS-013	18.22	5.72	5.77	7.04	20.75	0.39	n.d.	n.d.	41.24	n.d.	99.13
17-DECS-013	17.99	5.7	4.71	9.22	20.06	0.28	n.d.	n.d.	41.01	0.7	99.67

Sample Site	**Al_2O_3**	**CaO**	**Cr_2O_3**	**FeO**	**MgO**	**MnO**	**Na_2O**	**Sc_2O_3**	**SiO_2**	**TiO_2**	**Total**
17-DECS-013	18.13	6.1	4.9	8.58	19.71	0.33	n.d.	n.d.	40.58	0.74	99.07
17-DECS-013	18.11	5.66	6.23	6.93	21.29	0.3	n.d.	n.d.	41.19	n.d.	99.71
17-DECS-013	14.46	6.92	10.01	7.61	19.72	n.d.	n.d.	n.d.	40.28	0.54	99.54
17-DECS-013	17.7	5.82	5.5	7.75	20.61	n.d.	n.d.	n.d.	41.05	0.79	99.22
17-DECS-013	17.67	5.95	5.11	8.71	19.93	n.d.	n.d.	n.d.	40.95	0.77	99.09
17-DECS-013	19.34	5.01	3.95	7.35	21.07	n.d.	n.d.	n.d.	41.78	0.5	99
17-DECS-013	17.9	5.82	4.57	9.27	20.07	0.42	n.d.	n.d.	40.48	0.98	99.51
17-DECS-013	19.77	4.87	3.56	7.33	21.53	n.d.	n.d.	n.d.	41.74	0.36	99.16
17-DECS-013	17.87	5.8	6.08	7.39	20.6	0.35	n.d.	n.d.	40.92	n.d.	99.01
17-DECS-013	17.03	5.97	5.97	7.89	20.64	n.d.	n.d.	n.d.	41.53	0.74	99.77
17-DECS-013	18.48	5.84	5.85	7.3	20.38	0.31	n.d.	n.d.	40.84	n.d.	99
17-DECS-013	16.91	6.13	5.73	8.42	20.12	0.36	n.d.	n.d.	40.97	0.81	99.45
17-DECS-013	17.79	5.84	4.66	9.38	20.05	n.d.	n.d.	n.d.	40.33	0.96	99.01
17-DECS-013	17.33	5.64	5.05	7.81	20.94	0.35	n.d.	n.d.	40.94	0.77	98.83

Sample Site	Al_2O_3	CaO	Cr_2O_3	FeO	MgO	MnO	Na_2O	Sc_2O_3	SiO_2	TiO_2	Total
17-DECS-013	18.34	5.8	4.58	9.12	19.85	0.3	n.d.	n.d.	40.47	0.84	99.3
17-DECS-013	17.46	5.74	4.23	9.13	20.2	0.41	n.d.	n.d.	41.26	0.77	99.2
17-DECS-013	18.3	5.47	5.97	6.58	21.02	0.35	n.d.	n.d.	41.43	n.d.	99.12
17-DECS-013	16.9	5.66	5.67	7.74	21.23	n.d.	n.d.	n.d.	41.68	0.74	99.62
17-DECS-013	16.76	5.64	5.67	7.93	20.93	n.d.	n.d.	n.d.	41.38	0.74	99.05
17-DECS-013	14.09	5.14	10.32	7.25	21.19	n.d.	n.d.	n.d.	41.21	0.34	99.54
17-DECS-013	17.72	5.6	4.5	8.58	20.25	0.45	n.d.	n.d.	41.38	0.73	99.21
17-DECS-013	17.93	6.06	5.61	7.23	20.45	0.32	n.d.	n.d.	41.5	n.d.	99.1
17-DECS-013	16.23	6.33	7.09	7.66	20.09	n.d.	n.d.	n.d.	40.81	0.81	99.02
17-DECS-013	17.24	5.93	6.29	7.01	21.06	0.35	n.d.	n.d.	41.54	0.55	99.97
17-DECS-013	16.94	5.37	7.04	6.75	21.55	n.d.	n.d.	n.d.	41.41	n.d.	99.06
17-DECS-013	17.69	5.38	5.57	7.57	21.16	n.d.	n.d.	n.d.	41.6	0.46	99.43
17-DECS-013	17	5.79	5.76	7.51	21.2	n.d.	n.d.	n.d.	41.6	0.61	99.47
17-DECS-013	21.09	4.95	3.04	8.26	20.43	0.48	n.d.	n.d.	41.3	n.d.	99.55

Sample Site	Al_2O_3	CaO	Cr_2O_3	FeO	MgO	MnO	Na_2O	Sc_2O_3	SiO_2	TiO_2	Total
17-DECS-013	20.41	6.07	4.1	7.12	19.96	0.48	n.d.	n.d.	41.08	n.d.	99.22
17-DECS-013	19.66	5.17	3.37	7.4	21.6	0.29	n.d.	n.d.	41.65	0.26	99.4
17-DECS-013	18.97	4.78	4.11	7.13	22.06	n.d.	n.d.	n.d.	42.33	0.41	99.79
17-DECS-013	14.25	4.38	10.85	6.58	21.52	0.48	n.d.	n.d.	41.17	n.d.	99.23
17-DECS-013	12.77	7.21	10.92	7.43	19.72	n.d.	n.d.	n.d.	40.44	1	99.49
17-DECS-013	17.79	5.95	5.01	8.45	20.03	0.35	n.d.	n.d.	41.4	0.58	99.56
17-DECS-013	18.64	5.88	5.13	7.42	21.11	n.d.	n.d.	n.d.	41.66	n.d.	99.84
17-DECS-013	16.61	6.18	6.06	8.99	19.67	0.35	n.d.	n.d.	40.66	0.94	99.46
17-DECS-013	17.59	5.97	5.89	8.31	20.11	0.37	n.d.	n.d.	41.66	0.66	100.56
17-DECS-013	18.64	5.16	4.69	7.64	21.33	0.41	n.d.	n.d.	41.96	0.47	100.3
17-DECS-013	17.22	5.88	5.51	7.9	20.7	0.39	n.d.	n.d.	40.77	0.79	99.16
17-DECS-013	17.88	5.74	5.14	7.55	20.7	0.37	n.d.	n.d.	41.8	0.87	100.05
17-DECS-013	17.48	5.93	6.25	7.02	21.58	n.d.	n.d.	n.d.	42.15	0.57	100.98
17-DECS-013	17.63	5.59	5.24	7.63	21.49	n.d.	n.d.	n.d.	42.01	0.65	100.24

Sample Site	Al_2O_3	CaO	Cr_2O_3	FeO	MgO	MnO	Na_2O	Sc_2O_3	SiO_2	TiO_2	Total
17-DECS-013	17.32	5.95	5.83	8.22	19.98	0.39	n.d.	n.d.	41.21	0.63	99.79
17-DECS-013	18.02	5.84	6.06	7.07	21	0.31	n.d.	n.d.	41.45	n.d.	99.75
17-DECS-013	17.21	5.88	5.81	9.04	20.28	n.d.	n.d.	n.d.	40.77	0.97	99.96
17-DECS-013	17.57	5.32	5.25	7.74	20.95	n.d.	n.d.	n.d.	41.94	0.59	99.36
17-DECS-013	18.15	5.7	4.34	9.06	20.23	0.45	n.d.	n.d.	41.45	0.94	100.32
17-DECS-013	14.28	5.99	9.51	6.79	20.83	0.31	n.d.	n.d.	40.81	0.8	99.32
17-DECS-013	17.79	5.79	6.37	6.55	21.21	0.43	n.d.	n.d.	41.4	n.d.	99.54
17-DECS-013	17.75	5.81	4.46	9.24	20.23	0.38	n.d.	n.d.	40.73	0.92	99.52
17-DECS-013	21.37	5.32	3.32	7.5	20.43	0.39	n.d.	n.d.	41.42	n.d.	99.75
17-DECS-013	18.05	5.73	4.79	8.51	20.87	0.43	n.d.	n.d.	41.46	0.73	100.57
17-DECS-013	18.1	5.71	4.71	8.52	20.26	0.38	n.d.	n.d.	41.5	0.68	99.86
17-DECS-013	14.93	6.13	8.65	6.78	20.8	n.d.	n.d.	n.d.	41.12	0.74	99.15
17-DECS-013	17.14	5.63	5.57	7.48	20.75	0.42	n.d.	n.d.	41.65	0.51	99.15
17-DECS-013	18.2	5.77	3.98	9.75	19.84	0.35	n.d.	n.d.	41.14	0.92	99.95

Sample Site	Al_2O_3	CaO	Cr_2O_3	FeO	MgO	MnO	Na_2O	Sc_2O_3	SiO_2	TiO_2	Total
17-DECS-013	19	5.3	3.62	7.73	21.34	0.41	n.d.	n.d.	41.5	0.8	99.7
17-DECS-013	19.4	10.19	0.3	12.3	14.87	0.53	n.d.	n.d.	40.26	1.4	99.27
17-DECS-013	20.76	9.78	0.55	12.5	15.04	0.57	n.d.	n.d.	40.57	0.75	100.54
17-DECS-013	18.83	5.27	2.96	10.2	19.74	0.46	n.d.	n.d.	41.11	0.99	99.54
17-DECS-013	17.96	5.74	4.44	8.77	20.3	0.39	n.d.	n.d.	41.45	0.91	99.96
17-DECS-013	17.78	5.5	4.58	9.2	20.35	0.39	n.d.	n.d.	41.28	1.03	100.11
17-DECS-013	17.97	5.55	4.34	9.28	20.34	n.d.	n.d.	n.d.	41.07	1.03	99.58
17-DECS-013	17.87	5.6	4.13	9.54	19.99	0.31	n.d.	n.d.	40.58	1.27	99.29
17-DECS-013	18.14	5.83	3.85	9.67	19.58	0.32	n.d.	n.d.	40.94	1.06	99.39
17-DECS-013	17.6	6.12	5.21	9.07	20.3	n.d.	n.d.	n.d.	41.05	0.89	100.24
17-DECS-013	17.99	5.91	4.01	9.72	19.74	0.43	n.d.	n.d.	41.22	0.86	99.88
17-DECS-013	18.01	5.57	5.91	7.55	20.79	0.4	n.d.	n.d.	41.84	n.d.	100.07
17-DECS-013	20.68	3.18	n.d.	36.5	2.83	0.61	n.d.	n.d.	37.2	n.d.	100.95
17-DECS-013	18.01	5.57	5.91	7.55	20.79	0.4	n.d.	n.d.	41.84	n.d.	100.07

Sample Site	Al_2O_3	CaO	Cr_2O_3	FeO	MgO	MnO	Na_2O	Sc_2O_3	SiO_2	TiO_2	Total
17-DECS-013	18.02	5.84	4.85	8.47	19.9	0.37	n.d.	n.d.	41.26	0.69	99.4
17-DECS-013	17.98	6	5.09	8.73	20.47	0.41	n.d.	n.d.	41.32	0.54	100.54
17-DECS-013	16.65	5.98	6.54	7.12	21.02	n.d.	n.d.	n.d.	41.38	0.81	99.5
17-DECS-013	17.17	5.84	5.43	7.83	21.15	n.d.	n.d.	n.d.	42.03	0.74	100.19
17-DECS-013	21.22	5.66	3.17	7.6	20.38	0.55	n.d.	n.d.	41.34	n.d.	99.92
17-DECS-013	17.28	5.7	5.39	7.74	21.2	0.37	n.d.	n.d.	41.94	0.68	100.3
17-DECS-013	16.99	5.91	7.42	6.73	21.06	0.36	n.d.	n.d.	41.5	n.d.	99.97
17-DECS-013	15.25	5.39	8.8	6.77	21.18	0.35	n.d.	n.d.	41.02	0.52	99.28
17-DECS-013	17.47	5.88	5.2	8.5	20.74	0.32	n.d.	n.d.	41.44	0.82	100.37
17-DECS-013	18.33	5.56	4.18	8.11	21.11	n.d.	n.d.	n.d.	41.59	0.74	99.62
17-DECS-013	17.75	5.74	4.83	7.28	21.01	0.34	n.d.	n.d.	41.35	0.7	99
17-DECS-013	17.57	5.27	5.18	7.64	21.41	0.32	n.d.	n.d.	41.64	0.69	99.72
17-DECS-013	18.13	5.79	4.81	8.48	20.31	0.38	n.d.	n.d.	41.37	0.71	99.98
17-DECS-013	18.01	5.81	5.82	6.91	20.86	0.4	n.d.	n.d.	41.89	n.d.	99.7

Sample Site	Al_2O_3	CaO	Cr_2O_3	FeO	MgO	MnO	Na_2O	Sc_2O_3	SiO_2	TiO_2	Total
17-DECS-013	17.98	5.69	6.68	7.94	19.61	0.57	n.d.	n.d.	41.06	n.d.	99.53
17-DECS-013	16.43	5.73	5.91	8.51	21.75	0.44	n.d.	n.d.	39.98	0.81	99.56
17-DECS-013	17.51	5.49	4.86	9.25	21.47	0.38	n.d.	n.d.	39.64	0.72	99.32
17-DECS-013	16.65	5.79	6.41	8.18	21.69	n.d.	n.d.	n.d.	39.87	0.7	99.29
17-DECS-013	16.74	5.71	5.8	8.45	21.59	0.42	n.d.	n.d.	40.02	0.82	99.55
17-DECS-013	17.63	5.64	5.09	9.57	21.29	0.37	n.d.	n.d.	40.37	0.69	100.65
17-DECS-013	18.78	5.04	3.66	9.32	21.98	n.d.	n.d.	n.d.	41.1	0.69	100.57
17-DECS-013	17.49	5.76	5.51	9.32	21.17	0.28	n.d.	n.d.	40.3	0.84	100.67
17-DECS-013	16.43	6.09	5.95	9.3	20.82	0.3	n.d.	n.d.	39.84	0.91	99.64
17-DECS-013	17.75	5.81	4.96	9.31	21.12	n.d.	n.d.	n.d.	39.95	0.73	99.63
17-DECS-013	17.51	5.53	4.16	10.3	20.94	0.3	n.d.	n.d.	39.77	0.93	99.4
17-DECS-013	14.79	6.09	10.1	8.05	20.84	n.d.	n.d.	n.d.	39.78	0.52	100.17
17-DECS-013	18	5.56	5.61	8.12	21.83	0.39	n.d.	n.d.	40.29	n.d.	99.8
17-DECS-013	16.85	5.61	5.95	8.54	22.11	n.d.	n.d.	n.d.	40.17	0.69	99.92

Sample Site	Al_2O_3	CaO	Cr_2O_3	FeO	MgO	MnO	Na_2O	Sc_2O_3	SiO_2	TiO_2	Total
17-DECS-013	17.68	5.92	4.97	9.26	21.2	0.34	n.d.	n.d.	40.13	0.73	100.23
17-DECS-013	12.34	6.65	12.49	7.89	20.06	n.d.	n.d.	n.d.	39.47	0.63	99.53
17-DECS-013	17.23	5.74	5.16	9.43	21.06	n.d.	n.d.	n.d.	39.76	0.64	99.02
17-DECS-013	17.23	5.71	5.16	9.25	20.83	n.d.	n.d.	n.d.	40.16	0.77	99.11
17-DECS-013	17.35	5.9	5.04	9.49	21.31	0.35	n.d.	n.d.	40.73	0.74	100.91
17-DECS-013	17.65	5.56	4.23	9.67	21.38	0.5	n.d.	n.d.	40.16	0.91	100.06
17-DECS-013	16.15	6.19	7.25	8.6	21	0.43	n.d.	n.d.	39.52	0.74	99.88
17-DECS-013	20.77	7.82	0.6	11.1	16.92	0.49	n.d.	n.d.	40.69	0.97	99.38
17-DECS-013	18.1	5.83	4.7	8.34	20.5	0.4	n.d.	n.d.	41.79	0.84	100.5
17-DECS-013	18.16	5.65	4.65	8.62	20.57	n.d.	n.d.	n.d.	41.54	0.87	100.06
17-DECS-013	21.93	4.99	2.38	7.36	20.2	0.31	n.d.	n.d.	41.92	n.d.	99.09
17-DECS-013	18.14	5.82	5.1	8	19.86	0.33	n.d.	n.d.	41.23	0.8	99.28
17-DECS-013	17.3	5.88	5.92	7.28	20.84	0.38	n.d.	n.d.	41.54	0.84	99.98
17-DECS-013	16.5	6.03	7.48	6.63	20.63	n.d.	n.d.	n.d.	41.08	0.79	99.14

Sample Site	Al_2O_3	CaO	Cr_2O_3	FeO	MgO	MnO	Na_2O	Sc_2O_3	SiO_2	TiO_2	Total
17-DECS-013	17.71	5.56	5.02	8.81	19.64	0.44	n.d.	n.d.	41.28	1.11	99.57
17-DECS-013	17.86	5.78	5.47	7.79	20.04	0.47	n.d.	n.d.	41.41	0.68	99.5
17-DECS-013	17.82	5.57	4.78	8.28	19.91	0.38	n.d.	n.d.	41.6	0.8	99.14
17-DECS-013	17.86	5.89	5.03	8.9	20.23	n.d.	n.d.	n.d.	41.56	1.01	100.48
17-DECS-013	17.03	5.93	6.21	7.23	21.13	n.d.	n.d.	n.d.	42.19	0.67	100.39
17-DECS-013	17.55	6	5.96	7.29	20.41	0.31	n.d.	n.d.	41.09	0.7	99.31
17-DECS-013	16.93	5.78	6.08	7.65	20.77	0.33	n.d.	n.d.	41.47	0.72	99.73
17-DECS-013	17.31	5.65	6.1	7.28	20.79	n.d.	n.d.	n.d.	41.55	0.77	99.45
17-DECS-013	18.19	5.57	4.51	8.6	20.09	n.d.	n.d.	n.d.	41.31	1.07	99.34
17-DECS-013	18.07	5.82	4.8	8.46	20.32	0.35	n.d.	n.d.	41.62	0.9	100.34
17-DECS-013	17.6	5.68	5.21	9.1	19.37	n.d.	n.d.	n.d.	41.25	1.14	99.35
17-DECS-013	20.72	7.36		26.6	5.65	1.01	n.d.	n.d.	38.03	n.d.	99.32
17-DECS-013	17.87	5.79	4.17	9.3	19.78	n.d.	n.d.	n.d.	41.36	1.05	99.32
17-DECS-013	18.25	5.7	5.19	8.47	20.13	0.39	n.d.	n.d.	41.48	0.76	100.37

Sample Site	Al_2O_3	CaO	Cr_2O_3	FeO	MgO	MnO	Na_2O	Sc_2O_3	SiO_2	TiO_2	Total
17-DECS-013	16.6	14.9	7.63	6.28	14.78	n.d.	n.d.	n.d.	39.28	n.d.	99.47
17-DECS-013	20.13	0.59	n.d.	24.8	1.73	15.83	n.d.	n.d.	36.01	n.d.	99.12
17-DECS-013	20.7	7.89	n.d.	26.3	5.46	1.02	n.d.	n.d.	38.12	n.d.	99.52
17-DECS-013	20.45	9.87	0.65	12.1	14.72	0.54	n.d.	n.d.	40.28	0.87	99.43
17-DECS-013	20.57	7.12	n.d.	26.1	5.71	0.96	n.d.	n.d.	37.62	n.d.	98.04
17-DECS-013	20.26	0.44	n.d.	25.5	2.05	14.24	n.d.	n.d.	36.52	n.d.	99.01
17-DECS-013	20.67	7.18	n.d.	26.3	5.58	1.11	n.d.	n.d.	37.65	n.d.	98.46
17-DECS-013	20.5	7.56	n.d.	25.8	5.46	0.88	n.d.	n.d.	38.12	n.d.	98.33
17-DECS-013	21.18	8.28	0.4	11.3	16.27	0.52	n.d.	n.d.	40.67	0.8	99.4
17-DECS-013	21.39	7.55	n.d.	20.7	9.33	0.45	n.d.	n.d.	38.69	n.d.	98.14
17-DECS-013	22.06	6.39	n.d.	19.1	11.16	0.47	n.d.	n.d.	39.2	n.d.	98.39
17-DECS-013	20.34	0.39	n.d.	26.8	1.53	14.08	n.d.	n.d.	35.76	n.d.	98.87
17-DECS-013	21	6.79	n.d.	25.2	7.07	0.75	n.d.	n.d.	38.55	n.d.	99.33
17-DECS-013	19.9	6.2	0.56	12.3	17.88	0.41	n.d.	n.d.	41.17	1.48	99.86

Sample Site	Al_2O_3	CaO	Cr_2O_3	FeO	MgO	MnO	Na_2O	Sc_2O_3	SiO_2	TiO_2	Total
17-DECS-013	2.52	16.87	n.d.	12.1	16.1	0	n.d.	n.d.	51.82	0.78	100.18
17-DECS-013	20.74	7.36	n.d.	27.4	5.75	0.8	n.d.	n.d.	38.16	n.d.	100.23
17-DECS-013	20.95	6.92	n.d.	27.7	5.79	0.86	n.d.	n.d.	38.56	n.d.	100.76
17-DECS-013	21.35	8.68	n.d.	26.7	4.9	0.89	n.d.	n.d.	38.4	n.d.	100.96
17-DECS-013	21.06	7.06	n.d.	27	6.23	0.89	n.d.	n.d.	38.99	n.d.	101.2
17-DECS-013	21.19	6.94	n.d.	26.6	6.35	0.84	n.d.	n.d.	38.51	n.d.	100.39
17-DECS-013	21	7.01	n.d.	28.4	5.15	0.67	n.d.	n.d.	38.07	n.d.	100.31
17-DECS-013	20.85	7.83	n.d.	27.1	5.58	0.88	n.d.	n.d.	38.35	n.d.	100.54
17-DECS-013	21.36	6.81	n.d.	26.8	6.16	0.6	n.d.	n.d.	38.53	n.d.	100.3
17-DECS-013	20.66	1.31	n.d.	38.7	2.08	0.79	n.d.	n.d.	36.55	n.d.	100.1
17-DECS-013	20.49	0.29	n.d.	27.5	1.9	12.76	n.d.	n.d.	36.85	n.d.	99.78
17-DECS-013	20.69	0.3	n.d.	27.2	1.89	12.9	n.d.	n.d.	36.61	n.d.	99.6

Table 7.2: G Number classification based on criteria by Grütter et al. (2004) via excel functions *IF and AND.

Sample Site	**G Number**	**G1**	**G11**	**G10**	**G9**	**G12**	**G5**	**G4**	**G3**	**CA_INT**	**MGNUM**
17-DECS-016	G9	Negative	Negative	Negative	Positive	Negative	Negative	Negative	Negative	4.3775	0.8263
17-DECS-016	G9	Negative	Negative	Negative	Positive	Negative	Negative	Negative	Negative	4.6925	0.8132
17-DECS-016	G9	Negative	Negative	Negative	Positive	Negative	Negative	Negative	Negative	4.3675	0.8380
17-DECS-016	G9	Negative	Negative	Negative	Positive	Negative	Negative	Negative	Negative	4.5125	0.8023
17-DECS-016	G9	Negative	Negative	Negative	Positive	Negative	Negative	Negative	Negative	4.1400	0.8408
17-DECS-016	G9	Negative	Negative	Negative	Positive	Negative	Negative	Negative	Negative	5.0850	0.7799
17-DECS-016	G9	Negative	Negative	Negative	Positive	Negative	Negative	Negative	Negative	4.1875	0.8423
17-DECS-016	G9	Negative	Negative	Negative	Positive	Negative	Negative	Negative	Negative	3.5275	0.8088
17-DECS-016	G1	Positive	Negative	Negative	Negative	Negative	Negative	Negative	Negative	5.0725	0.7776
17-DECS-013	G9	Negative	Negative	Negative	Positive	Negative	Negative	Negative	Negative	4.0000	0.8309
17-DECS-013	G9	Negative	Negative	Negative	Positive	Negative	Negative	Negative	Negative	4.3500	0.7928
17-DECS-013	G9	Negative	Negative	Negative	Positive	Negative	Negative	Negative	Negative	3.6025	0.8509
17-DECS-013	G9	Negative	Negative	Negative	Positive	Negative	Negative	Negative	Negative	4.3750	0.8181

Sample Site	G Number	G1	G11	G10	G9	G12	G5	G4	G3	CA_INT	MGNUM
17-DECS-013	G9	Negative	Negative	Negative	Positive	Negative	Negative	Negative	Negative	4.5100	0.8122
17-DECS-013	G9	Negative	Negative	Negative	Positive	Negative	Negative	Negative	Negative	4.2900	0.8066
17-DECS-013	G9	Negative	Negative	Negative	Positive	Negative	Negative	Negative	Negative	4.9475	0.8393
17-DECS-013	G9	Negative	Negative	Negative	Positive	Negative	Negative	Negative	Negative	4.4375	0.7993
17-DECS-013	G9	Negative	Negative	Negative	Positive	Negative	Negative	Negative	Negative	4.3575	0.8069
17-DECS-013	G9	Negative	Negative	Negative	Positive	Negative	Negative	Negative	Negative	3.9750	0.8315
17-DECS-013	G10	Negative	Negative	Positive	Negative	Negative	Negative	Negative	Negative	2.8213	0.8314
17-DECS-013	G9	Negative	Negative	Negative	Positive	Negative	Negative	Negative	Negative	4.3800	0.8141
17-DECS-013	G9	Negative	Negative	Negative	Positive	Negative	Negative	Negative	Negative	4.4925	0.8066
17-DECS-013	G9	Negative	Negative	Negative	Positive	Negative	Negative	Negative	Negative	4.5375	0.8104
17-DECS-013	G10	Negative	Negative	Positive	Negative	Negative	Negative	Negative	Negative	2.7340	0.8457
17-DECS-013	G9	Negative	Negative	Negative	Positive	Negative	Negative	Negative	Negative	4.4500	0.8055
17-DECS-013	G9	Negative	Negative	Negative	Positive	Negative	Negative	Negative	Negative	4.4550	0.8050
17-DECS-013	G9	Negative	Negative	Negative	Positive	Negative	Negative	Negative	Negative	4.4000	0.7988

Sample Site	G Number	G1	G11	G10	G9	G12	G5	G4	G3	CA_INT	MGNUM
17-DECS-013	G9	Negative	Negative	Negative	Positive	Negative	Negative	Negative	Negative	4.1375	0.7984
17-DECS-013	G9	Negative	Negative	Negative	Positive	Negative	Negative	Negative	Negative	4.3300	0.8134
17-DECS-013	G9	Negative	Negative	Negative	Positive	Negative	Negative	Negative	Negative	4.1450	0.8318
17-DECS-013	G9	Negative	Negative	Negative	Positive	Negative	Negative	Negative	Negative	4.7125	0.7834
17-DECS-013	G9	Negative	Negative	Negative	Positive	Negative	Negative	Negative	Negative	4.1600	0.8301
17-DECS-013	G9	Negative	Negative	Negative	Positive	Negative	Negative	Negative	Negative	4.4575	0.8086
17-DECS-013	G9	Negative	Negative	Negative	Positive	Negative	Negative	Negative	Negative	4.1050	0.8314
17-DECS-013	G9	Negative	Negative	Negative	Positive	Negative	Negative	Negative	Negative	4.3850	0.8045
17-DECS-013	G9	Negative	Negative	Negative	Positive	Negative	Negative	Negative	Negative	3.9600	0.8404
17-DECS-013	G9	Negative	Negative	Negative	Positive	Negative	Negative	Negative	Negative	3.9550	0.8359
17-DECS-013	G9	Negative	Negative	Negative	Positive	Negative	Negative	Negative	Negative	4.3975	0.8008
17-DECS-013	G9	Negative	Negative	Negative	Positive	Negative	Negative	Negative	Negative	4.4650	0.8133
17-DECS-013	G9	Negative	Negative	Negative	Positive	Negative	Negative	Negative	Negative	4.1500	0.8323
17-DECS-013	G9	Negative	Negative	Negative	Positive	Negative	Negative	Negative	Negative	4.4625	0.8037

Sample Site	G Number	G1	G11	G10	G9	G12	G5	G4	G3	CA_INT	MGNUM
17-DECS-013	G9	Negative	Negative	Negative	Positive	Negative	Negative	Negative	Negative	4.5025	0.8019
17-DECS-013	G9	Negative	Negative	Negative	Positive	Negative	Negative	Negative	Negative	4.4625	0.7954
17-DECS-013	G9	Negative	Negative	Negative	Positive	Negative	Negative	Negative	Negative	4.4175	0.8043
17-DECS-013	G9	Negative	Negative	Negative	Positive	Negative	Negative	Negative	Negative	4.4800	0.8075
17-DECS-013	G9	Negative	Negative	Negative	Positive	Negative	Negative	Negative	Negative	4.5275	0.8121
17-DECS-013	G9	Negative	Negative	Negative	Positive	Negative	Negative	Negative	Negative	3.9800	0.8338
17-DECS-013	G9	Negative	Negative	Negative	Positive	Negative	Negative	Negative	Negative	4.5625	0.8083
17-DECS-013	G9	Negative	Negative	Negative	Positive	Negative	Negative	Negative	Negative	4.5225	0.8122
17-DECS-013	G10	Negative	Negative	Positive	Negative	Negative	Negative	Negative	Negative	3.0360	0.8362
17-DECS-013	G9	Negative	Negative	Negative	Positive	Negative	Negative	Negative	Negative	3.5875	0.8281
17-DECS-013	G9	Negative	Negative	Negative	Positive	Negative	Negative	Negative	Negative	3.6500	0.8483
17-DECS-013	G9	Negative	Negative	Negative	Positive	Negative	Negative	Negative	Negative	4.4275	0.8020
17-DECS-013	G10	Negative	Negative	Positive	Negative	Negative	Negative	Negative	Negative	2.9186	0.8377
17-DECS-013	G9	Negative	Negative	Negative	Positive	Negative	Negative	Negative	Negative	4.3975	0.8046

Sample Site	G Number	G1	G11	G10	G9	G12	G5	G4	G3	CA_INT	MGNUM
17-DECS-013	G9	Negative	Negative	Negative	Positive	Negative	Negative	Negative	Negative	4.3675	0.8339
17-DECS-013	G10	Negative	Negative	Positive	Negative	Negative	Negative	Negative	Negative	2.3563	0.8536
17-DECS-013	G9	Negative	Negative	Negative	Positive	Negative	Negative	Negative	Negative	4.1950	0.8362
17-DECS-013	G9	Negative	Negative	Negative	Positive	Negative	Negative	Negative	Negative	4.5600	0.8401
17-DECS-013	G9	Negative	Negative	Negative	Positive	Negative	Negative	Negative	Negative	3.8475	0.8437
17-DECS-013	G9	Negative	Negative	Negative	Positive	Negative	Negative	Negative	Negative	3.9950	0.8269
17-DECS-013	G9	Negative	Negative	Negative	Positive	Negative	Negative	Negative	Negative	4.1350	0.8257
17-DECS-013	G10	Negative	Negative	Positive	Negative	Negative	Negative	Negative	Negative	2.9170	0.8433
17-DECS-013	G10	Negative	Negative	Positive	Negative	Negative	Negative	Negative	Negative	2.9301	0.8361
17-DECS-013	G9	Negative	Negative	Negative	Positive	Negative	Negative	Negative	Negative	5.3250	0.8163
17-DECS-013	G9	Negative	Negative	Negative	Positive	Negative	Negative	Negative	Negative	4.5000	0.8083
17-DECS-013	G9	Negative	Negative	Negative	Positive	Negative	Negative	Negative	Negative	4.5025	0.8007
17-DECS-013	G9	Negative	Negative	Negative	Positive	Negative	Negative	Negative	Negative	3.6850	0.8445
17-DECS-013	G9	Negative	Negative	Negative	Positive	Negative	Negative	Negative	Negative	4.3325	0.8361

Sample Site	G Number	G1	G11	G10	G9	G12	G5	G4	G3	CA_INT	MGNUM
17-DECS-013	G9	Negative	Negative	Negative	Positive	Negative	Negative	Negative	Negative	4.4450	0.8057
17-DECS-013	G1	Positive	Negative	Negative	Negative	Negative	Negative	Negative	Negative	4.0750	0.7825
17-DECS-013	G1	Positive	Negative	Negative	Negative	Negative	Negative	Negative	Negative	4.5250	0.7840
17-DECS-013	G1	Positive	Negative	Negative	Negative	Negative	Negative	Negative	Negative	4.8500	0.7762
17-DECS-013	G1	Positive	Negative	Negative	Negative	Negative	Negative	Negative	Negative	4.2775	0.7793
17-DECS-013	G9	Negative	Negative	Negative	Positive	Negative	Negative	Negative	Negative	4.5100	0.7980
17-DECS-013	G3	Negative	Negative	Negative	Negative	Negative	Negative	Negative	Positive	9.1200	0.6836
17-DECS-013	G1	Positive	Negative	Negative	Negative	Negative	Negative	Negative	Negative	5.1850	0.7718
17-DECS-003	G12	Negative	Negative	Negative	Negative	Positive	Negative	Negative	Negative	6.0900	0.7958
17-DECS-015	G9	Negative	Negative	Negative	Positive	Negative	Negative	Negative	Negative	4.5225	0.8034
17-DECS-017	G9	Negative	Negative	Negative	Positive	Negative	Negative	Negative	Negative	4.2825	0.8275
17-DECS-018	G9	Negative	Negative	Negative	Positive	Negative	Negative	Negative	Negative	3.9975	0.8276
17-DECS-018	G9	Negative	Negative	Negative	Positive	Negative	Negative	Negative	Negative	4.4775	0.8090
17-DECS-013	G9	Negative	Negative	Negative	Positive	Negative	Negative	Negative	Negative	4.4575	0.7898

Sample Site	G Number	G1	G11	G10	G9	G12	G5	G4	G3	CA_INT	MGNUM
17-DECS-013	G9	Negative	Negative	Negative	Positive	Negative	Negative	Negative	Negative	4.1900	0.8446
17-DECS-013	G9	Negative	Negative	Negative	Positive	Negative	Negative	Negative	Negative	4.4100	0.8232
17-DECS-013	G9	Negative	Negative	Negative	Positive	Negative	Negative	Negative	Negative	4.3000	0.8244
17-DECS-013	G9	Negative	Negative	Negative	Positive	Negative	Negative	Negative	Negative	4.2775	0.8401
17-DECS-013	G9	Negative	Negative	Negative	Positive	Negative	Negative	Negative	Negative	4.5225	0.7950
17-DECS-013	G9	Negative	Negative	Negative	Positive	Negative	Negative	Negative	Negative	4.8750	0.8038
17-DECS-013	G9	Negative	Negative	Negative	Positive	Negative	Negative	Negative	Negative	4.1025	0.8456
17-DECS-013	G9	Negative	Negative	Negative	Positive	Negative	Negative	Negative	Negative	4.4175	0.8221
17-DECS-013	G9	Negative	Negative	Negative	Positive	Negative	Negative	Negative	Negative	4.4450	0.8258
17-DECS-013	G9	Negative	Negative	Negative	Positive	Negative	Negative	Negative	Negative	4.6725	0.8031
17-DECS-013	G1	Positive	Negative	Negative	Negative	Negative	Negative	Negative	Negative	4.0225	0.8364
17-DECS-013	G9	Negative	Negative	Negative	Positive	Negative	Negative	Negative	Negative	4.6775	0.7942
17-DECS-013	G1	Positive	Negative	Negative	Negative	Negative	Negative	Negative	Negative	3.9800	0.8397
17-DECS-013	G9	Negative	Negative	Negative	Positive	Negative	Negative	Negative	Negative	4.2800	0.8325

Sample Site	G Number	G1	G11	G10	G9	G12	G5	G4	G3	CA_INT	MGNUM
17-DECS-013	G9	Negative	Negative	Negative	Positive	Negative	Negative	Negative	Negative	4.4775	0.8234
17-DECS-013	G9	Negative	Negative	Negative	Positive	Negative	Negative	Negative	Negative	4.3775	0.8327
17-DECS-013	G9	Negative	Negative	Negative	Positive	Negative	Negative	Negative	Negative	4.6975	0.8099
17-DECS-013	G9	Negative	Negative	Negative	Positive	Negative	Negative	Negative	Negative	4.6750	0.7921
17-DECS-013	G9	Negative	Negative	Negative	Positive	Negative	Negative	Negative	Negative	4.3775	0.8270
17-DECS-013	G9	Negative	Negative	Negative	Positive	Negative	Negative	Negative	Negative	4.6550	0.7951
17-DECS-013	G9	Negative	Negative	Negative	Positive	Negative	Negative	Negative	Negative	4.6825	0.7978
17-DECS-013	G9	Negative	Negative	Negative	Positive	Negative	Negative	Negative	Negative	3.9775	0.8506
17-DECS-013	G9	Negative	Negative	Negative	Positive	Negative	Negative	Negative	Negative	4.2425	0.8302
17-DECS-013	G9	Negative	Negative	Negative	Positive	Negative	Negative	Negative	Negative	4.2225	0.8247
17-DECS-013	G10	Negative	Negative	Positive	Negative	Negative	Negative	Negative	Negative	2.9131	0.8390
17-DECS-013	G9	Negative	Negative	Negative	Positive	Negative	Negative	Negative	Negative	4.4750	0.8080
17-DECS-013	G9	Negative	Negative	Negative	Positive	Negative	Negative	Negative	Negative	4.6575	0.8345
17-DECS-013	G9	Negative	Negative	Negative	Positive	Negative	Negative	Negative	Negative	4.5575	0.8238

Sample Site	G Number	G1	G11	G10	G9	G12	G5	G4	G3	CA_INT	MGNUM
17-DECS-013	G9	Negative	Negative	Negative	Positive	Negative	Negative	Negative	Negative	4.3575	0.8427
17-DECS-013	G9	Negative	Negative	Negative	Positive	Negative	Negative	Negative	Negative	3.6100	0.8506
17-DECS-013	G9	Negative	Negative	Negative	Positive	Negative	Negative	Negative	Negative	3.9875	0.8329
17-DECS-013	G9	Negative	Negative	Negative	Positive	Negative	Negative	Negative	Negative	4.3500	0.8342
17-DECS-013	G9	Negative	Negative	Negative	Positive	Negative	Negative	Negative	Negative	4.1900	0.8151
17-DECS-013	G9	Negative	Negative	Negative	Positive	Negative	Negative	Negative	Negative	5.0450	0.8333
17-DECS-013	G9	Negative	Negative	Negative	Positive	Negative	Negative	Negative	Negative	4.3275	0.8388
17-DECS-013	G9	Negative	Negative	Negative	Positive	Negative	Negative	Negative	Negative	3.7525	0.8465
17-DECS-013	G10	Negative	Negative	Positive	Negative	Negative	Negative	Negative	Negative	2.4283	0.8536
17-DECS-013	G9	Negative	Negative	Negative	Positive	Negative	Negative	Negative	Negative	4.4800	0.8255
17-DECS-013	G9	Negative	Negative	Negative	Positive	Negative	Negative	Negative	Negative	4.6975	0.8087
17-DECS-013	G9	Negative	Negative	Negative	Positive	Negative	Negative	Negative	Negative	4.5975	0.8353
17-DECS-013	G9	Negative	Negative	Negative	Positive	Negative	Negative	Negative	Negative	4.6650	0.7960
17-DECS-013	G9	Negative	Negative	Negative	Positive	Negative	Negative	Negative	Negative	4.4975	0.8118

Sample Site	G Number	G1	G11	G10	G9	G12	G5	G4	G3	CA_INT	MGNUM
17-DECS-013	G9	Negative	Negative	Negative	Positive	Negative	Negative	Negative	Negative	3.9875	0.8327
17-DECS-013	G9	Negative	Negative	Negative	Positive	Negative	Negative	Negative	Negative	4.5025	0.8237
17-DECS-013	G9	Negative	Negative	Negative	Positive	Negative	Negative	Negative	Negative	4.4550	0.8302
17-DECS-013	G9	Negative	Negative	Negative	Positive	Negative	Negative	Negative	Negative	4.3675	0.8457
17-DECS-013	G9	Negative	Negative	Negative	Positive	Negative	Negative	Negative	Negative	4.2800	0.8339
17-DECS-013	G9	Negative	Negative	Negative	Positive	Negative	Negative	Negative	Negative	4.4925	0.8125
17-DECS-013	G9	Negative	Negative	Negative	Positive	Negative	Negative	Negative	Negative	4.3250	0.8412
17-DECS-013	G9	Negative	Negative	Negative	Positive	Negative	Negative	Negative	Negative	4.4275	0.8000
17-DECS-013	G9	Negative	Negative	Negative	Positive	Negative	Negative	Negative	Negative	4.0075	0.8283
17-DECS-013	G9	Negative	Negative	Negative	Positive	Negative	Negative	Negative	Negative	4.6150	0.7992
17-DECS-013	G9	Negative	Negative	Negative	Positive	Negative	Negative	Negative	Negative	3.6125	0.8454
17-DECS-013	G9	Negative	Negative	Negative	Positive	Negative	Negative	Negative	Negative	4.1975	0.8524
17-DECS-013	G9	Negative	Negative	Negative	Positive	Negative	Negative	Negative	Negative	4.6950	0.7961
17-DECS-013	G9	Negative	Negative	Negative	Positive	Negative	Negative	Negative	Negative	4.4900	0.8293

Sample Site	G Number	G1	G11	G10	G9	G12	G5	G4	G3	CA_INT	MGNUM
17-DECS-013	G9	Negative	Negative	Negative	Positive	Negative	Negative	Negative	Negative	4.5325	0.8139
17-DECS-013	G9	Negative	Negative	Negative	Positive	Negative	Negative	Negative	Negative	4.5325	0.8091
17-DECS-013	G9	Negative	Negative	Negative	Positive	Negative	Negative	Negative	Negative	3.9675	0.8454
17-DECS-013	G9	Negative	Negative	Negative	Positive	Negative	Negative	Negative	Negative	4.2375	0.8318
17-DECS-013	G1	Positive	Negative	Negative	Negative	Negative	Negative	Negative	Negative	4.7750	0.7839
17-DECS-013	G1	Positive	Negative	Negative	Negative	Negative	Negative	Negative	Negative	4.3950	0.8311
17-DECS-013	G1	Positive	Negative	Negative	Negative	Negative	Negative	Negative	Negative	4.5300	0.7756
17-DECS-013	G9	Negative	Negative	Negative	Positive	Negative	Negative	Negative	Negative	4.6300	0.8049
17-DECS-013	G9	Negative	Negative	Negative	Positive	Negative	Negative	Negative	Negative	4.3550	0.7977
17-DECS-013	G9	Negative	Negative	Negative	Positive	Negative	Negative	Negative	Negative	4.4650	0.7962
17-DECS-013	G9	Negative	Negative	Negative	Positive	Negative	Negative	Negative	Negative	4.5675	0.7888
17-DECS-013	G1	Positive	Negative	Negative	Negative	Negative	Negative	Negative	Negative	4.8675	0.7831
17-DECS-013	G9	Negative	Negative	Negative	Positive	Negative	Negative	Negative	Negative	4.8175	0.7996
17-DECS-013	G9	Negative	Negative	Negative	Positive	Negative	Negative	Negative	Negative	4.9075	0.7836

Sample Site	G Number	G1	G11	G10	G9	G12	G5	G4	G3	CA_INT	MGNUM
17-DECS-013	G9	Negative	Negative	Negative	Positive	Negative	Negative	Negative	Negative	4.0925	0.8308
17-DECS-013	G4	Negative	Negative	Negative	Negative	Negative	Negative	Positive	Negative	3.1800	0.1216
17-DECS-013	G9	Negative	Negative	Negative	Positive	Negative	Negative	Negative	Negative	4.0925	0.8308
17-DECS-013	G9	Negative	Negative	Negative	Positive	Negative	Negative	Negative	Negative	4.6275	0.8073
17-DECS-013	G9	Negative	Negative	Negative	Positive	Negative	Negative	Negative	Negative	4.7275	0.8070
17-DECS-013	G9	Negative	Negative	Negative	Positive	Negative	Negative	Negative	Negative	4.3450	0.8403
17-DECS-013	G9	Negative	Negative	Negative	Positive	Negative	Negative	Negative	Negative	4.4825	0.8281
17-DECS-013	G9	Negative	Negative	Negative	Positive	Negative	Negative	Negative	Negative	4.8675	0.8270
17-DECS-013	G9	Negative	Negative	Negative	Positive	Negative	Negative	Negative	Negative	4.3525	0.8300
17-DECS-013	G9	Negative	Negative	Negative	Positive	Negative	Negative	Negative	Negative	4.0550	0.8480
17-DECS-013	G10	Negative	Negative	Positive	Negative	Negative	Negative	Negative	Negative	3.2630	0.8480
17-DECS-013	G9	Negative	Negative	Negative	Positive	Negative	Negative	Negative	Negative	4.5800	0.8131
17-DECS-013	G9	Negative	Negative	Negative	Positive	Negative	Negative	Negative	Negative	4.5150	0.8227
17-DECS-013	G9	Negative	Negative	Negative	Positive	Negative	Negative	Negative	Negative	4.5325	0.8373

Sample Site	G Number	G1	G11	G10	G9	G12	G5	G4	G3	CA_INT	MGNUM
17-DECS-013	G9	Negative	Negative	Negative	Positive	Negative	Negative	Negative	Negative	3.9750	0.8332
17-DECS-013	G9	Negative	Negative	Negative	Positive	Negative	Negative	Negative	Negative	4.5875	0.8102
17-DECS-013	G9	Negative	Negative	Negative	Positive	Negative	Negative	Negative	Negative	4.3550	0.8433
17-DECS-013	G9	Negative	Negative	Negative	Positive	Negative	Negative	Negative	Negative	4.0200	0.8149
17-DECS-013	G9	Negative	Negative	Negative	Positive	Negative	Negative	Negative	Negative	4.2525	0.8200
17-DECS-013	G9	Negative	Negative	Negative	Positive	Negative	Negative	Negative	Negative	4.2750	0.8054
17-DECS-013	G9	Negative	Negative	Negative	Positive	Negative	Negative	Negative	Negative	4.1875	0.8254
17-DECS-013	G9	Negative	Negative	Negative	Positive	Negative	Negative	Negative	Negative	4.2600	0.8200
17-DECS-013	G9	Negative	Negative	Negative	Positive	Negative	Negative	Negative	Negative	4.3675	0.7986
17-DECS-013	G1	Positive	Negative	Negative	Negative	Negative	Negative	Negative	Negative	4.1250	0.8079
17-DECS-013	G9	Negative	Negative	Negative	Positive	Negative	Negative	Negative	Negative	4.3825	0.8020
17-DECS-013	G9	Negative	Negative	Negative	Positive	Negative	Negative	Negative	Negative	4.6025	0.7997
17-DECS-013	G9	Negative	Negative	Negative	Positive	Negative	Negative	Negative	Negative	4.5700	0.8018
17-DECS-013	G9	Negative	Negative	Negative	Positive	Negative	Negative	Negative	Negative	4.4900	0.7844

Sample Site	G Number	G1	G11	G10	G9	G12	G5	G4	G3	CA_INT	MGNUM
17-DECS-013	G9	Negative	Negative	Negative	Positive	Negative	Negative	Negative	Negative	3.5650	0.8219
17-DECS-013	G9	Negative	Negative	Negative	Positive	Negative	Negative	Negative	Negative	4.1575	0.8274
17-DECS-013	G9	Negative	Negative	Negative	Positive	Negative	Negative	Negative	Negative	4.1225	0.8219
17-DECS-013	G9	Negative	Negative	Negative	Positive	Negative	Negative	Negative	Negative	4.6775	0.8032
17-DECS-013	G9	Negative	Negative	Negative	Positive	Negative	Negative	Negative	Negative	3.5275	0.8193
17-DECS-013	G9	Negative	Negative	Negative	Positive	Negative	Negative	Negative	Negative	4.4500	0.7993
17-DECS-013	G9	Negative	Negative	Negative	Positive	Negative	Negative	Negative	Negative	4.4200	0.8006
17-DECS-013	G9	Negative	Negative	Negative	Positive	Negative	Negative	Negative	Negative	4.6400	0.8001
17-DECS-013	G9	Negative	Negative	Negative	Positive	Negative	Negative	Negative	Negative	4.5025	0.7976
17-DECS-013	G9	Negative	Negative	Negative	Positive	Negative	Negative	Negative	Negative	4.3775	0.8132
17-DECS-013	G9	Negative	Negative	Negative	Positive	Negative	Negative	Negative	Negative	4.6550	0.8142
17-DECS-013	G9	Negative	Negative	Negative	Positive	Negative	Negative	Negative	Negative	4.4875	0.8097
17-DECS-013	G9	Negative	Negative	Negative	Positive	Negative	Negative	Negative	Negative	4.3950	0.8303
17-DECS-013	G9	Negative	Negative	Negative	Positive	Negative	Negative	Negative	Negative	4.5450	0.8157

Sample Site	G Number	G1	G11	G10	G9	G12	G5	G4	G3	CA_INT	MGNUM
17-DECS-013	G9	Negative	Negative	Negative	Positive	Negative	Negative	Negative	Negative	4.4000	0.8362
17-DECS-013	G9	Negative	Negative	Negative	Positive	Negative	Negative	Negative	Negative	4.1600	0.8473
17-DECS-013	G9	Negative	Negative	Negative	Positive	Negative	Negative	Negative	Negative	4.3050	0.7990
17-DECS-013	G9	Negative	Negative	Negative	Positive	Negative	Negative	Negative	Negative	4.4125	0.8210
17-DECS-013	G9	Negative	Negative	Negative	Positive	Negative	Negative	Negative	Negative	4.3750	0.8109
17-DECS-013	G9	Negative	Negative	Negative	Positive	Negative	Negative	Negative	Negative	4.6325	0.8021
17-DECS-013	G9	Negative	Negative	Negative	Positive	Negative	Negative	Negative	Negative	4.3775	0.8390
17-DECS-013	G9	Negative	Negative	Negative	Positive	Negative	Negative	Negative	Negative	4.5100	0.8331
17-DECS-013	G9	Negative	Negative	Negative	Positive	Negative	Negative	Negative	Negative	4.2600	0.8288
17-DECS-013	G9	Negative	Negative	Negative	Positive	Negative	Negative	Negative	Negative	4.1250	0.8358
17-DECS-013	G9	Negative	Negative	Negative	Positive	Negative	Negative	Negative	Negative	4.4425	0.8064
17-DECS-013	G9	Negative	Negative	Negative	Positive	Negative	Negative	Negative	Negative	4.6200	0.8107
17-DECS-013	G9	Negative	Negative	Negative	Positive	Negative	Negative	Negative	Negative	4.3775	0.7914
17-DECS-013	G3	Negative	Negative	Negative	Negative	Negative	Negative	Negative	Positive	7.3600	0.2417

Sample Site	G Number	G1	G11	G10	G9	G12	G5	G4	G3	CA_INT	MGNUM
17-DECS-013	G9	Negative	Negative	Negative	Positive	Negative	Negative	Negative	Negative	4.7475	0.7913
17-DECS-013	G9	Negative	Negative	Negative	Positive	Negative	Negative	Negative	Negative	4.4025	0.8091
17-DECS-013	G12	Negative	Negative	Negative	Negative	Positive	Negative	Negative	Negative	12.9925	0.8075
17-DECS-013	G3	Negative	Negative	Negative	Negative	Negative	Negative	Negative	Positive	7.8900	0.2498
17-DECS-013	G3	Negative	Negative	Negative	Negative	Negative	Negative	Negative	Positive	7.1200	0.2809
17-DECS-013	G3	Negative	Negative	Negative	Negative	Negative	Negative	Negative	Positive	7.1800	0.2618
17-DECS-013	G3	Negative	Negative	Negative	Negative	Negative	Negative	Negative	Positive	7.5600	0.2232
17-DECS-013	G3	Negative	Negative	Negative	Negative	Negative	Negative	Negative	Positive	7.3600	0.2721
17-DECS-013	G3	Negative	Negative	Negative	Negative	Negative	Negative	Negative	Positive	6.9200	0.2716
17-DECS-013	G3	Negative	Negative	Negative	Negative	Negative	Negative	Negative	Positive	8.6800	0.2463
17-DECS-013	G3	Negative	Negative	Negative	Negative	Negative	Negative	Negative	Positive	7.0600	0.2917
17-DECS-013	G3	Negative	Negative	Negative	Negative	Negative	Negative	Negative	Positive	6.9400	0.2989
17-DECS-013	G3	Negative	Negative	Negative	Negative	Negative	Negative	Negative	Positive	7.0100	0.2443
17-DECS-013	G3	Negative	Negative	Negative	Negative	Negative	Negative	Negative	Positive	7.8300	0.2689

Sample Site	G Number	G1	G11	G10	G9	G12	G5	G4	G3	CA_INT	MGNUM
17-DECS-013	G3	Negative	Negative	Negative	Negative	Negative	Negative	Negative	Positive	6.8100	0.2904

Table 7.4: Composition of clinopyroxene in weight % oxide determined by SEM-EDX. Compositions are dominantly diopside (CaMgSi2O6). *- represents values below LOD

Sample	Cr_2O_3	Al_2O_3	TiO_2	FeO	MgO	CaO	MnO	Na_2O	SiO_2
A-003-S 2,1	0.45	1.42	-	5.92	14.67	24.25	-	-	52.55
A-003-S 4,1	-	0.92	-	12.68	10.52	24.29	0.51	-	51.17
A-003-S 3,2	-	3.69	-	5.62	13.76	25.08	0.82	0.33	51.04
A-003-S 2,2	-	1.36	-	7.09	14.1	24.76	0.26	0.38	52.42
A-003-S 1,2	0.4	1.81	-	4.76	15.26	24.06	-	0.55	52.61
A-004-do 2,1	-	4.49	-	6.34	13.02	24.79	0.27	0.6	51.01
A-004-do 5,1	-	-2.22	-	9.21	13.53	22.96	0.28	0.45	51.7
A-004-do 6,1	-	1.66	-	9.95	11.7	24.09	-	0.78	52.04
A-004-do 6,2	-	3.32	-	5.75	14.65	23.47	0.65	-	51.5
A-004-do 5,2	-	1.31	-	11.18	11.26	23.56	0.7	-	52.01
A-004-do 4,2	0.84	2.21	-	6.16	19.55	19.33	-	-	52.77
A-004-do 2,2	-	1	-	7.14	13.7	24.52	0.64	-	53.19
A-004-do 3,3	-	1.27	-	11.98	10.86	24.35	0.45	-	851.68

Sample	Cr_2O_3	Al_2O_3	TiO_2	FeO	MgO	CaO	MnO	Na_2O	SiO_2
A-004-do 4,3	-	1.29	-	6.19	14.53	25.04	0.41	-	53.07
A-004-do 6,3	-	1.91	-	7.59	14.31	23.61	0.41	-	52.31
A-004-do 6,4	-	1.27	-	8.98	13.45	22.07	0.44	1.1	52.34
A-004-do 4,4	0.6	2.65	0.51	5.28	15.45	22.73	-	0.46	51.83
c-013-do sp 14	0.27	1.3	-	5.19	15.63	23.75	-	0.35	52.55
C-002-do 2,4 1	0.47	2.52	-	8.08	17.46	19.86	-	-	52.23
C-002-do 2,4 2	0.45	2.56	-	7.81	17.1	19.23	-	-	51.22
C-002-do 2,4 4	0.75	3.82	0.57	7.43	15.98	19.9	-	-	49.57
C-002-do 2,4 3	0.89	3.58	0.58	7	16.35	19.9	0.35	-	49.41
17-DECS-013 odm	1.33	2.41	-	2.11	15.88	20.34	2.67	-	55.69
C-002-do 2,4 1	0.47	2.52	-	8.08	17.46	19.86	-	-	52.23
C-002-do 2,4 2	0.45	2.56	-	7.81	17.1	19.23	-	-	51.22
C-002-do 2,4 4	0.75	3.82	0.57	7.43	15.98	19.9	-	-	49.57
C-002-do 2,4 l	11.2	2.33	0.47	16.51	-	17.19	-	-	50.64

Sample	Cr_2O_3	Al_2O_3	TiO_2	FeO	MgO	CaO	MnO	Na_2O	SiO_2
C-002-do 2,4 3	0.89	3.58	0.58	7	16.35	19.9	0.35	-	49.41
17-decs-003	0.88	1.43	-	5.06	16.74	22.42	-	0.73	52.44

Table7.7.5: Composition of Chromite in till sample 17-DECS in wt. % oxides determined by SEM-EDX. *Values listed as 0 represent values below LOD

Sample	Al_2O_3	CaO	Cr_2O_3	FeO	MgO	MnO	TiO_2	V_2O_5	SiO_2	Total
17-DECS-016	0.55	0	1.45	40.52	8.69	0	47.83	0	0	99.04
17-DECS-013	4.41	0	61.54	22.85	10.49	0	0	0	0	99.29
17-DECS-013	21.47	0	45.8	20.71	11.13	0	0.83	0	0	99.94
17-DECS-013	8.74	0	60.29	20.57	11.35	0	0	0	0	100.95
17-DECS-013	8.84	0	60.5	20.31	11.14	0	0	0	0	100.79
17-DECS-013	14.87	0	42.08	25.93	15.55	0.58	1.01	0	0	100.02
17-DECS-013	24.32	0	37.59	19.51	17.42	0	0	0	0.62	99.46
17-DECS-013	14.89	0	50.59	21.93	11.3	0	0.65	0.44	0	99.8
17-DECS-013	14.93	0	51.17	21.58	11.31	0	0.87	0	0	99.86
17-DECS-013	27.25	0	42.72	14.16	13.91	0	0	0	0	98.04
17-DECS-013	12.72	0	58.21	14.27	13.74	0	0	0	0	98.94
17-DECS-013	17.68	0	43.07	20.86	15.01	0	1.58	0	0.6	98.8
17-DECS-013	17.46	0	40.92	24.43	16.13	0	0.28	0	0.71	99.93

Sample	Al_2O_3	CaO	Cr_2O_3	FeO	MgO	MnO	TiO_2	V_2O_5	SiO_2	Total
17-DECS-013	4.76	0	47.44	35.21	9.25	0	3.15	0	0	99.81
17-DECS-013	11.48	0	44.13	28.75	14.2	0	1.03	0	0.63	100.22
17-DECS-013	19.12	0	36	28.58	14.7	0	1.52	0	0	99.92
17-DECS-013	8.93	0	53.92	21.2	14.19	0	1.38	0	0.56	100.18
17-DECS-013	3.6	0	54.19	30.76	9.71	0	1.77	0	0	100.03
17-DECS-001	19.68	0	43.47	27.55	7.96	0	0.92	0	0	99.58
17-DECS-001	13.52	0	45.48	30.08	10.43	0	0.46	0	0	99.97
17-DECS-001	3.37	0	44.75	41.91	7.14	0	1.42	0	0	98.59
17-DECS-001	4.88	0.24	37.93	36.27	12.85	0	8.39	0	0	100.56
17-DECS-001	24.07	0	39.4	24.24	12.45	0	0	0	0	100.16
17-DECS-002	3.28	0	42.01	41.16	7.12	0	1.71	0	0	95.28
17-DECS-002	14.96	0	49.62	24.41	10.54	0	0	0	0	99.53
17-DECS-003	0.51	0	1.46	48.21	7.13	0	43.1	0.58	0	100.99
17-DECS-021	0.44	0	1.48	34.13	10.85	0	51.53	0	0	98.43

Sample	Al_2O_3	CaO	Cr_2O_3	FeO	MgO	MnO	TiO_2	V_2O_5	SiO_2	Total
17-DECS-021	0.42	0	1.57	34.59	10.88	0	51.82	0	0	99.28
17-DECS-021	0.47	0	1.4	33.51	11.82	0	52.37	0	0	99.57
17-DECS-021	0.47	0	1.29	34.66	11.11	0	52.56	0	0	100.09
17-DECS-021	0.49	0	1.3	33.86	11.21	0	52.56	0	0	99.42
17-DECS-013	0.5	0	1.86	30.81	11.5	0.32	55.11	0	0	100.1
17-DECS-013	0.63	0	1.89	30.76	11.19	0	54.84	0	0	99.31
17-DECS-013	0.55	0	2.12	30.36	11.37	0	54.71	0	0	99.11
17-DECS-016	0.54	0	0.95	35.58	10.94	0	51.75	0	0	99.76
17-DECS-017	0.5	0	1.52	42.09	9.63	0	47.07	0	0	100.81

Table 7.6: Composition of ilmenite from 17-DECS in wt. % oxides determined with SEM-EDX. *Values listed as 0 are values below LOD

Sample	Al_2O_3	CaO	Cr_2O_3	FeO	MgO	MnO	TiO_2	V_2O_5	SiO_2	Total
17-DECS-013	0.56	0	0	33.45	10.65	0	55.09	0	0	99.75
17-DECS-013	0.71	0	0	35.93	9.77	0	53.68	0	0	100.09
17-DECS-006	0	0	0	46.74	0	0.67	49.85	0	0	97.26
17-DECS-006	0	0	0	44.33	0	1.27	53.96	0	0	99.56
17-DECS-018	0	0	0	50.33	0	0.44	50.47	0	0	101.24
17-DECS-002	0	0	0	45.55	0	2.3	51.26	0	0	99.11
17-DECS-002	0	0	0	47.17	0.43	0	50.72	0	0.3	98.62

Appendix II LA-ICP-MS Results

Table 7.1: Rare earth element values for garnets from till sample 17-DECS-013,016 determined by SEM-EDX analysis. Cps= counts per second.

Sample	A-013-p3 spot 1	A-013-p3 spot 2	A-013-p3 spot 3	A-013-p3 spot 4	A-013-p3 spot 5	A-013-p3 spot 6	A-013-p3 spot 7
Ca (cps)	28370	33080	3.11E+04	25540	3.12E+04	3.15E+04	3.74E+04
Si (ppm)	2.32E+05	2.10E+05	2.22E+05	2.21E+05	2.16E+05	2.24E+05	2.15E+05
Ti (ppm)	388	4942	3304	1970	4272	3891	4550
Ni (ppm)	131.8	109.3	113.9	126.3	152.5	116.2	177.2
Y (ppm)	2.71	17.03	9.4	9.53	15.47	11.67	16.74
Zr (ppm)	9.63	47.1	29.9	28.1	43.8	41.5	44.2
La (ppm)	Below LOD	0.058	0.057	Below LOD	0.059	Below LOD	0.16
Ce (ppm)	0.463	0.589	0.478	0.376	0.603	0.52	1.329
Pr (ppm)	0.117	0.16	0.135	0.104	0.164	0.135	0.366
Nd (ppm)	1.32	1.5	1.08	1.12	1.62	1.39	2.47
Sm (ppm)	0.56	0.9	0.77	0.91	1.06	0.8	1.6
Eu (ppm)	0.196	0.621	0.328	0.398	0.489	0.304	0.804
Gd (ppm)	Below LOD	1.79	0.91	1.09	1.65	1.31	2.57
Tb (ppm)	0.072	0.434	0.203	0.258	0.368	0.297	0.516
Dy (ppm)	0.46	3.1	1.57	1.83	2.61	1.88	3.34
Ho (ppm)	0.129	0.628	0.39	0.371	0.623	0.528	0.701
Er (ppm)	0.316	1.97	1.23	1.13	2	1.42	1.7
Tm (ppm)	0.073	0.289	0.197	0.149	0.271	0.259	0.216
Yb (ppm)	0.54	2.1	1.56	1.21	1.88	1.89	1.42
Lu (ppm)	0.132	0.313	0.22	0.145	0.295	0.265	0.214

Sample	A-013-p3 spot 8	A-013-p3 spot 9	A-013-p3 spot 10	A-013-p3 spot 11	A-013-p3 spot 12	A-013-p3 spot 13	A-013-p3 spot 14
Ca (cps)	21580	23280	22330	26280	2.73E+04	2.78E+04	22310
Si (ppm)	2.15E+05	2.15E+05	2.24E+05	2.24E+05	2.18E+05	2.24E+05	2.14E+05
Ti (ppm)	136.7	1869	1321	528	2720	4040	687
Ni (ppm)	157.7	132.7	136.7	163.4	131.9	158.4	27.2
Y (ppm)	0.132	4.34	4.83	1.53	7.09	14.7	8.4
Zr (ppm)	Below LOD	11.72	16.83	16.67	23.03	38.6	7.89
La (ppm)	0.166	Below LOD	Below LOD	Below LOD	0.068	Below LOD	Below LOD
Ce (ppm)	0.846	0.295	0.388	0.478	0.385	0.625	0.185
Pr (ppm)	0.078	0.103	0.13	0.149	0.138	0.174	0.066
Nd (ppm)	0.21	0.82	0.67	1.26	0.92	1.37	0.64
Sm (ppm)	Below LOD	0.5	0.68	0.92	0.55	0.99	0.41
Eu (ppm)	Below LOD	0.159	0.239	0.352	0.295	0.575	0.13
Gd (ppm)	Below LOD	0.66	0.82	0.68	0.89	1.51	Below LOD
Tb (ppm)	Below LOD	0.133	0.139	0.11	0.241	0.352	0.13
Dy (ppm)	Below LOD	0.84	0.68	0.398	1.22	2.62	1.11
Ho (ppm)	Below LOD	0.184	0.205	0.054	0.273	0.562	0.3
Er (ppm)	Below LOD	0.544	0.574	0.124	0.83	1.82	1.12
Tm (ppm)	0.021	0.076	0.128	0.03	0.117	0.297	0.235
Yb (ppm)	0.24	0.7	1.03	0.27	1	2.19	1.9
Lu (ppm)	0.058	0.095	0.12	0.08	0.142	0.331	0.276

Sample	A-013-p3 spot 8	A-013-p3 spot 9	A-013-p3 spot 10	A-013-p3 spot 11	A-013-p3 spot 12	A-013-p3 spot 13	A-013-p3 spot 14
Ca (cps)	21580	23280	22330	26280	2.73E+04	2.78E+04	22310
Si (ppm)	2.15E+05	2.15E+05	2.24E+05	2.24E+05	2.18E+05	2.24E+05	2.14E+05
Ti (ppm)	136.7	1869	1321	528	2720	4040	687
Ni (ppm)	157.7	132.7	136.7	163.4	131.9	158.4	27.2
Y (ppm)	0.132	4.34	4.83	1.53	7.09	14.7	8.4
Zr (ppm)	Below LOD	11.72	16.83	16.67	23.03	38.6	7.89
La (ppm)	0.166	Below LOD	Below LOD	Below LOD	0.068	Below LOD	Below LOD
Ce (ppm)	0.846	0.295	0.388	0.478	0.385	0.625	0.185
Pr (ppm)	0.078	0.103	0.13	0.149	0.138	0.174	0.066
Nd (ppm)	0.21	0.82	0.67	1.26	0.92	1.37	0.64
Sm (ppm)	Below LOD	0.5	0.68	0.92	0.55	0.99	0.41
Eu (ppm)	Below LOD	0.159	0.239	0.352	0.295	0.575	0.13
Gd (ppm)	Below LOD	0.66	0.82	0.68	0.89	1.51	Below LOD
Tb (ppm)	Below LOD	0.133	0.139	0.11	0.241	0.352	0.13
Dy (ppm)	Below LOD	0.84	0.68	0.398	1.22	2.62	1.11
Ho (ppm)	Below LOD	0.184	0.205	0.054	0.273	0.562	0.3
Er (ppm)	Below LOD	0.544	0.574	0.124	0.83	1.82	1.12
Tm (ppm)	0.021	0.076	0.128	0.03	0.117	0.297	0.235
Yb (ppm)	0.24	0.7	1.03	0.27	1	2.19	1.9
Lu (ppm)	0.058	0.095	0.12	0.08	0.142	0.331	0.276

Sample	A-013-p3 spot 22	A-013-p3 spot 23	A-013-p3 spot 24	018 sp 28	018 sp 24	020 sp 1	B-013-o spot 1	B-013-o spot 2
Ca (cps)	2.81E+04	2.90E+04	3.01E+04	25630	28230	1.85E+05	3.42E+04	2.81E+04
Si (ppm)	2.14E+05	2.13E+05	2.12E+05	2.06E+05	2.22E+05	1.95E+05	2.01E+05	2.18E+05
Ti (ppm)	3847	3792	1707	4059	2337	1049	512	5610
Ni (ppm)	168.6	168.3	161.2	126.2	115	1.84	9.5	96.5
Y (ppm)	15.08	14.51	2.68	15.03	3.4	20.97	35.17	16.61
Zr (ppm)	40	35.9	22.48	41	19.97	1.23	11.46	47.6
La (ppm)	0.119	Below LOD	0.079	0.061	0.049	Below LOD	Below LOD	Below LOD
Ce (ppm)	0.688	0.603	0.782	0.538	0.384	Below LOD	Below LOD	0.346
Pr (ppm)	0.193	0.17	0.249	0.18	0.114	Below LOD	Below LOD	0.114
Nd (ppm)	1.48	1.43	2.29	1.39	1.04	Below LOD	0.27	1.41
Sm (ppm)	1	0.85	1.14	1.2	0.87	0.047	0.69	0.71
Eu (ppm)	0.477	0.365	0.441	0.477	0.351	Below LOD	0.485	0.481
Gd (ppm)	1.45	1.76	1.02	1.74	0.91	Below LOD	2.24	1.65
Tb (ppm)	0.354	0.363	0.138	0.329	0.124	0.082	0.693	0.425
Dy (ppm)	2.61	2.39	0.53	2.58	0.84	0.9	5.45	3.01
Ho (ppm)	0.63	0.592	0.124	0.621	0.12	0.501	1.34	0.66
Er (ppm)	1.73	1.56	0.267	1.81	0.359	2.58	3.73	2.1
Tm (ppm)	0.292	0.254	0.044	0.275	0.072	0.62	0.581	0.317
Yb (ppm)	2.09	1.7	0.229	2.05	0.49	6.26	4.17	2.13
Lu (ppm)	0.289	0.295	0.05	0.264	0.092	1.127	0.661	0.301

Sample	B-013-o spot 3	B-013-o spot 4	B-013-o spot 5	B-013-o spot 6	B-013-o spot 7	B-013-o spot 8	B-013-o spot 9	B-013-o spot 10
Ca (cps)	3.17E+04	35050	4.04E+04	4.34E+04	3.09E+04	3440	21550	4.20E+04
Si (ppm)	2.15E+05	2.06E+05	1.99E+05	1.94E+05	2.25E+05	2.10E+05	2.10E+05	2.02E+05
Ti (ppm)	5530	593	573	570	4728	185	229	467
Ni (ppm)	90.3	2.2	2.54	1.97	118.6	Below LOD	Below LOD	1.64
Y (ppm)	17.96	74.4	298.1	262.2	14.67	114.4	573	346
Zr (ppm)	51.7	24.08	17.47	20.98	42.6	44.7	1.67	11.03
La (ppm)	0.039	Below LOD	Below LOD	Below LOD	0.075	0.34	Below LOD	Below LOD
Ce (ppm)	0.384	0.137	0.445	0.719	0.511	0.93	Below LOD	0.338
Pr (ppm)	0.157	0.077	0.425	0.473	0.114	0.061	Below LOD	0.344
Nd (ppm)	1.27	1.34	7.72	8.35	1.2	0.26	Below LOD	6.25
Sm (ppm)	0.97	2	12.08	12.13	0.8	0.23	1.88	11.29
Eu (ppm)	0.44	1.04	2.87	3.02	0.438	Below LOD	1.23	2.87
Gd (ppm)	1.72	6.12	26	25.9	1.84	2.02	26.1	26.8
Tb (ppm)	0.398	1.6	5.86	5.56	0.342	1.28	9.62	6.17
Dy (ppm)	3.06	11.74	45.4	42.1	2.65	14.1	84.7	48.8
Ho (ppm)	0.75	2.94	11.23	9.36	0.619	3.46	22.33	12.72
Er (ppm)	2.22	8.53	33.7	26.2	1.66	11.4	72.2	40.3
Tm (ppm)	0.335	1.297	5.01	4.13	0.259	2.51	11.61	6.87
Yb (ppm)	2.24	9.52	38.2	29.4	1.64	24.9	83.3	52.9
Lu (ppm)	0.316	1.33	5.53	3.94	0.255	3.39	12.06	8.31

Sample	B-013-o spot 11	B-013-o spot 12	B-013-o spot 13	B-013-o spot 14	B-013-o spot 15	B-013-o spot 16	B-013-o spot 17
Ca (cps)	2600	3.98E+04	3.94E+04	3.58E+04	1910	2550	4.07E+04
Si (ppm)	1.88E+05	1.99E+05	2.08E+05	2.05E+05	3.07E+05	3.05E+06	9350
Ti (ppm)	168	638	619	564	165	5.60E+03	27.8
Ni (ppm)	Below LOD	2.23	Below LOD	Below LOD	Below LOD	Below LOD	Below LOD
Y (ppm)	585	291.7	268.7	187.6	835	10310	11.49
Zr (ppm)	10	25.11	26	24.1	17.7	228	1.027
La (ppm)	Below LOD	Below LOD	0.31	Below LOD	Below LOD	Below LOD	0.0048
Ce (ppm)	Below LOD	0.717	1.73	0.294	Below LOD	Below LOD	0.0276
Pr (ppm)	Below LOD	0.534	0.58	0.2	Below LOD	Below LOD	0.0185
Nd (ppm)	0.17	8.48	8.5	3.53	Below LOD	Below LOD	0.36
Sm (ppm)	0.77	12.09	12.81	5.59	0.46	6.9	0.541
Eu (ppm)	0.075	3.08	3.31	1.86	Below LOD	Below LOD	0.1318
Gd (ppm)	6.26	27.1	28.2	16.1	3.8	87	1.266
Tb (ppm)	4.13	6.02	6.32	3.78	3.25	60.2	0.274
Dy (ppm)	56.6	45.2	43.6	29.4	60.2	883	1.946
Ho (ppm)	19.1	10.89	9.51	7.46	26.7	323	0.405
Er (ppm)	84.7	32.1	25.96	22.8	169	1790	1.053
Tm (ppm)	21.6	4.72	4.02	3.66	55.6	573	0.159
Yb (ppm)	220	34.1	29.3	25.8	726	7180	1.036
Lu (ppm)	30.2	4.92	3.65	3.86	132	1310	0.1277

Sample	B-013-o spot 18	B-013-o spot 19	B-013-o spot 20	B-013-o spot 21	B-013-o spot 22	B-013-o spot 23	B-013-o spot 24
Ca (cps)	1450	18140	2.84E+04	4.96E+04	3.82E+04	36490	3.24E+04
Si (ppm)	2.42E+06	3.14E+05	3.88E+05	1.64E+05	2.07E+05	2.11E+05	2.19E+05
Ti (ppm)	1880	957	11560	2515	392	343	5490
Ni (ppm)	Below LOD	22.4	165.9	7.54	10.01	10.8	109.6
Y (ppm)	1740	15.67	29.6	26.07	27.3	20.17	18.88
Zr (ppm)	112	7.94	146.6	69.7	4	12.42	55.1
La (ppm)	Below LOD	Below LOD	Below LOD	Below LOD	Below LOD	Below LOD	Below LOD
Ce (ppm)	Below LOD	0.357	0.661	0.293	Below LOD	Below LOD	0.368
Pr (ppm)	Below LOD	0.071	0.198	0.108	Below LOD	Below LOD	0.116
Nd (ppm)	Below LOD	0.57	2.03	0.88	0.27	0.28	1.18
Sm (ppm)	5.8	0.77	1.58	0.91	0.52	0.75	0.72
Eu (ppm)	Below LOD	0.46	0.92	0.484	0.567	0.514	0.537
Gd (ppm)	32.2	1.68	3.16	2.16	2.05	2.34	1.44
Tb (ppm)	18.9	0.36	0.64	0.488	0.496	0.464	0.405
Dy (ppm)	217	2.99	5.21	4.19	3.87	3.5	3.19
Ho (ppm)	43	0.607	1.171	1.131	1.089	0.756	0.779
Er (ppm)	149	1.86	3.61	3.41	3.58	2.29	2.15
Tm (ppm)	36	0.32	0.529	0.604	0.538	0.362	0.374
Yb (ppm)	400	1.62	3.9	4.61	4.64	2.46	2.56
Lu (ppm)	53	0.272	0.609	0.677	0.676	0.361	0.343

Sample	B-013-o spot 25	B-013-o spot 26	B-013-o spot 27	B-013-o spot 28	B-013-o spot 29	B-013-o spot 30	B-013-o spot 31
Ca (cps)	4.50E+04	3.14E+04	2.74E+04	4.09E+04	5.76E+04	3.85E+04	7.11E+04
Si (ppm)	1.91E+05	2.25E+05	2.28E+05	1.96E+05	2.13E+05	1.95E+05	2.06E+05
Ti (ppm)	510	4698	6280	652	3950	493	7610
Ni (ppm)	2.29	123.4	70.8	2.2	16.2	6.07	26.83
Y (ppm)	336.8	16.48	15.22	216.2	36.6	135.4	43.9
Zr (ppm)	16.6	47.6	60.5	27.7	151.6	22.76	300.9
La (ppm)	Below LOD	Below LOD	Below LOD	Below LOD	Below LOD	Below LOD	0.1
Ce (ppm)	0.65	0.475	0.285	0.544	0.481	0.063	1.206
Pr (ppm)	0.382	0.133	0.094	0.467	0.2	0.054	0.422
Nd (ppm)	7.32	1.39	0.91	8.26	1.92	1.09	4.39
Sm (ppm)	11.1	1	0.73	12.74	1.68	1.55	3.13
Eu (ppm)	2.77	0.537	0.467	3	1.06	1.11	1.69
Gd (ppm)	28.8	1.76	1.25	27.5	3.79	5.2	5.75
Tb (ppm)	6.48	0.374	0.367	5.99	0.85	1.52	1.213
Dy (ppm)	53.7	3.04	2.44	38.7	6.25	16.79	8.45
Ho (ppm)	14.13	0.684	0.608	7.71	1.516	5.28	1.832
Er (ppm)	46.8	2	1.7	18.55	4.51	19.27	5
Tm (ppm)	7.18	0.301	0.289	2.5	0.687	3.37	0.65
Yb (ppm)	53	2.28	2.4	17.6	5.03	26.7	4.54
Lu (ppm)	9.06	0.351	0.288	2.07	0.773	4.25	0.587

Sample	B-013-o spot 32	B-013-o spot 33	B-013-o spot 34	B-013-o spot 35	B-013-o spot 36	B-013-o spot 37	B-013-o spot 38
Ca (cps)	5.09E+04	4.55E+04	4.86E+04	4.42E+04	2910	3.48E+04	31770
Si (ppm)	1.90E+05	1.92E+05	1.95E+05	2.09E+05	1.83E+05	2.17E+05	2.45E+05
Ti (ppm)	581	689	612	670	93.2	1170	3820
Ni (ppm)	Below LOD	3.34	1.86	Below LOD	Below LOD	Below LOD	144.6
Y (ppm)	213.9	179.8	245.7	270.7	440	69.5	11.06
Zr (ppm)	23.8	33.5	20.16	21.58	8.86	58	32.3
La (ppm)	0.089	Below LOD	Below LOD	Below LOD	Below LOD	0.047	0.07
Ce (ppm)	0.79	0.119	0.242	0.153	Below LOD	0.18	0.382
Pr (ppm)	0.44	0.074	0.282	0.225	Below LOD	0.075	0.091
Nd (ppm)	7.61	1.41	6.73	5.98	0.11	2.06	1.05
Sm (ppm)	10.6	2.15	11.35	9.43	0.48	3.5	0.82
Eu (ppm)	2.76	1.03	2.88	2.87	Below LOD	1.2	0.374
Gd (ppm)	25.7	7.69	25.7	22.7	4.81	9.17	1.56
Tb (ppm)	5.46	2.26	5.65	5.37	3.07	1.7	0.288
Dy (ppm)	37.5	21.9	41	40.8	40.3	12.57	1.97
Ho (ppm)	7.5	6.72	8.81	9.75	11.91	2.75	0.391
Er (ppm)	18.39	23.64	24.37	29.5	44.1	7.54	1.07
Tm (ppm)	2.67	4.1	3.53	4.5	9.72	1.079	0.18
Yb (ppm)	17.15	33.5	24.9	33.3	83.2	7.03	1.19
Lu (ppm)	2.1	5.24	3.18	4.95	8.59	1.016	0.211

Sample	B-013-o spot 39	B-013-o spot 40	B-013-o spot 41	B-013-o spot 42	B-013-o spot 43	B-013-o spot 44	B-013-o spot 45
Ca (cps)	4.44E+04	3.49E+04	4.49E+04	4.39E+04	4.02E+04	3.20E+04	5.83E+04
Si (ppm)	2.19E+05	2.50E+05	2.45E+05	2.72E+05	2.77E+05	3.32E+05	3.73E+05
Ti (ppm)	379	5050	685	648	678	4570	10180
Ni (ppm)	Below LOD	91.8	2.26	2.18	2.06	124.1	11.06
Y (ppm)	155.9	15.88	268.4	355	146.1	17.53	24.01
Zr (ppm)	9.81	44.1	28.4	20.2	43.1	43.5	138.4
La (ppm)	Below LOD	0.049	0.044	Below LOD	Below LOD	0.082	47.9
Ce (ppm)	0.088	0.451	0.642	0.592	0.43	0.669	76.5
Pr (ppm)	0.055	0.116	0.466	0.438	0.197	0.109	4.9
Nd (ppm)	1.59	1.15	8.12	8.04	3.62	1.24	22.41
Sm (ppm)	4.72	1.39	24.7	39.2	80	Below LOD	Below LOD
Eu (ppm)	1.71	0.545	3.46	3.59	2.43	0.69	2.35
Gd (ppm)	12.59	1.83	40.4	45.8	36.1	5.21	37.3
Tb (ppm)	2.63	0.321	6.27	6.54	3.74	0.398	0.764
Dy (ppm)	22.72	2.77	47	56.6	28.7	3.28	5.17
Ho (ppm)	5.95	0.668	9.62	13.73	5.62	0.687	0.933
Er (ppm)	19.14	1.79	25.47	43.3	15.04	2.22	2.46
Tm (ppm)	3.07	0.285	3.59	6.52	2.04	0.314	0.331
Yb (ppm)	23.93	2.22	23.7	52.3	12.65	2.41	2.35
Lu (ppm)	3.76	0.336	3.28	8.17	1.82	0.382	0.372

Sample	B-013-o spot 46	9-013 spot 1	9-013 spot 2	9-013 spot 3	9-013 spot 4	9-013 spot 5	9-013 spot 6	9-013 spot 7	9-013 spot 8
Ca (cps)	5.73E+04	18830	2.05E+04	16910	17510	18200	21070	20770	13780
Si (ppm)	4.37E+05	2.24E+05	2.17E+05	2.23E+05	2.13E+05	2.14E+05	2.26E+05	2.18E+05	2.22E+05
Ti (ppm)	10200	1696	4400	2085	4960	1698	343	4030	191
Ni (ppm)	10.16	159.1	161.7	164.5	119.8	160	110.1	162.4	160.2
Y (ppm)	23.26	2.54	13.88	0.58	17.31	2.66	2.8	14.6	0.57
Zr (ppm)	144.3	20.8	45.4	7.05	45.9	19.47	3.63	39.3	1.57
La (ppm)	68.7	0.105	0.076	0.071	Below LOD	0.092	Below LOD	Below LOD	0.07
Ce (ppm)	92.7	0.76	0.83	0.58	0.471	0.77	0.589	0.683	0.8
Pr (ppm)	4.66	0.232	0.221	0.214	0.166	0.205	0.141	0.186	0.185
Nd (ppm)	21.44	1.95	1.81	1.63	1.82	2.08	1.16	1.41	0.65
Sm (ppm)	Below LOD	0.97	1.08	0.53	1.22	1.03	0.33	1.04	Below LOD
Eu (ppm)	2.72	0.398	0.65	0.314	0.48	0.46	Below LOD	0.52	Below LOD
Gd (ppm)	Below LOD	0.96	1.6	Below LOD	1.71	1.01	0.62	1.63	Below LOD
Tb (ppm)	0.787	0.104	0.332	Below LOD	0.331	0.097	0.062	0.366	Below LOD
Dy (ppm)	5.4	0.67	3.01	0.132	3.08	0.61	0.51	2.42	0.125
Ho (ppm)	0.951	0.112	0.541	Below LOD	0.712	0.104	0.129	0.58	Below LOD
Er (ppm)	2.47	0.256	1.55	Below LOD	2	0.206	0.38	1.66	Below LOD
Tm (ppm)	0.308	Below LOD	0.22	Below LOD	0.321	Below LOD	0.094	0.31	Below LOD
Yb (ppm)	2.32	0.31	1.3	0.16	2.34	0.18	0.58	2.13	0.2
Lu (ppm)	0.405	0.064	0.19	Below LOD	0.343	0.073	0.112	0.306	0.05

Sample	9-013 spot 9	9-013 spot 10	9-013 spot 11	9-013 spot 12	9-013 spot 13	9-013 spot 14	9-013 spot 15	9-013 spot 16	9-013 spot 17
Ca (cps)	18190	19400	19090	21780	2.24E+04	20280	20390	2.95E+04	2.38E+04
Si (ppm)	2.15E+05	2.29E+05	2.31E+05	2.23E+05	2.20E+05	2.22E+05	2.18E+05	2.23E+05	2.18E+05
Ti (ppm)	4060	5140	2192	2482	3320	531	1672	5030	4600
Ni (ppm)	167.4	133.3	142.9	128.7	128	155.4	160.9	171.5	178.7
Y (ppm)	13.1	19.94	6.4	11.51	10.86	1.18	2.31	18.37	16.25
Zr (ppm)	36.1	48	14.53	23.2	25.1	18.08	19.61	52	47
La (ppm)	0.073	Below LOD	Below LOD	Below LOD	Below LOD	0.142	0.056	0.112	0.066
Ce (ppm)	0.618	0.329	0.323	0.475	0.678	1.2	0.748	0.941	0.745
Pr (ppm)	0.161	0.111	0.123	0.153	0.177	0.305	0.211	0.274	0.247
Nd (ppm)	1.44	0.83	0.83	1.24	1.54	3.32	2.1	2.41	2.12
Sm (ppm)	1	1.04	0.31	0.61	0.65	0.85	1.07	1.43	1.17
Eu (ppm)	0.419	0.432	0.277	0.46	0.359	0.402	0.374	0.77	0.613
Gd (ppm)	1.77	1.64	0.97	1.13	1.25	0.85	0.77	2.36	1.73
Tb (ppm)	0.272	0.402	0.151	0.251	0.287	0.088	0.123	0.517	0.43
Dy (ppm)	2.42	3.45	1.13	1.71	1.93	0.46	0.6	3.43	3.03
Ho (ppm)	0.519	0.779	0.201	0.421	0.445	0.054	0.101	0.694	0.647
Er (ppm)	1.48	2.58	0.657	1.25	1.4	Below LOD	0.293	2.23	1.7
Tm (ppm)	0.226	0.337	0.144	0.205	0.224	Below LOD	0.039	0.272	0.286
Yb (ppm)	1.24	2.74	0.94	1.72	1.57	Below LOD	0.21	2.14	1.82
Lu (ppm)	0.235	0.428	0.169	0.281	0.254	Below LOD	Below LOD	0.278	0.246

Sample	9-013 spot 18	9-013 spot 19	9-013 spot 20	4A-013 spot 1	4A-013 spot 2	4A-013 spot 3	4A-013 spot 4	4A-013 spot 5
Ca (cps)	22570	20980	22330	19800	14040	22050	19490	18670
Si (ppm)	2.19E+05	2.13E+05	2.23E+05	2.17E+05	2.52E+05	2.26E+05	2.18E+05	2.20E+05
Ti (ppm)	4880	4700	121.5	3930	127	4310	6360	3920
Ni (ppm)	114.8	123.5	15.9	110.6	31.8	133.8	106.5	114.1
Y (ppm)	17.57	13.7	0.88	11.42	16.38	10.06	17.6	12.12
Zr (ppm)	47.9	41	0.55	40.7	2.36	46.8	64.2	42.1
La (ppm)	0.065	0.062	Below LOD	Below LOD	Below LOD	Below LOD	Below LOD	Below LOD
Ce (ppm)	0.436	0.504	0.32	0.454	Below LOD	0.575	0.472	0.513
Pr (ppm)	0.143	0.154	0.101	0.137	Below LOD	0.188	0.16	0.128
Nd (ppm)	1.35	1.27	0.74	1.19	Below LOD	1.43	1.59	1.13
Sm (ppm)	0.86	0.91	0.31	0.76	Below LOD	0.95	1.09	0.62
Eu (ppm)	0.59	0.417	Below LOD	0.414	Below LOD	0.544	0.57	0.43
Gd (ppm)	1.81	1.42	Below LOD	1.11	Below LOD	1.64	1.93	1.19
Tb (ppm)	0.389	0.334	Below LOD	0.303	0.152	0.337	0.392	0.291
Dy (ppm)	2.89	2.65	Below LOD	1.9	2.19	2	2.96	1.86
Ho (ppm)	0.724	0.569	0.03	0.461	0.525	0.424	0.687	0.381
Er (ppm)	1.99	1.56	0.115	1.3	2.37	1.11	2.04	1.48
Tm (ppm)	0.341	0.254	Below LOD	0.224	0.417	0.18	0.329	0.259
Yb (ppm)	2.29	1.54	0.3	1.7	2.69	1.36	2.07	1.54
Lu (ppm)	0.319	0.203	0.117	0.281	0.49	0.167	0.316	0.205

Sample	4A-013 spot 6	4A-013 spot 7	4A-013 spot 8	4A-013 spot 9	4A-013 spot 10	4A-013 spot 11	4A-013 spot 12	4A-013 spot 13
Ca (cps)	20350	21650	24400	22080	20890	21500	21110	2.72E+04
Si (ppm)	2.11E+05	2.18E+05	2.09E+05	2.13E+05	2.20E+05	2.18E+05	2.26E+05	2.25E+05
Ti (ppm)	4380	4960	4660	3980	4120	4110	4230	4920
Ni (ppm)	112.6	112.3	115.1	165.8	170.7	100.7	181.6	121.2
Y (ppm)	13.52	17.06	17.12	15.48	14.76	11.91	16.69	15.67
Zr (ppm)	39.9	46.5	44.1	41.3	39.5	44.9	39.9	46.6
La (ppm)	Below LOD	Below LOD	Below LOD	0.063	Below LOD	Below LOD	Below LOD	0.051
Ce (ppm)	0.379	0.398	0.433	0.654	0.673	0.353	0.737	0.481
Pr (ppm)	0.1	0.152	0.117	0.209	0.166	0.117	0.176	0.182
Nd (ppm)	1.42	0.98	1.53	1.97	1.87	1.05	1.52	1.31
Sm (ppm)	0.92	1.1	0.96	1.04	1	0.81	1.05	0.97
Eu (ppm)	0.459	0.58	0.427	0.494	0.56	0.368	0.487	0.495
Gd (ppm)	1.38	1.42	1.45	1.96	1.56	1.4	1.87	1.65
Tb (ppm)	0.322	0.422	0.334	0.407	0.406	0.323	0.347	0.378
Dy (ppm)	2.33	2.89	2.69	2.71	2.58	2.03	2.62	2.91
Ho (ppm)	0.594	0.617	0.692	0.588	0.53	0.44	0.646	0.609
Er (ppm)	1.57	1.93	1.96	1.71	1.6	1.29	1.84	1.66
Tm (ppm)	0.264	0.292	0.288	0.261	0.253	0.216	0.297	0.294
Yb (ppm)	1.65	2.53	2.17	1.79	2.2	1.99	1.95	1.98
Lu (ppm)	0.235	0.362	0.326	0.26	0.288	0.185	0.34	0.324

Sample	4A-013 spot 14	4A-013 spot 15	4A-013 spot 16	4A-013 spot 17	4C-013 spot 1	4C-013 spot 2	4C-013 spot 3	4C-013 spot 4
Ca (cps)	24170	28210	24740	22370	19220	19150	17450	18210
Si (ppm)	2.25E+05	1.66E+05	2.15E+05	2.18E+05	2.24E+05	2.15E+05	2.26E+05	2.31E+05
Ti (ppm)	6190	411	5430	3870	3905	3850	3910	3990
Ni (ppm)	107.2	3.23	97.9	110.8	116.5	166.1	117.9	114.7
Y (ppm)	16.17	638	17.72	11.9	11.55	14.53	11.48	11.74
Zr (ppm)	65.8	12.97	48.5	40.7	42	37.9	42.2	42.3
La (ppm)	Below LOD	Below LOD	Below LOD	Below LOD	Below LOD	0.099	Below LOD	Below LOD
Ce (ppm)	0.484	0.06	0.376	0.46	0.575	0.768	0.492	0.45
Pr (ppm)	0.162	0.156	0.11	0.152	0.154	0.18	0.163	0.158
Nd (ppm)	1.87	4.3	1.1	1.32	1.74	1.72	0.92	1.32
Sm (ppm)	1.1	8.29	0.93	0.71	0.53	1	0.86	0.72
Eu (ppm)	0.58	2.05	0.482	0.351	0.437	0.53	0.41	0.397
Gd (ppm)	1.64	25.96	1.61	1.42	1.62	1.81	1.22	1.28
Tb (ppm)	0.37	8.02	0.401	0.285	0.306	0.315	0.242	0.285
Dy (ppm)	2.81	81.6	2.92	2.14	1.89	2.55	2.22	1.96
Ho (ppm)	0.713	24.19	0.654	0.45	0.503	0.626	0.454	0.451
Er (ppm)	2.09	83.4	2.17	1.37	1.5	1.65	1.49	1.55
Tm (ppm)	0.286	13.82	0.382	0.238	0.212	0.264	0.253	0.225
Yb (ppm)	2.02	105.7	2.31	1.65	1.79	1.75	1.75	1.52
Lu (ppm)	0.29	16.22	0.434	0.247	0.268	0.29	0.287	0.233

Sample	4C-013 spot 5	4C-013 spot 6	4C-013 spot 7	4C-013 spot 8	4C-013 spot 9	4C-013 spot 10	4C-013 spot 11	4C-013 spot 12
Ca (cps)	19170	20410	19580	19260	19320	22060	21220	23760
Si (ppm)	2.20E+05	2.29E+05	2.19E+05	2.21E+05	2.24E+05	2.16E+05	2.25E+05	2.17E+05
Ti (ppm)	3790	4140	4700	4890	4740	1990	3945	3880
Ni (ppm)	109.4	174.5	122.5	117	127.1	121.2	126.4	112.6
Y (ppm)	11.17	14.84	17.9	17.66	17.5	1.16	14.92	11.06
Zr (ppm)	41.1	42.1	47	48.8	45.8	13.94	32	42.5
La (ppm)	Below LOD	0.076	0.056	0.06	Below LOD	0.054	Below LOD	Below LOD
Ce (ppm)	0.451	0.628	0.501	0.459	0.539	0.427	0.324	0.525
Pr (ppm)	0.122	0.186	0.145	0.115	0.154	0.134	0.11	0.137
Nd (ppm)	1.01	1.91	1.49	1.67	0.9	1.14	1	1.35
Sm (ppm)	0.71	0.94	1.18	0.74	0.89	0.76	0.7	0.86
Eu (ppm)	0.45	0.461	0.455	0.483	0.464	0.281	0.436	0.321
Gd (ppm)	1.09	1.89	2.13	1.81	2.05	0.52	1.4	1.38
Tb (ppm)	0.278	0.346	0.418	0.41	0.391	0.053	0.272	0.283
Dy (ppm)	2.03	2.73	2.98	3.09	3.18	0.245	2.45	2.17
Ho (ppm)	0.495	0.588	0.757	0.727	0.73	0.043	0.573	0.507
Er (ppm)	1.45	1.52	2.17	2.17	2.09	0.128	1.54	1.4
Tm (ppm)	0.208	0.267	0.314	0.37	0.302	Below LOD	0.248	0.206
Yb (ppm)	1.44	1.77	2.39	2.27	2.57	0.54	1.89	1.62
Lu (ppm)	0.281	0.269	0.337	0.37	0.33	0.063	0.284	0.214

Sample	4C-013 spot 13	4C-013 spot 14	4C-013 spot 15	4C-013 spot 16	4C-013 spot 17	4C-013 spot 18	4C-013 spot 19	4C-013 spot 20
Ca (cps)	20160	2.61E+04	23390	2.61E+04	2.54E+04	24410	23100	23620
Si (ppm)	2.17E+05	2.09E+05	2.08E+05	2.22E+05	2.23E+05	2.15E+05	2.22E+05	2.19E+05
Ti (ppm)	4660	5050	3900	4130	6670	4190	3830	4130
Ni (ppm)	123	159.1	108.8	176.6	109.1	160.6	116.9	169.2
Y (ppm)	18.42	18.76	11.26	15.26	29.63	14.45	11.88	15.13
Zr (ppm)	48.3	54.9	39.1	42	77	42.1	42.6	41.1
La (ppm)	0.077	0.142	Below LOD	0.088	Below LOD	0.063	0.047	0.158
Ce (ppm)	0.559	1.073	0.469	0.736	0.524	0.687	0.494	0.821
Pr (ppm)	0.138	0.262	0.161	0.196	0.163	0.195	0.126	0.205
Nd (ppm)	1.43	2.38	1.03	2.12	1.46	1.88	1.5	1.74
Sm (ppm)	0.95	1.45	0.81	0.79	1.29	0.96	0.74	1.11
Eu (ppm)	0.6	0.73	0.356	0.6	0.65	0.467	0.335	0.509
Gd (ppm)	1.76	2.63	1.28	1.82	2.44	1.63	1.26	1.78
Tb (ppm)	0.394	0.522	0.227	0.308	0.677	0.414	0.293	0.337
Dy (ppm)	3.12	3.44	1.96	2.73	4.86	2.6	2.29	2.52
Ho (ppm)	0.776	0.791	0.475	0.618	1.156	0.541	0.5	0.608
Er (ppm)	2.08	2.08	1.35	1.69	3.58	1.75	1.48	1.82
Tm (ppm)	0.296	0.272	0.208	0.288	0.517	0.208	0.252	0.309
Yb (ppm)	2.38	1.99	1.49	2.08	3.7	1.82	1.71	1.88
Lu (ppm)	0.366	0.281	0.206	0.285	0.509	0.26	0.257	0.259

Sample	4D-013 spot 1	4D-013 spot 2	4D-013 spot 3	4D-013 spot 4	4D-013 spot 5	4D-013 spot 6	4D-013 spot 7	4D-013 spot 8
Ca (cps)	19260	17040	17420	18040	19760	19670	18880	19680
Si (ppm)	2.24E+05	2.14E+05	2.21E+05	2.35E+05	2.22E+05	2.25E+05	2.21E+05	2.13E+05
Ti (ppm)	4110	4220	4090	4200	3920	5940	4000	5200
Ni (ppm)	173.3	121.6	169.3	180	113.6	107.6	116	123.4
Y (ppm)	15.31	13.33	14.65	15.89	11.5	19.43	11.88	14.82
Zr (ppm)	41.9	40.2	40.2	43.6	41.2	51.7	41.7	44.3
La (ppm)	0.085	Below LOD	Below LOD	0.102	Below LOD	Below LOD	0.087	Below LOD
Ce (ppm)	0.636	0.539	0.671	0.695	0.584	0.336	0.442	0.545
Pr (ppm)	0.141	0.172	0.262	0.241	0.166	0.11	0.152	0.205
Nd (ppm)	1.56	1.34	1.66	1.75	1.15	0.81	1.32	1.46
Sm (ppm)	1.06	1.1	1.06	1.08	0.87	1.06	0.62	0.81
Eu (ppm)	0.52	0.41	0.48	0.49	0.383	0.5	0.4	0.474
Gd (ppm)	1.67	1.48	2.1	1.77	1.29	1.63	1.21	1.55
Tb (ppm)	0.307	0.36	0.363	0.339	0.244	0.468	0.259	0.387
Dy (ppm)	2.99	2.44	2.45	2.28	2.03	3.31	1.76	2.79
Ho (ppm)	0.597	0.596	0.634	0.695	0.422	0.785	0.456	0.58
Er (ppm)	1.9	1.63	1.56	1.96	1.4	2.26	1.41	1.51
Tm (ppm)	0.252	0.235	0.247	0.279	0.219	0.363	0.267	0.223
Yb (ppm)	1.81	1.78	1.48	2.19	1.75	2.62	1.65	1.89
Lu (ppm)	0.301	0.296	0.221	0.26	0.231	0.4	0.229	0.28

Sample	4D-013 spot 9	4D-013 spot 10	4D-013 spot 11	4D-013 spot 12	4D-013 spot 13	4D-013 spot 14	4D-013 spot 15	4D-013 spot 16
Ca (cps)	22080	19300	2.36E+04	19700	19840	22170	2.81E+04	2.90E+04
Si (ppm)	2.10E+05	2.14E+05	2.11E+05	2.17E+05	2.18E+05	2.28E+05	2.01E+05	2.13E+05
Ti (ppm)	3960	3900	2771	1394	3920	4140	3760	4320
Ni (ppm)	113.7	101.5	125.3	121.1	165.6	114.8	136.9	115.1
Y (ppm)	11.19	12.28	12.36	2.04	14.12	12.22	6.49	11.84
Zr (ppm)	39.6	32.5	26.7	8.55	37.3	44.5	43.6	44.7
La (ppm)	Below LOD	Below LOD	0.072	Below LOD	0.073	0.047	0.117	Below LOD
Ce (ppm)	0.502	0.447	0.678	0.37	0.612	0.5	0.929	0.499
Pr (ppm)	0.127	0.128	0.177	0.124	0.231	0.147	0.283	0.145
Nd (ppm)	1.11	1.21	1.57	1.13	1.41	1.09	2.31	1.46
Sm (ppm)	0.59	0.92	0.8	0.58	1.01	0.77	1.5	0.83
Eu (ppm)	0.442	0.325	0.368	0.157	0.463	0.405	0.68	0.463
Gd (ppm)	1.4	1.71	1.67	Below LOD	1.38	1.63	1.51	1.56
Tb (ppm)	0.291	0.252	0.337	0.058	0.351	0.36	0.22	0.281
Dy (ppm)	1.91	2	2.13	0.232	2.35	2.13	1.2	2.36
Ho (ppm)	0.418	0.439	0.478	0.064	0.541	0.415	0.224	0.492
Er (ppm)	1.54	1.2	1.44	0.373	1.67	1.49	0.77	1.4
Tm (ppm)	0.209	0.221	0.212	0.094	0.256	0.243	0.168	0.211
Yb (ppm)	1.28	1.68	1.72	0.41	1.85	1.79	1.19	1.66
Lu (ppm)	0.266	0.249	0.249	0.1	0.262	0.281	0.184	0.202

Sample	4D-013 spot 17	4D-013 spot 18	4D-013 spot 19	4D-013 spot 20	11-013 spot 1	11-013 spot 2	11-013 spot 3	11-013 spot 4
Ca (cps)	21710	21110	23460	2.30E+04	15880	16660	4.15E+04	14980
Si (ppm)	2.16E+05	2.27E+05	2.14E+05	2.16E+05	2.08E+05	2.28E+05	1.69E+05	2.11E+05
Ti (ppm)	5810	3820	3800	3840	5790	5040	5250	5850
Ni (ppm)	122.7	113	108.7	113.4	65.4	125	20.6	70.3
Y (ppm)	21.79	11.44	11.47	11.15	13.88	19.19	41.3	13.88
Zr (ppm)	53.5	41.4	39.3	41.1	52.9	44.9	267.8	56.5
La (ppm)	Below LOD	Below LOD	Below LOD	Below LOD	Below LOD	0.23	0.065	Below LOD
Ce (ppm)	0.427	0.491	0.456	0.452	0.243	0.73	1.02	0.27
Pr (ppm)	0.131	0.14	0.142	0.158	0.099	0.159	0.323	0.083
Nd (ppm)	1.35	1.3	1.01	1.33	0.68	1.46	3.64	0.9
Sm (ppm)	0.8	0.77	0.83	0.69	0.54	0.86	2.88	0.6
Eu (ppm)	0.538	0.342	0.3	0.294	0.38	0.48	1.59	0.335
Gd (ppm)	2.06	1.43	1.41	0.94	1.24	1.63	5.39	1.37
Tb (ppm)	0.518	0.256	0.247	0.299	0.233	0.433	1.195	0.289
Dy (ppm)	3.3	2.04	1.98	2.04	2.15	3.32	8.33	2.28
Ho (ppm)	0.822	0.466	0.425	0.466	0.532	0.761	1.76	0.548
Er (ppm)	2.41	1.42	1.35	1.44	1.65	2.37	4.58	1.53
Tm (ppm)	0.372	0.236	0.223	0.204	0.263	0.342	0.69	0.235
Yb (ppm)	2.49	1.82	1.52	1.86	1.61	2.37	3.86	1.52
Lu (ppm)	0.413	0.226	0.291	0.223	0.314	0.411	0.48	0.296

Sample	11-013 spot 5	11-013 spot 6	11-013 spot 7	11-013 spot 8	11-013 spot 9	11-013 spot 10	11-013 spot 11	5-013 spot 1	5-013 spot 2
Ca (cps)	16220	22650	18820	24220	3.58E+04	2.78E+04	3.18E+04	20800	2.95E+04
Si (ppm)	2.30E+05	2.11E+05	2.25E+05	2.29E+05	2.45E+05	2.09E+05	2.38E+05	2.18E+05	1.83E+05
Ti (ppm)	6760	6300	7860	6610	7740	4940	970	9150	458
Ni (ppm)	71.5	110.8	79.8	62.2	31.7	17.3	26.3	39	Below LOD
Y (ppm)	15.99	19.45	19.93	16.74	55.4	36.4	8.2	14.18	495
Zr (ppm)	64.7	55.3	85.4	66	270.3	147.3	10.23	203.7	12.67
La (ppm)	Below LOD	Below LOD	Below LOD	Below LOD	Below LOD	Below LOD	Below LOD	Below LOD	Below LOD
Ce (ppm)	0.198	0.331	0.386	0.343	0.473	0.428	0.366	0.638	0.166
Pr (ppm)	0.08	0.14	0.16	0.077	0.168	0.149	0.143	0.217	0.227
Nd (ppm)	1.08	1.16	1.27	1.08	1.93	1.56	1.77	1.73	4.29
Sm (ppm)	0.6	0.85	1.08	0.85	1.56	1.47	1.03	1.77	8.63
Eu (ppm)	0.409	0.47	0.56	0.365	1.04	0.79	0.586	0.85	2.33
Gd (ppm)	1.51	1.8	2.01	1.94	4.59	2.97	1.51	2.62	24.5
Tb (ppm)	0.391	0.425	0.443	0.401	1.22	0.805	0.259	0.464	7.01
Dy (ppm)	2.47	3.36	3.18	3.03	9.87	6.01	1.46	2.99	61.6
Ho (ppm)	0.642	0.792	0.716	0.669	2.24	1.5	0.312	0.554	18.73
Er (ppm)	2.02	2.19	2.33	1.77	6.24	4.56	0.8	1.25	63.6
Tm (ppm)	0.304	0.332	0.37	0.3	0.899	0.62	0.147	0.124	10.73
Yb (ppm)	2.01	2.23	2.53	2.28	5.8	4.89	0.87	0.63	84.3
Lu (ppm)	0.375	0.309	0.378	0.301	0.77	0.725	0.114	0.079	13.27

Sample	5-013 spot 3	5-013 spot 4	5-013 spot 5	a-013-p2 spot 1	a-013-p2 spot 2	a-013-p2 spot 3	a-013-p2 spot 4	a-013-p2 spot 5
Ca (cps)	28530	25250	3.28E+04	21500	19560	18750	16240	19840
Si (ppm)	1.84E+05	2.07E+05	1.95E+05	2.29E+05	2.08E+05	2.14E+05	2.45E+05	2.15E+05
Ti (ppm)	496	663	666	4200	269	4750	866	4710
Ni (ppm)	Below LOD	Below LOD	3.13	175.3	127.2	119.2	167.7	112.5
Y (ppm)	356	380	516	16.16	2.01	16.91	2.26	15.07
Zr (ppm)	8.8	16.65	15.2	43.2	6.8	46.8	5.25	43
La (ppm)	Below LOD	Below LOD	0.039	0.076	0.05	Below LOD	0.125	0.083
Ce (ppm)	0.242	0.27	0.33	0.749	0.467	0.482	1.01	0.538
Pr (ppm)	0.295	0.367	0.35	0.221	0.153	0.185	0.252	0.172
Nd (ppm)	5.9	7.84	6.32	1.93	1.27	1.47	1.96	1.28
Sm (ppm)	9.75	11.5	10.7	0.85	0.55	1.17	0.72	0.82
Eu (ppm)	2.73	3.02	2.61	0.51	0.239	0.533	0.307	0.531
Gd (ppm)	24.7	28.7	27.6	1.89	Below LOD	1.96	0.85	1.74
Tb (ppm)	5.81	6.79	7.12	0.384	0.036	0.386	0.072	0.352
Dy (ppm)	48.6	55.6	67.4	2.8	0.214	3.02	0.35	2.63
Ho (ppm)	13.13	15.02	20.72	0.653	0.072	0.679	0.055	0.566
Er (ppm)	44	50.5	78.2	1.89	0.275	1.91	0.23	1.82
Tm (ppm)	7.27	8.02	13.14	0.315	0.08	0.279	Below LOD	0.249
Yb (ppm)	57.4	62.2	98.3	2.32	0.52	2.28	0.42	2.35
Lu (ppm)	9.38	10.63	16.84	0.301	0.107	0.311	0.063	0.314

Sample	a-013-p2 spot 6	a-013-p2 spot 7	a-013-p2 spot 8	a-013-p2 spot 9	a-013-p2 spot 10	a-013-p2 spot 11	a-013-p2 spot 12
Ca (cps)	22880	19770	19280	19080	440	17830	2.22E+04
Si (ppm)	2.13E+05	2.21E+05	2.10E+05	2.25E+05	no value	3.13E+05	2.27E+05
Ti (ppm)	3660	985	4940	4260	no value	2832	3990
Ni (ppm)	154.6	110.3	114.7	117.4	no value	200.4	113.7
Y (ppm)	12.51	2.11	16.58	12.55	no value	9.63	12.14
Zr (ppm)	35.2	7.44	44.5	42.4	no value	23.3	41.5
La (ppm)	0.062	Below LOD	Below LOD	Below LOD	no value	Below LOD	Below LOD
Ce (ppm)	0.587	0.408	0.406	0.58	no value	0.43	0.5
Pr (ppm)	0.198	0.1	0.124	0.111	no value	0.154	0.15
Nd (ppm)	1.13	0.88	1.3	1.63	no value	0.97	1.32
Sm (ppm)	0.85	0.3	0.99	0.82	no value	0.8	0.65
Eu (ppm)	0.494	0.149	0.458	0.4	no value	0.306	0.456
Gd (ppm)	1.36	Below LOD	1.9	1.16	no value	1.08	1.1
Tb (ppm)	0.317	0.031	0.4	0.26	no value	0.237	0.336
Dy (ppm)	2.02	0.274	2.83	1.99	no value	1.62	2.17
Ho (ppm)	0.49	0.079	0.616	0.434	no value	0.444	0.441
Er (ppm)	1.59	0.34	1.88	1.52	no value	1.07	1.27
Tm (ppm)	0.25	0.041	0.381	0.257	no value	0.196	0.221
Yb (ppm)	1.96	0.34	2.3	1.86	no value	1.68	1.36
Lu (ppm)	0.278	0.099	0.335	0.229	no value	0.283	0.236

Sample	a-013-p2 spot 13	a-013-p2 spot 14	a-013-p2 spot 15	a-013-p2 spot 16	a-013-p2 spot 17	a-013-p2 spot 18
Ca (cps)	20410	2.39E+04	18640	24320	17730	21330
Si (ppm)	2.34E+05	1.60E+05	2.34E+05	1.85E+05	2.66E+05	2.31E+05
Ti (ppm)	4140	2160	1292	4130	2519	984
Ni (ppm)	166.7	91.2	130.5	98.9	164.3	127.9
Y (ppm)	14.78	4.63	4.85	15.17	9.85	1.24
Zr (ppm)	39.6	28.4	4.21	39.8	19.58	9.11
La (ppm)	0.058	0.055	0.061	Below LOD	0.084	Below LOD
Ce (ppm)	0.67	0.642	0.551	0.416	0.379	0.442
Pr (ppm)	0.166	0.207	0.183	0.133	0.134	0.187
Nd (ppm)	1.58	1.9	1.33	1.09	0.91	1.44
Sm (ppm)	0.91	0.82	0.38	0.98	0.53	0.48
Eu (ppm)	0.41	0.428	0.151	0.436	0.351	0.212
Gd (ppm)	1.55	0.99	0.61	1.55	0.99	Below LOD
Tb (ppm)	0.357	0.186	0.099	0.335	0.26	0.052
Dy (ppm)	2.62	1.06	0.87	2.55	1.44	0.244
Ho (ppm)	0.639	0.189	0.202	0.628	0.369	0.043
Er (ppm)	1.6	0.353	0.51	1.79	1.16	0.184
Tm (ppm)	0.34	0.063	0.107	0.268	0.209	0.034
Yb (ppm)	2.29	0.56	1.24	1.87	1.88	0.46
Lu (ppm)	0.275	0.055	0.162	0.305	0.192	0.081

Sample	a-013-p2 spot 20	a-013-p2 spot 21	a-013-p2 spot 22	a-013-p2 spot 23	a-013-p2 spot 24	a-013-p2 spot 25	a-013-p4 spot 1
Ca (cps)	21550	2.46E+04	23160	2.31E+04	22040	2.31E+04	19740
Si (ppm)	2.36E+05	2.31E+05	2.19E+05	2.26E+05	2.20E+05	2.25E+05	2.62E+05
Ti (ppm)	4430	4920	3631	4960	4710	598	2876
Ni (ppm)	188	121.5	164.4	123.7	146	124.1	184.8
Y (ppm)	16.53	16.24	14	17.8	16.87	2.06	12.57
Zr (ppm)	44.2	46.4	36.3	47.4	50.5	4.42	26
La (ppm)	0.058	0.063	Below LOD	0.068	0.08	Below LOD	Below LOD
Ce (ppm)	0.662	0.492	0.583	0.458	0.666	0.513	0.39
Pr (ppm)	0.196	0.128	0.207	0.137	0.224	0.184	Below LOD
Nd (ppm)	1.71	1.45	1.37	1.36	1.69	1.33	1.23
Sm (ppm)	1.23	1.15	0.95	0.87	1.16	0.59	0.62
Eu (ppm)	0.69	0.542	0.503	0.572	0.652	0.171	0.33
Gd (ppm)	1.75	1.55	1.62	1.94	1.92	0.47	1.32
Tb (ppm)	0.415	0.377	0.332	0.37	0.456	0.029	0.267
Dy (ppm)	2.74	2.95	2.16	2.66	2.83	0.38	2.31
Ho (ppm)	0.633	0.614	0.608	0.674	0.692	0.063	0.587
Er (ppm)	1.78	1.91	1.63	1.92	1.98	0.279	1.55
Tm (ppm)	0.315	0.313	0.228	0.32	0.287	0.039	0.252
Yb (ppm)	2.06	1.92	1.69	2.01	2.08	0.49	1.78
Lu (ppm)	0.335	0.304	0.321	0.352	0.31	0.086	0.313

Sample	a-013-p4 spot 2	a-013-p4 spot 3	a-013-p4 spot 4	a-013-p4 spot 5	a-013-p4 spot 6	a-013-p4 spot 7	a-013-p4 spot 8
Ca (cps)	2.49E+04	21970	20210	21330	22630	22680	20110
Si (ppm)	2.18E+05	1.97E+05	2.23E+05	1.82E+05	2.24E+05	2.01E+05	2.02E+05
Ti (ppm)	5500	3562	4580	3170	4610	4680	423
Ni (ppm)	155.7	129	190.8	107.5	175.3	138.5	126.6
Y (ppm)	12.84	7.03	17.66	9.8	19.93	16.78	1.22
Zr (ppm)	46.4	31.84	46	31.5	48.4	46.4	Below LOD
La (ppm)	Below LOD	Below LOD	0.101	0.06	0.08	0.086	0.082
Ce (ppm)	0.584	0.524	0.82	0.508	0.685	0.74	0.613
Pr (ppm)	0.191	0.207	0.213	0.154	0.199	0.242	0.174
Nd (ppm)	1.56	1.55	2.07	1.2	1.81	1.85	1.15
Sm (ppm)	0.85	0.93	0.91	0.91	1.27	1.06	0.23
Eu (ppm)	0.558	0.49	0.58	0.231	0.56	0.588	Below LOD
Gd (ppm)	1.72	1.38	1.87	1.27	2.31	2.11	Below LOD
Tb (ppm)	0.401	0.231	0.395	0.202	0.497	0.415	Below LOD
Dy (ppm)	2.58	1.49	3.3	1.67	3.33	3.01	Below LOD
Ho (ppm)	0.492	0.276	0.75	0.434	0.819	0.678	0.027
Er (ppm)	1.37	0.83	2.16	1.37	2.23	1.82	0.185
Tm (ppm)	0.198	0.122	0.327	0.239	0.327	0.349	0.047
Yb (ppm)	1.75	0.86	1.81	1.48	2.75	1.95	0.45
Lu (ppm)	0.215	0.113	0.344	0.196	0.4	0.336	0.129

Sample	a-013-p4 spot 10	a-013-p4 spot 11	a-013-p4 spot 12	a-013-p4 spot 13	a-013-p4 spot 14	a-013-p4 spot 15	a-013-p4 spot 16
Ca (cps)	2.45E+04	2.40E+04	21510	6700	25220	7.02E+04	1.08E+05
Si (ppm)	2.04E+05	1.83E+05	2.07E+05	8.35E+05	2.24E+05	1.52E+05	4.07E+04
Ti (ppm)	5210	4300	1108	109	4770	216.8	8.5
Ni (ppm)	117.3	166.3	125.2	Below LOD	155.6	246.7	Below LOD
Y (ppm)	18.17	14.61	2.94	10780	13.58	243.6	10.37
Zr (ppm)	49	44.6	14.79	2.73E+06	46.9	236.7	0.13
La (ppm)	Below LOD	Below LOD	Below LOD	500	Below LOD	248	1.916
Ce (ppm)	0.546	0.738	0.618	1550	0.612	241.8	6.52
Pr (ppm)	0.114	0.187	0.146	87	0.156	234.5	0.935
Nd (ppm)	1.24	2.32	1.46	320	1.36	231.7	4.31
Sm (ppm)	0.94	1.47	0.81	76	1	247.5	0.721
Eu (ppm)	0.56	0.614	0.241	19.7	0.627	248.2	1.65
Gd (ppm)	1.72	2.22	0.72	155	1.86	238.3	1
Tb (ppm)	0.399	0.416	0.094	45.1	0.416	238.7	0.174
Dy (ppm)	3.29	2.84	0.5	605	2.64	233.3	1.3
Ho (ppm)	0.725	0.607	0.107	285	0.535	241.1	0.323
Er (ppm)	2.49	1.49	0.33	1730	1.61	229.1	1.002
Tm (ppm)	0.358	0.234	0.069	518	0.266	227.4	0.151
Yb (ppm)	2.38	1.27	0.55	5950	1.66	238.1	1.28
Lu (ppm)	0.411	0.242	0.113	927	0.233	233.7	0.181

Sample	a-013-p4 spot 17	a-013-p4 spot 18	a-013-p4 spot 19	w-013-p spot 1	w-013-p spot 2	w-013-p spot 3	w-013-p spot 4
Ca (cps)	24320	26320	2.30E+04	19080	17890	18040	20730
Si (ppm)	2.02E+05	1.86E+05	1.96E+05	2.13E+05	2.09E+05	2.18E+05	2.23E+05
Ti (ppm)	4170	4280	4240	3960	367	3890	549
Ni (ppm)	119.2	167.5	182.3	165	25.4	166.1	113.8
Y (ppm)	13.05	11.53	16.67	15.5	7.39	14.33	3.42
Zr (ppm)	46.9	38.5	45	40.8	2.81	37.2	5.29
La (ppm)	0.073	0.101	0.095	0.073	Below LOD	0.086	0.066
Ce (ppm)	0.535	0.926	0.646	0.633	0.187	0.566	0.615
Pr (ppm)	0.155	0.244	0.187	0.152	0.056	0.149	0.184
Nd (ppm)	1.64	2.12	1.88	1.86	0.83	1.37	1.93
Sm (ppm)	0.93	1.05	1.17	0.99	0.201	1.31	0.47
Eu (ppm)	0.443	0.491	0.47	0.532	0.164	0.47	0.198
Gd (ppm)	1.53	2.04	1.99	2.2	Below LOD	1.27	Below LOD
Tb (ppm)	0.333	0.289	0.352	0.32	0.127	0.352	0.094
Dy (ppm)	2.32	2.34	2.98	2.61	1.05	2.4	0.51
Ho (ppm)	0.518	0.469	0.65	0.679	0.298	0.603	0.112
Er (ppm)	1.35	1.01	1.98	1.82	1.06	1.79	0.474
Tm (ppm)	0.272	0.145	0.322	0.311	0.15	0.283	0.094
Yb (ppm)	1.83	1.2	2.27	2.2	1.13	1.89	0.46
Lu (ppm)	0.252	0.198	0.348	0.341	0.175	0.307	0.092

Sample	w-013-p spot 5	w-013-p spot 6	w-013-p spot 7	w-013-p spot 8	w-013-p spot 9	w-013-p spot 10	w-013-p spot 11
Ca (cps)	2.02E+04	17970	19570	20020	19760	22570	23830
Si (ppm)	2.05E+05	2.34E+05	2.05E+05	2.25E+05	2.18E+05	2.08E+05	2.09E+05
Ti (ppm)	3760	4210	4180	3070	3510	3680	938
Ni (ppm)	124.6	134.6	130	169.8	141.2	106.3	112.7
Y (ppm)	10.41	15.56	14.48	7.81	14.12	10.95	0.505
Zr (ppm)	35	44.5	40.7	43.5	36.6	39.4	3.8
La (ppm)	Below LOD	Below LOD	0.072	0.105	0.073	Below LOD	Below LOD
Ce (ppm)	0.475	0.45	0.529	0.885	0.636	0.582	0.418
Pr (ppm)	0.101	0.112	0.147	0.258	0.175	0.145	0.122
Nd (ppm)	1.05	1.08	1.55	2.49	1.45	1.37	0.79
Sm (ppm)	0.69	0.58	0.96	0.89	0.85	0.83	0.128
Eu (ppm)	0.4	0.301	0.49	0.52	0.52	0.321	Below LOD
Gd (ppm)	1.27	1.62	1.7	1.72	1.55	1.43	Below LOD
Tb (ppm)	0.326	0.344	0.361	0.328	0.274	0.192	Below LOD
Dy (ppm)	2.12	2.8	2.72	1.83	2.32	2.13	Below LOD
Ho (ppm)	0.461	0.53	0.599	0.302	0.621	0.484	0.02
Er (ppm)	1.22	1.97	1.92	0.69	1.8	1.49	Below LOD
Tm (ppm)	0.187	0.327	0.302	0.069	0.3	0.22	Below LOD
Yb (ppm)	1.4	2.53	2	0.55	1.99	1.69	0.272
Lu (ppm)	0.207	0.272	0.262	0.104	0.24	0.306	0.04

Sample	w-013-p spot 12	b-013-p spot 1	b-013-p spot 2	b-013-p spot 3	b-013-p spot 4	b-013-p spot 5	17-decs-016 spot 1
Ca (cps)	23130	23930	22550	6040	20970	3860	2.40E+04
Si (ppm)	2.15E+05	1.85E+05	1.93E+05	3.29E+05	1.87E+05	1.66E+05	1.94E+05
Ti (ppm)	393	3750	3970	67.4	1060	21.1	2618
Ni (ppm)	23.6	102.4	105.7	Below LOD	93.1	Below LOD	97.9
Y (ppm)	7.62	11.87	12.13	21	2.56	144.6	4.11
Zr (ppm)	23.1	42.3	45.1	13.1	18.56	1.34	20.73
La (ppm)	Below LOD	Below LOD	Below LOD	Below LOD	0.057	Below LOD	0.068
Ce (ppm)	0.473	0.464	0.559	Below LOD	0.484	Below LOD	0.337
Pr (ppm)	0.136	0.121	0.121	Below LOD	0.146	Below LOD	0.131
Nd (ppm)	0.82	1.06	1.58	0.78	1.66	Below LOD	1.04
Sm (ppm)	0.88	0.85	0.75	4.71	0.52	0.146	0.75
Eu (ppm)	0.47	0.349	0.365	3.13	0.29	Below LOD	0.245
Gd (ppm)	1.33	1.28	1.73	8.2	0.81	3.01	0.94
Tb (ppm)	0.215	0.256	0.307	1.17	0.104	1.66	0.135
Dy (ppm)	1.41	2.03	1.63	5.49	0.44	20	0.76
Ho (ppm)	0.252	0.423	0.46	0.72	0.094	5.98	0.147
Er (ppm)	0.84	1.53	1.37	1.49	0.265	17.8	0.45
Tm (ppm)	0.121	0.208	0.216	0.146	0.066	2.4	0.074
Yb (ppm)	0.96	1.4	1.64	1.11	0.45	16.2	0.48
Lu (ppm)	0.12	0.227	0.167	0.139	0.088	2.52	Below LOD

Sample	17-decs-016 spot 2	17-decs-016 spot 3	17-decs-016 spot 4	17-decs-016 spot 5	17-decs-016 spot 6	17-decs-016 spot 7
Ca (cps)	22020	21120	20410	22110	2.71E+04	19350
Si (ppm)	2.14E+05	1.97E+05	1.83E+05	2.06E+05	1.99E+05	2.01E+05
Ti (ppm)	5350	1455	4980	4110	5710	1302
Ni (ppm)	128.2	116.8	94.5	162.9	96.3	98.7
Y (ppm)	19.57	2.25	13	15.14	16.78	2.89
Zr (ppm)	48	8.37	51.9	39.5	49.3	13.2
La (ppm)	Below LOD	Below LOD	Below LOD	0.09	Below LOD	Below LOD
Ce (ppm)	0.398	0.413	0.331	0.517	0.486	0.376
Pr (ppm)	0.147	0.157	0.099	0.161	0.141	0.117
Nd (ppm)	1.32	1.1	0.85	1.4	1.66	1.02
Sm (ppm)	0.99	0.61	0.94	0.96	1.07	0.52
Eu (ppm)	0.56	0.213	0.39	0.61	0.57	0.174
Gd (ppm)	1.8	0.83	1.66	1.56	2.11	Below LOD
Tb (ppm)	0.392	0.059	0.309	0.401	0.38	0.092
Dy (ppm)	3.38	0.36	2.15	2.66	3.02	0.41
Ho (ppm)	0.701	0.097	0.524	0.585	0.604	0.088
Er (ppm)	2.36	0.284	1.47	1.78	1.76	0.348
Tm (ppm)	0.351	0.046	0.187	0.257	0.242	0.065
Yb (ppm)	2.16	0.39	1.48	1.9	2.37	0.79
Lu (ppm)	0.354	0.076	0.196	0.308	0.22	0.093

Sample	17-decs-016 spot 8	17-decs-016 spot 9	4B- 013 spot 1	4B- 013 spot 2	4B- 013 spot 3	4B- 013 spot 4	4B- 013 spot 5
Ca (cps)	20190	2.52E+04	2.61E+04	2.91E+04	26400	2.56E+04	27770
Si (ppm)	2.02E+05	1.98E+05	2.14E+05	2.25E+05	2.13E+05	2.13E+05	2.21E+05
Ti (ppm)	60	6830	4430	4900	4650	5090	3794
Ni (ppm)	20.5	64.8	114.4	133.7	113.3	115.3	114.1
Y (ppm)	0.255	17.45	14.15	22.13	18.05	18.85	11.9
Zr (ppm)	Below LOD	76.9	39.8	46.2	46.9	48.3	42.4
La (ppm)	Below LOD	Below LOD	0.098	Below LOD	Below LOD	Below LOD	0.056
Ce (ppm)	0.417	0.377	0.546	0.476	0.462	0.368	0.475
Pr (ppm)	0.089	0.114	0.162	0.148	0.135	0.109	0.145
Nd (ppm)	0.48	1.47	1.28	1.2	1.43	1.01	1.1
Sm (ppm)	Below LOD	0.78	0.87	0.96	0.79	0.72	0.56
Eu (ppm)	Below LOD	0.449	0.52	0.49	0.623	0.443	0.313
Gd (ppm)	Below LOD	1.89	1.62	1.82	1.59	1.38	0.96
Tb (ppm)	Below LOD	0.416	0.325	0.436	0.461	0.377	0.289
Dy (ppm)	Below LOD	2.54	2.55	3.36	3.08	2.82	2.03
Ho (ppm)	Below LOD	0.675	0.548	0.822	0.707	0.699	0.457
Er (ppm)	Below LOD	2.12	1.71	2.76	1.91	2.27	1.48
Tm (ppm)	Below LOD	0.314	0.26	0.442	0.309	0.303	0.246
Yb (ppm)	0.28	2.29	2.29	3.06	2.56	2.64	1.75
Lu (ppm)	0.044	0.303	0.284	0.363	0.344	0.346	0.271

Sample	4B- 013 spot 6	4B- 013 spot 7	4B- 013 spot 8	4B- 013 spot 9	4B- 013 spot 10	4B- 013 spot 11	4B- 013 spot 12	4B- 013 spot 13
Ca (cps)	25350	2.85E+04	25830	26360	23520	31530	32830	27360
Si (ppm)	2.14E+05	2.29E+05	2.20E+05	2.17E+05	2.12E+05	2.14E+05	1.92E+05	2.20E+05
Ti (ppm)	1980	3960	4391	3339	450	3643	118.7	4780
Ni (ppm)	164.4	116.9	114.2	114	41.8	110.6	23.7	128.4
Y (ppm)	6.74	12.59	16.05	9.42	0.86	11.42	3.04	17.44
Zr (ppm)	26.94	42.8	42	30.6	9.86	40.6	14.99	47
La (ppm)	0.103	0.07	0.053	Below LOD	0.303	Below LOD	0.058	0.067
Ce (ppm)	0.593	0.47	0.467	0.489	1.27	0.444	0.825	0.382
Pr (ppm)	0.213	0.162	0.132	0.166	0.235	0.144	0.315	0.104
Nd (ppm)	1.45	1.32	1.28	1.06	1.78	1.12	3.24	1.09
Sm (ppm)	0.86	0.73	0.78	0.65	0.53	0.59	1.33	0.88
Eu (ppm)	0.43	0.375	0.422	0.327	0.185	0.373	0.441	0.492
Gd (ppm)	1.32	1.43	1.69	1.14	0.6	0.83	0.76	1.55
Tb (ppm)	0.213	0.297	0.349	0.261	0.068	0.281	0.123	0.4
Dy (ppm)	1.4	1.79	2.74	1.78	0.208	1.88	0.558	2.85
Ho (ppm)	0.254	0.464	0.566	0.356	0.043	0.445	0.112	0.693
Er (ppm)	0.81	1.46	1.78	1.12	0.095	1.3	0.414	1.94
Tm (ppm)	0.136	0.208	0.302	0.21	0.032	0.209	0.063	0.314
Yb (ppm)	0.64	1.67	2.21	1.42	0.319	1.56	0.6	2.32
Lu (ppm)	0.122	0.288	0.369	0.209	0.057	0.225	0.138	0.401

Sample	4B- 013 spot 14	4B- 013 spot 15	4B- 013 spot 16	4B- 013 spot 17	4B- 013 spot 18	4B- 013 spot 19	4B- 013 spot 20
Ca (cps)	3.18E+04	3.03E+04	32900	30630	3.80E+04	3.10E+04	2.97E+04
Si (ppm)	2.43E+05	2.18E+05	2.20E+05	2.16E+05	2.07E+05	2.32E+05	2.22E+05
Ti (ppm)	4305	3958	3688	3999	4119	7000	4046
Ni (ppm)	126.1	167.9	115.4	149.4	157.7	98	171.2
Y (ppm)	13.09	15.36	12.17	15.42	10.32	18.36	15.47
Zr (ppm)	46.3	41.3	41.6	44.6	34.8	82	43.7
La (ppm)	0.057	0.049	Below LOD	Below LOD	0.101	Below LOD	0.088
Ce (ppm)	0.519	0.57	0.445	0.566	0.892	0.396	0.608
Pr (ppm)	0.148	0.17	0.128	0.163	0.27	0.168	0.186
Nd (ppm)	1.24	1.67	1.13	1.44	1.9	1.41	1.48
Sm (ppm)	0.82	0.91	0.86	1.02	1.13	0.92	0.91
Eu (ppm)	0.501	0.532	0.385	0.528	0.531	0.502	0.592
Gd (ppm)	1.7	1.6	1.23	1.68	1.56	1.62	1.75
Tb (ppm)	0.277	0.335	0.274	0.373	0.3	0.422	0.368
Dy (ppm)	2.21	2.8	1.98	2.68	1.92	3.16	2.63
Ho (ppm)	0.548	0.641	0.502	0.574	0.456	0.838	0.596
Er (ppm)	1.61	1.7	1.27	1.78	0.97	2.23	1.9
Tm (ppm)	0.274	0.314	0.244	0.276	0.145	0.344	0.302
Yb (ppm)	1.81	2.06	1.57	1.81	0.99	2.44	2.16
Lu (ppm)	0.242	0.326	0.231	0.285	0.143	0.391	0.328

Sample	17-DEC-015 Grt-1	17-DEC-017 Grt-1	17-DEC-017 Grt-2
Ca (cps)	13720	16490	1.27E+04
Si (ppm)	2.33E+05	2.46E+05	2.24E+05
Ti (ppm)	5060	349	4820
Ni (ppm)	134.1	140.2	135.6
Y (ppm)	14.88	1.11	9.67
Zr (ppm)	46	2.28	36.8
La (ppm)	Below LOD	0.101	Below LOD
Ce (ppm)	0.511	0.59	0.4
Pr (ppm)	0.178	0.14	0.158
Nd (ppm)	1.55	0.94	0.88
Sm (ppm)	1.05	0.42	0.97
Eu (ppm)	0.65	Below LOD	0.63
Gd (ppm)	2.03	Below LOD	1.7
Tb (ppm)	0.371	Below LOD	0.278
Dy (ppm)	3.19	0.33	1.81
Ho (ppm)	0.71	Below LOD	0.45
Er (ppm)	1.68	0.15	0.92
Tm (ppm)	0.234	Below LOD	0.159
Yb (ppm)	2.11	0.46	0.75
Lu (ppm)	0.3	Below LOD	0.218

Appendix III Maps and Charts

(1) Grütter et al. (2004) and Hardman et al (2018a) classification per map sheet

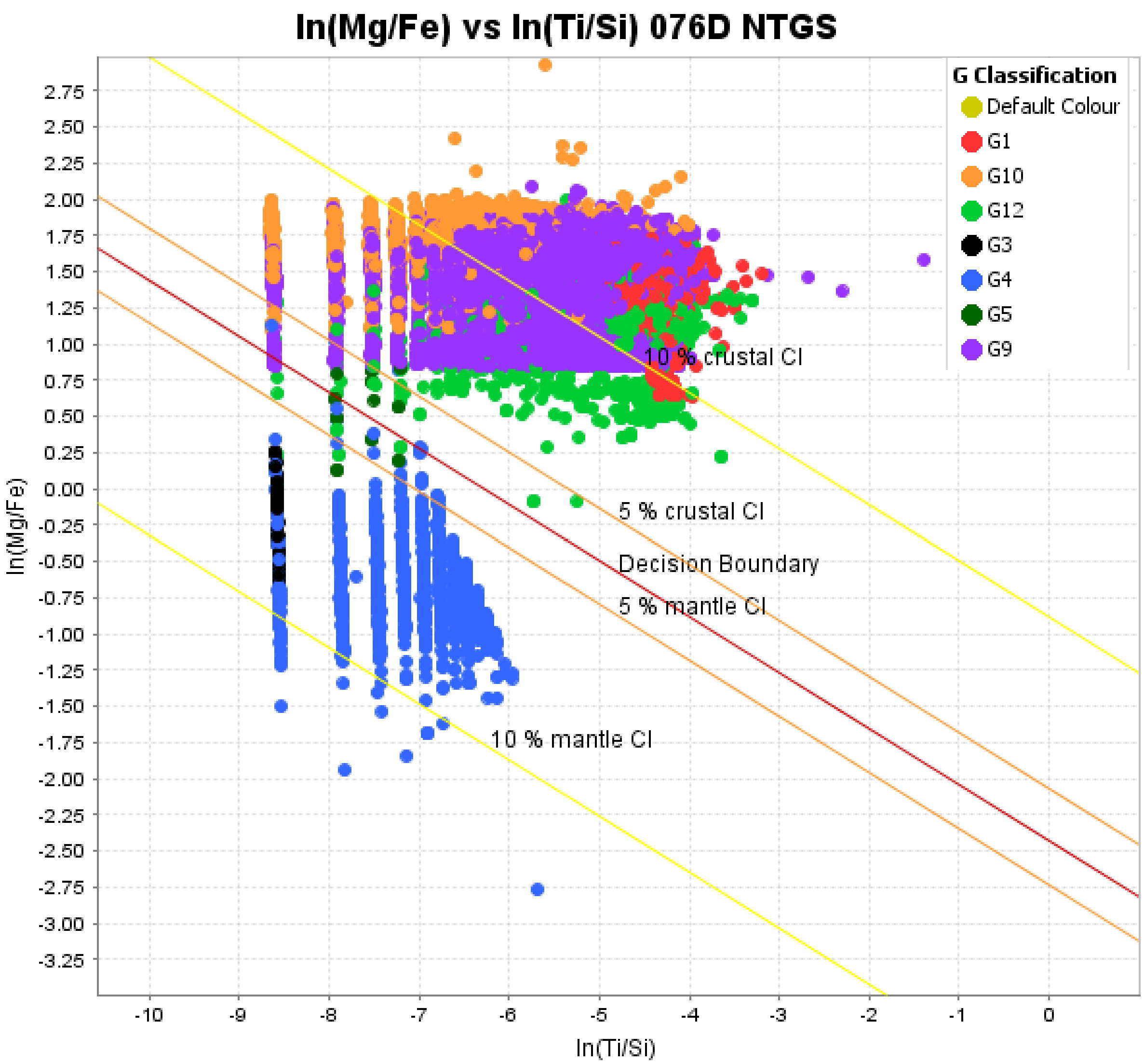

Figure 7.1: Garnets in surficial sediment samples from NTS map sheet 076D classified using G-number scheme of Grutter et al. (2004) and plotted on the discrimination biplot of mantle vs crustal of Hardman et al. (2018a).

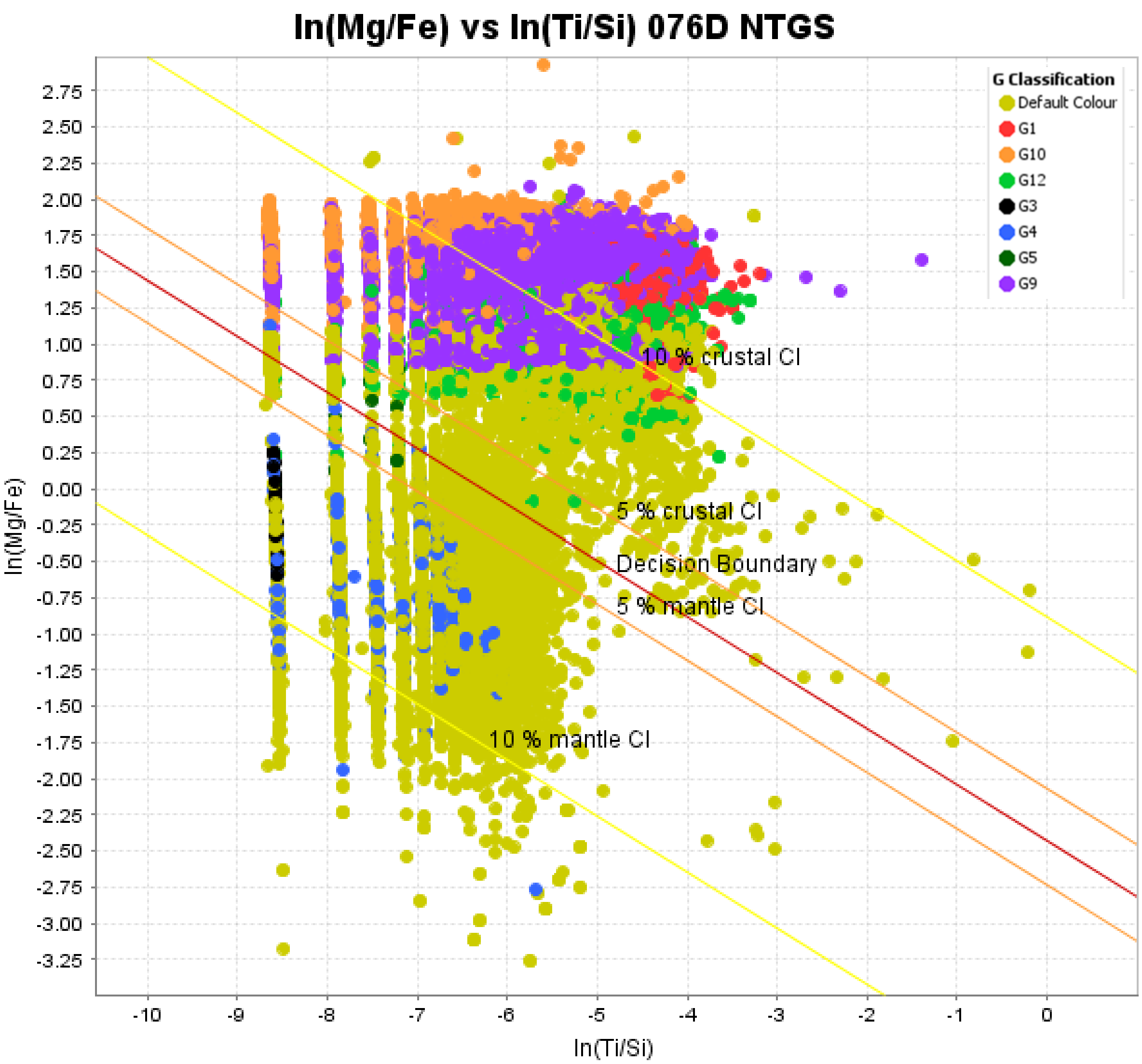

Figure 7.2: Garnets in surficial sediment samples from NTS map sheet 076D classified using G-number scheme of Grutter et al. (2004) and plotted on the discrimination biplot of mantle vs crustal of Hardman et al. (2018a).

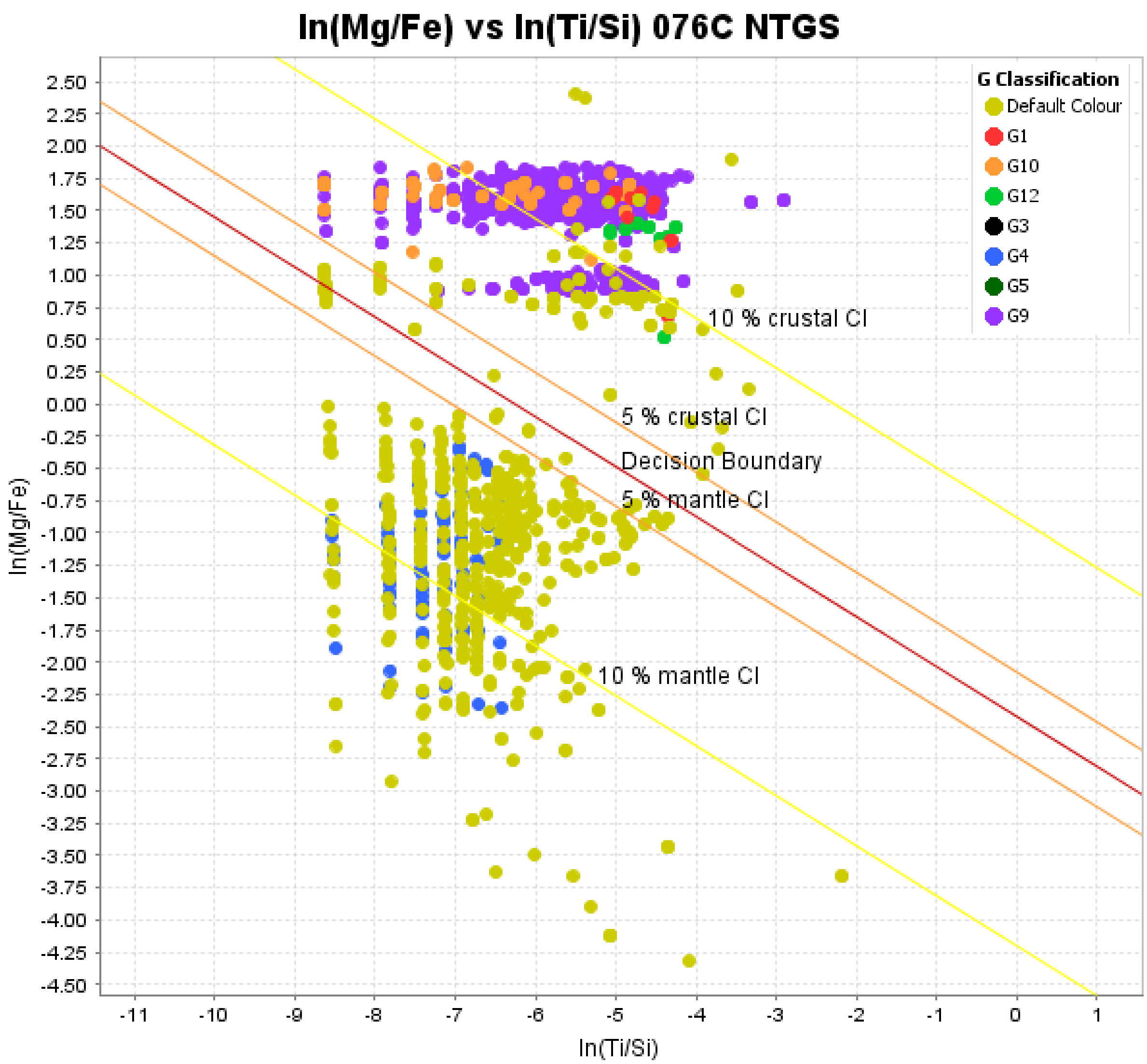

Figure 7.3: Garnets in surficial sediment samples from NTS map sheet 076C classified using G-number scheme of Grutter et al. (2004) and plotted on the discrimination biplot of mantle vs crustal of Hardman et al. (2018a).

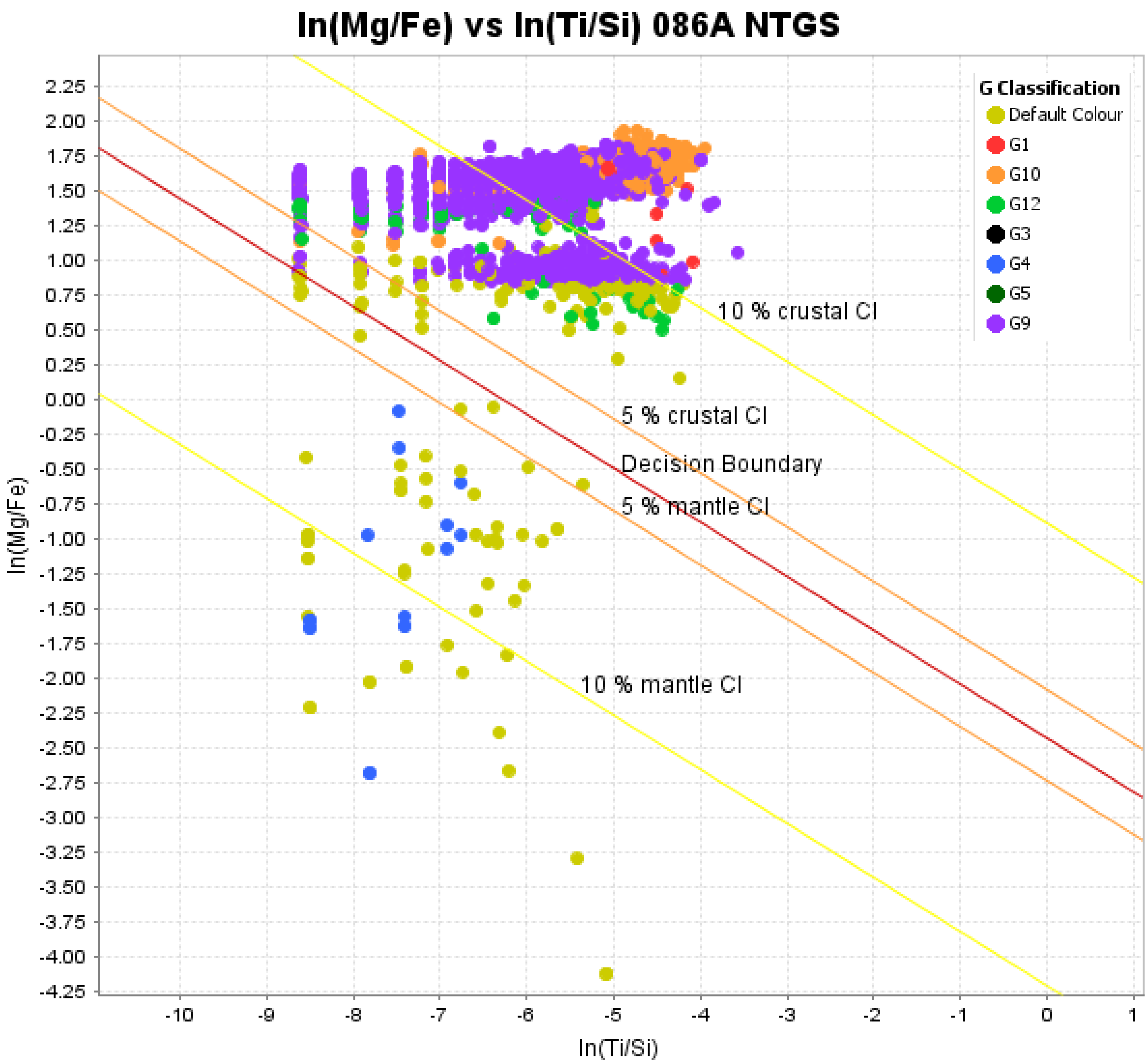

Figure 7.4: Garnets in surficial sediment samples from NTS map sheet 086A classified using G-number scheme of Grutter et al. (2004) and plotted on the discrimination biplot of mantle vs crustal of Hardman et al. (2018a).

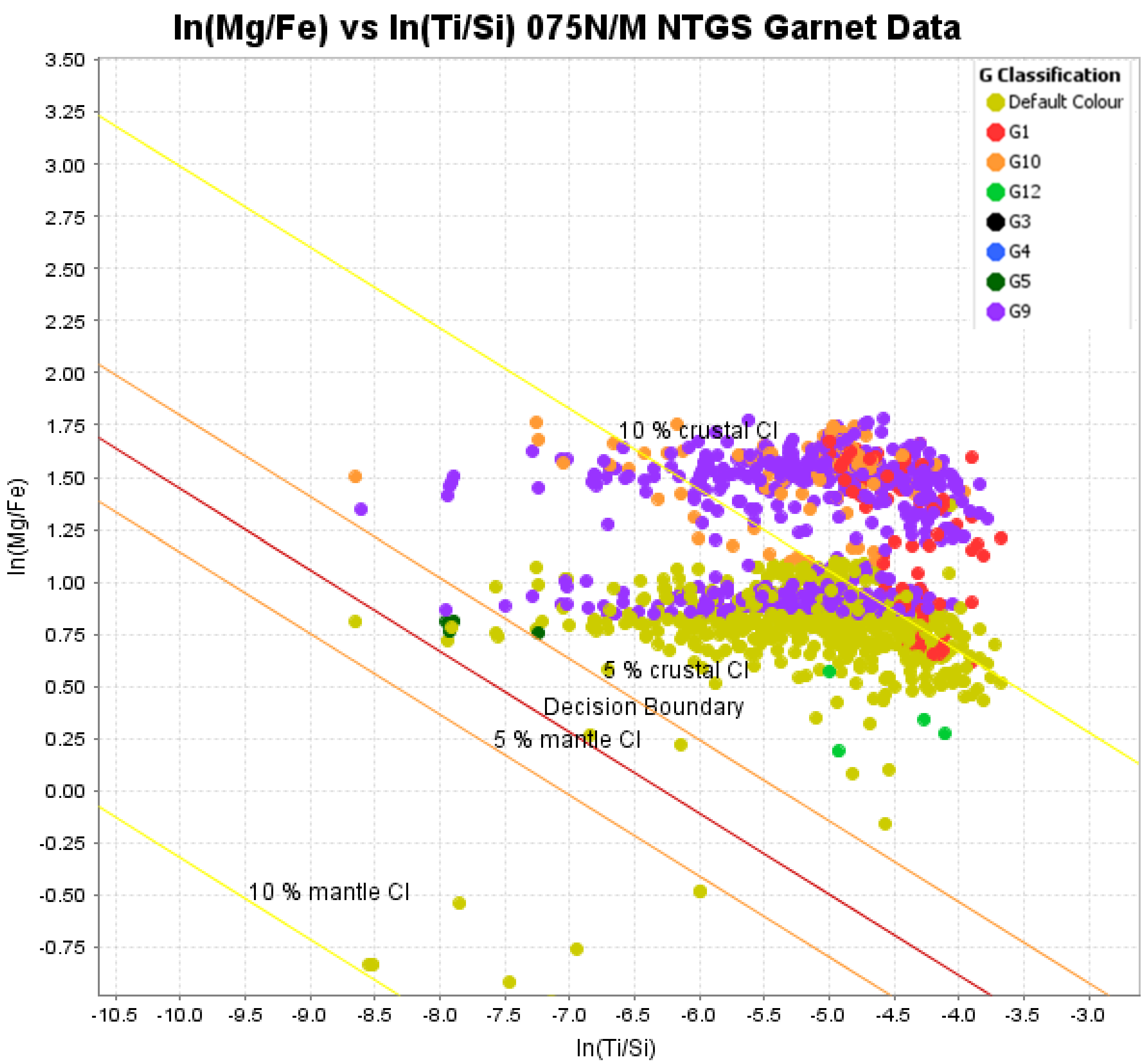

Figure 7.5: Garnets in surficial sediment samples from NTS map sheet 075N/M classified using G-number scheme of Grutter et al. (2004) and plotted on the discrimination biplot of mantle vs crustal of Hardman et al. (2018a).

(2) Grütter et al. (2004) vs Hardman et al. (2018)

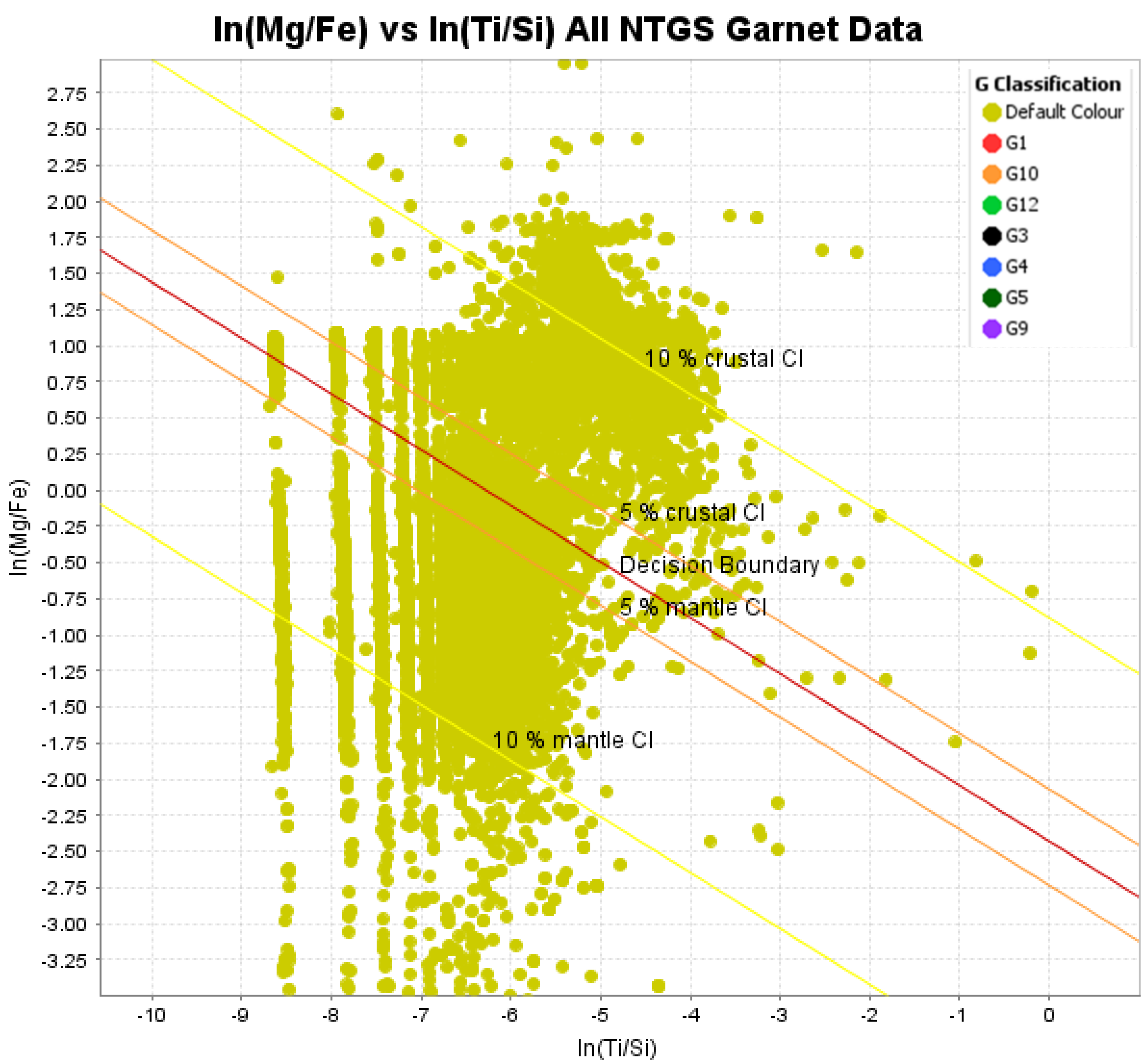

Figure 7.6: Unclassified garnet (Grutter et al., 2004) plotted on the discrimination biplot by Hardman et al. (2018a).

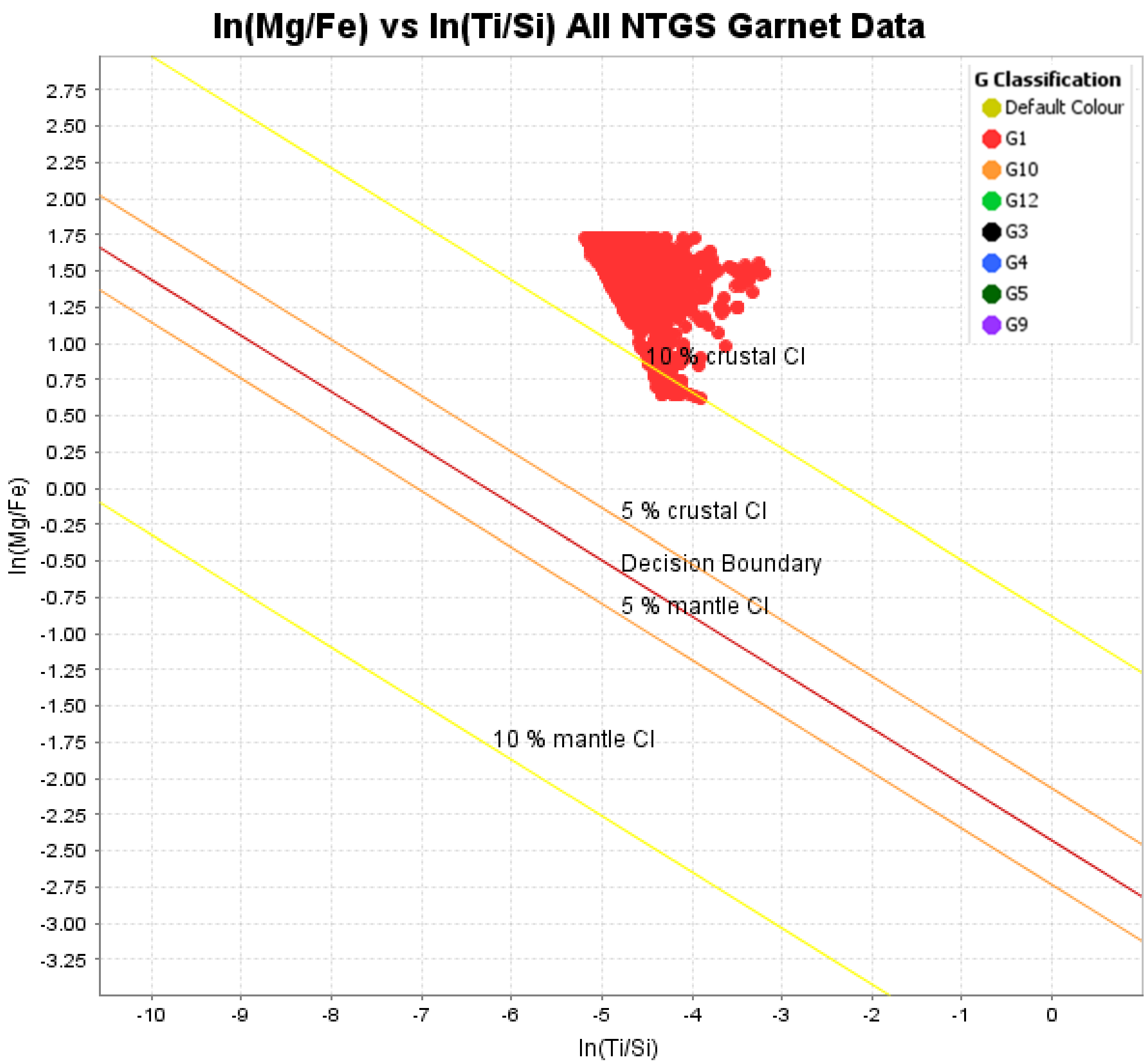

Figure 7.7: G1 garnet (Grutter et al., 2004) plotted on the discrimination biplot by Hardman et al. (2018a).

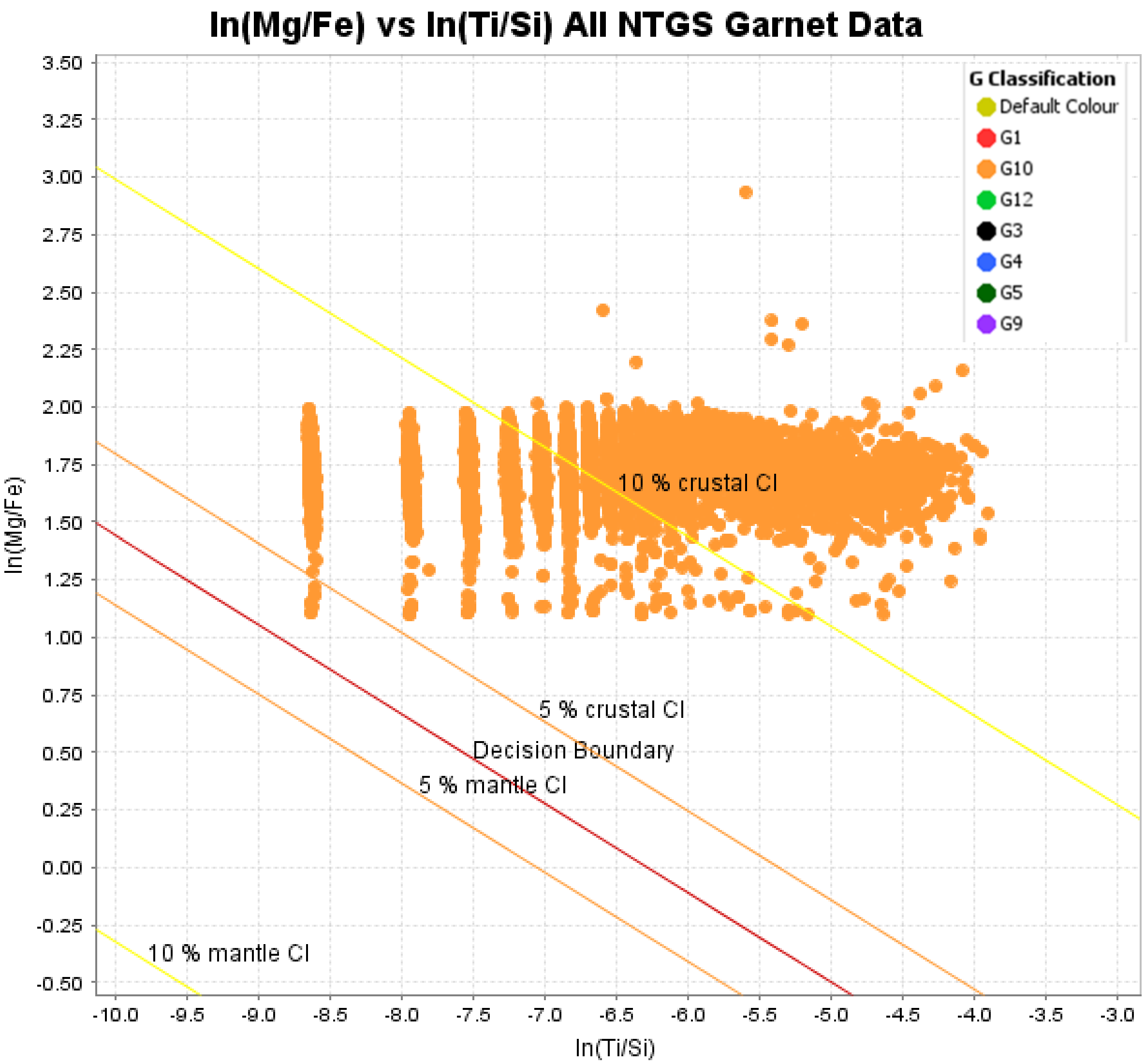

Figure 7.8: G10 garnet (Grutter et al., 2004) plotted on the discrimination biplot by Hardman et al. (2018a).

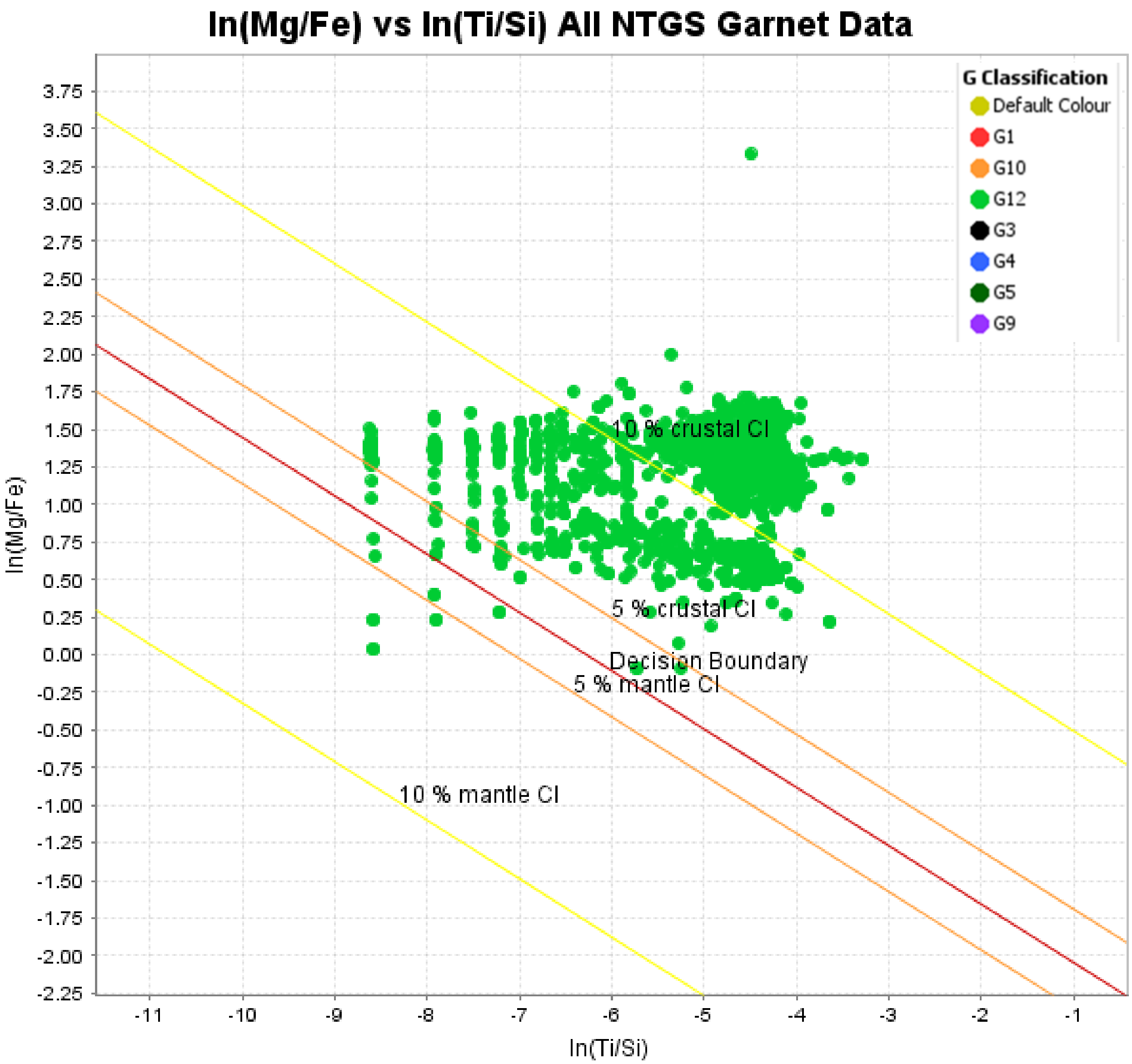

Figure 7.9: G12 garnet (Grutter et al., 2004) plotted on the discrimination biplot by Hardman et al. (2018a).

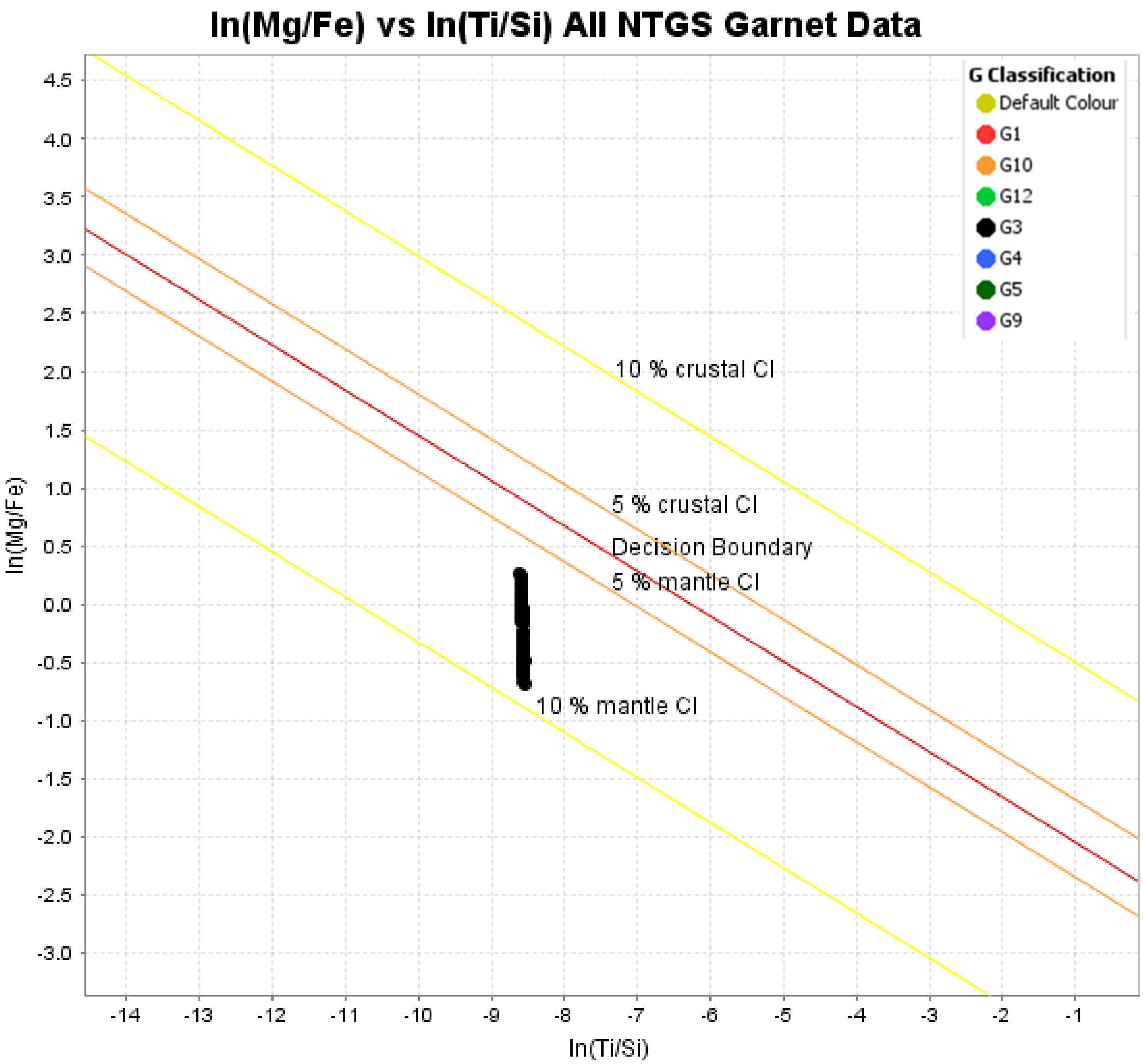

Figure 7.10: G3 garnet (Grutter et al., 2004) plotted on the discrimination biplot by Hardman et al. (2018a).

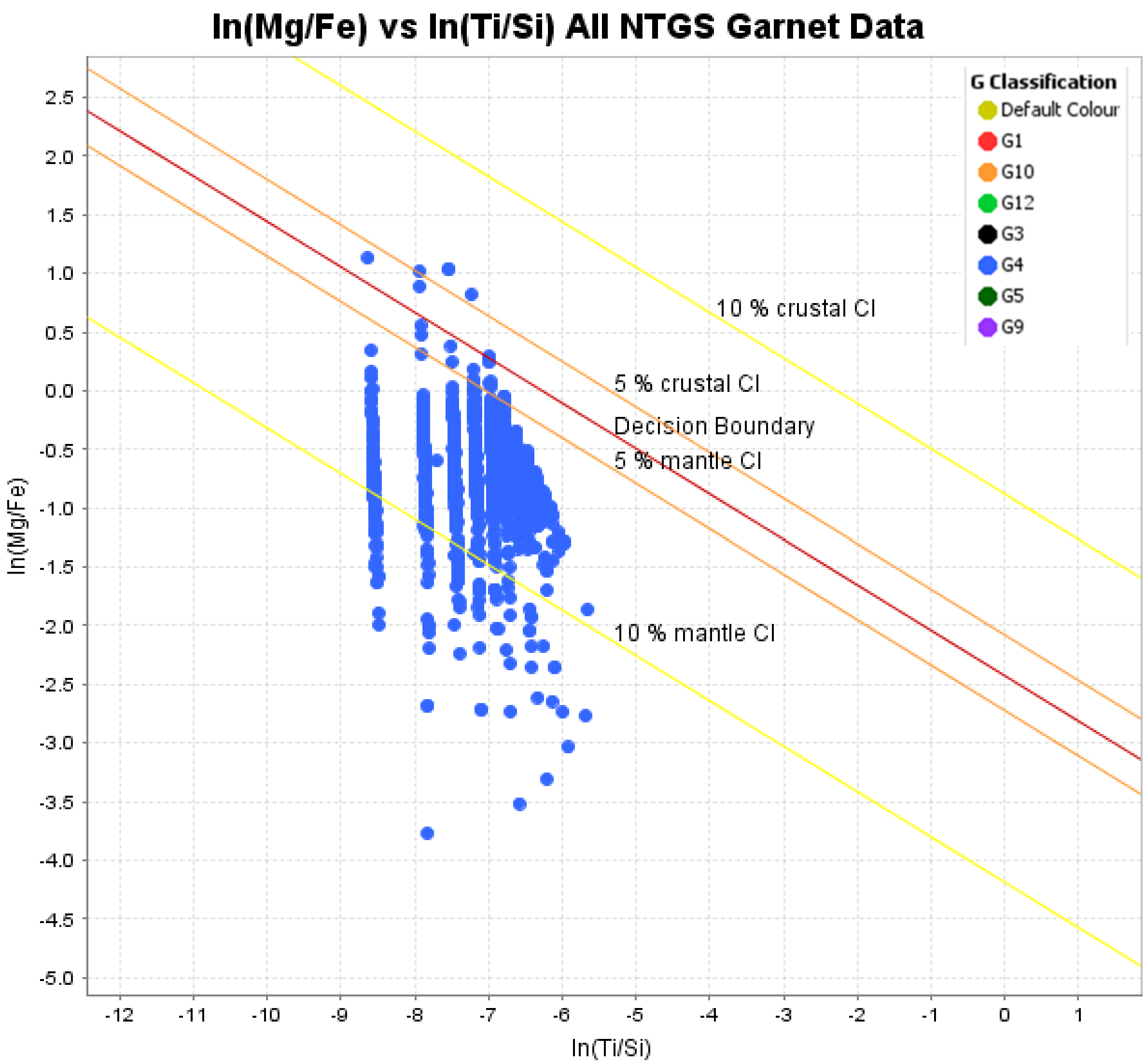

Figure 7.11: G4 garnet (Grutter et al., 2004) plotted on the discrimination biplot by Hardman et al. (2018a).

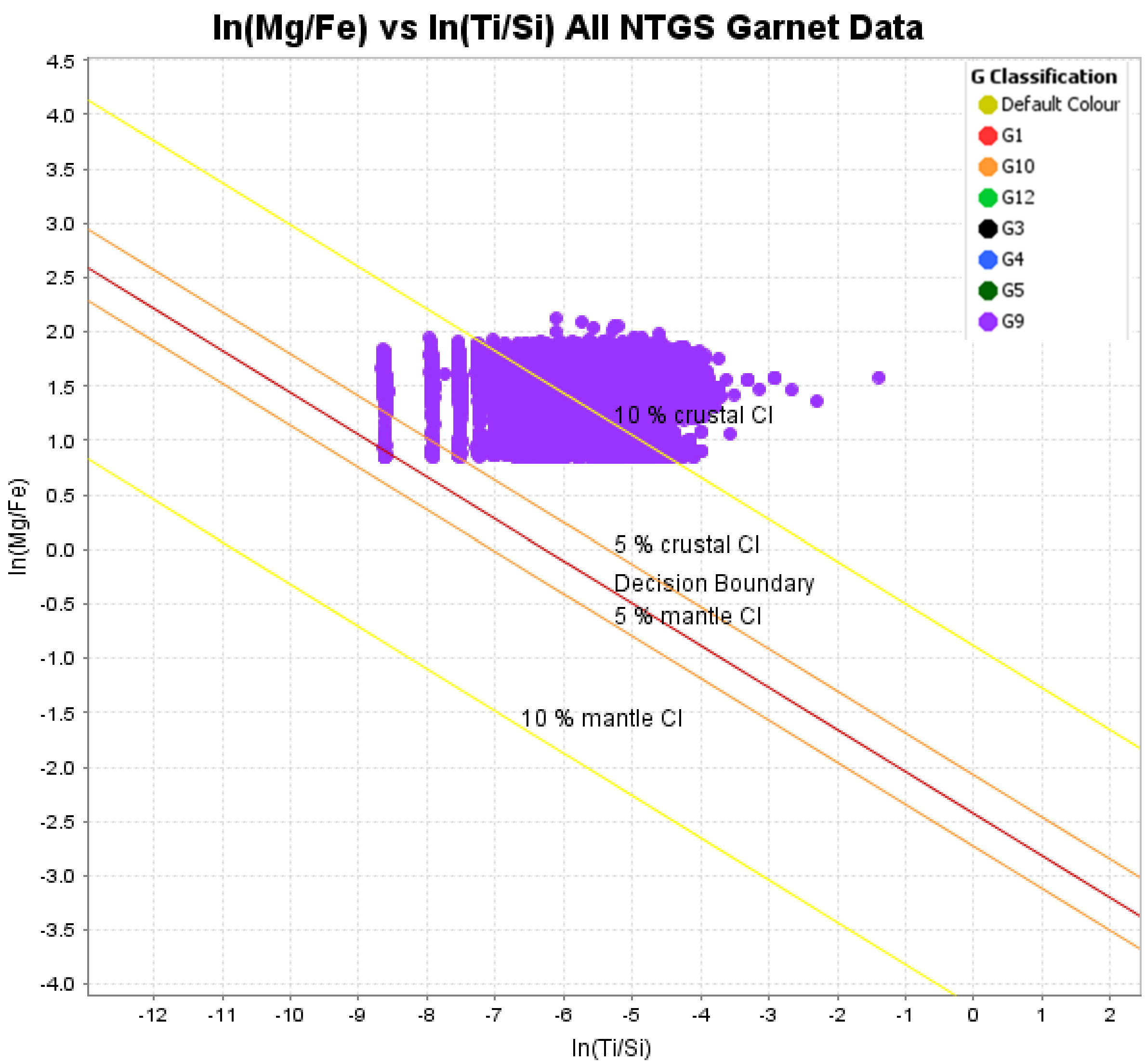

Figure 7.12: G9 garnet (Grutter et al., 2004) plotted on the discrimination biplot by Hardman et al. (2018a).

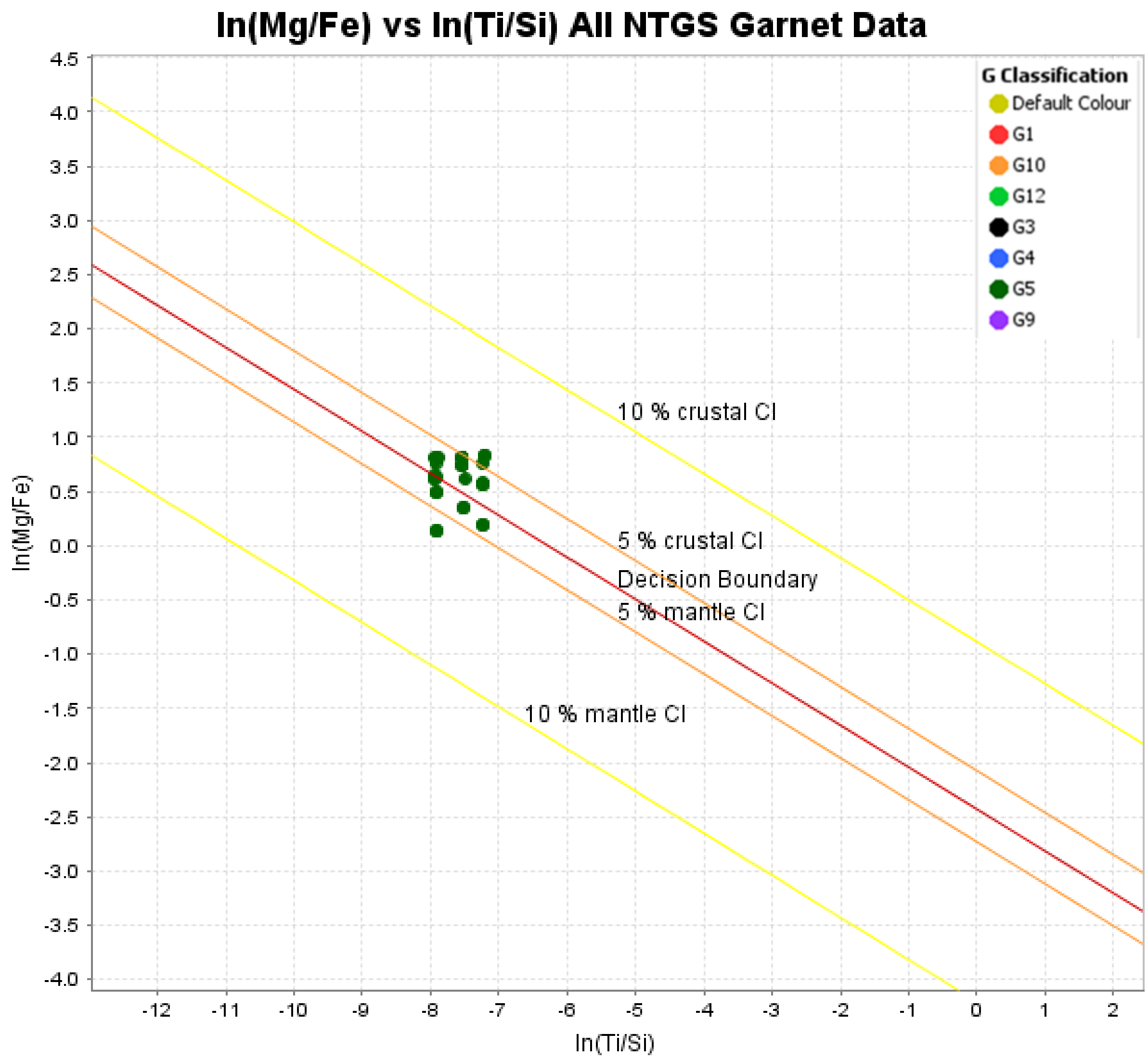

Figure 7.13: G5 garnet (Grutter et al., 2004) plotted on the discrimination biplot by Hardman et al. (2018a).

Appendix IV Field Observations

(1) 17-DECS-001

Date: July 15, 2017	Samplers: Dana Campbell, Barrett Elliott, Robin Mckillop, Dave Sacco	Weather: Overcast
Sample: 001	Zone: 12 V Easting: 0555756 UTM Northing: 7035243	Elevation (m asl): 400
Till Description: Light gray soil with mild to moderate oxidation. Silty sand, angular to sub-rounded 10-15% clasts.		
Vegetation: Shrubs and lichen.		
Exposure: Hand dug pit	Note: Sample between two roche moutonnées.	
Topographic position: Uphill between two outcrops.		




(2) 17-DECS-002

Date: July 15, 2017	Samplers: Dana Campbell, Barrett Elliott, Robin Mckillop, Dave Sacco	Weather: Overcast
Sample: 002	12 V 0556208 UTM 7024102	Elevation(m asl): 418
Till Description: Gray brown till silty sand with mild oxidation. Sub-angular to sub-rounded clasts, 35-40% clasts.		
Vegetation: Shrubs		
Exposure: Pit	Note:	
Topographic position: Side of hill.		

(3) 17-DECS-003

Date: July 16, 2017	Samplers: Dana Campbell, Barrett Elliott, Robin Mckillop, Dave Sacco	Weather: Cloudy
Sample: 003	12 V 0556171 UTM 7023310	Elevation(m asl): 429
Till Description: Light gray silty sand. Angular-subangular clasts 5-10% clasts.		
Vegetation: Shrubs.		
Exposure: Pit	Note: Topographic high	
Topographic Position: Topographic high, top of hill.		




(4) 17-DECS-004

Date: July 17, 2017	Samplers: Dana, Dave, Robin	Weather: Overcast
Sample: 17-DECS-004	12 V 0557857 UTM 7067721	Elevation(m asl): 412
Till Description: Light brown soil with weak oxidation. Silty sand. Angular to subangular clasts. 30-35% clasts. Sizes variable with dominantly cobbles.		
Vegetation: Shrubs.		
Exposure: Pit	Note: Sample area has exposed outcrop as well as abundant boulders and minor erratic's.	
Topographic position: On the top of a small slope.		




(5) 17-DECS-005

Date: July 13, 2017	Samplers: Dana, Dave, Robin	Weather: Overcast
Sample: 17-DECS-005	12 V 0559902 UTM 7064215	Elevation(m asl): 412
Till Description: Light gray to blueish gray sandy clayey silt with approximately 10% clasts. Clasts are sub-rounded.		
Vegetation: Sedges and Grasses		
Exposure: Pit	Note: Down ice of suspected mag anomaly. High moisture content.	
Topographic position: Low lying swampy area.		

(6) 17-DECS-006

Date: July 13, 2017	Samplers: Dana, Dave, Robin	Weather: Overcast
Sample: 17-DECS-006	12 V 0559834 UTM 7064227	Elevation(m asl): 405
Till Description: Gray Silty Sand, sub rounded to rounded elongate clasts. Most clasts had schistose foliations. 15-20% clasts. Fine grain to pebbles and cobbles.		
Vegetation: Shrubs.		
Exposure: Pit	Note: Sampled relict frostboil.	
Topographic position: On a ridge near outcrop.		

(7) 17-DECS-007

Date: July 13, 2017	Samplers: Dana Campbell, Robin, Dave	Weather: Overcast
Sample: 17-DECS-007	12 V 0559528 UTM 7064262	Elevation(m asl): 418
Till Description: Silty sand, subangular clasts, 20-25% clasts. Fine- cobbles.		
Vegetation: Shrubs.		
Exposure: Pit	Note: Bouldery area. Surrounded by boulder nets. Sampled on frost boil.	
Topographic position: ridge.		

(8) 17-DECS-008

Date: July 13, 2017	Samplers: Dana Campbell, Robin, Dave	Weather: overcast
Sample: 17-DECS-008	12 V 0557601 UTM 7064775	Elevation(m asl): 422
Till Description: Light brown-gray, 15-30% clasts, clasts are subangular.		
Vegetation: Shrubs.		
Exposure: Pit	Note: Relict frostboil .	
Topographic position: Up hill.		

(9) 17-DECS-009A+B

Date: July 13, 2017	Samplers: Dana Campbell, Robin, Dave	Weather: overcast
Sample: 17-DECS-009A+B	12 V 0557785 UTM 7064799	Elevation(m asl): 411
Till Description: light brown-gray till, 25-30% clasts. Clasts are angular to subangular.		
Vegetation: Dominantly shrubs.		
Exposure: Pit	Note: relict frostboil.	
Topographic position: side of a hill, middle of the slope.		

(10) 17-DECS-010

Date: July 13, 2017	Samplers: Dana, Dave, Robin	Weather: Overcast
Sample: 17-DECS-010	12 V 0557820 UTM 7064824	Elevation(m asl): 404
Till Description: Light brown silty sand. Low clast content 10-15%, with dominantly subangular to angular clasts.		
Vegetation: Shrub dominated.		
Exposure: Pit	Note: Down slope of known magnetic anomaly. Taken from inactive frostboil ~5m in diameter.	
Topographic position: Down slope.		

(11) 17-DECS-011

Date: July 13, 2017	Samplers: Dana Campbell, Robin, Dave	Weather: Overcast
Sample: 17-DECS-011	12 V 0557418 UTM 7054371	Elevation(m asl): 400
Till Description: Light brown gray silty sand, 10-15% subangular clasts. Fine to cobble sized clasts with low boulder concentration on surface.		
Vegetation: Shrubs.		
Exposure: Pit	Note: Mapped as a moraine. Relict frostboils abundant.	
Topographic position: flat lying area moderately high relative to surrounding area.		

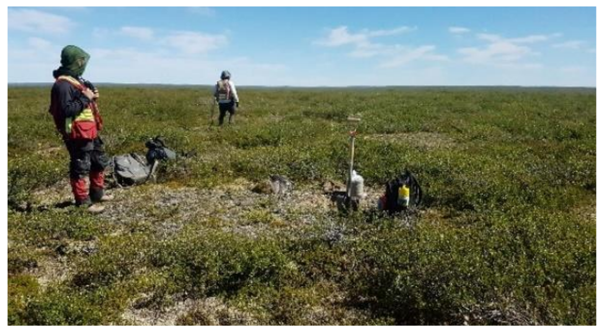

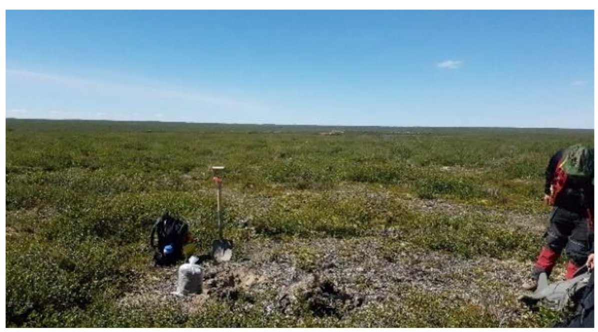

(12) 17-DECS-012

Date: July 16, 2017	Samplers: Dana Campbell, Brent Ward	Weather: Clear Skies and windy
Sample: 17-DECS-012	12 V 0555756 UTM 7035243	Elevation(m asl): 400
Till Description: Till is light gray to brown; oxidation is moderate at depth. Sandy with minor silt. Pebbles abundant. Clasts are subangular to sub rounded. 10-20% clasts.		
Vegetation: Shrubs		
Exposure: Pit	Note: Sample is located within previously defined high KIM count zone. Surface has abundant boulders. Inactive frostboil.	
Topographic position: Topographic high		




(13) 17-DECS-013

Date: July 16, 2017	Samplers: Dana Campbell, Brent Ward	Weather: Clear Skies and windy
Sample: 17-DECS-013	12 V 0540545 UTM 7049304	Elevation (m asl): 434
Till Description: Till is brown. 20-25% clasts. Abundant pebbles. Silty sand with subangular clasts. Heavily Oxidized.		
Vegetation: Shrubs.		
Exposure: Pit	Note: Relict frostboil- regrowth of vegetation over frostboil.	
Topographic position: Relative low between two bedrock highs on a stoss slope, high topographic position.		

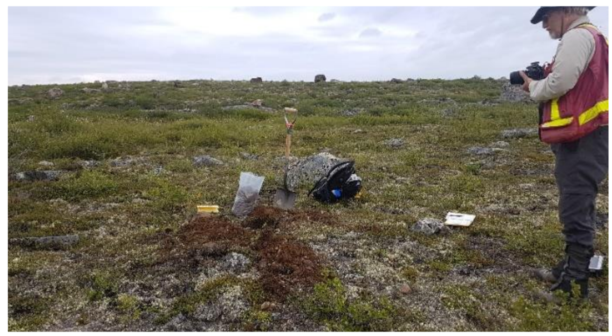

(14) 17-DECS-014

Date: July 16, 2017	Samplers: Dana Campbell, Brent Ward	Weather: Clear Skies and windy
Sample: 17-DECS-014	12 V 0549208 UTM 7053872	Elevation: 437
Till Description: Sandy silt 15-20% clasts. Fine to pebbly. Sub rounded to subangular clasts.		
Vegetation: Shrubs.		
Exposure: Pit	Note: Boulders present at surface, frostboil sampled.	
Topographic position: Mid to down slope.		

(15) 17-DECS-015

Date: July 21, 2017	Samplers: Dana Campbell, Barrett Elliot, Andy Wickham, Bianca Iulianella Phillips	Weather: Clear Skies
Sample: 17-DECS-015	12 V 0542015 UTM 7049802	Elevation(m asl): 407
Till Description: Light gray silty sand, 10-15% clasts, clasts are subangular and up to pebble sized. Matrix is notably rich in micas.		
Vegetation: Shrubs.		
Exposure: Pit	Note: Boulders present at surface. Relict frostboils.	
Topographic position: Topographic high, mid slope.		

(16) 17-DECS-016

Date: July 21, 2017	Samplers: Dana Campbell, Barrett Elliot, Andy Wickham, Bianca Iulianella Phillips	Weather: Clear Skies
Sample: 17-DECS-016	12 V 0536363 UTM 7047396	Elevation: 439
Till Description: light gray silty sand, 20-25% clasts, clasts are angular to subangular. Pebble and cobble sized clasts. Granitic and Microcline clasts are dominant.		
Vegetation: Shrubs and blueberry bushes.		
Exposure: Pit	Note: Till is vesicular in nature. Bedrock is shallow and exposed at surface.	
Topographic position: Topographic high, flat region.		

(17) 17-DECS-017

Date: July 21, 2017	Samplers: Dana Campbell, Barrett Elliot, Andy Wickham, Bianca Iulianella Phillips	Weather: Clear Skies
Sample: 17-DECS-017	12 V 0526750 UTM 7045011	Elevation(m asl): 438
Till Description: Light brown gray soil, 15-20% clasts, clasts are subangular, up to cobbles. Clasts are granitic and felsic in composition.		
Vegetation: Shrubs		
Exposure: Pit	Note: Boulders present at surface. Relict frostboil.	
Topographic position: Topographic high, flat.		

(18) 17-DECS-018

Date: July 21, 2017	Samplers: Dana Campbell, Barrett Elliot, Andy Wickham, Bianca Iulianella Phillips	Weather: Clear Skies
Sample: 17-DECS-018	12 V 0517312 UTM 7042461	Elevation(m asl): 424
Till Description: Silty sand with minor gleying. 15-20% clasts, sub rounded up to pebbles and cobbles in grain size.		
Vegetation: Mosses and shrubs.		
Exposure: Pit	Note: Rare boulders at surface. Active frostboil.	
Topographic position: Flat lying area.		

(19) 17-DECS-019

Date: July 22, 2017	Samplers: Dana Campbell, Barrett Elliot, Sara McPeak	Weather: Cloudy with moderate wind
Sample: 17-DECS-019	12 V 0558977 UTM 7065547	Elevation(m asl): 400
Till Description: Light gray brown silty sand, 20-25% clasts, clasts angular to subangular up to cobbles in grain size.		
Vegetation: Shrubs and small conifers.		
Exposure: Pit	Note: Boulders coming to surface via cryoturbation.	
Topographic position: Flat lying area.		

(20) 17-DECS-020

Date: July 22, 2017	Samplers: Dana Campbell, Barrett Elliot, Sara McPeak	Weather: Cloudy
Sample: 17-DECS-020	12 V 0545789 UTM 7059473	Elevation(m asl): 423
Till Description: Light gray brown, clast dominated, 15-20% fines (sandy silt). Clasts sub rounded to subangular, up to cobbles.		
Vegetation: Shrubs and mosses.		
Exposure: Pit	Note: Boulders abundant at surface.	
Topographic position: Topographic high.		

(21) 17-DECS-021

Date: July 22, 2017	Samplers: Dana Campbell, Barrett Elliot, Sara McPeak	Weather: Cloudy
Sample: 17-DECS-021	12 V 0541212 UTM 7054536	Elevation(m asl): 445
Till Description: Light gray brown silty sand, 20-25% clasts, clasts are subangular.		
Vegetation: Shrubs and minor amounts of moss.		
Exposure: Pit	Note: Boulders are abundant at surface and rounded. Small relict frostboils.	
Topographic position: Topographic high, adjacent to slope.		

Appendix V External Lab Data

Overburden Drilling Management Ltd. Data analysis of 17-DECS

Gold Grain Summary									
Client: Northwest Territories Geological Survey									
File Name: 20187745 - NTGO - Elliott - (17-DECS) - 21 KIM - March 2018									
Total Number of Samples in this Report: 21									
ODM Batch Number(s): 7745									
Sample Number	Number of Visible Gold Grains				Nonmag HMC	Calculated PPB Visible Gold in HMC			
	Total	Reshaped	Modified	Pristine	Weight (g)*	Total	Reshaped	Modified	Pristine
17-DECS-001	0	0	0	0	42.0	0	0	0	0
17-DECS-002	0	0	0	0	37.6	0	0	0	0
17-DECS-003	0	0	0	0	41.2	0	0	0	0
17-DECS-004	2	2	0	0	28.0	3	3	0	0
17-DECS-005	2	1	1	0	58.4	1	1	<1	0
17-DECS-006	0	0	0	0	42.8	0	0	0	0
17-DECS-007	1	1	0	0	44.8	0	1282	0	0
17-DECS-008	1	1	0	0	37.6	15	15	0	0

17-DECS-009	2	2	0	0	24.4	18	18	0	0
17-DECS-010	0	0	0	0	22.4	0	0	0	0
17-DECS-011	2	2	0	0	47.2	30	30	0	0
17-DECS-012	0	0	0	0	36.8	0	0	0	0
17-DECS-013	0	0	0	0	36.0	0	0	0	0
17-DECS-014	3	3	0	0	36.0	1	1	0	0
17-DECS-015	0	0	0	0	33.2	0	0	0	0
17-DECS-016	0	0	0	0	30.4	0	0	0	0
17-DECS-017	0	0	0	0	39.6	0	0	0	0
17-DECS-018	0	0	0	0	42.0	0	0	0	0
17-DECS-019	0	0	0	0	38.8	0	0	0	0
17-DECS-020	1	1	0	0	36.4	1	1	0	0
17-DECS-021	0	0	0	0	34.8	0	0	0	0

Detailed Gold Grain Data

Client: Northwest Territories Geological Survey

File Name: 20187745 - NTGO - Elliott - (17-DECS) - 21 KIM - March 2018

Total Number of Samples in this Report: 21

ODM Batch Number(s): 7745

Sample Number	Dimensions (µm)				Number of Visible Gold Grains				Nonmag HMC Weight* (g)	Calculated V.G. Assay in HMC (ppb)	Metallic Minerals in Pan Concentrate
	Thickness		Width	Length	Reshaped	Modified	Pristine	Total			
17-DECS-001	No Visible Gold										No sulphides.
17-DECS-002	No Visible Gold										No sulphides.
17-DECS-003	No Visible Gold										Tr (5 grains) pyrite (25-150 µm).
17-DECS-004	5	C	25	25	1			1		1	Tr (1 grain) pyrite (75 µm).
	8	C	25	50	1			1		3	
								2	28.0	3	
17-DECS-005	3	C	15	15		1		1		<1	No sulphides.
	8	C	25	50	1			1		1	
								2	58.4	1	
17-DECS-006	No Visible Gold										No sulphides.

17-DECS-007	175	M	175	250	1	1		1282	No sulphides.
						1	44.8	1282	
17-DECS-008	15	C	50	100	1	1		15	No sulphides.
						1	37.6	15	
17-DECS-009	8	C	25	50	1	1		3	No sulphides.
	13	C	50	75	1	1		15	
						2	24.4	18	
17-DECS-010	No Visible Gold								No sulphides.
17-DECS-011	5	C	25	25	1	1		1	No sulphides.
	20	C	75	125	1	1		30	
						2	47.2	30	
17-DECS-012	No Visible Gold								No sulphides.
17-DECS-013	No Visible Gold								No sulphides.
17-DECS-014	3	C	15	15	1	1		<1	Tr (5 grains) pyrite (25-75 µm).
	5	C	25	25	2	2		1	
						3	36.0	1	
17-DECS-015	No Visible Gold								No sulphides.
17-DECS-016	No Visible Gold								No sulphides.

17-DECS-017	No Visible Gold								No sulphides.
17-DECS-018	No Visible Gold								No sulphides.
17-DECS-019	No Visible Gold								No sulphides.
17-DECS-020	5	C	25	25	1	1		1	No sulphides.
						1	36.4	1	
17-DECS-021	No Visible Gold								No sulphides.

Primary Sample Processing Weights and Descriptions

Client: Northwest Territories Geological Survey

File Name: 20187745 - NTGO - Elliott - (17-DECS) - 21 KIM - March 2018

Total Number of Samples in this Report: 21

ODM Batch Number(s): 7745

						Screening and Shaking Table Sample Descriptions												
						Clasts (+2.0 mm)					Matrix (-2.0 mm)							
	Weight (kg wet)						Percentage				Distribution					Colour		
Sample Number	Bulk Rec'd	Archived Split	Table Split	+2.0 mm Clasts	Table Feed	Size	V/S	GR	LS	OT	S/U	SD	ST	CY	ORG	SD	CY	Class
17-DECS-001	12.3	0.3	12.0	1.5	10.5	P	10	90	0	0	U	Y	+	-	Y	OC	OC	TILL
17-DECS-002	12.1	0.3	11.8	2.4	9.4	P	20	80	0	0	U	Y	+	-	Y	DOC	DOC	TILL
17-DECS-003	13.2	0.3	12.9	2.6	10.3	P	20	80	0	0	U	Y	+	-	Y	DOC	DOC	TILL
17-DECS-004	11.1	0.3	10.8	3.8	7.0	P	80	20	0	0	U	Y	Y	Y	N	OC	OC	TILL
17-DECS-005	16.0	0.3	15.7	1.1	14.6	P	50	50	0	0	U	Y	+	-	N	BE	BE	TILL
17-DECS-006	12.8	0.3	12.5	1.8	10.7	P	70	30	0	0	U	Y	Y	-	N	LOC	LOC	TILL
17-DECS-007	13.4	0.3	13.1	1.9	11.2	P	70	30	0	0	U	Y	+	-	N	LOC	LOC	TILL

17-DECS-008	14.5	0.3	14.2	4.8	9.4	P	80	20	0	0	U	Y	+	-	N	LOC	LOC	TILL
17-DECS-009	7.8	0.3	7.5	1.4	6.1	P	90	10	0	0	U	Y	+	-	N	OC	OC	TILL
17-DECS-010	7.1	0.3	6.8	1.2	5.6	P	70	30	0	0	U	Y	+	-	N	OC	OC	TILL
17-DECS-011	13.6	0.3	13.3	1.5	11.8	P	70	30	0	0	U	Y	+	-	N	OC	OC	TILL
17-DECS-012	11.6	0.3	11.3	2.1	9.2	P	20	80	0	0	U	Y	Y	-	N	OC	OC	TILL
17-DECS-013	10.8	0.3	10.5	1.5	9.0	P	20	80	0	0	U	+	Y	-	N	OC	OC	TILL
17-DECS-014	11.0	0.3	10.7	1.7	9.0	P	5	95	0	0	U	Y	+	-	N	LOC	LOC	TILL
17-DECS-015	10.5	0.3	10.2	1.9	8.3	P	30	70	0	0	U	Y	Y	-	N	DOC	DOC	TILL
17-DECS-016	9.6	0.3	9.3	1.7	7.6	P	0	100	0	0	U	Y	Y	-	N	DOC	DOC	TILL
17-DECS-017	12.5	0.3	12.2	2.3	9.9	P	0	100	0	0	U	Y	+	-	Y	OC	OC	TILL
17-DECS-018	13.6	0.3	13.3	2.8	10.5	P	0	100	0	0	U	Y	+	-	N	OC	OC	TILL
17-DECS-019	13.1	0.3	12.8	3.1	9.7	P	95	5	0	0	U	Y	+	-	Y	OC	OC	TILL
17-DECS-020	12.3	0.3	12.0	2.9	9.1	P	95	5	0	0	U	Y	+	-	N	OC	OC	TILL
17-DECS-021	11.5	0.3	11.2	2.5	8.7	P	50	50	0	0	U	Y	+	Y	N	DOC	DOC	TILL

Laboratory Processing Weights

Client: Northwest Territories Geological Survey

File Name: 20187745 - NTGO - Elliott - (17-DECS) - 21 KIM - March 2018

Total Number of Samples in this Report: 21

ODM Batch Number(s): 7745

	Weight of -2.0 mm Table Concentrate (g)												
			0.25 to 2.0 mm Heavy Liquid Separation S.G. 3.20										
					HMC S.G.>3.20								
								Nonferromagnetic HMC					
									Processed Split				
									Total				
Sample Number	Total	-0.25 mm	Total	Lights S.G. <3.2	Total	-0.25 mm (wash)	Mag	Total	%	Weight	0.25 to 0.5 mm	0.5 to 1.0 mm	1.0 to 2.0 mm
17-DECS-001	870.7	678.4	192.3	188.2	4.1	0.4	1.6	2.1	100	2.1	1.5	0.5	0.1
17-DECS-002	1119.7	717.1	402.6	396.2	6.4	1.5	2.6	2.3	100	2.3	1.6	0.6	0.1
17-DECS-003	1118.5	625.0	493.5	483.0	10.5	1.6	4.4	4.5	100	4.5	2.3	1.5	0.7
17-DECS-004	732.6	438.0	294.6	291.2	3.4	0.3	0.4	2.7	100	2.7	1.4	0.9	0.4
17-DECS-005	1110.7	748.8	361.9	355.2	6.7	0.9	0.7	5.1	100	5.1	3.5	1.2	0.4
17-DECS-006	699.8	428.3	271.5	263.2	8.3	0.7	1.5	6.1	100	6.1	3.3	2.0	0.8

17-DECS-007	1001.3	561.5	439.8	429.9	9.9	0.8	1.6	7.5	100	7.5	4.0	2.4	1.1
17-DECS-008	754.4	427.2	327.2	321.1	6.1	0.5	1.0	4.6	100	4.6	2.7	1.5	0.4
17-DECS-009	675.9	402.8	273.1	270.1	3.0	0.2	0.4	2.4	100	2.4	1.4	0.7	0.3
17-DECS-010	598.6	317.6	281.0	277.5	3.5	0.3	0.5	2.7	100	2.7	1.7	0.8	0.2
17-DECS-011	927.9	479.3	448.6	437.8	10.8	1.0	1.7	8.1	100	8.1	5.3	2.2	0.6
17-DECS-012	1096.2	494.6	601.6	599.3	2.3	0.4	0.8	1.1	100	1.1	0.7	0.3	0.1
17-DECS-013	677.7	481.2	196.5	191.5	5.0	0.66	3.3	1.04	100	1.04	0.7	0.3	0.04
17-DECS-014	898.4	606.6	291.8	283.1	8.7	0.8	1.7	6.2	100	6.2	3.9	1.8	0.5
17-DECS-015	1117.7	470.2	647.5	646.7	0.8	0.06	0.3	0.44	100	0.44	0.3	0.1	0.04
17-DECS-016	763.1	427.4	335.7	330.9	4.8	0.37	3.5	0.93	100	0.93	0.7	0.2	0.03
17-DECS-017	953.2	405.0	548.2	544.8	3.4	0.43	1.8	1.17	100	1.17	0.8	0.3	0.07
17-DECS-018	1007.7	547.1	460.6	454.6	6.0	0.6	2.6	2.8	100	2.8	2.1	0.6	0.1
17-DECS-019	649.9	398.2	251.7	249.8	1.9	0.1	0.6	1.2	100	1.2	0.7	0.4	0.1
17-DECS-020	730.2	386.1	344.1	341.2	2.9	0.2	0.8	1.9	100	1.9	1.1	0.6	0.2
17-DECS-021	938.6	502.3	436.3	434.7	1.6	0.2	0.3	1.1	100	1.1	0.7	0.3	0.1

Kimberlite Indicator Mineral Counts

Client: Northwest Territories Geological Survey

File Name: 20187745 - NTGO - Elliott - (17-DECS) - 21 KIM - March 2018

Total Number of Samples in this Report: 21

ODM Batch Number(s): 7745

Number of Grains

Sample Number	Selected MMSIMs 1.0 to 2.0 mm Low-Cr diopside		Cpy		Gh		0.5 to 1.0 mm Low-Cr diopside		Cpy		Gh		0.25 to 0.5 mm Low-Cr diopside		Cpy		Gh		KIMs 1.0 to 2.0 mm GP		GO		DC		IM		CR		FO		0.5 to 1.0 mm GP		GO		DC		IM		CR		FO		0.25 to 0.5 mm GP		GO		DC		IM		CR		FO		Total (KIMs)	
	T	**P**	**T**	**P**	**T**	**P**	**T**	**P**	**T**	**P**	**T**	**P**	**T**	**P**	**T**	**P**	**T**	**P**	**T**	**P**	**T**	**P**	**T**	**P**	**T**	**P**	**T**	**P**	**T**	**P**	**T**	**P**	**T**	**P**	**T**	**P**	**T**	**P**	**T**	**P**	**T**	**P**	**T**	**P**	**T**	**P**	**T**	**P**	**T**	**P**	**T**	**P**	**T**	**P**	**T**	**P**
17-DECS -001	0	0	0	0	0	0	0	0	0	0	0	0	0	0	0	0	1	1	0	0	0	0	0	0	0	0	0	0	0	0	0	0	0	0	0	0	0	0	0	0	0	0	0	0	0	0	0	0	0	0	5	5	0	0	5	5
17-DECS-002	0	0	0	0	0	0	0	0	0	0	0	0	0	0	0	0	0	0	0	0	0	0	0	0	0	0	0	0	0	0	0	0	0	0	0	0	0	0	0	0	0	0	0	0	0	0	0	0	0	0	3	3	0	0	3	3
17-DECS-003	0	0	0	0	0	0	0	0	0	0	0	0	1	1	0	0	0	0	0	0	0	0	0	0	0	0	0	0	0	0	0	0	0	0	0	0	0	0	0	0	0	0	1	1	0	0	0	0	1	1	0	0	0	0	2	2
17-DECS-004	0	0	0	0	0	0	0	0	0	0	0	0	0	0	0	0	0	0	0	0	0	0	0	0	0	0	0	0	0	0	0	0	0	0	0	0	0	0	0	0	0	0	0	0	0	0	0	0	0	0	0	0	0	0	0	0
17-DECS-005	0	0	0	0	0	0	0	0	0	0	0	0	0	0	0	0	0	0	0	0	0	0	0	0	0	0	0	0	0	0	0	0	0	0	0	0	0	0	0	0	0	0	0	0	0	0	0	0	0	0	0	0	0	0	0	0
17-DECS-006	0	0	0	0	0	0	0	0	0	0	0	0	0	0	0	0	0	0	0	0	0	0	0	0	0	0	0	0	0	0	0	0	0	0	0	0	0	0	0	0	0	0	0	0	0	0	0	0	0	0	0	0	0	0	0	0
17-DECS-007	0	0	0	0	0	0	0	0	0	0	0	0	0	0	0	0	0	0	0	0	0	0	0	0	0	0	0	0	0	0	0	0	0	0	0	0	0	0	0	0	0	0	0	0	0	0	0	0	0	0	0	0	0	0	0	0
17-DECS-008	0	0	0	0	0	0	0	0	0	0	0	0	0	0	0	0	1	1	0	0	0	0	0	0	0	0	0	0	0	0	0	0	0	0	0	0	0	0	0	0	0	0	0	0	0	0	0	0	0	0	0	0	0	0	0	0
17-DECS-009	0	0	0	0	0	0	0	0	0	0	0	0	0	0	0	0	0	0	0	0	0	0	0	0	0	0	0	0	0	0	0	0	0	0	0	0	0	0	0	0	0	0	0	0	0	0	0	0	0	0	0	0	0	0	0	0
17-DECS-010	0	0	0	0	0	0	0	0	0	0	0	0	0	0	0	0	0	0	0	0	0	0	0	0	0	0	0	0	0	0	0	0	0	0	0	0	0	0	0	0	0	0	0	0	0	0	0	0	0	0	1	1	0	0	1	1
17-DECS-011	0	0	0	0	0	0	0	0	0	0	0	0	0	0	0	0	0	0	0	0	0	0	0	0	0	0	0	0	0	0	0	0	0	0	0	0	0	0	0	0	0	0	0	0	0	0	0	0	0	0	0	0	0	0	0	0
17-DECS-012	0	0	0	0	0	0	0	0	0	0	0	0	0	0	0	0	0	0	0	0	0	0	0	0	0	0	0	0	0	0	0	0	0	0	0	0	0	0	0	0	0	0	0	0	0	0	0	0	0	0	0	0	0	0	0	0
17-DECS-013	0	0	0	0	0	0	0	0	0	0	0	0	0	0	0	0	0	0	5	5	0	0	0	0	1	1	0	0	0	0	82	82	17	17	0	0	3	3	6	6	0	0	600	20	50	20	1	1	5	5	11	11	0	0	781	171
17-DECS-014	0	0	0	0	0	0	0	0	0	0	0	0	0	0	0	0	0	0	0	0	0	0	0	0	0	0	0	0	0	0	0	0	0	0	0	0	0	0	0	0	0	0	0	0	0	0	0	0	0	0	0	0	0	0	0	0
17-DECS-015	0	0	0	0	0	0	0	0	0	0	0	0	0	0	0	0	0	0	0	0	0	0	0	0	0	0	0	0	0	0	1	1	0	0	0	0	0	0	0	0	0	0	0	0	0	0	0	0	0	0	0	0	0	0	1	1
17-DECS-016	0	0	0	0	0	0	0	0	0	0	0	0	0	0	0	0	0	0	0	0	0	0	0	0	0	0	0	0	0	0	0	0	0	0	0	0	2	2	0	0	0	0	8	8	0	0	0	0	2	2	0	0	0	0	12	12
17-DECS-017	0	0	0	0	0	0	0	0	0	0	0	0	0	0	0	0	0	0	0	0	0	0	0	0	0	0	0	0	0	0	0	0	0	0	0	0	0	0	0	0	0	0	2	2	0	0	0	0	1	1	0	0	0	0	3	3
17-DECS-018	0	0	0	0	0	0	0	0	0	0	0	0	0	0	0	0	0	0	0	0	0	0	0	0	0	0	0	0	0	0	0	0	0	0	0	0	0	0	0	0	0	0	2	2	0	0	0	0	1	1	0	0	0	0	3	3
17-DECS-019	0	0	0	0	0	0	0	0	0	0	0	0	0	0	0	0	1	1	0	0	0	0	0	0	0	0	0	0	0	0	0	0	0	0	0	0	0	0	0	0	0	0	0	0	0	0	0	0	0	0	0	0	0	0	0	0
17-DECS-020	0	0	0	0	0	0	0	0	0	0	0	0	0	0	0	0	0	0	0	0	0	0	0	0	0	0	0	0	0	0	0	0	0	0	0	0	0	0	0	0	0	0	0	0	0	0	0	0	0	0	0	0	0	0	0	0
17-DECS-021	0	0	0	0	0	0	0	0	0	0	0	0	0	0	0	0	0	0	0	0	0	0	0	0	0	0	0	0	0	0	0	0	0	0	0	0	0	0	0	0	0	0	0	0	0	0	0	0	2	2	0	0	0	0	2	2

T = Total number of grains in sample. Total is estimated if number is greater than number of picked grains.

P = Number of picked grains in sample.

Kimberlite Indicator Mineral Remarks			
Client: Northwest Territories Geological Survey			
File Name: 20187745 - NTGO - Elliott - (17-DECS) - 21 KIM - March 2018			
Total Number of Samples in this Report: 21			
ODM Batch Number(s): 7745			
Sample Number	Remarks	INPUT ASSEMBLAGE	INPUT REMARKS
17-DECS-001	Almandine-augite-hematite/staurolite-apatite-epidote assemblage. SEM checks from 0.25-0.5 mm fraction: 1 GO versus almandine candidates = 1 almandine; 4 IM versus crustal ilmenite candidates = 3 crustal ilmenite and 1 CR; 4 CR candidates = 4 CR; 2 blue-green gahnite versus spinel candidates = 1 gahnite and 1 spinel; and 1 loellingite candidate = 1 Ni-loellingite.	Almandine-augite-hematite/staurolite-apatite-epidote	SEM checks from 0.25-0.5 mm fraction: 1 GO versus almandine candidates = 1 almandine; 4 IM versus crustal ilmenite candidates = 3 crustal ilmenite and 1 CR; 4 CR candidates = 4 CR; 2 blue-green gahnite versus spinel candidates = 1 gahnite and 1 spinel; and 1 loellingite candidate = 1 Ni-loellingite.
17-DECS-002	Almandine-augite-hematite/staurolite-epidote assemblage. SEM checks from 0.25-0.5 mm fraction: 3 IM versus crustal ilmenite candidates = 2 crustal ilmenite and 1 CR.	Almandine-augite-hematite/staurolite-epidote	SEM checks from 0.25-0.5 mm fraction: 3 IM versus crustal ilmenite candidates = 2 crustal ilmenite and 1 CR.
17-DECS-003	Almandine-augite/staurolite assemblage. SEM check from some size or other: 1 GP versus zircon candidate = 1 GP.	Almandine-augite/staurolite	SEM check from some size or other: 1 GP versus zircon candidate = 1 GP.
17-DECS-004	Almandine-hornblende-augite/staurolite-epidote assemblage.	Almandine-hornblende-augite/staurolite-epidote	
17-DECS-005	Hornblende-augite-almandine/staurolite-apatite-epidote assemblage.	Hornblende-augite-almandine/staurolite-apatite-epidote	
17-DECS-006	Hornblende-almandine-augite/staurolite-epidote-apatite assemblage.	Hornblende-almandine-augite/staurolite-epidote-apatite	

17-DECS-007	Almandine-hornblende/staurolite-apatite-epidote assemblage.	Almandine-hornblende/staurolite-apatite-epidote	
17-DECS-008	Almandine-hornblende-augite/staurolite-apatite-sillimanite assemblage. SEM checks from 0.25-0.5 mm fraction: 3 GP versus almandine candidates = 3 almandine; and 2 blue-green gahnite versus spinel candidates = 1 gahnite and 1 spinel.	Almandine-hornblende-augite/staurolite-apatite-sillimanite	SEM checks from 0.25-0.5 mm fraction: 3 GP versus almandine candidates = 3 almandine; and 2 blue-green gahnite versus spinel candidates = 1 gahnite and 1 spinel.
17-DECS-009	Almandine-hornblende-augite/staurolite-epidote-apatite assemblage.	Almandine-hornblende-augite/staurolite-epidote-apatite	
17-DECS-010	Almandine-hornblende-augite/staurolite-apatite-epidote assemblage.	Almandine-hornblende-augite/staurolite-apatite-epidote	
17-DECS-011	Hornblende-almandine-augite/staurolite-epidote-apatite assemblage. SEM checks from 0.25-0.5 mm fraction: 3 GP versus almandine candidates = 3 almandine; and 1 blue-green gahnite versus spinel candidates = 1 spinel.	Hornblende-almandine-augite/staurolite-epidote-apatite	SEM checks from 0.25-0.5 mm fraction: 3 GP versus almandine candidates = 3 almandine; and 1 blue-green gahnite versus spinel candidates = 1 spinel.
17-DECS-012	Hornblende-augite-almandine/apatite-epidote assemblage.	Hornblende-augite-almandine/apatite-epidote	
17-DECS-013	Augite-almandine-hornblende/epidote-GP assemblage. SEM checks from 0.25-0.5 mm fraction: 13 IM versus crustal ilmenite candidates = 5 IM and 8 CR; and 1 blue-green gahnite versus spinel candidate = 1 knorringite (Mg3Cr2 (SiO4)3). 4 GP and 1 IM from 1.0-2.0 mm; 55 GP, 12 GO and 1 IM from 0.5-1.0 mm; and 30% of GP and 25% of GO from 0.25-0.5 mm fractions have alteration mantles.	Augite-almandine-hornblende/epidote-GP	SEM checks from 0.25-0.5 mm fraction: 13 IM versus crustal ilmenite candidates = 5 IM and 8 CR; and 1 blue-green gahnite versus spinel candidate = 1 knorringite (Mg3Cr2 (SiO4)3). 4 GP and 1 IM from 1.0-2.0 mm; 55 GP, 12 GO and 1 IM from 0.5-1.0 mm; and 30% of GP and 25% of GO from 0.25-0.5 mm fractions have alteration mantles.
17-DECS-014	Hornblende-almandine-augite/staurolite-apatite-epidote assemblage.	Hornblende-almandine-augite/staurolite-apatite-epidote	

17-DECS-015	Goethite/epidote-apatite assemblage. SEM check from 0.25-0.5 mm fraction: 1 GP versus almandine candidate = 1 almandine.	Goethite/epidote-apatite	SEM check from 0.25-0.5 mm fraction: 1 GP versus almandine candidate = 1 almandine.
17-DECS-016	Hornblende-augite/epidote-apatite-staurolite assemblage.	Hornblende-augite/epidote-apatite-staurolite	
17-DECS-017	Horblende-augite/apatite assemblage.	Horblende-augite/apatite	
17-DECS-018	Hornblende-augite-almandine/titanite-apatite-diopside assemblage.	Hornblende-augite-almandine/titanite-apatite-diopside	
17-DECS-019	Almandine-hornblende/staurolite-apatite assemblage. SEM check from 0.25-0.5 mm fraction: 1 blue-green gahnite versus spinel candidate = 1 gahnite.	Almandine-hornblende/staurolite-apatite	SEM check from 0.25-0.5 mm fraction: 1 blue-green gahnite versus spinel candidate = 1 gahnite.
17-DECS-020	Almandine-augite-hornblende/staurolite-apatite-sillimanite assemblage. SEM checks from 0.25-0.5 mm fraction: 1 GO versus grossular candidate = 1 grossular; and 1 blue-green gahnite versus spinel candidate = 1 gahnite.	Almandine-augite-hornblende/staurolite-apatite-sillimanite	SEM checks from 0.25-0.5 mm fraction: 1 GO versus grossular candidate = 1 grossular; and 1 blue-green gahnite versus spinel candidate = 1 gahnite.
17-DECS-021	Almandine-hornblende/apatite-staurolite assemblage. SEM checks from 0.25-0.5 mm fraction: 2 GO versus grossular candidates = 2 almandine; and 4 IM versus crustal ilmenite candidates = 2 IM and 2 crustal ilmenites.	Almandine-hornblende/apatite-staurolite	SEM checks from 0.25-0.5 mm fraction: 2 GO versus grossular candidates = 2 almandine; and 4 IM versus crustal ilmenite candidates = 2 IM and 2 crustal ilmenites.

Northwest Territories Geological Survey Published maps (Mirza and Elliott, 2017):

..\Tilt Derivative East_Elliott.pdf

..\Total Residual Magnetic Field_Elliott.pdf

Table 7.7: 2015 Munn Lake Property Samples- Microprobe Results (Miller, 2016)

Sample	UTME	UTMN	Type	G9	G10	Eclogite	Cr-Diopside	Olivine	Ilmenite	Chromite
120651	558779	7066304	Basal Till	0	0	0	0	0	0	1
120652	558766	7066344	Basal Till	0	0	0	0	0	0	1
120653	558750	7066382	Basal Till	0	0	0	0	0	0	0
120654	558755	7066455	Basal Till	0	0	0	0	0	0	0
120655	558741	7066494	Basal Till	1	0	0	0	0	0	0
120656	551397	7063954	Basal Till	0	0	0	0	0	0	0
120657	551413	7063865	Basal Till	0	0	0	0	0	0	0
120658	551481	7063780	Basal Till	0	0	0	0	0	0	0
120659	551455	7063723	Basal Till	0	0	0	0	0	0	0
120665	545328	7060162	Basal Till	0	0	0	0	0	0	0
120666	545321	7060127	Basal Till	0	0	0	0	0	0	0
120667	545303	7060073	Basal Till	0	0	0	0	0	0	0
120675	557698	7065023	Basal Till	0	0	0	0	0	0	0
120676	558567	7066343	Basal Till	0	0	0	0	0	0	0
120683	551182	7063852	Basal Till	0	0	0	0	0	0	0
120684	551176	7063800	Basal Till	0	0	0	0	0	0	0
120685	551169	7063762	Basal Till	0	0	0	0	0	0	0
120686	556786	7067427	Basal Till	0	0	0	0	0	0	0
120687	556802	7067373	Basal Till	0	0	0	0	0	0	0
120688	556817	7067325	Basal Till	0	0	0	0	0	0	0
120689	556831	7067274	Basal Till	0	0	0	0	0	0	0
120690	556843	7067224	Basal Till	0	0	0	0	0	0	0
120691	549048	7062134	Basal Till	0	0	0	0	0	11	0
120692	549044	7062084	Basal Till	0	0	0	0	0	3	0
120693	549043	7062030	Basal Till	0	0	0	0	0	0	0
120694	544197	7060165	Basal Till	0	0	0	0	0	0	0
120695	544187	7060216	Basal Till	0	0	0	0	0	3	0
120696	544195	7060276	Basal Till	1	0	0	0	0	6	0
120697	554929	7066826	Basal Till	4	0	0	0	0	1	0
120698	556111	7067029	Basal Till	0	0	0	0	0	0	0

120699	556094	7067080	Basal Till	1	0	0	0	0	0	0
120700	556076	7067139	Basal Till	1	0	1	0	0	1	0
120701	556065	7067183	Basal Till	0	0	0	0	0	0	0
120702	556056	7067235	Basal Till	1	0	0	0	0	1	0
120703	557697	7064983	Basal Till	3	1	0	0	0	22	0
120704	557692	7064887	Basal Till	1	0	1	0	0	604	3
120705	557705	7064942	Basal Till	0	0	0	0	0	1	0
120706	557702	7064833	Basal Till	0	0	1	0	0	0	0